UNIVERSIDAD AUTÓNOMA DE NUEVO LEÓN

FACULTAD DE CIENCIAS FÍSICO MATEMÁTICAS

DIVISIÓN DE ESTUDIOS DE POSTGRADO

QUANTUM ENTANGLEMENT OF PARTICLES IN BLACK HOLE NEIGHBORHOODS

THESIS

SUBMITTED IN PARTIAL FULFILLMENT
OF THE REQUIREMENTS FOR THE DEGREE OF

PH.D.
IN INDUSTRIAL PHYSICS ENGINEERING

BY

FELIPE ANGEL ROBLEDO PADILLA

CIUDAD UNIVERSITARIA   NOVEMBER 2014

Universidad Autónoma de Nuevo León
Facultad de Ciencias Físico-Matemáticas

División de Estudios de Postgrado
Doctorado en Ciencias en Ingeniería Física Industrial

Thesis committee members recommend the present thesis *Quantum Entanglement of Particles in Black Hole Neighborhoods* written by Felipe Angel Robledo Padilla, with student number 809745, to be accepted in partial fulfillment of the requirements for the degree of **Ph.D. in Industrial Physics Engineering**

Thesis Committee

José Rubén Morones Ibarra, Ph.D.
President/Thesis director

Héctor Hugo García Compeán, Ph.D.
Secretary/Thesis Co-director

Edgar Martínez Guerra, Ph.D.
1st. Examiner

Manuel García Méndez, Ph.D.
2nd. Examiner

Manuel A. Jiménez Lizárraga, Ph.D.
3rd. Examiner

Romeo Selvas Aguilar, Ph.D.
Sub-Director of División de Estudios de Posgrado

November de 2014

Abstract

The aim of this thesis is to obtain the spin precession angle for an Einstein-Podolsky-Rosen pair of spin-1/2 particles in circular orbits in a general axially symmetric spacetime. In order to achieve this purpose, hovering observers are introduced for ensuring fixed reference frames to perform suitable reliable measurements. Frame-dragging of spinning holes is explicitly incorporated relative to hovering observers. The spin-singlet state is found to be mixed with the spin-triplet by acceleration and gravity effects, which deteriorate the perfect anti-correlation of an entangled pair of spins measured by hovering observers. Finally, an algorithm to calculate spin precession for a general axially symmetric spacetime is proposed. This algorithm is applied to study the complete list of expanding and twisting Type D Plebański-Demiański black holes and their descendent limiting solutions with lower parameters.

This thesis has two main contributions on the subject of quantum entanglement and general relativity. The first one is the incorporation of the frame-dragging in the velocity of the particles suspended viewed from observers. This analysis was not included in the literature review. The second contribution is the construction of the algorithm able to quickly calculate the spin precession for any metric of spacetime that is desired. This generalization is valuable because it not only allows you to make calculations for the proposed black holes, but also for another curvatures of space-time unforeseen.

Resumen

El propósito de esta tesis es obtener el ángulo de precesión de espín de un par de partículas EPR de espín-$\frac{1}{2}$, moviéndose en órbitas circulares en un espacio-tiempo con simetría axial. Para lograr este objetivo, se introducen observadores suspendidos para asegurar que sus marcos de referencia estén fijos y realizar así mediciones confiables. Con respecto a estos observadores suspendidos se incorpora explícitamente el arrastre del sistema de coordenadas en presencia de los agujeros negros. Se encuentra que el estado singlete de espín se mezcla con el estado triplete de espín por los efectos de la aceleración y gravedad sobre las partículas, lo cual deteriora la perfecta anticorrelación del par de espines entrelazados medidos por los observadores suspendidos. Finalmente, se propone un algoritmo para calcular la precesión de espín de las partículas en un espacio-tiempo general con simetría axial. Este algoritmo se utiliza para estudiar una lista completa de agujeros negros Tipo D de Plebański-Demiański con expansión y torsión, así como sus subcasos particulares con menor número de parámetros.

Esta tesis tiene dos principales contribuciones en el tema del entrelazamiento cuántico y la relatividad general. La primera es la incorporación del arrastre de coordenadas en la velocidad de las partículas visto desde los observadores suspendidos. Este análisis no se había incluido en la bibliografía revisada. La segunda contribución es la construcción del algoritmo capaz de calcular rápidamente la precesión de espín para cualquier métrica de espacio-tiempo que se desee. Esta generalización es valiosa porque no sólo permite hacer cálculos para los agujeros negros propuestos, sino también para otras curvaturas de espacio-tiempo no previstas.

Acknowledgement

To my parents.

To the medical and nurse staff of IMSS Clinica 25 and specially to the anonymous and altruistic donor of june 2010.

To my thesis director, José Rubén Morones Ibarra, Ph.D. who opened the opportunity of a degree and renewed my love for Theoretical Physics, when I thought there was no more chances in life.

And to Héctor Hugo García Compeán, Ph.D. who support me with infinite patience and advise me in this thesis, who give me access to a whole Universe.

To the faculty of the Industrial Physics Engineering Ph.D. and the staff of Centre for Research in Physical and Mathematical Sciences of Universidad Autónoma de Nuevo León.

ༀ་མ་ཎི་པདྨེ་ཧཱུྃ།

Contents

List of Figures

Chapter 1

Introduction

Entanglement of quantum states is a very interesting subject which has had a great deal of attention as a fundamental issue in physics since Einstein-Podolsky-Rosen (EPR) famous paper [1]. With the work by Bohm-Aharanov [2] for spin-entangled particles and Bell's hidden variables [3] it was possible to realize that quantum mechanics is actually the correct description of the quantum phenomena and eventual experimental results [4, 5, 6] confirmed this fact. In recent years a great deal of research on entangled states has been focused on quantum communication and teleportation [7, 8, 9], quantum computation [10, 11, 12, 13] and quantum cryptography [14, 15].

The quantum states of matter in a classical gravitational background have been of great interest in physical models. One of the famous experimental examples in this situation are the experiments of neutron interferometry in laboratories on the Earth. In such experiments it is possible to capture the effects of the gravitational field into quantum phases associated to the possible trajectories of a beam of neutrons, following paths with different intensity of the gravitational field. The phase differences have information about how the gravitational field of Earth do affect the quantum states of neutrons [16]. Experiments using atomic interferometry were also reported later [17, 18]. Another instance of the description of quantum states of matter in classical gravitational fields is Hawking's radiation [19, 20] describing the process of black hole evaporation. This process involves relativistic quantum particles and uses quantum field theory in curved spacetimes (see for instance, [21, 22]).

For many years the general behavior of the entangled quantum states has been studied in the literature. In particular, the entanglement of a pair of non-relativistic spin-1/2 particles have been extended to Special Relativity [23, 24, 25, 26, 27, 28] through the uses of the Wigner rotation [29, 30]. More recently the entanglement was integrated within the framework of General Relativity for the Schwarzschild spacetime [31] and for the Kerr-Newman spacetime

[32].

In particular for the Schwarzschild black hole, Terashima and Ueda [31] considered a pair of spinning particles in an entangled state moving on equatorial motion. Their results showed that the acceleration and the gravitational effects spoiled the EPR correlation [1] precisely in the directions that are the same than in non-relativistic theory, and it apparently decrease the degree of the violation of Bell's inequality. This effect leads to a decrement in Bell's inequality degree of violation given by the quantum spin directions is written as

$$\langle \mathcal{Q}'\mathcal{S}' \rangle + \langle \mathcal{R}'\mathcal{S}' \rangle + \langle \mathcal{R}'\mathcal{T}' \rangle - \langle \mathcal{Q}'\mathcal{T}' \rangle = 2\sqrt{2}\cos^2 \Delta.$$

All the information of the gravitational field is encoded in the precession angle Δ, which depends in general on all the parameters of the black hole of interest, on the radius r and on the frame-dragging velocity (if any). The case with $\Delta = 0$ corresponds with the result consistent with quantum mechanics. For $\Delta \neq 0$ and large, there is a deterioration of the perfect anti-correlation of the entangled pair of spin-1/2 particles.

For the simplest case of the Schwarzschild black hole studied by Terashima and Ueda [31], it depends only on the mass m parameter, and its strongest effect is localized on the Schwarzschild event horizon due an extremely (infinite) rapid spin precession with $|\Delta_S| \to \infty$ producing the mentioned decrement of the Bell's inequality. In this case there is not frame-dragging, however Δ_S still depends on the local velocity of the particles with respect to the hovering observers. In the whole process it is observed that the choices of the four-velocity vector and of the vierbein are important in order to be able of communicating non-locally in a curved spacetime using these spinning particles. Similar results, but also with subtle and important differences, were found for the case of Kerr-Newman black holes [32] and Kerr-Newman metric with frame-dragging [33].

The approach used in the present thesis follows mainly that of Terashima and Ueda in analysis, notations and conventions. The main idea is to look at the structure behind a Wigner rotation on the spin quantum state, which is locally well defined in the non-relativistic theory. This transformation must preserve quantum probabilities of finding the spin state in the particular direction measured on a local inertial frame. In order to guarantee this, the transformation changing quantum state from a point to another one, must be unitary. The Wigner rotation matrix [29] precisely achieves this. This rotation is composed by infinitesimal Lorentz transformations, which consist of a boost along the radial direction and a rotation in the angle direction of the orbital particle.

The aim of this work is to extend the description of spin precession mentioned above to the Plebański-Demiański black hole [34], which is the most general axially symmetric expanding

and twisting Type-D solution of the Einsten-Maxwell equations according the Petrov-Penrose classification (see for instance, [35]). In order to do that, it is more convenient to write down the metric in Boyer-Lindquist coordinates. This description was studied by Griffiths and Podolský in a series of papers [36, 37, 38] (and reviewed in Refs. [39, 40]) with the purpose of clarifying the physical meaning of the parameters entering in the solution.

The Plebański-Demiański solution has been worked out previously in the literature connecting with higher dimensional theories. Some time ago, there was some interest of this metric in the study of some generalizations of the AdS/CFT correspondence [41, 42, 43]. More recently has been a great deal of work in the context of higher-dimensional solutions the Kerr-NUT-(anti-)de Sitter black hole in the context of brane and string theory [44, 45, 46, 47, 48, 49, 50, 51].

The Plebański-Demiański family of Type D solutions of the Einstein field equation describes a configuration of the gravitational fields characterized by seven parameters [34]. These configurations have null congruences of geodesic curves characterized in general by non-vanishing expansion, twist and shear parameters. In the present thesis we will consider only expanding and twisting solutions. Under certain non-degenerate coordinate transformations of the original metric and the setting of constraints, the metric is turned out into a new suitable form in Boyer-Lindquist coordinates and depending on seven parameters with almost direct physical interpretation [36, 37, 38, 39, 40].

Other kind of models involving the effects of the gravitational field on quantum matter properties precisely in Plebański-Demiański backgrounds is discussed in Ref. [52]. In that paper the phase shift of charged particles interferometry described by complex scalar fields was computed. In there it was also adopted the mentioned new form of the Plebański-Demiański spacetimes and it was shown that all physical parameters contribute to the phase shift. The consideration of the interferometry of spin-1/2 particles in this context was worked out in Ref. [53].

In this work the final result is a spin precession of a particle moving in circular motion in curved spacetime due the acceleration of the particle by an external force and due to the difference between local inertial frames at different points. These enable us to find a precession angle Δ for a general axially symmetric spacetime. These results are then applied to describe the spin precession angle of an EPR pair of particles moving on the equator of a expanding and twisting Plebański-Demiański black hole. We will find that this angle depends on all the physical parameters of the black hole. Moreover, by making appropriate reductions we obtain the precession angle for all known subfamilies of this Plebański-Demiański black hole.

This thesis is organized as follows. In Chapter 2 it is reviewed the background needed to solve the general problem of Quantum Mechanics of Entanglement in gravitational classical backgrounds. In particular for General Relativity it is reviewed the Type-D solution of the Einstein-Maxwell field equations according the Petrov-Penrose classification of Weyl tensor.

Also in Chapter 2 the Entanglement is described, as a counterexample proposed by Einstein [1] of Quantum Mechanics validity and it is reviewed the Entanglement until today and the experimental results. Then the Spin Correlation measurements and Bell's Inequality of the metric are introduced.

In Chapter 3 the effect of the axially symmetric component is reviewed and the frame-dragging corrections over the velocity of a particles are calculated. The Zero Angular Momentum Observers (ZAMO's) are introduced. There is also presented a gedanken experiment to describe the entangled pair of particles in circular orbit around a general axially symmetric black hole. Moreover, in this same section an algorithm to find the spin precession angle without reference to any particular spacetime metric is proposed. It is calculated the EPR correlation by Wigner rotations due the motion of the particles in a generalized spacetime.

Finally all results are integrated in the Section 4 to illustrate the use of the algorithm to get the spin precession angle for the Plebański-Demiański black hole. From this general case the spin precession angle of the EPR pair is obtained for the complete list of subfamilies of Einstein's equation expanding solutions. It is found that for the most general case, this angle depends on all the physical parameters of the solution. Conclusions and final remarks are presented in Section 5.

There is included at the end two appendixes. The Appendix A is dedicated to clarify the importance of the Lorentz Transformation and how to get it in Spetial Relativity. And in Appendix B the Wigner rotation for General Relativity, is presented and developed.

1.1   The general problem to solve

The aim of the present work is to study the spin state of a pair of entangled particles moving in a gravitational field to show its decoherence by the effects of General Relativity.

The spin in General Relativity can be defined only locally by invoking the rotational symmetry of the local inertial frame. As a consequence of this local definition, the motion of the particles is accompanied by a continuous succession of local Lorentz transformations [54].

These continuous succession of transformations is caused by the spacetime curvature. This means that even if the state of the spin is pure at one spacetime point, it, in general,

becomes mixed at an other spacetime point, e.g. from singlet to triplet.

As Terashima and Ueda [31] showed, the acceleration and the gravitational effects in a Schwarzschild spacetime spoiled the EPR correlation precisely in the directions that are the same than in non-relativistic theory, and it apparently decrease the degree of the violation of Bell's inequality.

This thesis extend this previous work and address the problem of finding the precession of spin of a pair of particles moving in a general curved spacetime. The precession of spin is caused by the acceleration of the particles by an external force and due to the difference between local inertial frames at different points.

1.2 The particular problem to solve

From the work of Terashima-Ueda [31] we know that gravity destroys the quantum entanglement. And more important, we are able to measure this effect and therefore make predictions with the knowledge of the position and the velocity of a pair of entangled particles.

The aim of this thesis is extend the previous research with more parameters besides the mass. We shall see that the extra parameters modify the spacetime metric and consequently the entanglement of a pair of particles in circular orbits around a black hole. This research is an exploration with an initial hypothesis that quantum entanglement shall be reduced as more parameters are incorporated into the metric.

For this purpose, a Plebański-Demiański black hole is used as spacetime background to calculate the precession angle of the entangled particles traveling in circular orbits around this black hole. The Plebański-Demiański spacetime is the most general axially symmetric expanding and twisting Type-D solution of the Einstein-Maxwell equations according the Petrov-Penrose classification (see for instance, [35]). It is important because the Plebański-Demiański spacetime covers a wide range of spacetimes that can be found in nature. Also, it could be possible to test in the future some implication of this model in some level.

In the present work we consider two observers and an EPR particle source on the equator plane $\theta = \pi/2$ of the Plebański-Demiański spacetime. The observers are placed at azimuthal angles $\phi = \pm\Phi$ and the EPR source is located at $\phi = 0$. The observers and the EPR source are assumed to be hovering over the black hole in order to keep them "at rest" in the coordinate system. The EPR source emits a pair of entangled particles in opposite directions, describing a circular orbit on the equator at constant radius. We suppose that this EPR source is accelerated on the equator in order to keep a constant radius, in such a way that they are not influenced by the frame-dragging. The gedanken experiment depicting

this situation is shown in Fig. 1.1.
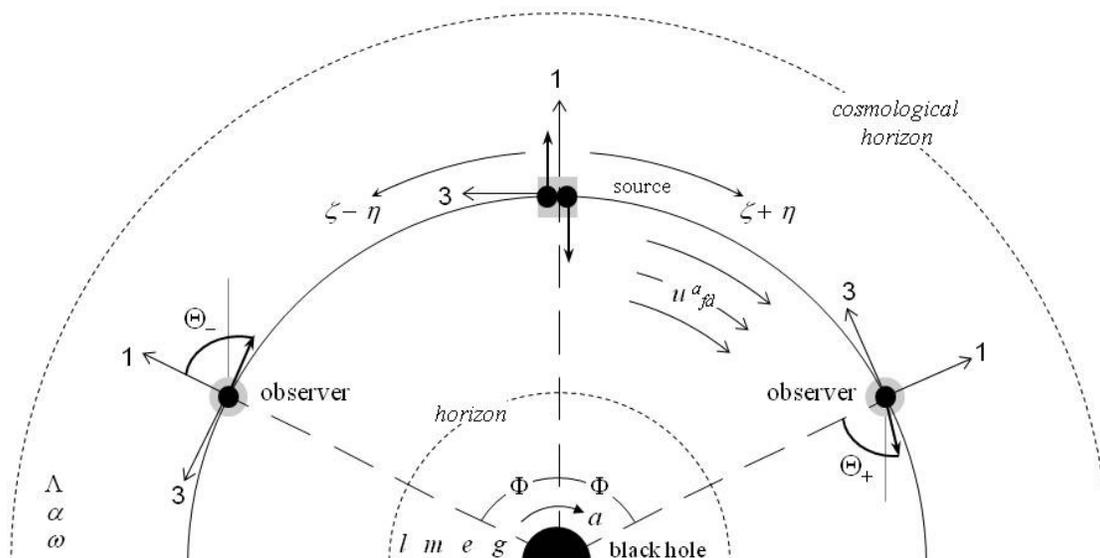
Figure 1.1: An EPR gedanken experiment in an axially symmetric spacetime.

The pair of entangled particles has a quantum state defined by the four-momentum and spins that shall be measured by each hovering observer. The spin-singlet state for entangled particles is given by

$$|\psi\rangle = \frac{1}{\sqrt{2}}[|p_+^a, \uparrow; \phi\rangle|p_-^a, \downarrow; \phi\rangle - |p_+^a, \downarrow; \phi\rangle|p_-^a, \uparrow; \phi\rangle], \tag{1.1}$$

where the sign on the lineal momentum stand for the direction of each particle and the arrows corresponds to the up and down of spin direction. The azimuthal position is represented by the ϕ coordinate, where for simplicity it shall equal zero.

Therefore, the objective of this research is to calculate the quantum state that the observers measure over the entangled particles as they travel starting from the initial state defined by equation (1.1). The Lorentz transformations shall determine the measurement of the quantum states and the cumulative sum of these transformations must show whether the curvature of spacetime modifies the initial state.

Chapter 2

Background

2.1 Quantum Entanglement

In May 1935, Albert Einstein, Boris Podolsky and Nathan Rosen published [1] an argument that quantum mechanics fails to provide a complete description of physical reality. This article was one of the last intent Einstein did to argue against the interpretation of the quantum mechanics and the uncertainty principle.

Throughout his life, Einstein was faithful to three principles that he believed they must be part of a good description of nature [55]:

1. The fundamental level of nature should be described in principle by a deterministic theory, even though gaps in human knowledge about initial and boundary conditions may force human beings to resort to probability in making predictions about the outcomes of observations.

2. The theory should include all elements of reality.

3. The theory should be local: what happens here depends on elements of reality located here, and whatever happens there depends on elements of reality located there.

Since 1920's Bohr and Einstein debated about the interpretation of the reality that the quantum mechanics can give. At Solvay congress or another meetings, Einstein brought thought experiments that seemed to destroy the quantum model and the Copenhaguen interpretation, specially the probabilistic description of nature. But after some hard work Bohr always found a counterargument in the logical sequence that Einstein missed, just to find an another mental experiment proposed by Einstein in the next occasion.

In particular, in the Solvay congress of 1933 Einstein proposed a thought experiment with an illustration of an unfamiliar feature of quantum mechanics:

"Suppose two particles are set in motion towards each other with the same, very large, momentum, and that they interact with each other for a very short time when they pass at known positions. Consider now an observer who gets hold of one of the particles, far away from the region of interaction, and measures its momentum; then, from the conditions of the experiment, he will obviously be able to deduce the momentum of the other particle. If, however, he chooses to measure the position of the first particle, he will be able to tell where the other particle is. This is a perfectly correct and straightforward deduction from the principles of quantum mechanics; but is it not very paradoxical? How can the final state of the second particle be influenced by a measurement performed on the first, after all physical interaction has ceased between them? [55]"

For first time, the quantum *entanglement* concept is used for complicated quantum states, because they use both position and momentum of two particles that have interacted in the past and thus are correlated. Their argument is basically a description of quantum entanglement for position and momentum.

This argumentation finally take form in the article of 1935 in *Physical Review* [1], where essentially take as central point the assumption of *locality*. What happens in one place does not immediately affect what happens in another place. The authors said:

"If, without in any way disturbing a system, we can predict with certainty (i.e., with probability equal to unity) the value of a physical quantity, then there exists an element of physical reality corresponding to this physical quantity."

This condition is satisfied when a measurement of position is made on particle 1 and also when a measurement of momentum is made of the same particle. In each case, we can predict with certainty the position (or momentum) of the other particle. This permits us the inference of the existence of an element of physical reality. Now, since particle 2 is unaffected by what is done to particle 1, and the element of reality, the position, of this particle is inferred in one case, and of momentum in the other, both position and momentum are elements of physical reality of particle 2. Thus the EPR "paradox". We have two particles that are related to each other. We measure one and we know about the other. Thus, the theory that allows us to do that is incomplete [55].

Bohr sent an answer few months later to *Physical Review* with the exactly same title of the original EPR article[1] where he argued that the experiment proposed by Einstein has two quantities (position and momentum) that cannot be measured simultaneously. He argued

---

[1] Can Quantum-Mechanical Description of Physical Reality be Considered Complete? [56].

that the EPR experiment contains an essential ambiguity when it is applied to quantum phenomena. He pointed out that, even if the EPR thought-experiment excludes any direct physical interaction of the system with the measuring apparatus, the measurement process has an essential influence on the conditions on which the very definition of the physical observables in question rest. And these conditions must be considered as an inherent element of any phenomenon to which the term "physical reality" can be unambiguously applied. Bohr acknowledged that it is possible to determine experimental arrangements such that the measurement of the position or of the momentum of one particle automatically determines the position or the momentum of the other. But each time the experimental arrangements for measuring moment and position are incompatible [57]. Although position and momentum of first particle obey the Uncertainly Principle, the momentum of particle 1 conmutes to position of particle 2 and it is possible to assign values simultaneously to both particles. Hence we are forced to consider a measurement as a whole. Then, the assumption of EPR for physical element of reality is wrong. He finally argued that the EPR paradox did not present a practical challenge to the application of quantum theory to real physical problems.

This discussion was eventually forgot until two decades after Bohm and Aharonov [2] review the EPR problem and simplify the ideal experiment from two quantum quantities (momentum and position) to one variable of interest (spin). Their version of the EPR thought experiment would be the one most often used by experimentalists and theorists studying entanglement in the following decades. They consider a molecule of total spin zero consisting of two atoms, each of spin one-half. The two atoms are then separated by a method that does not influence the total spin [55]. After they have separated enough so that they cease to interact, any desired component of the spin of the first particle is measured. Then, because the total spin is still zero, it can immediately be concluded that the same component of the spin of the other particle is opposite to that of first particle. In other words, the two spin vectors are correlated as EPR proposed.

We can describe this situation for example by a two-electron system in a spin-singlet state, that is, with a total spin of zero [58]. The state ket can be written as

$$|\psi\rangle = \frac{1}{\sqrt{2}}(|\hat{z}+;\hat{z}-\rangle - |\hat{z}-;\hat{z}+\rangle), \tag{2.1}$$

where the spin quantization z-direction is indicated as $\hat{z}$. Here, $|\hat{z}+;\hat{z}-\rangle$ means that electron 1 is in the spin-up state and electron 2 is in the spin-down state. The same is true for $|\hat{z}-;\hat{z}+\rangle$.

If we make a measurement on the spin component of one of the electrons, there is a 50-50 chance of getting either up or down because the composite system may be in $|\hat{z}+;\hat{z}-\rangle$

or $|\hat{z}-;\hat{z}+\rangle$ with equal probabilities. But if one of the components is shown to be in the spin-up state, the other is necessarily in the spin-down state, and vice versa. When the spin component of the electron 1 is shown to be up, the measurement apparatus has selected the first term, $|\hat{z}+;\hat{z}-\rangle$ of Eq. (2.1); a subsequent measurement of the spin component of the electron 2 must ascertain that the state ket of the composite system is given by $|\hat{z}+;\hat{z}-\rangle$.

This situation is depicted in Figure 2.1. Observer A specializes in measuring S_z of particle 1 (moving the left), while observer B specializes in measuring S_z of particle 2 (moving to the right). In this situation the observer A finds S_z to be positive (spin-up state) for particle 1. Then she can predict, even before B performs any measurement, the outcome of B's measurement which certainty: B must find S_z to be negative (spin-down state) of particle 2. On the other hand, if A makes no measurement, B has a 50-50 chance of getting S_z+ or S_z-.
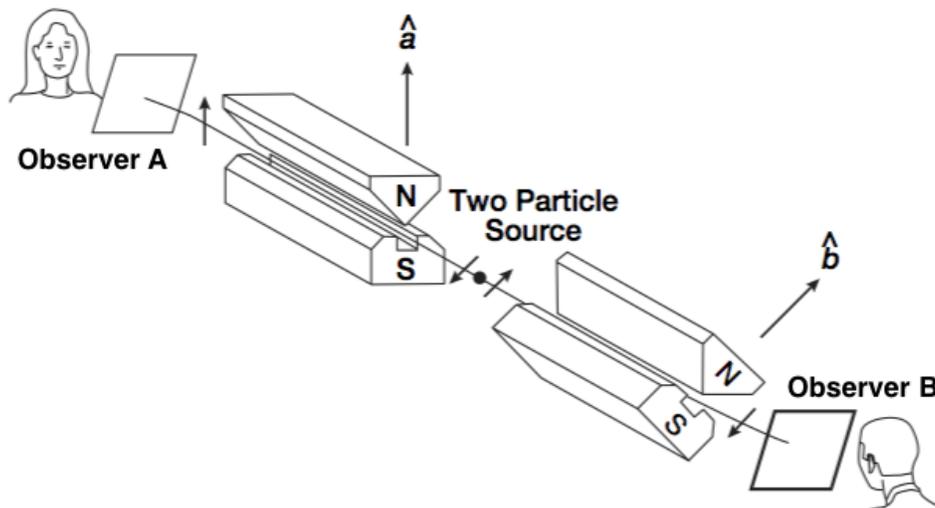
Figure 2.1: Spin correlation in a spin-singlet state (image credit: [55]). Note the Stern-Gerlach array that emphasizes the spin measurement of the particles. Each array is oriented to an arbitrary direction $\hat{\mathbf{a}}$ or $\hat{\mathbf{b}}$.

As Sakurai remarks [58]: "This is by itself might not be so peculiar. One may say, it is just like an urn known to contain one black ball and one white ball. When we blindly pick one of them, there is a 50-50 chance of getting black or white. But if the first ball we pick is black, then we can predict with certainty that the second ball will be white."

But the quantum-mechanical situation is quite complicated than that. This is because observers may choose to measure at any moment S_x in place of S_z, just by turning around the longitudinal axis the array of Figure 2.1. That is, the spin-$\frac{1}{2}$ system S_x are related to S_z

as follows:

$$|\hat{x}\pm\rangle = \frac{1}{\sqrt{2}}(|\hat{z}+\rangle \pm |\hat{z}-\rangle), \quad |\hat{z}\pm\rangle = \frac{1}{\sqrt{2}}(|\hat{x}+\rangle \pm |\hat{x}-\rangle). \tag{2.2}$$

Therefore the spin-singlet ket Eq. (2.1) can be rewritten by choosing the x-direction as the axis of quantization[2]:

$$|\psi\rangle = \frac{1}{\sqrt{2}}(|\hat{x}-;\hat{x}+\rangle - |\hat{x}+;\hat{x}-\rangle). \tag{2.3}$$

Let us now suppose that observer A can choose to measure S_z or S_x of particle 1 by changing the orientation of her spin analyzer (direction vector $\hat{\mathbf{a}}$), while observer B always specializes in measuring S_x of particle 2 (direction vector $\hat{\mathbf{b}}$). As we know by entangled particles, the outcome of B depends on the A measurement, that is:

I.   If A measures S_z and B measures S_x, there is completely random correlation between the two measurements.

II. If A measures S_x and B measures S_x, there is a 100% (opposite sign) correlation between the two measurements.

III. If A makes no measurement, B's measurements show random results.

It is important to note that the separation distance between the observers is not included in the quantum state. A and B can be kilometers apart with no possibility of communications or mutual interactions. Observer A can decide how to orient her spin-analyzer apparatus long after the two particles have separated. It seems like particle 2 knows which spin component of particle 1 is being measured.

The orthodox quantum-mechanical interpretation of this situation is that the measurement is a selection process. When S_z of particle 1 is measured to be positive, then component $|\hat{z}+;\hat{z}-\rangle$ is selected. A subsequent measurement of the other particle's S_z merely ascertains that the system is still in $|\hat{z}+;\hat{z}-\rangle$. We must accept that a measurement on what appears to be a part of the system is to be regarded as a measurement on the whole system [58].

All the previous discussion could be just a theoretical problem with no more implications in the Physics if there is no way to produce a entangled particles as experimental problem. But there are different ways of producing spin-$\frac{1}{2}$ entangled particles. This is certainly the case for a $J = 0$ system disintegrating spontaneously into two half-spin particles with no relative orbital angular momentum, because angular-momentum conservation must hold in the disintegration process. An example of this would be a rare decay of the η meson (mass 549 MeV/c^2) into a muon pair $\eta \to \mu^+ + \mu^-$. Another example is a proton-proton scattering

---

[2]This is because the spin-singlet states have no preferred direction in space

at low kinetic energies. The Pauli principle forces the interacting proton to be in $^1S_0$ (orbital angular momentum 0, spin-singlet state) [58].

Also, Kocher and Commins in 1967 [59] used the atomic cascade method for producing correlated photons. Here an atom is excited and emits two photons as it decays into two levels down; and the two photons are entangled. The source of the photons was a beam of calcium atoms emanating from a hot oven. The atoms in the beam were bombarded by strong ultraviolet radiation. As a response to this radiation, electrons in the calcium atoms were exited to higher levels, and when they descended again, they released pairs of correlated photons. Such a process is called an atomic cascade because an electron cascades down from a high level, through an intermediate level, down to a final level, releasing a photon at each of the two steps down. Because the initial and the final levels are both states of zero total angular momentum, and angular momentum is a conserved quantity, the emitted photon pair has zero angular momentum, and that is a state of high symmetry and strong polarization correlation between the photons. The idea of such an atomic cascade is shown in the Figure 2.2.
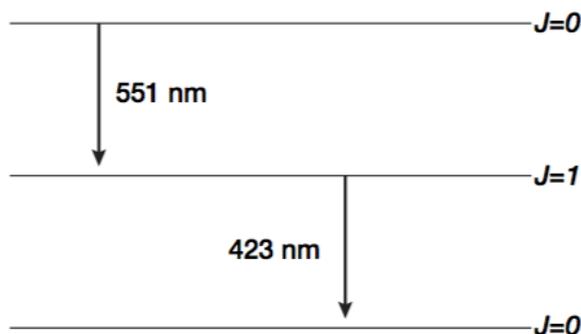
Figure 2.2: Kocher and Commins calcium atomic cascade.

In 1994 Cirac and Zoller [60] showed an alternative way to prepare a singlet state, by allowing two atoms, 1 and 2, initially in their excited $|+\rangle$ and ground $|-\rangle$ states respectively, to interact with a resonant cavity mode in the vacuum state. Through the Jaynes-Cummings model, where the excitation and ground states are conserved, the particles experience vacuum Rabi oscillations, which depend on the interaction time of each particle in the cavity field, the atomic velocity of the particles and the length of the cavity. Now a last question is raised. Why this situation is considered a paradox? Philosophically speaking, the Einsteninian separability is part and parcel of the philosophy of physical realism, which Einstein defended throughout his life. This is the philosophy that considers physical objects to be real independent of each other and of their measurement or observation. But in quantum mechanics the idea of the reality of physical objects independent of

our measurement of them is difficult to uphold. Thus EPR's motive was to discredit quantum mechanics and reestablish physical realism as the undergirding philosophy of physics. EPR's result is a paradox from the point of view of physical realism; it seems to say that we have to choose between locality or separability and the completeness of quantum mechanics, and this is no choice at all since separability is imperative. The resolution of the EPR paradox is to realize an essential inseparability of quantum objects; measurement of one of two correlated particles affects its correlated partner (this was essentially Bohr's answer [56] to EPR). When observer A colapse the spin state of particle 1 by measuring it, the other wave function of particle 2 is collapsed also. The collapse is nonlocal, just as the correlation is nonlocal. EPR entangled objects have a non-local ontological connection (inseparability) with a signalless instantaneous influence upon each other, as hard as it is to believe from the point of view of physical realism and the locality principle. Separability is the result of collapse; only after collapse are there independent objects [61].

This EPR paradox was not a paradox at all, as everybody called it. Einstein pointed out that Quantum Mechanics, localism and realism was contradictory, and both posture cannot be true at the same time. The Quantum Mechanics was not incomplete, instead of that if Quantum Mechanics was true, locality was not. If we want to hold the localism there has something wrong in the quantum theory. We must consider the possibility of alternative realistic interpretation of the Quantum Mechanics. One such interpretation is based on the idea of *hidden variables*, i.e. hidden unknown parameters that should provide a realistic ontological description of quantum objects, trajectories and all. In 1964 John Bell takes the EPR argument in order to complete Quantum Mechanics [3], introducing supplementary parameters, the hidden variables, given to the two particles at their initial preparation in an entangled state, and carried along by each particle after separation. A crucial hypothesis in Bell's reasoning is the *locality hypothesis* which needs to be fulfilled by the supplementary parameter models to lead to a conflict with quantum mechanics. This very natural assumption asserts that there is no direct non-local, interaction between the two measuring apparatuses far from each other. In other words, the conflict arises only if the result of a measurement on the first particle does not depend on the setting of the second measuring apparatus. As Bell remarks in his paper, this very natural hypothesis would become a direct consequence of Einstein's views that no influence can travel faster than light, in an experimental scheme where the settings of the measuring apparatus are rapidly changed while the particles are flying between the source and the measuring apparatus.

To establish the incompatibility between quantum mechanics and the local hidden variable theories, Bell showed that the correlations predicted by any local hidden variable model

are limited by inequalities that are violated by certain quantum predictions. It became possible to settle the question experimentally, by looking carefully at measurements of correlations between entangled particles [62]. This inequalities are now called Bell's inequalities.

Going back to the spin-$\frac{1}{2}$ particles, it can be derived the Bell's inequalities as follows. As we previously saw, it is impossible to determine S_x and S_z simultaneously. However, when we have a large number of particles with spin-$\frac{1}{2}$, we would assign a certain fraction of them to have the following properties:

- If S_z is measured, we obtain a plus sign with certainty.

- If S_x is measured, we obtain a minus sign with certainty.

A particle satisfying this property is said to belong to the type $(\hat{z}+, \hat{x}-)$. It is important to note here that it is not asserting that we can simultaneously measure S_z and S_x to be $+$ and $-$, respectively. When we measure S_z, we do not measure S_x, and vice versa. We are assigning definite values of spin component in more than one direction with the understanding that only one or the other of the components can actually be measured. For a particular pair, there must be a perfect matching between particle 1 and particle 2 to ensure zero total angular momentum: If particle 1 is of type $(\hat{z}+, \hat{x}-)$, the particle 2 must belong to type $(\hat{z}-, \hat{x}+)$, and so forth. The results of correlation measurements can be reproduced if particle 1 and particle 2 are matched as follows:

$$
\begin{array}{ccc}
\text{particle 1} & & \text{particle 2} \\
(\hat{z}+, \hat{x}-) & \leftrightarrow & (\hat{z}-, \hat{x}+) \\
(\hat{z}+, \hat{x}+) & \leftrightarrow & (\hat{z}-, \hat{x}-) \\
(\hat{z}-, \hat{x}+) & \leftrightarrow & (\hat{z}+, \hat{x}-) \\
(\hat{z}-, \hat{x}-) & \leftrightarrow & (\hat{z}+, \hat{x}+)
\end{array} \tag{2.4}
$$

with equal population, that is 25% each of them. A very important assumption is used here. Suppose a particular pair belongs to the first pair of (2.4) and observer A (see Fig. 2.1) decides to measure S_z of particle 1; then she necessarily obtains a plus sign regardless of whether B decides to measure S_z or S_x. It is in this sense that Einstein's locality and realism are incorporated in this model, because we assumed from the beginning that there is a reality behind any result of measurement, reality that is predetermining the result of both particles simultaneously, like the black or white balls example.

The next step is to consider a more complicated situation. This time observers A and B can choose to measure the spin in three possible directions, indicated by unit vectors $\hat{\mathbf{a}}$, $\hat{\mathbf{b}}$ and $\hat{\mathbf{c}}$, which are, in general, not mutually orthogonal. In this way some arbitrary particle

can start in the $(\hat{\mathbf{a}}-, \hat{\mathbf{b}}+, \hat{\mathbf{c}}+)$ state, which means that if $\mathbf{S} \cdot \hat{\mathbf{a}}$ is measured, we obtain a minus sign with certainty; if $\mathbf{S} \cdot \hat{\mathbf{b}}$ is measured, we obtain a plus sign with certainty; and if $\mathbf{S} \cdot \hat{\mathbf{c}}$ is measured, we obtain a plus sign with certainty. Again there must be a perfect matching in the sense that the other particle necessarily belongs to the type $(\hat{\mathbf{a}}+, \hat{\mathbf{b}}-, \hat{\mathbf{c}}-)$ to ensure zero total angular momentum, in the same sense of (2.4).

Let $P[\hat{\mathbf{a}}+, \hat{\mathbf{b}}-]$ be the probability that, in a random selection, observer A measures $\mathbf{S} \cdot \hat{\mathbf{a}}$ to be $+$ and $\mathbf{S} \cdot \hat{\mathbf{b}}$ to be $-$. Therefore, in agreement with the hypothesis of realism there must be a reality, which are simultaneous behind each measurement. This particular kind of particles can be present in two subtypes of probabilities related to unit vector $\hat{\mathbf{c}}$, that is particles of the type $(\hat{\mathbf{a}}+, \hat{\mathbf{b}}-, \hat{\mathbf{c}}+)$ and $(\hat{\mathbf{a}}+, \hat{\mathbf{b}}-, \hat{\mathbf{c}}-)$. The same conclusion can be obtained for the rest permutations of unitary vector. We can generalize this results in the next equations:

$$P_1(\hat{\mathbf{a}}+, \hat{\mathbf{b}}-) = P_1(\hat{\mathbf{a}}+, \hat{\mathbf{b}}-, \hat{\mathbf{c}}+) + P_1(\hat{\mathbf{a}}+, \hat{\mathbf{b}}-, \hat{\mathbf{c}}-), \tag{2.5}$$

$$P_1(\hat{\mathbf{a}}+, \hat{\mathbf{c}}-) = P_1(\hat{\mathbf{a}}+, \hat{\mathbf{c}}-, \hat{\mathbf{b}}+) + P_1(\hat{\mathbf{a}}+, \hat{\mathbf{c}}-, \hat{\mathbf{b}}-), \tag{2.6}$$

$$P_1(\hat{\mathbf{b}}-, \hat{\mathbf{c}}+) = P_1(\hat{\mathbf{b}}-, \hat{\mathbf{c}}+, \hat{\mathbf{a}}+) + P_1(\hat{\mathbf{b}}-, \hat{\mathbf{c}}+, \hat{\mathbf{a}}-). \tag{2.7}$$

Here the subindex 1 is used to emphasized the observer A measures the spin of the particle 1 on different directions, which are predetermined by "hidden variables", regardless the measurement of observer B. At this moment it is not important what kind of theory can determine the values of the hidden variables. Bell just used the predictions that that kind of theory could give.

Therefore, because the all is always greater that the parts, from equations (2.6) and (2.7) we can get

$$P_1(\hat{\mathbf{a}}+, \hat{\mathbf{c}}-) \geq P_1(\hat{\mathbf{a}}+, \hat{\mathbf{c}}-, \hat{\mathbf{b}}-), \tag{2.8}$$

$$P_1(\hat{\mathbf{b}}-, \hat{\mathbf{c}}+) \geq P_1(\hat{\mathbf{b}}-, \hat{\mathbf{c}}+, \hat{\mathbf{a}}+), \tag{2.9}$$

and summing up both inequalities,

$$P_1(\hat{\mathbf{a}}+, \hat{\mathbf{c}}-) + P_1(\hat{\mathbf{b}}-, \hat{\mathbf{c}}+) \geq P_1(\hat{\mathbf{a}}+, \hat{\mathbf{c}}-, \hat{\mathbf{b}}-) + P_1(\hat{\mathbf{b}}-, \hat{\mathbf{c}}+, \hat{\mathbf{a}}+). \tag{2.10}$$

Returning back to Eq. (2.5) it follows

$$P_1(\hat{\mathbf{a}}+, \hat{\mathbf{b}}-) \leq P_1(\hat{\mathbf{a}}+, \hat{\mathbf{c}}-) + P_1(\hat{\mathbf{b}}-, \hat{\mathbf{c}}+). \tag{2.11}$$

Now we want to know the probability of $P(\hat{\mathbf{a}}+, \hat{\mathbf{b}}+)$ from $P_1(\hat{\mathbf{a}}+, \hat{\mathbf{b}}-)^3$. That is, particle 1 with spin up in direction $\hat{\mathbf{a}}$ and particle 2 with spin up in direction $\hat{\mathbf{b}}$ also, but with particle 1 predeterminated in the state of Eq. (2.11).

To know how can we get this result, first we have to realize that the whole probability is preceded for the random election of two directions, one for each particle 1 and 2, between the three posible directions $\hat{\mathbf{a}}$, $\hat{\mathbf{b}}$ and $\hat{\mathbf{c}}$. This doble election can be done by nine different ways, each one with the same probability by construction. Therefore, the probability to get the a-direction for particle 1 and the b-direction for the particle 2 is $\frac{1}{9}$. Nevertheless, once a mesure over particle 1 is selected in a-direction, the sign of the spin for this particle will be $+$, since the starting particle is the "reality" of $(\hat{\mathbf{a}}+, \hat{\mathbf{b}}-)$ from our initial assumption. In the same way, once b-direction is selected for particle 2, the sign that we will measure for the spin have to be $+$, since the perfect anticorrelation between particle 1 and 2.

Thus, once the selected random directions are the previous mentioned (a for particle 1 and b for particle 2), the whole state of the system is defined as $[\hat{\mathbf{a}}+, \hat{\mathbf{b}}+]$. In the other hand, this state $[\hat{\mathbf{a}}+, \hat{\mathbf{b}}+]$ can only come form a reality of the individual state $(\hat{\mathbf{a}}+, \hat{\mathbf{b}}-)$ of particle 1. Consequently, the probability to get $[\hat{\mathbf{a}}+, \hat{\mathbf{b}}+]$ from $(\hat{\mathbf{a}}+, \hat{\mathbf{b}}-)$ will be $\frac{1}{9}$. In other words,

$$
\begin{aligned}
P_1(\hat{\mathbf{a}}+, \hat{\mathbf{b}}-) &= 9P[\hat{\mathbf{a}}+, \hat{\mathbf{b}}+], \\
P_1(\hat{\mathbf{a}}+, \hat{\mathbf{c}}-) &= 9P[\hat{\mathbf{a}}+, \hat{\mathbf{c}}+], \\
P_1(\hat{\mathbf{c}}+, \hat{\mathbf{b}}-) &= 9P[\hat{\mathbf{c}}+, \hat{\mathbf{b}}+].
\end{aligned}
\tag{2.12}
$$

Finally, grouping (2.12) and (2.11) we get

$$
P[\hat{\mathbf{a}}+, \hat{\mathbf{b}}+] \leq P[\hat{\mathbf{a}}+, \hat{\mathbf{c}}+] + P[\hat{\mathbf{c}}+, \hat{\mathbf{b}}+],
\tag{2.13}
$$

that is, the Bell's inequality in the form of Wigner-D'Espagnat [63]. This equation is then suitable to test Quantum Mechanics against the Realism y Localism as demanded by EPR (points 2 and 3 at the beginning of this Chapter), because each particle has an predefined spin in any direction (element of Reality) and a measure on particle 1 does not affect the measure of particle 2 (Locality).

Now, returning back to Quantum Mechanics, we want to evaluate $P[\hat{\mathbf{a}}+, \hat{\mathbf{b}}+]$. Following [58], suppose observer A finds $\mathbf{S_1} \cdot \hat{\mathbf{a}}$ to be positive. Because the perfect anticorrelation, B's measurement of $\mathbf{S_2} \cdot \hat{\mathbf{a}}$ will be a minus sign. But to calculate $P[\hat{\mathbf{a}}+, \hat{\mathbf{b}}+]$ we must consider a new quantization axis $\hat{\mathbf{b}}$ that makes an angle θ_{ab} with $\hat{\mathbf{a}}$. The probability that the $\mathbf{S_2} \cdot \hat{\mathbf{b}}$

---

[3]Here the brackets are used to emphasized the fact we are talking about the whole system of 2 particles, instead of the state for particle 1 or 2, where parenthesis are used. The first element between brackets represents particle 1 and the last one is for particle 2

measurement yields $+$ when particle 2 is known to be in an eigenket of $\mathbf{S_2} \cdot \hat{\mathbf{a}}$ with negative eigenvalue is given by

$$\cos^2\left[\frac{(\pi - \theta_{ab})}{2}\right] = \sin^2\left(\frac{\theta_{ab}}{2}\right). \tag{2.14}$$

As a result, we obtain

$$P[\hat{\mathbf{a}}+, \hat{\mathbf{b}}+] = \left(\frac{1}{2}\right)\sin^2\left(\frac{\theta_{ab}}{2}\right), \tag{2.15}$$

where the factor $\frac{1}{2}$ arises from the probability of initially obtaining $\mathbf{S_1} \cdot \hat{\mathbf{a}}$ to be positive.

Similarly the other two terms of Eq. (2.13) can be obtained to write the Bell's inequality as

$$\sin^2\left(\frac{\theta_{ab}}{2}\right) \leq \sin^2\left(\frac{\theta_{ac}}{2}\right) + \sin^2\left(\frac{\theta_{cb}}{2}\right). \tag{2.16}$$

For simplicity let suppose that $\hat{\mathbf{a}}$, $\hat{\mathbf{b}}$ and $\hat{\mathbf{c}}$ to lie in a plane, and let $\hat{\mathbf{c}}$ bisect the two direction defined by $\hat{\mathbf{a}}$ and $\hat{\mathbf{b}}$, that is,

$$\theta_{ab} = 2\theta, \quad \theta_{ac} = \theta_{cb} = \theta, \tag{2.17}$$

It is easy to show that inequality (2.16) is violated for $0 < \theta < \frac{\pi}{2}$. Then the Quantum Mechanics predictions are not compatible with Bell's inequality. There is a real observable difference between quantum mechanics and the alternative theories satisfying EPR locality principle.

In a series of experiments in the decade of 1980's, Alain Aspect and his collaborators [5, 64, 65] provided the experiment to reply to the EPR proposal under conditions in which Bell's type of analysis apply. They showed that the quantum theory predictions were indeed obeyed. In these experiments the two spin-$\frac{1}{2}$ particles are replaced by a pair of photons, which polarization playing the role of spin for entanglement. The pairs are emitted by calcium atoms in a radiative cascade after suitable pumping by lasers. Because the initial and final atomic states have $J = 0$, quantum theory predicts that the photons will be found to have the same polarization if they are measured along the same direction. But if the polarizations are measured at 120° angles, then theory predicts that they will be the same only a quarter of the time.

There are some remarkable features of these experiments. The two polarization analyzers were placed as far as 13 meters apart without producing any noticeable change in the results. In [65] the authors used a mechanism for rapidly switching the directions along which the polarizations of each photon are measured as follows. Each photon go into to its detector through a volume of water that supports an ultrasonic standing wave. Depending on the

instantaneous amplitude of the wave, the photon either passed directly into a polarizer with one orientation or is Bragg reflected into another with a different orientation. The standing waves that determine the choice of orientation at each detector are independently driven and have frequencies so high that several cycles take place during the light travel time form one detector to the other.

All this corresponds to a refinement of the *gedanken* demonstration in which, to be absolutely safe, the switches are not given their random setting until after the parcels have departed from their photon common source [66]. This additional feature ensures that there is no influence at distance can be transmitted over particle 2 when the direction of measurement for particle 1 is setting when it flies apart.

In the theoretical field the entangled quantum phenomena continue as an active research subject and eventually the research of this topic moves to include relativity theory in a coherent model. The first steps was taken in Special Relativity with moving relativistic particles [23, 24, 25, 26, 27, 28]. Later, these works were the basis for Terashima and Ueda [31] to extend the analysis to in the framework of General Relativity, where they proposed an *gedankenexperiment* in a Schwarzschild spacetime. This is the most simple case that describe a black hole which only include one parameter, which is its mass.

This thesis follows the efforts of Terashima and Ueda to describe the Entanglement in the framework of any black holes of the Type-D solution (with expansion and twist) of the Einstein-Maxwell equations.

Before we continue with the Quantum Entanglement, it is important to review some features of General Relativity and Black Holes.

2.2   Black holes

The term black hole has a very recent origin. It was coined in 1969 by the American scientist John Wheeler as the graphic description of an idea that dates back at least two hundred years, at a time when there were two theories of light: one, preferred by Newton, who assumed that the light is composed of particles, and the other one which was assumed to be formed by waves. Today, we know that both theories are correct. Due to the wave-particle duality of quantum mechanics, light can be considered as a wave and as a particle as well. In wave light theory, it was not clear how light would respond to gravity. But if light is composed of particles, one might expect that these were affected by gravity in the same way as are the bullets, rockets and planets. At first, it was thought that the particles of light travel with infinite speed, so that gravity had not been able to stop them, but the discovery

of Römer that light traveled at a finite speed, meant that gravity might have a significant effect on the light.

Under this assumption, a professor from Cambridge, John Michell, wrote in 1783 an article in the *Philosophical Transactions of the Royal Society of London* in which he stated that a star that was sufficiently massive and compact would have such a strong gravitational field that light could not escape: the light emitted from the surface of that star would be dragged back to the center by the gravitational attraction of the star, before it could get very far. Michell suggested that there could be a large number of stars of this type. Although we would not be able to see them because their light would not reach us, we would notice their gravitational attraction. These objects are what today we call black holes, because this is precisely what they are: black holes in space. A similar suggestion was made a few years later by the French scientist the Marquis de Laplace, it seems that independently of Michell. It is quite interestigs that Laplace included this idea only in te first and second edition of his book *The World System*, and not in subsequents editions. Maybe he considered that was a absurd idea. It's important to remember that the particle theory of light was in disuse in XIX century because everything was described by wave theory and, in consequence it was no clear if light is affected by gravity.

To understand how it could form a black hole, we have to have some knowledge about the life cycle of a star. A star forms when a large amount of gas, mostly hydrogen, starts to collapse on itself due to its gravitational pull. Under the contraction, the atoms begin to collide with each other, with increasing frequency and at higher speeds and then the gas is heated. Eventually, the gas would be so hot that when hydrogen atoms collide, they don't bounce back, but will merge to form helium. The heat released by the reaction makes the star shine. This additional heat also increases the gas pressure until it is sufficient to balance the pull of gravity , and the gas stops shrinking. The stars remain stable in this form for a long period, with the heat of nuclear reactions balancing the gravitational attraction. Finally however, the star will consume all its hydrogen and other nuclear fuels. The more fuel has a star at first, soon runs out . This is because the more massive the star, it must be hotter to counteract the gravitational attraction, and the hotter the star is, uses its fuel faster. When a star runs out of fuel, begins to cool and thereby to contract. What can happen from this point only began to understand the end of 1920's.

In 1928, an Indian graduate student, Subrahmanyan Chandrasekhar calculated how big it could become a star that was able to withstand its own gravity, once it had spent all its fuel. The idea was this: when the star is reduced in size, material particles are very close to each other, and so, according to the Pauli exclusion principle, must have very different

SINGULARITY

LIGHT RAY EMITTED WHEN THE
EVENTS HORIZON IS CREATED

LIGHT RAY EMITTED AFTER
THE EVENTS HORIZON IS
CREATED

LIGHT CONES

LIGHT RAY EMITTED BEFORE
THE EVENTS HORIZON IS
CREATED

INTERIOR OF THE STAR

TIME

0

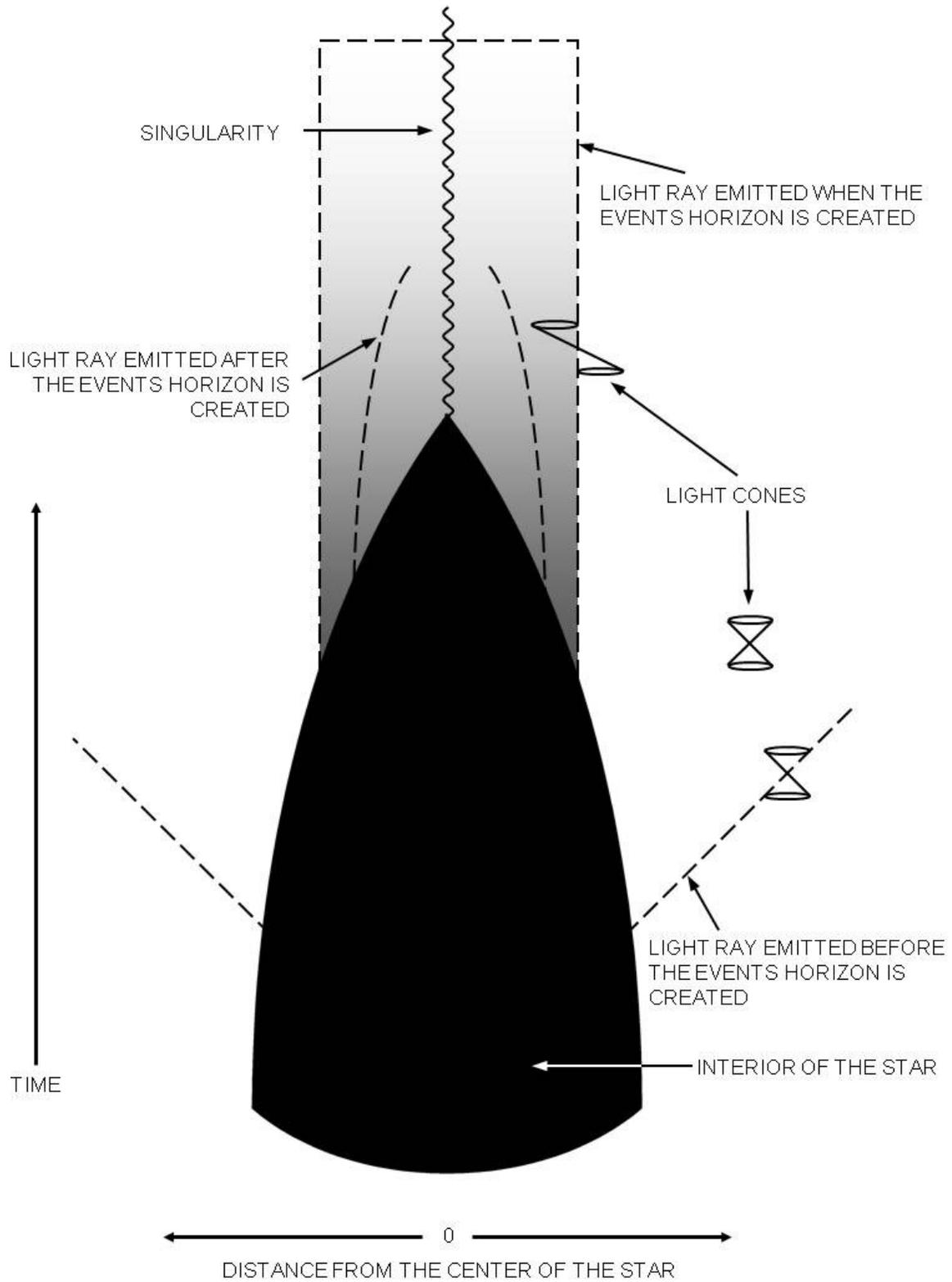DISTANCE FROM THE CENTER OF THE STAR

Figure 2.3: Star colapse into a black hole (image credit: [67]).

speeds. This causes to move away from each other, which tends at expand at the star. A star can, therefore, be maintained to a constant radius because a balance between gravitational attraction and repulsion arises exclusion principle, in the same way as before gravity was compensated by heat.

Chandrasekhar realized, however, that there is a limit to the repulsion that the exclusion principle can provide. The theory of relativity limits the maximum difference between the velocities of the material particles from the star at the speed of light. This means that when the star is sufficiently dense, the repulsion due to the exclusion principle would be less than the pull of gravity. Chandrasekhar calculated that a cold star of more than about one and a half times the mass of the Sun would not be able to support its own gravity.[4]

If a star has less than the Chandrasekhar mass limit can finally cease to contract and stabilize at a possible final state, as a "white dwarf" star, with a radius of a few thousand kilometers and a density of tens tons per cubic centimeter. A white dwarf is supported by the repulsion due to the exclusion principle between electrons of the material.

Russian scientist Lev Davidovich Landau also noted that there was another possible final state for a star, also with a mass limit of one or two times the mass of the Sun but much smaller even than a white dwarf. These stars are maintained by the repulsion due to the exclusion principle between neutrons and protons, rather than between electrons. For this reason they were called neutron stars. Would have a radius of about ten miles and a density of tens of millions of tons per cubic centimeter.

Stars with masses above the Chandrasekhar limit are a big problem when they run out of fuel. In some cases they explode or loose enough material to reduce weight below the limit and avoid a catastrophic gravitational collapse. Chandrasekhar had shown that the exclusion principle could not stop the collapse of a massive star beyond the Chandrasekhar limit, but the problem of understanding what would happen to such a star, according to general relativity, was first time solved by Robert Oppenheimer, in 1939: the gravitational field of the star changes the paths of light rays in spacetime, for such would have been if the star had not been present. The light-cones that indicate the paths followed in space and time by flashes of light emitted from its vertices, incline slightly inward near the surface of the star. When the star contracts, the gravitational field at its surface is more intense and the light-cones are more inclined inward. This makes it harder to escape the light of the star, and the light turns weaker and red to a distant observer. Finally, when the star has shrunk to a certain critical radius, the gravitational field at the surface becomes so strong that the light-cones are tilted inward so that light can not escape. According to the theory

---

[4]This mass is known today as the Chandrasekhar limit.

of relativity, nothing can travel faster than light. So if light can not escape, neither can any other object, that is, everything is driven by the gravitational field. Therefore, there is a set of events, a region of spacetime from which you can not escape and reach a distant observer. This region is what we now call black hole. Its boundary is called the event horizon coincides with the paths of light rays that are just about to escape the black hole [67].

The natural description of a black hole occurs in the frame of General Relativity developed by Einstein at the beginning of the XX century. After he worked with inertial frames in Special Relativity, Einstein struggled with the problem of gravity and how must it be included in the description of the spacetime. The bold hypothesis he proposed was that *the spacetime metric is not flat, as it was assumed in special relativity. The world lines of freely falling bodies in a gravitational field are simply the geodesics of the curved spacetime metric* [68]. He finally came to the conclusion that the laws of Physics in General Relativity are governed by two basic principles:

I. The principle of general covariance, which states that the spacetime metric, g_{ab}, and quantities derivable form it are the only spacetime quantities that can appear in the equations of Physics.

II. The requirement that equations must reduce to the equations satisfied in special relativity in the case where g_{ab} is flat.

This spacetime metric g_{ab} is the solution of the Einstien-Maxwell equation of General Relativity

$$G_{ab} \equiv R_{ab} - \frac{1}{2}Rg_{ab} = 8\pi T_{ab}. \tag{2.18}$$

Therefore, in general relativity, the spacetime is a manifold M on which is defined a Lorentz metric g_{ab}. The curvature of g_{ab}, left hand side of (2.18), is related to matter and energy distribution in that spacetime (i.e. T_{ab}).

There are some important remarks on Einstein's equation that are worth to mention [69]:

• Mathematical character: Einstein's equation is a nonlinear second order partial differential equation for the metric components g_{ab}. For a metric of Lorentz signature, these equations have a hyperbolic (i.e. wave equations) character.

• Point of view: in ones sense, Einstein's equation is analogous to Maxwell's equation with the stress tensor T_{ab} serving as the source of the gravitational field, in much the same way as the current j_a serves as a source of the electromagnetic field. But in General Relativity, we can not solve Einstein's equation by specifying T_{ab} first and then finding g_{ab}, because until g_{ab} is known, we do not know how to physically interpret T_{ab}. One must solve simultaneously for the spacetime metric and the matter distribution.

- Equations of motion of matter: Einstein's equation alone implies the *geodesic hypothesis* that the world-lines of test bodies are geodesics of the spacetime metric.

The eq. (2.18) can describe the Universe by idealized cosmologies. Astronomical observations reveal that the universe is homogeneous and isotropic on scales of $\sim 10^8$ light years and larger. Taking a "fine-scale" point of view, one sees the agglomeration of matter into stars, galaxies, and clusters of galaxies in regions of size ~ 1 light year, $\sim 10^6$ light years, and $\sim 3 \times 10^7$ light years, respectively. But taking instead a "large-scale" viewpoint, one sees little difference between an elementary volume of the universe of the order of 10^8 light years on a side centered on the Earth and other elementary volumes of the same size located elsewhere [70]. By taking the large-scale viewpoint, we can treat galaxies as "particles" of a "gas" that fills the universe. We can remove the particulate structure of the gas from view by treating it in the perfect-fluid approximation. Thus, we can characterize the gas by a 4-velocity[5] u^μ, by a density of mass-energy[6] ρ and by a pressure[7] p. In this way, the right size of eq. (2.18) can be assumed as a stress-energy tensor for this "fluid of galaxies" of the form

$$T_{\mu\nu} = (\rho + p)u_\mu u_\nu + pg_{\mu\nu}, \tag{2.19}$$

For physical reasons, it should be assumed that $\rho \geq p \geq 0$. Also, it is useful to restrict attention to the case in which the equation of state takes the linear form

$$p = (\gamma - 1)\rho, \tag{2.20}$$

where $1 \leq \gamma \leq 2$ is an appropriately chosen constant. This include special cases, like a pressureless fluid, which is usually refereed to a *dust*, when $\gamma = 1$. When $\gamma = 0$, then $\rho = -p$. If this is constant, then $8\pi\rho$ is exactly equivalent to the presence of a cosmological constant Λ (see section 4.3.5). In addition, it may be noted that, in a perfect fluid spacetime with any equation of state, a cosmological constant can always be included by setting $\rho \to \rho + \Lambda/8\pi$ and $p \to p - \Lambda/8\pi$.

With the 4-velocity of the fluid denoted by u_μ, such that $u_\mu u^\mu = -1$, its expansion θ and acceleration a^μ are given by

$$\begin{aligned} \theta &= \nabla_\mu u^\mu, \\ a^\mu &= u^\nu \nabla_\nu u^\mu. \end{aligned} \tag{2.21}$$

---

[5]The 4-velocity of an observer who sees the galaxies in his neighborhood to have no mean motion.
[6]The soothed-out density of mass-energy seen in the frame with 4-velocity u^μ; this includes the rest mass plus kinetic energy of the galaxies in a unit volume, divided by the volume.
[7]The kinetic pressure of the galaxies, which is assumed to be isotropic.

It is then convenient to introduce a new tensor

$$h_{\mu\nu} = g_{\mu\nu} + u_\mu u_\nu, \tag{2.22}$$

which satisfies $h_{\mu\nu}u^\nu = 0$, $h_{\mu\alpha}h^\alpha{}_\nu = h_{\mu\nu}$ and $h^\mu{}_\mu = 3$. A shear tensor $\sigma_{\mu\nu}$ and rotation (twist) tensor $\omega_{\mu\nu}$ are then defined by

$$
\begin{aligned}
\sigma_{\mu\nu} &= \left[\frac{1}{2}(\nabla_\alpha u_\beta + \nabla_\beta u_\alpha) - \frac{1}{3}\nabla_\gamma u^\gamma h_{\alpha\beta}\right] h^\alpha{}_\mu h^\beta{}_\nu, \\
\omega_{\mu\nu} &= \frac{1}{2}(\nabla_\alpha u_\beta + \nabla_\beta u_\alpha) h^\alpha{}_\mu h^\beta{}_\nu.
\end{aligned}
\tag{2.23}
$$

Scalar quantities representing the local shear and rotation of the fluid are then given, respectively, by

$$\sigma = \sqrt{\sigma^{\mu\nu}\sigma_{\mu\nu}}, \quad \omega = \sqrt{\omega^{\mu\nu}\omega_{\mu\nu}}. \tag{2.24}$$

Finally, the stress-energy tensor can also represent a general class of pure radiation fields,

$$T^{\mu\nu} = \rho k^\mu k^\nu, \tag{2.25}$$

where k^μ is a null vector and ρ is its radiation density. This is generally taken to describe some kind of field that propagates at the speed of light, that could represent a null electromagnetic field. It could also represent an incoherent beam of photons or some kinds of idealized (massless) neutrino fields. A source of this type is sometimes referred to as "null dust", since it can be considered to be a limiting case of a pressureless perfect fluid in which the 4-velocity becomes null [40].

The term R_{ab} in eq. (2.18) is known as the Ricci tensor, that is a trace of the Riemann curvature tensor $R_{abc}{}^d$. This tensor is defined in terms of the failure of successive operations of differentiation to commute when applied to a dual vector field. This tensor is directly related to the path-dependent nature of parallel transport; specifically, the failure of a vector to return to its original value when parallel transported around a small closed loop is governed by the Riemann tensor. The Riemann tensor also fully describes the failure of initially parallel geodesics to remain parallel. This tensor is defined by

$$R_{abc}{}^d \omega_d = \nabla_a \nabla_b \omega_c - \nabla_b \nabla_a \omega_c, \tag{2.26}$$

where ω_c is a dual vector field.

It is useful to decompose the Riemann tensor in a "trace part" and "trace free part". The

trace part over the second and fourth indices of eq. (2.26) defines the *Ricci tensor*,

$$R_{ac} = R_{abc}{}^{b} \tag{2.27}$$

The trace free part is called the *Weyl tensor*, C_{abcd}, and is defined for manifolds of dimension $n \geq 3$ by the equation

$$R_{abcd} = C_{abcd} + \frac{2}{n-2}(g_{a[c}R_{d]b} - g_{b[c}R_{d]a}) - \frac{2}{(n-1)(n-2)}Rg_{a[c}g_{d]b}, \tag{2.28}$$

where R is the *scalar curvature*, defined as the trace of the Ricci tensor, i.e. $R = R_a{}^a$, and the square brackets indicates anti-symmetrization operations. The Weyl tensor is also called *conformal tensor*, because behaves in a very simple manner under conformal transformations of the metric [69].

In essence, Einstein's equation (2.18) says

"curvature of spacetime" = "energy density of matter"

Thus, Einstein provided us with a truly remarkable and beautiful theory of gravitation. The effects of gravitation are fully expressed in terms of the structure of spacetime and the structure of spacetime is related to the distribution of matter [71]. It should be mentioned that in practice it has been difficult to obtain exact solutions of Einstein's equation. The Weyl tensor (2.28) has ten independent components, however, is determined only indirectly from the field equations. These components may therefore be understood as representing "free components" of the gravitational field that also arise from non-local sources. In seeking to interpret any exact solution physically, these components need to be investigated explicitly [40], as we shall do next.

A spacetime is said to be *conformally flat* if its Weyl tensor vanishes, i.e. if $C_{abcd} = 0$. Otherwise, gravitational fields are usually classified according to the Petrov-Penrose classification of their Weyl tensor. This is based on the number of its distinct principal null directions and the number of times these are repeated.

It is frequently important, at any event (or point in spacetime), to determine the components of vectors or tensors in particular directions. For this, it is first appropriate to introduce a normalized orthonormal tetrad $(t,\ x,\ y,\ z)$, composed of a timelike and three spacelike vectors. From these, it is convenient to construct a null tetrad $(k, l, m, \bar{m})$, with the two null vectors $k = \frac{1}{\sqrt{2}}(t + z)$ and $l = \frac{1}{\sqrt{2}}(t - z)$ and the complex vector $m = \frac{1}{\sqrt{2}}(x - iy)$ and its conjugate $\bar{m} = \frac{1}{\sqrt{2}}(x + iy)$, which span the 2-space orthogonal to k and l. These null tetrad vectors are mutually orthogonal except that $k_a l^b = -1$ and $m_a \bar{m}^a = 1$. With these

conditions, the metric tensor can be expressed in terms of its null tetrad components in the form

$$g_{ab} = -k_a l_b - l_a k_b + m_a \bar{m}_b + \bar{m}_a m_b. \tag{2.29}$$

Such a null tetrad may be Lorentz transformed into the following ways:

$$k' = k, \quad l' = l + L\bar{m} + \bar{L}m + L\bar{L}k, \quad m' = m + Lk, \tag{2.30}$$

$$k' = k + K\bar{m} + \bar{K}m + K\bar{K}l, \quad l' = l, \quad m' = m + KL, \tag{2.31}$$

$$k' = Bk, \quad l' = B^{-1}l, \quad m' = e^{i\Phi}m, \tag{2.32}$$

where L and K are complex and B and Φ are real parameters. Together, these represent the six-parameter Lorentz group transformations.

The ten independent components previously mentioned of the Weyl tensor (2.28) are determined by the five complex scalar functions defined as

$$
\begin{aligned}
\Psi_0 &= C_{\kappa\lambda\mu\nu}k^\kappa m^\lambda k^\mu m^\nu, \\
\Psi_1 &= C_{\kappa\lambda\mu\nu}k^\kappa l^\lambda k^\mu m^\nu, \\
\Psi_2 &= C_{\kappa\lambda\mu\nu}k^\kappa m^\lambda \bar{m}^\mu l^\nu, \\
\Psi_3 &= C_{\kappa\lambda\mu\nu}l^\kappa k^\lambda l^\mu \bar{m}^\nu, \\
\Psi_4 &= C_{\kappa\lambda\mu\nu}l^\kappa \bar{m}^\lambda l^\mu \bar{m}^\nu.
\end{aligned} \tag{2.33}
$$

By considering the equation of geodesic derivation in a suitably adapted frame, these components (in vacuum spacetime) may be shown generally to have the following physical meanings:

Ψ_0 is a transverse component propagating in the l direction,

Ψ_1 is a longitudinal component in the l direction,

Ψ_2 is a Coulomb-like component,

Ψ_3 is a longitudinal component in the k direction,

Ψ_4 is a transverse component propagating in the k direction.

A null vector k is said to be a *principal null direction* of the gravitational field if it satisfies the property

$$k_{[\rho}C_{\kappa]\lambda\mu[\nu}k_{\sigma]}k^\lambda k^\mu = 0. \tag{2.34}$$

If k is a member of the null tetrad defined above, then the condition (2.34) is equivalent to the $\Psi_0 = 0$. It may then be noted that, under a transformation (2.31) of the tetrad

which keeps l fixed, but changes the direction of k, the component Ψ_0 of the Weyl tensor transforms as

$$\Psi_0 = \Psi_0' - 4K\Psi_1' + 6K^2\Psi_2' - 4K^3\Psi_3' + K^4\Psi_4'. \tag{2.35}$$

The condition for k to be a principal null direction (i.e. that $\Psi = 0$) is thus equivalent to the existence of a root K such that

$$\Psi_0' - 4K\Psi_1' + 6K^2\Psi_2' - 4K^3\Psi_3' + K^4\Psi_4' = 0. \tag{2.36}$$

Since this is a quartic expression in K, there are four (complex) roots to this equation, although these do not need to be distinct.

Each root of (2.36) corresponds to a principal null direction which can be constructed using (2.31), and the multiplicity of each principal null direction is the same as the multiplicity of the corresponding root. For a principal null direction k of multiplicity 1, 2, 3 or 4, it can be shown that, respectively

$$
\begin{aligned}
k_{[\rho}C_{\kappa]\lambda\mu[\nu}k_{\sigma]}k^\lambda k^\mu = 0 &\quad\Leftrightarrow\quad & \Psi_0 = 0, &\quad & \Psi_1 \neq 0, \\
C_{\kappa\lambda\mu[\nu}k_{\sigma]}k^\lambda k^\mu = 0 &\quad\Leftrightarrow\quad & \Psi_0 = \Psi_1 = 0, &\quad & \Psi_2 \neq 0, \\
C_{\kappa\lambda\mu[\nu}k_{\sigma]}k^\mu = 0 &\quad\Leftrightarrow\quad & \Psi_0 = \Psi_1 = \Psi_2 = 0, &\quad & \Psi_3 \neq 0, \\
C_{\kappa\lambda\mu\nu}k^\mu = 0 &\quad\Leftrightarrow\quad & \Psi_0 = \Psi_1 = \Psi_2 = \Psi_3 = 0, &\quad & \Psi_4 \neq 0.
\end{aligned}
$$

If a spacetime admits four distinct principal null directions (*pnds*), it is said to be *algebraically general*, or of type I. Otherwise it is *algebraically special*. The different algebraic types can be summarized as follows:

type I: four distinct *pnds*

type II: one *pnd* of multiplicity 2, others distinct

type D: two distinct *pnds* of multiplicity 2

type III: one *pnd* of multiplicity 3, other distinct

type N: one *pnds* of multiplicity 4

type O: conformally flat

If either of the basis vectors k or l are aligned with principal null directions, either $\Psi_0 = 0$ or $\Psi_4 = 0$, respectively. If the vector k is aligned with the repeated principal null direction of an algebraically special spacetime, then $\Psi_0 = 0 = \Psi_1$. If k and l are both aligned with the two repeated principal null directions of a type D spacetime, then the only non-zero component of the Weyl tensor is Ψ_2. For a type N spacetime with repeated principal null direction k, the only non-zero component of the Weyl tensor is Ψ_4 [40].

The Plebański-Demiański family of solutions of the Einstein field equations associated with the gravitational fields of isolated massive objects is known to completely exhaust the Petrov type D spacetimes. The expanding and twisting axially symmetric solutions are characterized by seven parameters which under certain circumstances are related to mass, angular momentum, cosmological constant, electric and magnetic charges, NUT parameter and acceleration. This includes black hole spacetimes like Kerr-NUT-(A)dS spacetimes and the C-metric describing accelerating sources. The non-accelerating Plebański-Demiański solutions possess the outstanding property that they allow separable Hamilton-Jacobi equations and, thus, integrability of the geodesic equation. This also extends to higher dimensions. Higher dimensional solutions of this type became popular in the connection of string theories and braneworld models [52].

As was explained in the Introduction chapter, the aim of this thesis is to calculate the entangled quantum state (1.1) when two particles travels over a Plebański-Demiański spacetime. As a secondary objetive, here will be obtained an expression for the Bell's inequality (2.13) to know how each parameter of the Plebański-Demiański spacetime affects the inequality and the perfect anticorrelation of the two particles.

Chapter 3

Methodology

It is usual to find examples in relativity theory that employ fictitious observers who send and receive signals. These "observers" should not be thought of as human beings, but rather as ordinary physical emitters and detectors. Their role is to label and locate events in spacetime. The speed of transmission of these signals is bounded by the velocity of light c because information needs a material carrier, and the latter must obey the laws of physics.

However, the mere existence of an upper bound on the speed of propagation of physical effects does not do justice to the fundamentally new concepts that were introduced by Albert Einstein. He showed that simultaneity had no absolute meaning, and that distant events might have different time orderings when referred to observers in relative motion. Relativistic kinematics is all about information transfer between observers in relative motion [72].

3.1   Spin for curved spacetime

The EPR paradox previously mentioned seems to show that at the quantum level there is a violation of locality of physical events, suggesting that the measurement of spin in a particular direction, affects the quantum state (in this case the spin) of the second particle in the same direction or axis, regardless of the distance between the two particles, thus obtaining the effect that act at distance and called quantum entanglement, which can be described is terms of a quantum correlation of both systems.

It is necessary to clarify the nature of this non-locality considering the EPR effect on a pair of spinor particles propagating in an external gravitational field. It is not evident that the correlation should exist in this case because there is no "Natural" correspondence between the two regions spatially separated in curved spacetime. In Ref. [73] the authors conclude that nonlocal quantum correlation EPR is indeed a correlation between the results

of measuring two spatially separated systems. That is, this phenomenon apparently nonlocal is preceded by 1) the establishment of quantum correlation between two systems in a starting point and then 2) the correlation is carried out during the propagation of particles of two spatially separated points. Both operations are local and therefore the final correlation is prepared in the journey of the particles by local processes.

These authors demonstrates that the determination of correlation can be made only in terms of the world-lines of the particles, and in general terms, a perfect correlation EPR can not exist in gravitational fields. They concluded that the reason for, this is that different local processes are superimposed coherently given by the different particle trajectories.

These same observations are indicated in the work of Terashima and Ueda [54], which shows that the entropy in the spin of a pair of entangled particles increases very rapidly in the vicinity of the horizon of a Schwarzschild black hole when are moving in a circular orbit. This means that the EPR correlation is lost between the particles and the spin can not be used as a qubit[1] within intense gravitational field in quantum information processing.

Later, these same authors extend this work in [31] and they show that the acceleration and gravity effects deteriorate the EPR correlation in the direction of the spins that would be equal in a non-relativistic theory, and that there is a decrement in the violation of Bell inequalities.

Also they find that near the horizon of a Schwarzschild black hole a small uncertainty in identifying the positions of the observers, lead to a fatal error in identifying the direction of measurement necessary to maintain the perfect correlation EPR, because there are a very fast spin precession near horizon.

This implies that in order to maintain a non-local quantum communication in curved space-time using a pair of EPR particles, it is important the proper selection of the 4-vector velocity of the particles and the frame system that they are referred to. By this means is possible to compensate for the effects of gravity on the twisted pair. We shall see later these effects of the pair of particles velocity and the reference systems.

Thus, this thesis extends the work of Terashima and Ueda by adding more physical and theoretical parameters to curved spacetime used by them, obtaining more complicated black holes than those previously analyzed in the literature. We will see that these parameters impact the spacetime curvature, as well as defining new event horizons.

---

[1]Qubit is an acronym for "quantum bit". In classical computation a bit is the basic unit of information and it can have one of two possible values, 0 or 1. Similarly in quantum information, a qubit can also have the values 0 or 1 or a superposition of both simultaneously.

3.1.1   Special Relativity Quantum states: Lorentz transformations

First it is necessary to address the problem of describing the spin of a particle in the scheme of Special Relativity. To do this we define the quantum state $|\phi\rangle$ of a massive particle from a classical non-relativistic frame with spin j,

$$|\phi\rangle = |p^a(x), \sigma; x\rangle, \tag{3.1}$$

where x represents the position, $p^a(x)$ the lineal 4-momentum and $\sigma \in \{-j, -j+1, ..., j\}$ are the spin component of the particle measured in one of the axes in the static inertial frame of the particle [74].

The physical observables linked with quantum objects are represented by hermitian operators that act over the quantum states [61]. It is said that an operator $\mathbf{A}$ is hermitian if its eigenvalues are real, that is, $\mathbf{A}$ satisfies

$$\mathbf{A} = \mathbf{A}^\dagger,$$
$$\langle\phi|\mathbf{A}|\phi\rangle = \langle\phi|\mathbf{A}|\phi\rangle^*. \tag{3.2}$$
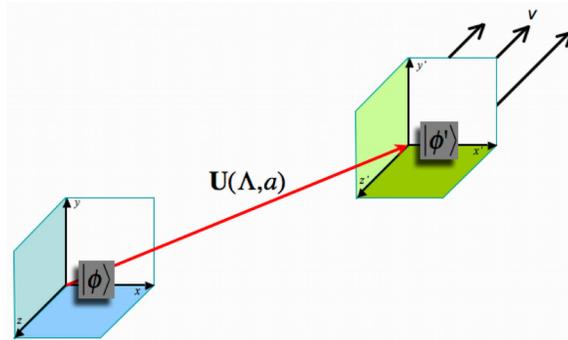
Figure 3.1: Description of the quantum state $|\phi\rangle$ in an inertial frame in relation with another inertial frame (primed).

Through operators is how we can, for example, translate a quantum state from a frame of reference to another, do evolve over time, know the momentum, determine its spin, or any other observable. In particular we are interested in describing the same state from different frames of reference, that is moving relative to each other with constant velocity.

Let propose the following scenario, an observer in the inertial frame measures a quantum state in its frame. Also, another inertial observer moving relative to the first one measures the same state and both observers must coincide in their measures (see Figure 3.1). It is important to remember that the observations correspond to statistical probabilities given by quantum states, defined by the product $\langle\phi|\mathbf{A}|\phi\rangle$, such that the operator $\mathbf{A}$ connects state

$|\phi\rangle$ in an inertial frame to another one moving inertial system $|\phi'\rangle$, i.e.

$$|\phi\rangle \rightarrow |\phi'\rangle = \mathbf{A}|\phi\rangle. \tag{3.3}$$

Thus it is desirable that both observers agree on their observations regardless of the state of inertial motion they have, which means $\langle\phi|\phi\rangle = \langle\phi'|\phi'\rangle$. With equation (3.3) therefore we can see that

$$\langle\phi|\phi\rangle = \langle\phi|\mathbf{A}|\phi\rangle, \tag{3.4}$$

and therefore we expect that the operator $\mathbf{A}$ must be a unitary operator.

A unitary operator $\mathbf{U}$ is a symmetry operation that changes the point of view of the experimenter (reference system) but does not change the results of possible experiments. This operator is defined in a Hilbert space, acts linearly and its adjoint satisfies [75]

$$\mathbf{U}^\dagger \mathbf{U} = \mathbf{U}\mathbf{U}^\dagger = \mathbf{1}. \tag{3.5}$$

As an example, let consider now a massive particle with mass M traveling with a velocity v in x direction with respect to a laboratory. A second observer moves away from the laboratory towards z with velocity V. This situation is described in Fig. 3.2.

In the framework of the particle 4-momentum is given by the momentum at rest $k^\mu = (Mc, 0, 0, 0)$. In this frame of reference the state (3.1) is defined by[2] $|k, \sigma\rangle$ and it is characterized for the eigenvalues of the Hamiltonian $\mathbf{H}$, the momentum operator $\mathbf{P}$ and the z component of the total angular momentum by the operator $\mathbf{J}$, that is,

$$\begin{aligned}
\mathbf{H}|k, \sigma\rangle &= Mc^2|k, \sigma\rangle, \\
\mathbf{P}|k, \sigma\rangle &= 0, \\
\mathbf{J}^3|k, \sigma\rangle &= \sigma\hbar|k, \sigma\rangle.
\end{aligned} \tag{3.6}$$

Because that the momentum k^μ is invariant under the group of spatial rotations $SO(3)$, a rotation is represented by the unitary matrix $D^{(j)}(R)$ with dimension $(2j + 1)$,

$$U(R)|k, \sigma\rangle = \sum_{\sigma'} D^{(j)}_{\sigma'\sigma}(R)|k, \sigma'\rangle, \tag{3.7}$$

where j is an integer or a half integer and $-j \leq \sigma \leq j$. Note that j is the spin of the particle and σ is its component in the z-axis because the orbital angular momentum is not present in the particle frame [76].

---

[2]For simplicity it is omitted the position index x from $|p^a(x), \sigma; x\rangle$.
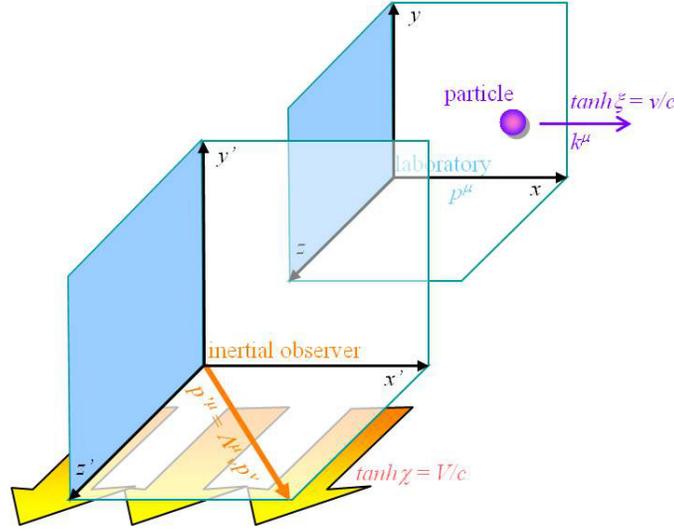
Figure 3.2: A particle has an quantum state $|k, \sigma\rangle$ and travels in x direction as seen by a "fixed" observer in a laboratory. There the state is measure as $|p, \sigma\rangle = U(L(p))|k, \sigma\rangle$. Then a moving inertial observer in z-axis relative to the laboratory (primed system) measure the state of the same particle as $|p', \sigma'\rangle = U(\Lambda)|p, \sigma\rangle$.

However, in the laboratory reference frame, the 4-momentum of the particle is $p^\mu = (\sqrt{|\vec{p}|^2 + M^2 c^2}, p^1, p^2, p^3)$, which is obtained by a standar Lorentz transformation $L(p)^\mu{}_\nu$ over the rest momentum k^u, that is, $p^\mu = L(p)^\mu{}_\nu k^\nu$, where $\mu, \nu = 0, 1, 2, 3$ and the repeated index are added according to the Einstein summation convention. The Lorentz transformation is expressed as [76],

$$
\begin{aligned}
L(p)^0{}_0 &= \gamma, \\
L(p)^0{}_i &= L(p)^i{}_0 = p^i/Mc, \\
L(p)^i{}_k &= \delta_{ik} + (\gamma - 1)p^i p^k/|\vec{p}|^2,
\end{aligned}
\tag{3.8}
$$

where $\gamma = \sqrt{|\vec{p}|^2 + M^2 c^2}/Mc$ and the index can take the spatial coordinates values $i, j = 1$, 2, 3. In Appendix A the previous transformations are obtained.

Thus, the state of the particle is $|p, \sigma\rangle = U(L(p))|k, \sigma\rangle$ measured by a laboratory observer, where $U(L(p))$ is the unitary operator which correspond to $L(p)^\mu{}_\nu k^\nu$. This means that both reference frames (of the particle and of the laboratory) are connected by a unitary transformation defined by a Lorentz transformation. In this operation the spin z-component is not affected because the particle and the laboratory have their reference frames connected only by a coordinate transformation in the x-axis (see Fig. 3.2).

But for an observer moving in the z direction, it is necessary to proceed carefully to compare the spin of the particle with respect to the laboratory and the other inertial observer.

Then, consider an additional observer moving in z direction with V velocity from the perspective of the laboratory and let $\Lambda^\mu{}_\nu$ its Lorentz transformation that connect the reference frame of the laboratory with the reference frame of the moving observer (see Fig. 3.2). For this moving observer, the state of the particle is described by $U(\Lambda)|p,\sigma\rangle = U(L(\Lambda p))U(W(\Lambda,p))|k,\sigma\rangle$, where we will define

$$W(\Lambda,p)^\mu{}_\nu = [L^{-1}(\Lambda p)\Lambda L(p)]^\mu{}_\nu, \tag{3.9}$$

as the Wigner rotation [29]. In Appendix B.1 is shown how to get it.

It is important to emphasize that the Wigner rotation is an element of the special group rotations $SO(3)$, because it leaves the momentum k^μ without changes [76], that is, $k' = W(\Lambda,p)k$. This group of rotations is called the *little group* of Wigner for massive particles, that is, is the group that leaves the 4-momentum invariant in the particle reference frame [74]. We shall see that the Wigner rotation is essential for the description of the spin entangled quantum states under a curved spacetime influence, because in this background it is not clear in what direction must be measured the spin, as previously mentioned. The Wigner rotation will be the instrument that we will use to link the direction of the spin from one place to another, because it will be the guide to indicate how much the initial coordinate system has rotated with respect to the final state, that is, how the measure instrument is moving away from the original position in the curve spacetime.

From Eq. (3.7) follows

$$U(\Lambda)|p,\sigma\rangle = \sum_{\sigma'} D^{(j)}_{\sigma'\sigma}(W(\Lambda,p))|\Lambda p,\sigma'\rangle, \tag{3.10}$$

where Λp are the spatial components of the 4-momentum under the operation of Lorentz transformations, that is,, $p^{\mu'} = \Lambda^\mu{}_\nu p^\nu$. The term $D^{(j)}_{\sigma'\sigma}(W(\Lambda,p))$ is the spinor matrix $(2j+1) \times (2j+1)$ of the rotation group $SO(3)$ and $W(\Lambda,p)$ is called the Wigner rotation angle [74]. We will work with spinor 2×2 matrices for our analysis of particles with spin. We shall see in section 3.2.1 the application of this.

So, lets take the case of a massive particle with a half-spin with 4-momentum $p^\mu = (Mc\cosh\xi, Mc\sinh\xi, 0, 0)$ in the laboratory reference frame (see Fig. 3.2). The speed is described by ξ and is related to the velocity v by the hyperbolic relation $v/c = \tanh\xi$ (see

A.9 of Appendix A). In this case, as it is shown in (A.10), the Lorentz transformation is[3]

$$L(p)^\mu{}_\nu = \begin{bmatrix} \cosh\xi & \sinh\xi & 0 & 0 \\ \sinh\xi & \cosh\xi & 0 & 0 \\ 0 & 0 & 1 & 0 \\ 0 & 0 & 0 & 1 \end{bmatrix}. \tag{3.11}$$

An additional observer comes on the scene and moves away from the laboratory in the z-axis (see Fig. 3.2). Following the Appendix A is possible to get the Lorentz transformation that describe this extra observer[4], that is,

$$\Lambda^\mu{}_\nu = \begin{bmatrix} \cosh\chi & 0 & 0 & -\sinh\chi \\ 0 & 1 & 0 & 0 \\ 0 & 0 & 1 & 0 \\ -\sinh\chi & 0 & 0 & \cosh\chi \end{bmatrix}. \tag{3.12}$$

It is important to note that the function $L(p)^\mu{}_\nu$ acts over the momentum k^u of the particle, meanwhile $\Lambda^\mu{}_\nu$ acts over the description of the position.

Thereby, the Wigner rotation (3.9) is reduced to a simple rotation around y-axis, where the rotation angle, that we shall call δ, is given by

$$\tan\delta = \frac{\sinh\xi \sinh\chi}{\cosh\xi + \cosh\chi}. \tag{3.13}$$

In the Appendix B.2 it can review the steps to get this angle of rotation. In the non-relativistic limit, when $\xi \to 0$ and $\chi \to 0$, the angle $\delta \to \xi\chi/2$. This implies that everyday speeds (i.e. non-relativistic), the moving observer will measure a negligible spin rotation with respect to the observer in the laboratory, which we already expected. On the other hand, if $\xi = \chi = 0$ the angle $\delta = 0$ and there is no Wigner transformation as expected. This is the case of "static" observers that do not have movement respect the particle reference frame.

However, when the observers and their reference frames move away at near speed light velocity, that is $\xi \to \infty$ and $\chi \to \infty$, we get that the denominator of the Eq. (3.13) tends to zero and therefore $\delta = \pi/2$. Then, there is no possible to get a finite Wigner rotation.

---

[3]The sign that precedes the hyperbolic function $\sinh\xi$ is positive now, in contrast to Eq. (A.10) that was negative. This is because now we start from the particle reference frame and we connect with the laboratory reference frame with $L(p)^\mu{}_\nu$, which "moves away" from the left of the particle. In the Appendix A the reference frame O' moves away from the right of O.

[4]Now the sign of $\sinh\chi$ is negative according to Eq. (A.10).

This ultimately means that a coordinate transformation between the reference frames cannot be established, as can be seen more clearly in Wigner rotation of the equations (B.16) and (B.17).

Finally, Eq. (3.10) tells us which is the quantum vector state of the particle that the observer measure in the z-axis. This state is composed of the sum of the matrix components of spinors $D^{(j)}_{\sigma'\sigma}$ that has been rotated an angle δ which is defined by $W(\Lambda, p)$. That is, in order to compare the original state of the particle against his/her own recessional speed, the moving observer can calculate the state of the particle (momentum and spin) at the beginning and then in the final position as moves away. This equation of states for the case of special relativity can be found in the references [23, 76].

In the next section we will discuss the case of the observers that are no longer moving inertially, but they are accelerating, i.e., subject to general relativity.

3.1.2 Local inertial frames

In the previous section we saw that inertial observers do not get the same measurement of the spin component in a particular direction, but among these observers there is a rotation of coordinates given by the Wigner rotation (3.10). Ultimately however, they can connect the description of quantum states throughout unitary Lorentz transformations.

For the case of General Relativity, where spacetime is curved, it is not possible to define a coordinate system that is equivalent from one point to another one.

As mentioned in Section 2.2, in General Relativity, the spacetime curvature is obtained as derivatives of $g_{\mu\nu}(x)$, which is the solution of the Einstein field equations

$$G_{\mu\nu} = R_{\mu\nu} - \frac{1}{2}Rg_{\mu\nu} = 8\pi T_{\mu\nu}, \tag{3.14}$$

where the Einstein tensor $G_{\mu\nu}$ is related to the mass and energy distribution $T_{\mu\nu}$ on the spacetime itself [69].

Therefore it is possible to define a differential element that allow us to measure lengths and time intervals in the spacetime throughout the curvature defined by the matter distribution in Eq. 3.14).

Then, in spherical coordinates, the axial metric is defined by:

$$ds^2 = g_{00}dt^2 + 2g_{03}dtd\phi + g_{11}dr^2 + g_{22}d\theta^2 + g_{33}d\phi^2, \tag{3.15}$$

where $g_{30} = g_{03}$, the coordinate t are related to the time axis, r to the radial coordinate, θ

to the radial angle and ϕ for the azimutal angle.

Moreover, the elements of the inverse of the metric are defined by

$$
\begin{aligned}
g^{00} &= \frac{g_{33}}{g_{33}g_{00} - g_{03}^2}, \\
g^{03} &= g^{30} = -\frac{g_{03}}{g_{33}g_{00} - g_{03}^2}, \\
g^{11} &= \frac{1}{g_{11}}, \\
g^{22} &= \frac{1}{g_{22}}, \\
g^{33} &= \frac{g_{00}}{g_{33}g_{00} - g_{03}^2}.
\end{aligned}
\tag{3.16}
$$

In order to define the spin in the curved spacetime we introduce a local inertial reference frame in each point through an *vierbein*[5] that complies the next conditions [77]:

$$
\begin{aligned}
e_a{}^{\mu}(x)e_b{}^{\nu}(x)g_{\mu\nu}(x) &= \eta_{ab}, \\
e^a{}_{\mu}(x)e_a{}^{\nu}(x) &= \delta_{\mu}{}^{\nu}, \\
e^a{}_{\mu}(x)e_b{}^{\mu}(x) &= \delta^a{}_b,
\end{aligned}
\tag{3.17}
$$

where the latin indexes are Lorentz indexes and take the values of $0, 1, 2, 3$; the greek indexes correspond to the four coordinates of General Relativity (t, r, θ, ϕ), and the repeated indexes follow the Einstein sum convention.

The term $e_a{}^{\mu}$ is defined to be the matrix that transforms from a general coordinate system x^{μ} to the local inertial frame x^a at each point. The vierbein is a 4×4 matrix, with 16 independent components. The inverse vierbein is denoted by $e^a{}_{\mu}$.

For example, the 4-momentum $p^{\mu}(x)$ in the general coordinate system can be transformed into the local inertial frame at x^{μ} via the relation $p^a(x) = e^a{}_{\mu}(x)p^{\mu}(x)$.

The choice of the local inertial frame is not unique, since the inertial frame remains inertial under the Lorentz transformation. The choice of the vierbein therefore has the same degree of freedom known as the local Lorentz transformation. It is this degree of freedom that transforms the spin of a particle. Namely a $\frac{1}{2}$-spin particle in a curved spacetime is defined as a particle whose one-particle states furnish the $\frac{1}{2}$-spin representation of the Lorentz transformation, not of the general coordinate transformation. Note that the Dirac field in the curved spacetime is spinor under the Lorentz transformation, whereas it is a scalar under the general coordinate transformation. Usually, the definition of a particle is not unique in quantum field theory in curved spacetime, because we cannot uniquely choose

---

[5]From german "4 legs". This is the reference frame that it is mounted on the particle instant by instant. That was mentioned at the beginning of this chapter.

the time coordinate to define the positive energy [54]. However, in the present formulation, our particle is specified by the choice of the vierbein, since $e_0{}^\mu$ generates a preferred global time coordinate from the local inertial time coordinate (the 0-axis).

3.1.3 Quantum states in classical backgrounds: Wigner rotations

Since the spin of a particle is defined locally relative to the local inertial frame, we must consider the change of the spin when a particle moves form one point to another one in curved spacetime. We have already seen in Section 3.1.1 how to compare the quantum state of a particle for inertial frames through Lorentz transformations. But for accelerated frames in curve spacetime the process is quite different as we shall see.
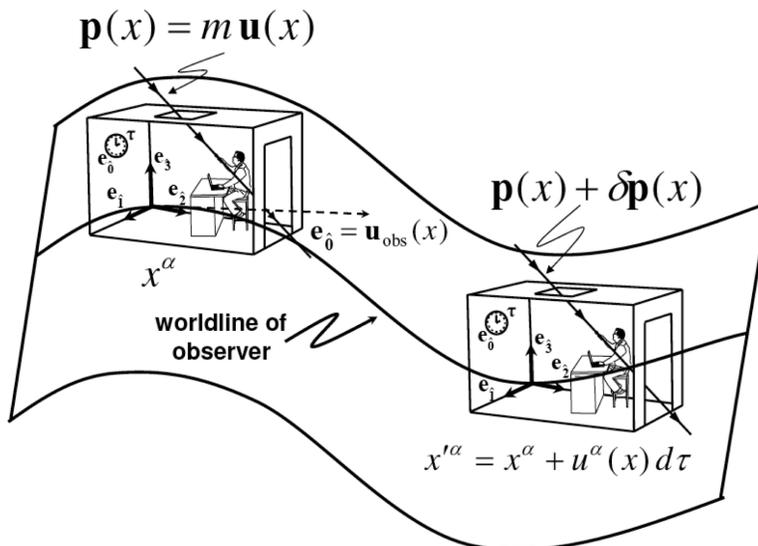
Figure 3.3: Laboratory frame for curved spacetime. The observer's local laboratory (small box with man) at the curved spacetime point x, defined by the orthonormal vierbein $e_a{}^\mu(x)$. The three spatial axes $e_i(x)$, $i = (1, 2, 3)$ are located at the origin of the observer's laboratory, while $e_0(x) = u_{obs}(x)$ is the temporal axis, defined as his 4-velocity, or the tangent to his geodesic trajectory (image credit: [78]).

Let us consider how the spin changes as we move from one point in curved spacetime to another along an arbitrary word line trajectory. Let our particle initially be at a spacetime point with coordinate x and 4-momentum $p(x) = mu(x)$. At a small proper time $d\tau$ later the particle has moved along its trajectory with tangent u to the point with coordinates $x' = x + u(x)d\tau$ and new 4-momentum $p(x) + \delta p(x)$ (see Fig. 3.3). Since the spin of the particle is defined locally with respect to the observer's reference frame, and defined by the tetrad that is carried along with him at the laboratory's origin, the 4-momentum changes in

the form of[6]

$$\delta p^a(x) = \lambda^a{}_b(x) p^b(x) d\tau, \tag{3.18}$$

where $\lambda^a{}_b(x)$ is a infinitesimal local Lorentz transformation (see Appendix A),

$$\Lambda^a{}_b(x) = \delta^a{}_b(x) + \lambda^a{}_b(x) d\tau. \tag{3.19}$$

From the definition of the local 4-momentum in the observer's reference frame as projection of the world 4-momentum onto the local axes $p^a(x) = e^a{}_\mu(x) p^\mu(x)$ we have

$$\delta p^a(x) = \delta p^\mu(x) e^a{}_\mu(x) + p^\mu(x) \delta e^a{}_\mu(x), \tag{3.20}$$

where the term $\delta p^\mu(x)$ is the chance of the world 4-momentum components $p^\mu(x)$ as the particles moves from $x^\mu \to x'^\mu$ in the underlying curved spacetime, and the term $\delta e^a{}_\mu(x)$ is the change in the vierbein components $e^a{}_\mu(x)$ which are used to project the world 4-momentum components onto the observer's local laboratory axes, $p^\mu(x) \to p^a(x)$.

The first term is simply given by

$$\delta p^\mu(x) = u^\nu(x) \nabla_\nu p^\mu(x) d\tau = m a^\mu(x) d\tau, \tag{3.21}$$

where we have used the definition of the 4-momentum in terms of the 4-velocity, i.e. $p(x) = mu(x)$, and the definition of the acceleration,

$$\begin{aligned} a^\mu(x) &= u^\nu(x) \nabla_\nu u^\mu(x), \\ a^b(x) &= a^\mu(x) e_\mu{}^b(x). \end{aligned} \tag{3.22}$$

The symbol ∇_μ denotes the covariant derivative for a contravariant vector V^ν, that is,

$$\nabla_\mu V^\nu = \frac{\partial V^\nu}{\partial x^\mu} + V^\sigma \Gamma^\nu_{\sigma\mu}, \tag{3.23}$$

where

$$\Gamma^\nu_{\sigma\mu} = \frac{1}{2} \left(\frac{\partial g_{\nu\sigma}}{\partial x^\mu} + \frac{\partial g_{\sigma\mu}}{\partial x^\nu} - \frac{\partial g_{\nu\mu}}{\partial x^\sigma} \right) \tag{3.24}$$

are the Christoffel's symbols.

Since $p^\mu(x) p_\mu(x) = -m^2$ and $p^\mu(x) a_\mu(x) = 0$ (particles no subject to no-external forces

---

[6]Note the latin indices because we are working in local inertial frame for infinitesimal proper time $d\tau$.

traveling on a geodesic), where m is the mass of the particle, we can write Eq. (3.21) as

$$\delta p^\mu(x) = -\frac{1}{m}[a^\mu(x)p_\nu(x) - p^\mu(x)a_\nu(x)]p^\nu(x)d\tau. \tag{3.25}$$

For the second term in Eq. (3.20), the change in the local inertial frame (vierbein components) is given by

$$\begin{aligned}
\delta e^a{}_\mu(x) &= \nabla_\mu e^a{}_\mu(x)d\tau, \\
&= u^\nu(x)\nabla_\nu e^a{}_\mu(x)d\tau, \\
&= -u^\nu(x)\omega_\nu{}^a{}_b(x)e^b{}_\mu(x)d\tau, \\
&= \chi^a{}_b(x)e^b{}_\mu(x)d\tau,
\end{aligned} \tag{3.26}$$

where the term $\chi^a{}_b(x) = -u^\nu\omega_\nu{}^a{}_b(x)$ was defined as the change in the local inertial frame along u^μ, and

$$\omega_\mu{}^a{}_b(x) = -e_b{}^\nu(x)\nabla_\mu e^a{}_\nu(x) = e^a{}_\nu(x)\nabla_\mu e_b{}^\nu(x) \tag{3.27}$$

is the connection one-form or spin connection. The second equality in Eq. (3.27) results from the first definition in Eq. (3.17) and $\nabla_\mu g_{\nu\rho}(x) = 0$, giving $\chi_{ab}(x) = -\chi_{ba}(x)$.

Returning back to Eq. (3.20), collecting the previous results from equations (3.25) and (3.26), we obtain

$$\delta p^a(x) = \lambda^a{}_b(x)p^b(x)d\tau, \tag{3.28}$$

where $\lambda^a{}_b(x)$ is the infinitesimal local Lorentz transformation

$$\lambda^a{}_b(x) = -\frac{1}{m}[a^a(x)p_b(x) - p^a(x)a_b(x)] + \chi^a{}_b(x). \tag{3.29}$$

We can now calculate the components of the local Wigner rotation (3.10), but for curved spacetimes, which determines how the spin of the particle precesses locally as the particle moves from $x^\mu \to x'^\mu$, as previously mentioned.

From the definition of the Wigner rotation Eq. (3.9), we can perform the calculation to first order in $d\tau$ to get the infinitesimal Wigner rotation using

$$W^a{}_b(x) = \delta^a{}_b + \vartheta^a{}_b(x)d\tau, \tag{3.30}$$

where $\vartheta^0{}_0(x) = \vartheta^0{}_i(x) = \vartheta^i{}_0(x) = 0$ (see [78] for an extensive calculation review) and

$$\vartheta^i{}_k(x) = \lambda^i{}_k(x) + \frac{\lambda^i{}_0(x)p_k(x) - \lambda_{k0}(x)p^i(x)}{p^0(x) + m}. \tag{3.31}$$

For a particle of spin-j the rotation matrix $D^{(j)}_{\sigma'\sigma}(W(x))$ of Eq. (3.10) is given by

$$D^{(j)}_{\sigma'\sigma}(W(x)) = I + i[\vartheta_{23}J_1 + \vartheta_{31}J_2 + \vartheta_{12}J_3]d\tau, \tag{3.32}$$

where $[J_i, J_j] = -i\epsilon_{ijk}J_k$ are the commutation relations for SU(2) with the constant flat spacetime spin-j matrices J_i.

For the case of spin-$\frac{1}{2}$, in our modem, we have $J_i = \frac{1}{2}\sigma_i$ where σ_i are the usual flat spacetime constant Pauli matrices. The infinitesimal unitary transformation of the state Eq. (3.1) as the particle moves from $x^\mu \to x'^\mu$ is given by Eq. (3.10)

$$\begin{aligned}
U(\Lambda(x))|p^i(x),\uparrow\rangle &= \left(I + \frac{i}{2}\vartheta_{23}(x)d\tau\right)|p^i(x'),\uparrow\rangle \\
&\quad -\frac{1}{2}\left(\vartheta_{31}(x) - i\vartheta_{23}(x)\right)d\tau|p^i(x'),\downarrow\rangle,
\end{aligned} \tag{3.33}$$

$$\begin{aligned}
U(\Lambda(x))|p^i(x),\downarrow\rangle &= \frac{1}{2}\left(\vartheta_{31}(x) + i\vartheta_{23}(x)\right)d\tau|p^i(x'),\uparrow\rangle \\
&\quad +\left(I - \frac{i}{2}\vartheta_{23}(x)d\tau\right)|p^i(x'),\downarrow\rangle,
\end{aligned} \tag{3.34}$$

where we have used the notation $\sigma = \{\frac{1}{2}, -\frac{1}{2}\} = \{\uparrow, \downarrow\}$.

The next step is to iterate the formula for infinitesimal local Wigner rotation to obtain the finite rotation between an initial and final point in spacetime, that is $\{x(\tau_i), x(\tau_f)\}$, for a finite proper time. By a Dyson serie (like in time-dependent perturbation theory), we can break up the trajectory into N infinitesimal time steps of length $\tau_{f,i}/N$ where

$$\tau_{f,i} = \int_{\tau_i}^{\tau_f} d\tau = \int_{\tau_i}^{\tau_f} [g_{\mu\nu}(x)dx^\mu dx^\nu]^{1/2} \tag{3.35}$$

is the total proper time between the two events, and

$$x_k^\mu = x^\mu(\tau_i + k\tau_{f,i}/N). \tag{3.36}$$

Therefore the finite Wigner rotation is given by

$$\begin{aligned}
W^a{}_b(x_f, x_i) &= \lim_{N\to\infty} \prod_{k=0}^{N} \left[\delta^a{}_b + \vartheta^a{}_b(x_k)\frac{k\tau_{f,i}}{N}\right] \\
&= T\exp\left[\int_{\tau_i}^{\tau_f} \vartheta^a{}_b(x(\tau))d\tau\right].
\end{aligned} \tag{3.37}$$

In the last expression the time ordering operator T is required since, in general, the

infinitesimal local Wigner rotations $\vartheta^a{}_b(x(\tau))$ do not commute at different positions $x^\mu(\tau)$ along the trajectory. The exponential refers not to the exponential of each component but to that of the whole matrix.

The Eq. (3.37) is finally the expression needed to calculate the finite Wigner rotation in a curved spacetime.

Before continue with the spin precession of the entangled particles, it is important to review a particular feature of the curved axialsymmetrical spacetimes, which induce a additional correction in the dynamics of the particles.

3.1.4 Frame-dragging

There is another effect that an axialsymmetrical metric induces over particles traveling in this kind of spacetimes. When a rotation black hole is considered, it is important to be aware that the spacetime itself around the black hole is rotating too. Therefore any object is under the influence of this effect. This phenomena is known as "frame-dragging" and it has to be considered in any analysis where transformation of coordinates are involved.

Thus, consider a freely falling test particle with four-velocity u^μ in the exterior of a rotating black hole. For an observer at infinite, this particle has two conserved quantities: the relativistic energy per unit mass $E = -u_t$ and the angular momentum per unit mass $L_z = u_\phi$. Both quantities has an key relevance for understanding the dynamics of spin particles in an arbitrary spacetime.

We will see in Section 4.1 that in general, $g_{\mu\nu}$ is independent of ϕ, but the trajectory of the particle still conserves angular momentum u_ϕ. Furthermore, the presence of $g_{03} \neq 0$ in the metric introduces a new effect on the particle trajectories [79]. It is worth to mention in advance that Section 4.1 analyzes the Plebański-Demiański Spacetime, which, as we already said, is the most important family of Type D solutions among the solutions of the Einstein-Maxwell equations. Thus the analysis of frame-dragging in this section is valid for extensive range of real spacetimes. In this section we will see how this effect has an relevant influence for particles and over the spacetime itself.

From the ordinary definition of the four-velocity of any particle, we know that

$$
\begin{aligned}
\frac{dt}{d\tau} &= u^t = g^{00}u_t + g^{03}u_\phi, \\
\frac{d\phi}{d\tau} &= u^\phi = g^{03}u_t + g^{33}u_\phi.
\end{aligned}
\tag{3.38}
$$

We consider also that the test particle would be falling from infinity with originally zero angular momentum, i.e. $u_\phi = 0$. Despite the fact that initially the particle falls radially

with no angular momentum, it will acquire an angular motion during the in fall [80], that is, from (3.38) the angular velocity as seen by a distant observer is given by

$$\omega(r, \theta) = \frac{d\phi}{dt} = \frac{d\phi/d\tau}{dt/d\tau} = \frac{u^\phi}{u^t} = \frac{g^{03}}{g^{00}}. \tag{3.39}$$

Equation (3.39) stands for a rotating relativistic body influences the surrounding matter through its rotation. The metric element $g_{03} \neq 0$ introduces an axial symmetry in a static spacetime, and it is interpreted as a rotation of the spacetime itself, like a Kerr black hole for example. Thus a particle dropped in a rotating black hole from infinity (large distances) is dragged just by the influence of gravity so that it acquires an angular velocity ω in the same direction of rotation of the black hole. This effect decreases with distance [79]. From a physical point of view we can interpret this phenomenon as a dragging of the local inertial frames by the rotating hole.[7]

Therefore we have showed that for a rotating spacetime, any free falling particle acquires angular moment. This effect is known as frame-dragging [80]. Consider now a particle in circular orbit around the rotating black hole $(u_r = u_\theta = 0)$. From Eqs. (3.38) we get

$$u^\phi_{fd} = -\frac{g_{03}}{g_{33}} u^t_{fd} = \omega u^t_{fd}, \tag{3.40}$$

where we now identify u^μ_{fd} as the velocity of the particle due this frame-dragging.[8] Using the normalization condition for velocities $u^\mu u_\mu = -1$, it can be shown that

$$u^t_{fd} = \sqrt{\frac{-g_{33}}{g_{00}g_{33} - (g_{03})^2}}. \tag{3.41}$$

Both Eqs. (3.40) and (3.41) constitute the components of the four-velocity of a test particle due the frame-dragging as seen by a distant observer in the general frame.

Then, after some arrange the terms, the four-velocity due the frame-dragging for a free-falling particle, as seen by the same distant observers, is given as

$$u^\mu_{\text{fd}} = \sqrt{\frac{-g_{33}}{g_{00}g_{33} - (g_{03})^2}} \left(1, \ 0, \ 0, \ -\frac{g_{03}}{g_{33}} \right). \tag{3.42}$$

On the other hand, we shall see later that the spin precession angle is calculated by infinitesimal Lorentz transformations of the velocity of a particle in a local inertial frame, because the spin is only defined in this kind of frames. Thus, in order to find the velocity

---

[7]We shall see below that this effect due the axial symmetry appears too in more general spacetimes.
[8]The subindex "fd" will be used to identify the local inertial velocity due the frame-dragging effect.

of a particle in a local inertial frame, we will consider a convenient set of hovering observers that will be useful to measure or prepare the relevant spin states.

But first, the contravariant four-velocity of these hovering observers[9] as seen at infinity is

$$u_h^\mu = (dt/d\tau,\ 0,\ 0,\ 0) = ((-g_{00})^{-1/2},\ 0,\ 0,\ 0), \tag{3.43}$$

and their covariant four-velocity is obtained by lowering indices, that is

$$u_{\mu_h} = \left(-\sqrt{-g_{00}},\ 0,\ 0,\ \frac{g_{03}}{\sqrt{-g_{00}}}\right). \tag{3.44}$$

It is worth to mention that this hovering observer is at rest in their local frame ($u_h^a = \eta^{ab}e_b{}^\mu u_{\mu h}$) too, because the selected vierbein (3.17) ensures this condition. By both requirement (hovering observers at rest in general frame Eq. (3.43) and at local frame) we can be sure that the measures of the local infinitesimal Lorentz transformations of spin precession will be correct, which shall be a medullar point in Section 3.1.5.

Now, the energy of a particle with respect to the local hovering observer with four-velocity u_{μ_h} is the time component of the four-momentum of the particle in the observer's frame of reference. It is obtained by projecting the four-momentum mu_{fd}^μ of the test particle on the four-velocity of the hovering observer, that is

$$u_{fd}^\mu u_{\mu_h} = -E = -\gamma_{fd}, \tag{3.45}$$

where $\gamma_{fd} = (1 - v_{fd}^2)^{-1/2}$ is the usual relativistic gamma factor and v_{fd} the local velocity (speed) of the particle subject to the frame-dragging. E is interpreted as the relativistic energy per unit mass of the particle relative to a hovering observer.

The scalar product (3.45) is an invariant and its value is independent of the coordinate system used to evaluate it. That means that this physical quantity will be connected by a Lorentz transformation between two different local frames, even though one or both of the frames may be accelerating.

The local frame-dragging velocity is then obtained from Eq. (3.45), and can be expressed as hyperbolic relativistic functions by $\tanh \eta = v_{fd}$. That is, the local inertial velocity due the frame-dragging and measured by a hovering observer will be

$$u_{fd}^a = (\cosh \eta, 0, 0, \sinh \eta). \tag{3.46}$$

Further on we will see that it is a suitable way of expressing the frame-dagging velocity

---

[9]The subindex "h" will be used for "hovering observers".

when this effect shall be incorporated on spin precession angle in Section 3.2.1.

Finally, the hyperbolic functions are obtained after some algebra from equations (3.42, 3.43, 3.45) and are equivalent to

$$
\begin{aligned}
v_{\text{fd}} = \tanh \eta &= \frac{g_{03}}{\sqrt{(g_{03})^2 - g_{00}g_{33}}}, \\
\gamma_{\text{fd}} = \cosh \eta &= \sqrt{\frac{g_{00}g_{33} - (g_{03})^2}{g_{00}g_{33}}}, \\
\sinh \eta &= \sqrt{\frac{-(g_{03})^2}{g_{00}g_{33}}}.
\end{aligned}
\tag{3.47}
$$

3.1.5 Spin precession

As previously mentioned at the beginning in Sec. 1.2, in the present work it is considered two observers and an EPR particles source on the equator plane $\theta = \pi/2$ of a black hole. The observers are placed at azimuthal angles $\phi = \pm\Phi$ and the EPR source is located at angle $\phi = 0$. The observers and the EPR source are assumed to be hovering satisfying Eq. (3.43) over the black hole in order to keep them "at rest" in the Boyer-Linquist coordinate system (4.4). The EPR source emits a pair of entangled particles in opposite directions, describing a circular orbit on the equator at constant radio. The vierbein (4.6) works as a reference frame to prepare the spin state in the EPR source and to measure the new quantum states of the particles from the perspective of the hovering observers. This vierbein is defined at each point of spacetime since the observers, and consequently, the EPR source is accelerated on the equator and keeping a constant radius, in such a way that they are not influenced by the frame-dragging, as previously stated. The gedanken experiment depicting this situation is shown in Fig. 3.4.

Now we will introduce another kind of observers that are mounted in a frame that is rotating around the black hole due the frame-dragging, These observers are known as *zero angular momentum observers* (ZAMO).

A ZAMO has a local velocity described by Eq. (3.46), as seen by the hovering observers. Moreover it has angular speed $\omega = -g_{03}/g_{33}$, maintaining their r and θ coordinates constant. The events at the same time t are simultaneous for them, that means the world-lines of this kind of observers are orthogonal to the surface of constant t (i.e. $dx_\mu u_{fd}^\mu = 0$), and the angular momentum of any particle is conserved in their local inertial frame [33, 80], that is why they called like that.

Due this last feature, we will adopt a ZAMO observer as a preliminary step before we calculate the total local inertial velocity of entangled particles measured by the hovering
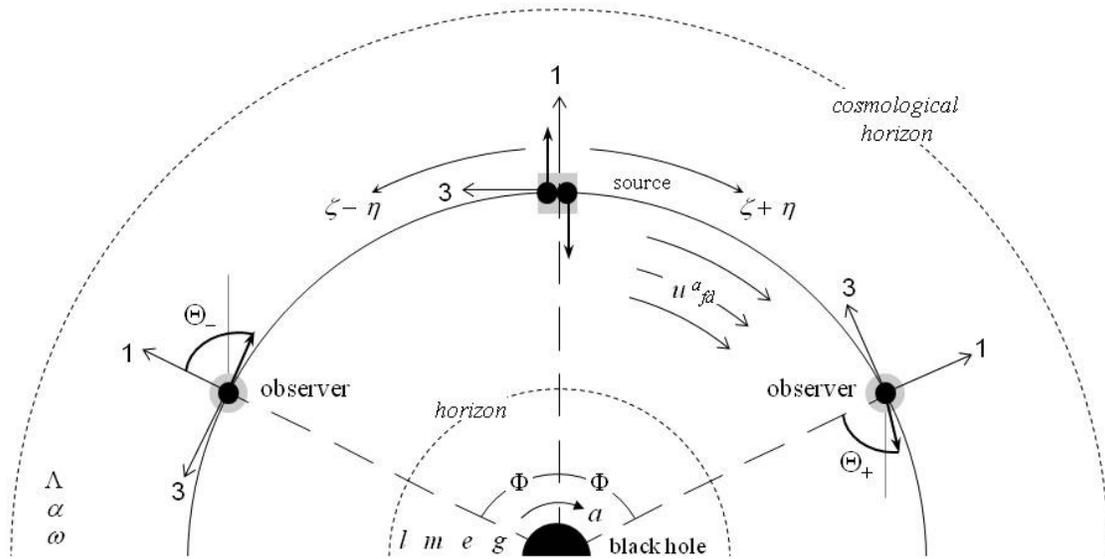
Figure 3.4: An EPR gedanken experiment in an axially symmetric spacetime. Two hovering observers (indicated by gray circles) and a static EPR source (gray square and hovering too) are located at $\phi = \pm\Phi$ and 0, respectively. The expanding and twisting Plebański-Demiański metric, represents a spacetime described through seven parameters: mass m, electric and magnetic charges e, g, rotation parameter a, cosmological constant Λ, NUT-like parameter l, acceleration-like parameter α. Both entangled particles feel a frame-dragging with respect the observers and they leave the source with a local velocity $\tanh(\zeta \pm \eta)$, which the positive sign stands for the particle traveling in the same direction than the rotation and the negative sign corresponds to the opposite one.

observer.

From the perspective of a ZAMO, the local velocity of the entangled particles is given by

$$u_{\text{EPR}}^a = (\cosh\zeta,\ 0,\ 0,\ \sinh\zeta), \qquad (3.48)$$

where $v_{\text{EPR}} = \tanh\zeta$ is the speed of particles in the local inertial frame of the ZAMO.

When the particles leave behind the EPR source, their local velocity u_{EPR}^a remains constant in any ZAMO's frame with the same radius r and angle θ.

Now, from the point of view of a hovering observer, the particles have a local inertial frame velocity given by the relativistic addition of the velocity of the ZAMO (3.46) plus the velocity of the particles measured by ZAMOs (3.48). That is, we define a total velocity $\tanh\xi$, where $\xi = \zeta \pm \eta$ is the total speed of the particle in the local inertial frame (see Fig. 3.4). The plus sign corresponds to the particle traveling in direction of the rotation of the black hole, meanwhile the minus sign is for the other particle that travels in opposite direction. In this way, the gravitational and frame-dragging effects are taken in account.

After the pair of entangled spin-$1/2$ particles is generated at the EPR source, they leave it and follow a circular path around a black hole. In spherical coordinates on the equatorial plane $\theta = \pi/2$, the velocity of the particles has two relevant components, the temporal one and the spatial one with ϕ-coordinate at constant radius r. Thus, for the hovering observer, the motion is measured by the proper-velocity with $v = \tanh\xi$. That is, $u^a = (\cosh\xi, 0, 0, \sinh\xi)$. Applyng the vierbein Eq. (3.17) to transforms for local frame to general frame, the general contravariant four-vector velocity is

$$
\begin{aligned}
u^t &= e_0{}^t \cosh\xi + e_3{}^t \sinh\xi, \\
u^\phi &= e_3{}^\phi \sinh\xi,
\end{aligned}
\qquad (3.49)
$$

which satisfies the normalization condition $u^\mu u_\mu = -1$.

In the Sec. 3.2.1 the frame-dragging will be incorporated on the local inertial frame velocity u^a affecting the previous local velocity transformation and then the total velocity will be written as $u_\pm^a = (\cosh\xi_\pm, 0, 0, \sinh\xi_\pm)$. Here, the argument $\xi_\pm = \zeta \pm \eta$, contains ζ, which is now related to the velocity of the EPR process instead of ξ.

In order the particles describe circular motion, we must apply an external force that compensates both the centrifugal force and the gravity.[10] The acceleration due to this external force is obtained from Eq. (3.22). Thus, on the equatorial plane the acceleration

---

[10]In this work it is not relevant the kind of mechanical system needed to apply this external force, either a rocket or some interaction force fields. The important fact here is that the particles are forced to keep a circular orbit by a unknown means.

becomes

$$
\begin{aligned}
a^r &= (e_0{}^t)^2 \Gamma^1_{00} \cosh^2 \xi \\
&\quad + \left[(e_3{}^t)^2 \Gamma^1_{00} + (e_3{}^\phi)^2 \Gamma^1_{33} + 2 e_3{}^t e_3{}^\phi \Gamma^1_{03} \right] \sinh^2 \xi \\
&\quad + 2 e_0{}^t (e_3{}^\phi \Gamma^1_{03} + e_3{}^t \Gamma^1_{00}) \sinh \xi \cosh \xi.
\end{aligned}
\tag{3.50}
$$

Once the frame-dragging velocity is incorporated into acceleration, it is interesting to note that (3.47) does not affect the structure of (3.50), i.e., the covariant derivatives in Eq. (3.22) act only over coordinates t and ϕ, and those variables are not present on frame-dragging velocity. In the rest of this work, there will be no place where the frame-dragging does affect another computation.

The change of the local inertial frame consists of a boost along the 1-axis and a rotation about the 2-axis calculated by

$$
\chi^a{}_b = -u^\nu \omega_\nu{}^a{}_b,
\tag{3.51}
$$

where the connection one-forms $\omega_\nu{}^a{}_b$ was defined in Eq. (3.27).

In our particular situation, the connections of interest are given by:

$$
\begin{aligned}
\omega_t{}^0{}_1 &= e_1{}^r e^0{}_t \Gamma^0_{01} + e_1{}^r e^0{}_\phi \Gamma^3_{01}, \\
\omega_t{}^1{}_3 &= e_3{}^t e^1{}_r \Gamma^1_{00} + e_3{}^\phi e^1{}_r \Gamma^1_{03}, \\
\omega_\phi{}^0{}_1 &= e_1{}^r e^0{}_t \Gamma^0_{13} + e_1{}^r e^0{}_\phi \Gamma^3_{13}, \\
\omega_\phi{}^1{}_3 &= e_3{}^t e^1{}_r \Gamma^1_{03} + e_3{}^\phi e^1{}_r \Gamma^1_{33}.
\end{aligned}
\tag{3.52}
$$

The relevant boost is described by

$$
\chi^0{}_1 = -e_0{}^t e_1{}^r (e^0{}_t \Gamma^0_{01} + e^0{}_\phi \Gamma^3_{01}) \cosh \xi - e_1{}^r \left[e_3{}^\phi (e^0{}_t \Gamma^0_{13} + e^0{}_\phi \Gamma^3_{13}) + e_3{}^t (e^0{}_t \Gamma^0_{01} + e^0{}_\phi \Gamma^3_{01}) \right] \sinh \xi,
\tag{3.53}
$$

while the rotation about the 2-axis is given by

$$
\chi^1{}_3 = -e_0{}^t e^1{}_r (e_3{}^t \Gamma^1_{00} + e_3{}^\phi \Gamma^1_{03}) \cosh \xi - e^1{}_r \left[e_3{}^t (e_3{}^t \Gamma^1_{00} + e_3{}^\phi \Gamma^1_{03}) + e_3{}^\phi (e_3{}^t \Gamma^1_{03} + e_3{}^\phi \Gamma^1_{33}) \right] \sinh \xi.
\tag{3.54}
$$

The infinitesimal Lorentz transformation Eq. (3.29) can be calculated easily by adding the rotation of the local four-momentum $p^a(x) = m u^a(x)$ on the plane traced by the general four-vectors of velocity and acceleration, thus the boost along the 1-axis and the rotation

about the 2-axis are respectively

$$
\begin{aligned}
\lambda^0{}_1 &= e^1{}_r \left[(e_0{}^t)^2 \Gamma^1_{00} \cosh^2 \xi + ((e_3{}^t)^2 \Gamma^1_{00} + (e_3{}^\phi)^2 \Gamma^1_{33} + 2 e_3{}^t e_3{}^\phi \Gamma^1_{03}) \sinh^2 \xi \right. \\
&\quad \left. + 2 e_0{}^t (e_3{}^\phi \Gamma^1_{03} + e_3{}^t \Gamma^1_{00}) \sinh \xi \cosh \xi \right] \cosh \xi \\
&\quad - e_0{}^t e_1{}^r (e^0{}_t \Gamma^0_{01} + e^0{}_\phi \Gamma^3_{01}) \cosh \xi \\
&\quad - e_1{}^r \left[e_3{}^\phi (e^0{}_t \Gamma^0_{13} + e^0{}_\phi \Gamma^3_{13}) + e_3{}^t (e^0{}_t \Gamma^0_{01} + e^0{}_\phi \Gamma^3_{01}) \right] \sinh \xi, \\
\lambda^1{}_3 &= -e^1{}_r \left[(e_0{}^t)^2 \Gamma^1_{00} \cosh^2 \xi + ((e_3{}^t)^2 \Gamma^1_{00} + (e_3{}^\phi)^2 \Gamma^1_{33} + 2 e_3{}^t e_3{}^\phi \Gamma^1_{03}) \sinh^2 \xi \right. \\
&\quad \left. + 2 e_0{}^t (e_3{}^\phi \Gamma^1_{03} + e_3{}^t \Gamma^1_{00}) \sinh \xi \cosh \xi \right] \sinh \xi \\
&\quad - e_0{}^t e^1{}_r (e_3{}^t \Gamma^1_{00} + e_3{}^\phi \Gamma^1_{03}) \cosh \xi \\
&\quad - e^1{}_r \left[e_3{}^t (e_3{}^t \Gamma^1_{00} + e_3{}^\phi \Gamma^1_{03}) + e_3{}^\phi (e_3{}^t \Gamma^1_{03} + e_3{}^\phi \Gamma^1_{33}) \right] \sinh \xi.
\end{aligned}
\tag{3.55}
$$

The change of the spin is obtained by computing Eq. (3.31). In particular, the rotation about the 2-axis through a certain angle reads:

$$
\begin{aligned}
\vartheta^1{}_3 &= -e^1{}_r \left[(e_0{}^t)^2 \Gamma^1_{00} \cosh^2 \xi + ((e_3{}^t)^2 \Gamma^1_{00} + (e_3{}^\phi)^2 \Gamma^1_{33} + 2 e_3{}^t e_3{}^\phi \Gamma^1_{03}) \sinh^2 \xi \right. \\
&\quad \left. + 2 e_0{}^t (e_3{}^\phi \Gamma^1_{03} + e_3{}^t \Gamma^1_{00}) \sinh \xi \cosh \xi \right] \sinh \xi \\
&\quad - e_0{}^t e^1{}_r (e_3{}^t \Gamma^1_{00} + e_3{}^\phi \Gamma^1_{03}) \cosh \xi \\
&\quad - e^1{}_r \left[e_3{}^t (e_3{}^t \Gamma^1_{00} + e_3{}^\phi \Gamma^1_{03}) + e_3{}^\phi (e_3{}^t \Gamma^1_{03} + e_3{}^\phi \Gamma^1_{33}) \right] \sinh \xi \\
&\quad + \left(\frac{\sinh \xi}{\cosh \xi + 1} \right) \left\{ e^1{}_r \left[(e_0{}^t)^2 \Gamma^1_{00} \cosh^2 \xi + ((e_3{}^t)^2 \Gamma^1_{00} + (e_3{}^\phi)^2 \Gamma^1_{33} + 2 e_3{}^t e_3{}^\phi \Gamma^1_{03}) \sinh^2 \xi \right. \right. \\
&\quad \left. + 2 e_0{}^t (e_3{}^\phi \Gamma^1_{03} + e_3{}^t \Gamma^1_{00}) \sinh \xi \cosh \xi \right] \cosh \xi \\
&\quad - e_0{}^t e_1{}^r (e^0{}_t \Gamma^0_{01} + e^0{}_\phi \Gamma^3_{01}) \cosh \xi \\
&\quad \left. - e_1{}^r \left[e_3{}^\phi (e^0{}_t \Gamma^0_{13} + e^0{}_\phi \Gamma^3_{13}) + e_3{}^t (e^0{}_t \Gamma^0_{01} + e^0{}_\phi \Gamma^3_{01}) \right] \sinh \xi \right\}.
\end{aligned}
\tag{3.56}
$$

Finally, from the vierbein given in Eq. (4.6), it can be shown, after some algebra, that the previous expression (3.56), can be expressed only in terms of the metric components

$$
\begin{aligned}
\vartheta^1{}_3 &= -\frac{\cosh(2\xi)}{2 g_{00} \sqrt{g_{11} [(g_{03})^2 - g_{00} g_{33}]}} \left(g_{03} \frac{\partial g_{00}}{\partial r} - g_{00} \frac{\partial g_{03}}{\partial r} \right) \\
&\quad - \frac{\sinh(2\xi)}{4 g_{00} [(g_{03})^2 - g_{00} g_{33}] \sqrt{g_{11}}} \left[g_{00} \left(g_{33} \frac{\partial g_{00}}{\partial r} - g_{00} \frac{\partial g_{33}}{\partial r} \right) + 2 g_{03} \left(g_{03} \frac{\partial g_{00}}{\partial r} - g_{00} \frac{\partial g_{03}}{\partial r} \right) \right].
\end{aligned}
\tag{3.57}
$$

Thus the complete rotation matrix due the infinitesimal Lorentz transformations is given by

$$
\vartheta^a{}_b(x) = \begin{pmatrix} 0 & 0 & 0 & 0 \\ 0 & 0 & 0 & \vartheta^1{}_3 \\ 0 & 0 & 0 & 0 \\ 0 & -\vartheta^1{}_3 & 0 & 0 \end{pmatrix}.
\tag{3.58}
$$

3.2 EPR correlation and Bell inequalities

3.2.1 EPR correlation

As previously mentioned in Section 3.1, in the case of the curved spacetime, the one-particle quantum states $|p^a(x), \sigma; x\rangle$ transforms under a local Lorentz transformation as [29, 30]

$$U(\Lambda(x))|p^a(x), \sigma; x\rangle = \sum_{\sigma'} D^{(1/2)}_{\sigma'\sigma}(W(x))|\Lambda p^a(x), \sigma'; x\rangle, \tag{3.59}$$

where σ represents the spin state and $W^a{}_b(x) \equiv W^a{}_b(\Lambda(x), p(x))$ is the so called local finite Wigner rotation.

If a particle moves along a path $x^\mu(\tau)$ from $x^\mu_i(\tau_i)$ to $x^\mu_f(\tau_f)$, we can iterate Eq. (3.37) for infinitesimal transformations, where the time-ordering operator $T = 1$, the term $\vartheta^a{}_b(x(\tau))$ is defined by Eq. (3.58) and $u^\phi d\tau = \Phi$. After a proper time $\Phi/u^\phi_\pm$, each particle reaches the corresponding observer. Thus, the Wigner rotation becomes a rotation about the 2-axis

$$W^a{}_b(\pm\Phi, 0) = \exp\left(\int_0^\Phi \frac{\vartheta^a{}_b(x)}{\varphi^1{}_3(x)} d\phi\right) = \exp\left(\frac{\Phi}{u^\phi}\vartheta^a{}_b\right). \tag{3.60}$$

Then, for matrix expansion series

$$
\begin{aligned}
\exp(\frac{\Phi}{u^\phi}\vartheta^a{}_b) &= \mathbb{I} + \frac{\Phi\vartheta^a{}_b}{u^\phi} + \frac{1}{2!}\left(\frac{\Phi\vartheta^a{}_b}{u^\phi}\right)^2 + \frac{1}{3!}\left(\frac{\Phi\vartheta^a{}_b}{u^\phi}\right)^3 + \frac{1}{4!}\left(\frac{\Phi\vartheta^a{}_b}{u^\phi}\right)^4 + \cdots \\[2mm]
&= \begin{pmatrix} 1 & 0 & 0 & 0 \\ 0 & 1 & 0 & 0 \\ 0 & 0 & 1 & 0 \\ 0 & 0 & 0 & 1 \end{pmatrix} + \begin{pmatrix} 0 & 0 & 0 & 0 \\ 0 & 0 & 0 & \frac{\Phi\vartheta^1{}_3}{u^\phi} \\ 0 & 0 & 0 & 0 \\ 0 & -\frac{\Phi\vartheta^1{}_3}{u^\phi} & 0 & 0 \end{pmatrix} + \frac{1}{2!}\begin{pmatrix} 0 & 0 & 0 & 0 \\ 0 & 0 & 0 & \frac{\Phi\vartheta^1{}_3}{u^\phi} \\ 0 & 0 & 0 & 0 \\ 0 & -\frac{\Phi\vartheta^1{}_3}{u^\phi} & 0 & 0 \end{pmatrix}^2 \\[2mm]
&+ \frac{1}{3!}\begin{pmatrix} 0 & 0 & 0 & 0 \\ 0 & 0 & 0 & \frac{\Phi\vartheta^1{}_3}{u^\phi} \\ 0 & 0 & 0 & 0 \\ 0 & -\frac{\Phi\vartheta^1{}_3}{u^\phi} & 0 & 0 \end{pmatrix}^3 + \frac{1}{4!}\begin{pmatrix} 0 & 0 & 0 & 0 \\ 0 & 0 & 0 & \frac{\Phi\vartheta^1{}_3}{u^\phi} \\ 0 & 0 & 0 & 0 \\ 0 & -\frac{\Phi\vartheta^1{}_3}{u^\phi} & 0 & 0 \end{pmatrix}^4 + \cdots
\end{aligned}
\tag{3.61}
$$

Then, summing up term by term of each element of matrix we get

$$\exp\left(\tfrac{\Phi}{u^\phi}\vartheta^a{}_b\right) =$$

$$\begin{pmatrix} 1 & 0 & 0 & 0 \\ 0 & 1 - \tfrac{1}{2!}\left(\tfrac{\Phi\vartheta^1{}_3}{u^\phi}\right)^2 + \tfrac{1}{4!}\left(\tfrac{\Phi\vartheta^1{}_3}{u^\phi}\right)^4 + \cdots & 0 & \left(\tfrac{\Phi\vartheta^1{}_3}{u^\phi}\right) - \tfrac{1}{3!}\left(\tfrac{\Phi\vartheta^1{}_3}{u^\phi}\right)^3 + \tfrac{1}{5!}\left(\tfrac{\Phi\vartheta^1{}_3}{u^\phi}\right)^5 + \cdots \\ 0 & 0 & 1 & 0 \\ 0 & -\left(\tfrac{\Phi\vartheta^1{}_3}{u^\phi}\right) + \tfrac{1}{3!}\left(\tfrac{\Phi\vartheta^1{}_3}{u^\phi}\right)^3 - \tfrac{1}{5!}\left(\tfrac{\Phi\vartheta^1{}_3}{u^\phi}\right)^5 + \cdots & 0 & 1 - \tfrac{1}{2!}\left(\tfrac{\Phi\vartheta^1{}_3}{u^\phi}\right)^2 + \tfrac{1}{4!}\left(\tfrac{\Phi\vartheta^1{}_3}{u^\phi}\right)^4 + \cdots \end{pmatrix}.$$

$$(3.62)$$

Therefore we can identify to power series for sine and cosine, that is,

$$W^a{}_b(\pm\Phi, 0) = \begin{pmatrix} 1 & 0 & 0 & 0 \\ 0 & \cos\Theta & 0 & \pm\sin\Theta \\ 0 & 0 & 1 & 0 \\ 0 & \mp\sin\Theta & 0 & \cos\Theta \end{pmatrix}, \qquad (3.63)$$

where the angle of rotation is given by $\Theta = \Phi\vartheta^1{}_3/u^\phi$ and $\vartheta^1{}_3$ of Eq. (3.57), that is

$$\begin{aligned} \Theta &= \frac{\Phi}{2\sqrt{-(g_{00})^3 g_{11}}} \left\{ \left(g_{03}\frac{\partial g_{00}}{\partial r} - g_{00}\frac{\partial g_{03}}{\partial r} \right) \frac{\cosh(2\xi)}{\sinh(\xi)} \right. \\ &\left. + \left[g_{00}\left(g_{00}\frac{\partial g_{33}}{\partial r} - g_{33}\frac{\partial g_{00}}{\partial r} \right) + 2g_{03}\left(g_{03}\frac{\partial g_{00}}{\partial r} - g_{00}\frac{\partial g_{03}}{\partial r} \right) \right] \frac{\cosh(\xi)}{\sqrt{(g_{03})^2 - g_{00}g_{33}}} \right\}. \end{aligned}$$

$$(3.64)$$

The total argument Φ is obtained by integrating out $\delta\phi = u^\phi d\tau$, and in this case, the operator T is not needed because $\vartheta^a{}_b$ is time-independent during the motion. Therefore, the velocity u^ϕ represents a trivial rotation about the 2-axis, i.e. $u^\phi = \varphi^1{}_3 = -\varphi^3{}_1$, since the curved spacetime defines the parallel transport needed to compare local inertial frames in two different points.

In Sec. 3.1.5 we saw that $\tanh\xi = \tanh(\zeta \pm \eta)$, where the $\pm$ sign depends on the direction of motion of each particle. Therefore we can define the four-momentum of the particle as seen by each hovering observer. Thus, the spin-singlet state for entangled particles is given by

$$|\psi\rangle = \frac{1}{\sqrt{2}}[|p^a_+, \uparrow; 0\rangle|p^a_-, \downarrow; 0\rangle - |p^a_+, \downarrow; 0\rangle|p^a_-, \uparrow; 0\rangle], \qquad (3.65)$$

where the sign on the lineal momentum stand for the direction of each particle and the arrows corresponds to the up and down of spin direction, as was mentioned in Sec. 1.2. For notational simplicity it was written only the evaluation at $\phi = 0$ in the arguments of the position.

Thus the Wigner rotation from Eq. (3.37) can be written as

$$
W^a{}_b(\pm\Phi, 0) =
\begin{pmatrix}
1 & 0 & 0 & 0 \\
0 & \cos\Theta_\pm & 0 & \pm\sin\Theta_\pm \\
0 & 0 & 1 & 0 \\
0 & \mp\sin\Theta_\pm & 0 & \cos\Theta_\pm
\end{pmatrix}.
\tag{3.66}
$$

Once again, the sign of the angle $\Theta_\pm$ depends if the motion of the entangled particle is in direction (or in its opposite sense) of the frame-dragging. Thus one has

$$
\begin{aligned}
\Theta_+ &= \frac{\Phi}{2\sqrt{-(g_{00})^3 g_{11}}} \left\{ \left(g_{03}\frac{\partial g_{00}}{\partial r} - g_{00}\frac{\partial g_{03}}{\partial r} \right) \frac{\cosh(2\zeta + 2\eta)}{\sinh(\zeta + \eta)} \right. \\
&\quad \left. + \left[g_{00}\left(g_{00}\frac{\partial g_{33}}{\partial r} - g_{33}\frac{\partial g_{00}}{\partial r} \right) + 2g_{03}\left(g_{03}\frac{\partial g_{00}}{\partial r} - g_{00}\frac{\partial g_{03}}{\partial r} \right) \right] \frac{\cosh(\zeta + \eta)}{\sqrt{(g_{03})^2 - g_{00}g_{33}}} \right\}, \\
\Theta_- &= \frac{\Phi}{2\sqrt{-(g_{00})^3 g_{11}}} \left\{ \left(g_{03}\frac{\partial g_{00}}{\partial r} - g_{00}\frac{\partial g_{03}}{\partial r} \right) \frac{\cosh(2\zeta - 2\eta)}{\sinh(\zeta - \eta)} \right. \\
&\quad \left. + \left[g_{00}\left(g_{00}\frac{\partial g_{33}}{\partial r} - g_{33}\frac{\partial g_{00}}{\partial r} \right) + 2g_{03}\left(g_{03}\frac{\partial g_{00}}{\partial r} - g_{00}\frac{\partial g_{03}}{\partial r} \right) \right] \frac{\cosh(\zeta - \eta)}{\sqrt{(g_{03})^2 - g_{00}g_{33}}} \right\}.
\end{aligned}
\tag{3.67}
$$

The required Wigner rotation is given in the following form

$$
D^{(1/2)}_{\sigma'\sigma}(W(\pm\Phi, 0)) = \exp\left(\mp i\frac{\sigma_y}{2}\Theta_\pm \right),
\tag{3.68}
$$

where σ_y is the Pauli matrix.

Therefore, each particle state is transformed through the corresponding Wigner rotation, and the new total quantum state is given by $|\psi'\rangle = W(\pm\Phi)|\psi\rangle$. Consequently in the local inertial frame at the corresponding positions $\phi = \Phi$ and $-\Phi$, each particle state can be written as

$$
\begin{aligned}
|p^a_\pm, \uparrow; \pm\Phi\rangle' &= \cos\frac{\Theta_\pm}{2}|p^a_\pm, \uparrow; \pm\Phi\rangle \pm \sin\frac{\Theta_\pm}{2}|p^a_\pm, \downarrow; \pm\Phi\rangle,
\end{aligned}
\tag{3.69}
$$

$$
\begin{aligned}
|p^a_\pm, \downarrow; \pm\Phi\rangle' &= \mp\sin\frac{\Theta_\pm}{2}|p^a_\pm, \uparrow; \pm\Phi\rangle + \cos\frac{\Theta_\pm}{2}|p^a_\pm, \downarrow; \pm\Phi\rangle.
\end{aligned}
\tag{3.70}
$$

Thus the entangled state is described by the combination

$$
\begin{aligned}
|\psi\rangle' = \frac{1}{\sqrt{2}} \left[\cos\left(\frac{\Theta_+ + \Theta_-}{2} \right) (|p^a_+, \uparrow; \Phi\rangle|p^a_-, \downarrow; -\Phi\rangle - |p^a_+, \downarrow; \Phi\rangle|p^a_-, \uparrow; -\Phi\rangle) \right. \\
\left. + \sin\left(\frac{\Theta_+ + \Theta_-}{2} \right) (|p^a_+, \uparrow; \Phi\rangle|p^a_-, \uparrow; \Phi-\rangle + |p^a_+, \downarrow; \Phi\rangle|p^a_-, \downarrow; -\Phi\rangle) \right].
\end{aligned}
\tag{3.71}
$$

Now, in order to eliminate the spurious effect of the evident rotation of the local inertial frames leading to angles $\pm\Phi$, one has to compensate the rotation. That can be achieved as one perform a second transformation

$$
|p_\pm^a, \uparrow; \pm\Phi\rangle'' \;=\; \cos\frac{\Phi}{2}|p_\pm^a, \uparrow; \pm\Phi\rangle \pm \sin\frac{\Phi}{2}|p_\pm^a, \downarrow; \pm\Phi\rangle, \tag{3.72}
$$

$$
|p_\pm^a, \downarrow; \pm\Phi\rangle'' \;=\; \mp\sin\frac{\Phi}{2}|p_\pm^a, \uparrow; \pm\Phi\rangle + \cos\frac{\Phi}{2}|p_\pm^a, \downarrow; \pm\Phi\rangle. \tag{3.73}
$$

It easy to see that this quantum state reads

$$
\begin{aligned}
|\psi\rangle'' = \frac{1}{\sqrt{2}}[&\cos\Delta(|p_+^a, \uparrow; \Phi\rangle'|p_-^a, \downarrow; -\Phi\rangle' - |p_+^a, \downarrow; \Phi\rangle'|p_-^a, \uparrow; -\Phi\rangle')\\
+ &\sin\Delta(|p_+^a, \uparrow; \Phi\rangle'|p_-^a, \uparrow; \Phi-\rangle' + |p_+^a, \downarrow; \Phi\rangle'|p_-^a, \downarrow; -\Phi\rangle')].
\end{aligned} \tag{3.74}
$$

Where $\Delta = (\Theta_+ + \Theta_-)/2 - \Phi$, that can be simplified as by [81],

$$
\Delta = \Phi\left[(2A\sinh\zeta + B\cosh\zeta)\cosh\eta - A\frac{\sinh\zeta\cosh\eta}{\cosh^2\eta - \cosh^2\zeta} - 1\right], \tag{3.75}
$$

where

$$
\begin{aligned}
A =\;& \frac{1}{2\sqrt{-(g_{00})^3 g_{11}}}\left(g_{03}\frac{\partial g_{00}}{\partial r} - g_{00}\frac{\partial g_{03}}{\partial r}\right),\\
B =\;& \frac{1}{2\sqrt{-(g_{00})^3 g_{11}[(g_{03})^2 - g_{00}g_{33}]}}\left[g_{00}\left(g_{00}\frac{\partial g_{33}}{\partial r} - g_{33}\frac{\partial g_{00}}{\partial r}\right) + 2g_{03}\left(g_{03}\frac{\partial g_{00}}{\partial r} - g_{00}\frac{\partial g_{03}}{\partial r}\right)\right].
\end{aligned} \tag{3.76}
$$

The spin precession angle Δ contains the gravitational, acceleration and frame-dragging effects that deteriorate the perfect anti-correlation of the entangled particles [31]. It can be observed in the Eq. (3.74) that the spin-singlet state is mixed up with the spin-triplet state, which it is easy to proof when $\Delta \to 0$, that is, in the plane spacetime and low speed. This is because while the spin-singlet state is invariant under spatial rotations, it is not invariant under Lorentz transformations (3.55). It is evident that this formula can be applied to any axially symmetric black hole, and in the next chapter it will be applied to the type-D solution of Einstein equations.

As it was pointed out in [31], this deterioration is a consequence of the manifest difference between the rotation matrix element $\vartheta^1{}_3$ and trivial rotation $\varphi^1{}_3$. It is important to note that the entanglement is still invariant under local unitary operations, and then it does not mean to put away the nonlocal correlation. Because the relativistic effect arises from acceleration, gravity and frame-dragging, the perfect anticorrelation can still be employed

for quantum communication, by rotating the direction of measurement about the 2-axis through the angles $\mp\Theta$ in the local inertial frames of the hovering observers. The parallel transport in general relativity (3.51) does not give the directions that maintain the perfect anticorrelation, because the rotation matrix elements (3.58) and the components of the change in local inertial frame (3.51) are not equal.

3.2.2 Bell's inequalities

In previous sections it was observed the importance of the hovering observers as systems of reference for the measurement of the infinitesimal Lorentz transformation and subsequently the Wigner rotation, in order to obtain the spin precession angle.

Moreover, it is from the perspective of these observers that the velocity of the entangled particles are measured in first instance. Thus, the hovering observers can in principle adjust their local frame in order to measure the perfect anti-correlation in the entangled spin of the particles. All they have to do is to calculate the spin precession (3.75) for the particular position r where they are placed. Therefore they can rotate their instruments of measurement against the angle Δ calculated, thereby compensating the dynamical and gravitational spacetime effects. Hence they can reestablish the quantum communication for instance.

Nevertheless as we will see, near the horizon of the black hole, and the static limit and the asymptotic region defined by the frame-dragging coupling, this precession angle Δ would oscillate too fast, making impossible any compensation, plus the fact that any small variation of the position Φ will be reflected as a huge uncertainty in the Δ calculus, that is

$$\delta\Theta = \delta\Phi \left| 1 + \frac{\Delta}{\Phi} \right|. \tag{3.77}$$

And then, in order to adjust the EPR correlation $\delta\Theta$ by the observers, it must be less than π [31], therefore there must satisfy

$$\delta\Phi < \pi \left| 1 + \frac{\Delta}{\Phi} \right|^{-1}. \tag{3.78}$$

By this means, a decrement in Bell's inequity degree of violation follows by the dynamic and gravitational effects of the spacetime determinated by

$$\langle \mathcal{Q}'\mathcal{S}' \rangle + \langle \mathcal{R}'\mathcal{S}' \rangle + \langle \mathcal{R}'\mathcal{T}' \rangle - \langle \mathcal{Q}'\mathcal{T}' \rangle = 2\sqrt{2}\cos^2\Delta, \tag{3.79}$$

where the trivial rotations of the local inertial frames $\pm\Phi$ has been discarded, and the spin

components of one particle are measured in the directions

$$
\begin{aligned}
\mathcal{Q}' &= (\cos\Phi,\ 0,\ -\sin\Phi), \\
\mathcal{R}' &= (0,1,0), \\
\mathcal{S}' &= \left(\frac{-\cos\Phi}{\sqrt{2}},\ \frac{-1}{\sqrt{2}},\ \frac{-\sin\Phi}{\sqrt{2}}\right), \\
\mathcal{T}' &= \left(\frac{\cos\Phi}{\sqrt{2}},\ \frac{-1}{\sqrt{2}},\ \frac{-\sin\Phi}{\sqrt{2}}\right).
\end{aligned}
\tag{3.80}
$$

Then, the hovering observers must take into account all the effects reviewed in previous sections, i.e. gravity, acceleration and frame-dragging. As Terashima-Ueda shown [31], the component of one particle at $\phi = \Phi$ must be measured in the $(\cos\Theta,\ 0,\ -\sin\Theta)$ direction, or also in the $(0,\ 1,\ 0)$ direction, in the local inertial frame.

The spin for the other particle at $\phi = -\Phi$. must be measured in the $(-\cos\Theta,\ -1,\ -\sin\Theta)/\sqrt{2}$ direction, or also in the $(\cos\Theta,\ -1,\ \sin\Theta)/\sqrt{2}$ direction.

It is important to emphasize once again that if the observers are located near the horizon or the asymptotic static limits, it should be almost impossible to keep their positions at Φ, and a small uncertainty on $\delta\Phi$ will reflect in an uncertainty on $\delta\Theta$ in equation (3.77). This error in Θ decreases the degree of violation in Bell's inequality as $2\sqrt{2}\cos^2\delta\Theta$, and this error must be greater than 2 in order to restore the maximum violation of the inequality. Therefore, the quantities from Eq. (3.77), $\delta\Phi$ and r, must be adjusted at least

$$
\delta\Phi < \sqrt{2}\left|1 + \frac{\Delta}{\Phi}\right|^{-1}.
\tag{3.81}
$$

If these quantities cannot be adjusted, the uncertainty in position Φ must be high and it should not be possible to compensate the direction of the measure instruments of the observers to extract the maximum violation of Bell's inequality. Contrary to equation (3.78) that only accounts the precession of the spin, the equation (3.81) takes care of the position of the observers to get reliable measurements for any suitable use of the perfect EPR anticorrelation.

In Section 4.5 we will see the effects of spacetime curvature over the perfect anticorrelation and the precession angle.

Chapter 4

Results

4.1 Plebański-Demiański spacetime

The complete family of expanding solutions of the original Plebański-Demiański spacetime [34] is characterized by seven parameters which are not all directly related to the physical parameters of a black hole. A new look of this metric Refs. [39, 40], allowed to give a Boyer-Lindquist form of the Plebański-Demiański metric in terms of the the physical parameters, namely: a mass-like parameter m, a cosmological constant Λ, a rotation-like parameter a, a NUT-like parameter l, the electric and magnetic charges e and g, and an acceleration-like parameter α (or the twist parameter ω).

4.1.1 Metric and Tetrad

Thus the line element can be represented in real coordinates describing the spacetime with non-vanishing cosmological constant of a rotating and accelerating mass with the three types of charge, electric, magnetic and gravitomagnetic. The metric is given by

$$
\begin{aligned}
ds^2 = \quad & \frac{1}{\Omega^2}\left(-\frac{D}{\rho^2}(dt-(a\sin^2\theta+2l(1-\cos\theta))d\phi)^2+\frac{\rho^2}{D}dr^2\right.\\
& \left.+\frac{P}{\rho^2}(adt-(r^2+(a+l)^2)d\phi)^2+\rho^2\frac{\sin^2\theta}{P}d\theta^2\right),
\end{aligned}
\tag{4.1}
$$

with

$$
\begin{aligned}
\rho^2 &= r^2 + (l + a\cos\theta)^2, \\
\Omega &= 1 - \frac{\alpha}{\omega}(l + a\cos\theta)r, \\
P &= \sin^2\theta(1 - a_3\cos\theta - a_4\cos^2\theta), \\
D &= (\kappa + e^2 + g^2) - 2mr + \epsilon r^2 - 2n\frac{\alpha}{\omega}r^3 - \left(\frac{\alpha^2}{\omega^2}\kappa + \frac{\Lambda}{3}\right)r^4,
\end{aligned}
\tag{4.2}
$$

and where

$$
\begin{aligned}
a_3 &= 2a\frac{\alpha}{\omega}m - 4al\frac{\alpha^2}{\omega^2}(\kappa + e^2 + g^2) - 4\frac{\Lambda}{3}al, \\
a_4 &= -a^2\frac{\alpha^2}{\omega^2}(\kappa + e^2 + g^2) - \frac{\Lambda}{3}a^2, \\
\epsilon &= \frac{\kappa}{a^2 - l^2} + 4l\frac{\alpha}{\omega}m - (a^2 + 3l^2)\left(\frac{\alpha^2}{\omega^2}(\kappa + e^2 + g^2) + \frac{\Lambda}{3}\right), \\
n &= \frac{\kappa l}{a^2 - l^2} - (a^2 - l^2)\frac{\alpha}{\omega}m + (a^2 - l^2)l\left(\frac{\alpha^2}{\omega^2}(\kappa + e^2 + g^2) + \frac{\Lambda}{3}\right), \\
\kappa &= \frac{1 + 2l\frac{\alpha}{\omega}m - 3l^2\frac{\alpha^2}{\omega^2}(e^2 + g^2) - l^2\Lambda}{\frac{1}{a^2 - l^2} + 3l^2\frac{\alpha^2}{\omega^2}}.
\end{aligned}
\tag{4.3}
$$

In addition, for the rest of this work, we will consider the physics parameters and space-time metric expressed in normalized geometric units, that is, by defining the gravitational constant as $G = 1$ and the speed of light as $c = 1$.

For simplicity and for continuation of Chapter 3, it is suitable to work with equation (4.1) as the line element Eq. (3.15), that is:

$$
ds^2 = g_{00}dt^2 + 2g_{03}dtd\phi + g_{11}dr^2 + g_{22}d\theta^2 + g_{33}d\phi^2,
\tag{4.4}
$$

with a non-diagonal element induced by the axial symmetry of the metric are:

$$
\begin{aligned}
g_{00} &= \frac{-D + Pa^2}{\Omega^2\rho^2}, \\
g_{0i}dx^i &= \frac{1}{\Omega^2}\left[\frac{D}{\rho^2}(a\sin^2\theta + 2l(1 - \cos\theta)) - \frac{P}{\rho^2}a(r^2 + (a + l)^2)\right]d\phi, \\
g_{ij}dx^idx^j &= \frac{\rho^2}{\Omega^2 D}dr^2 + \rho^2\frac{\sin^2\theta}{\Omega^2 P}d\theta^2 + \frac{1}{\Omega^2}\left[-\frac{D}{\rho^2}(a\sin^2\theta + 2l(1 - \cos\theta))^2\right. \\
&\quad \left.+ \frac{P}{\rho^2}(r^2 + (a + l)^2)^2\right]d\phi^2.
\end{aligned}
\tag{4.5}
$$

We shall use it for this and the next section, and in this work the signature $(-1, 1, 1, 1)$ is adopted, i.e. $\eta_{ab} = (-1, 1, 1, 1)$ is the Minkowski metric .

In order to describe the motion of spinning particles in a curved spacetime, the local

inertial frame at each point is defined by a vierbein chosen as [52]:

$$
\begin{aligned}
e_0{}^\mu(x) &= \frac{1}{\sqrt{-g_{00}}}(1,0,0,0), & e^0{}_\mu &= \sqrt{-g_{00}}\left(1,0,0,\frac{g_{03}}{g_{00}}\right), \\
e_1{}^\mu(x) &= \frac{1}{\sqrt{g_{11}}}(0,1,0,0), & e^1{}_\mu &= \sqrt{g_{11}}(0,1,0,0), \\
e_2{}^\mu(x) &= \frac{1}{\sqrt{g_{22}}}(0,0,1,0), & e^2{}_\mu &= \sqrt{g_{22}}(0,0,1,0), \\
e_3{}^\mu(x) &= \sqrt{\frac{-g_{00}}{g_{03}^2 - g_{00}g_{33}}}\left(-\frac{g_{03}}{g_{00}},0,0,1\right), & e^3{}_\mu &= \sqrt{\frac{g_{03}^2 - g_{00}g_{33}}{-g_{00}}}(0,0,0,1.),
\end{aligned}
\tag{4.6}
$$

where μ runs over the spacetime coordinates $\{t, r, \theta, \phi\}$. It is easy to show that this vierbein satisfy the standard conditions of equations (3.17).

4.1.2   Spin precession

In the present section we study the spin precession angle of the spin-$1/2$ systems of entangled particles in the spacetime black hole described by the Plebański-Demiański metric (4.1) with frame-dragging (3.47).

From the last chapter, it is easy to show that the coefficients functions A and B of equation (3.76) on equator $(\theta = \pi/2)$ are

$$
\begin{aligned}
A_{\text{PD}} &= \frac{a\sqrt{D}}{2(r^2+l^2)(D-a^2)^{3/2}}[(r^2+l^2)D' - 2r(D-a^2)], \\
B_{\text{PD}} &= \frac{1}{2(r^2+l^2)(D-a^2)^{3/2}}[4Dr(D-a^2) - (a^2r^2 + Dr^2 + Dl^2 + a^2l^2)D'],
\end{aligned}
\tag{4.7}
$$

where

$$
D' = \frac{\partial D}{\partial r} = -4\left(\frac{\alpha^2\kappa}{\omega^2} + \frac{\Lambda}{3}\right)r^3 - \frac{6n\alpha r^2}{\omega} + 2\epsilon r - 2m. \tag{4.8}
$$

Moreover, the frame-dragging local inertial frame velocity is given by

$$
\cosh\eta_{\text{PD}} = (r^2+l^2)\sqrt{\frac{D}{(D-a^2)\left[(r^2+a^2+2al+l^2)^2 - (a+2l)^2D\right]}}, \tag{4.9}
$$

Thus, the coefficients A_{PD}, B_{PD}, the spin precession angle Δ_{PD} and the frame-dragging $\cosh\eta_{\text{PD}}$ are finally written in terms of the 7 parameters arising in the metric and which have a direct physical interpretation. It is well known from Refs. [39, 40] that the metric (4.1) represents a pair of accelerating black holes with the rotation, NUT parameter,cosmological constant parameters, charge and mass. It is also known that in this situation there are

two very different spacetime solutions. The first case is the one with $|l| \geq |a|$, which has non-singular curvature, this gives rise to an *accelerating NUT solution with rotation*. This also corresponds to the right branch of the diagram 1 of Ref. [39, 40]. In the second case with $|l| \leq |a|$ we have an *accelerating and rotating black hole* including also the rest of the parameters. The type of solutions arising here corresponds to the left branch and they are of singular nature. It can be shown that the coefficients A_{PD}, B_{PD} and Δ_{PD} have the correct asymptotic limits.

We will analyze the spin precession angle associated of these two branches of these Type D solutions of the Einstein equations. We start from the right branch and follows with the left one. The more evident contribution to the spin precession angle will come from the exterior event, the cosmological and the acceleration horizons (obtained from the condition that the quartic polynomial in D of the parameters (4.2) has at least two real roots which define the inner and outer horizons. The other vanishing terms define the cosmological and acceleration horizons). We will see that the main contribution to Δ_{PD} comes from precisely these horizons. Beside of the horizon contribution, we will have an additional possibly non-trivial contribution coming from the frame-dragging at $\cosh \eta_{\mathrm{PD}} = \cosh \zeta$ in Eq. (3.75). In order to give a more detailed account of the entanglement behavior on these horizons we shall study below the different limiting cases.

4.2   Previous results: Schwarzschild spacetime

As Terashima and Ueda showed [31] for a Schwarzschild black hole, the acceleration and gravity deteriorate the EPR correlation for particles in a circular motion on the equatorial plane. We summarize their results by describing in four important regions relative the black hole plotted in Fig. 4.1.

Region I: $r \to \infty$, $v \to 0$, or far away the black hole (no gravitational effects) and static particles. This region corresponds to the non-relativistic limit, where there are no corrections to quantum mechanics and where EPR proposed their *gedanken* experiment [1]. The precession angle vanishes ($\Delta = 0$) and we get the maximal violation of Bell's inequality.

Region II: $r \to \infty$, $v \to 1$, it is still far away from the black hole but relativistic corrections should be taken into account, which were also studied by Terashima and Ueda in Ref. [76]. The angle Δ is positive and becomes infinite. It is no possible to maintain perfect anti-correlation and the particles cannot be used for quantum communication.

Region III: $r \to r_{\rm s}$, where $r_{\rm s} = 2m$ is the Schwarzschild radius (event horizon). Indepen-
dently of local inertial velocity of the particles, the precession angle becomes
infinite ($\Delta \to -\infty$). The static observers cannot extract the EPR correlation
from circularly moving particles unless they have infinite accuracy in their
own positions. To exploit the EPR correlation on and beyond the horizon,
the observers must choose a four-velocity and a non-singular vierbein at the
horizon, and thus the observers must fall into the black hole together with the
particles.

Region IV: Although acceleration and gravity deteriorate the EPR correlation as
Terashima and Ueda showed, it is still possible to find a combination of local
inertial velocity and position with respect to the black hole keeps the perfect
anti-correlation. They defined a path where at radius $r = r_0$ the angle Δ
vanishes. We will identify this path as an additional region and it is between
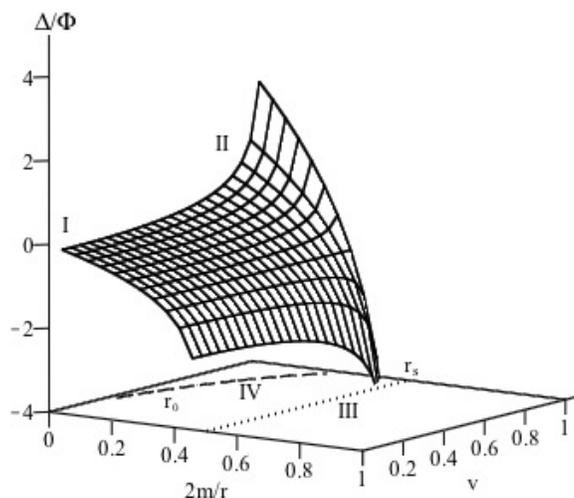the other three regions.

Figure 4.1: The angle Δ/Φ for a Schwarzschild black hole as function of $2m/r$ and
v, which is asymptotic to the event horizon $r_{\rm s} = 2m$, indicated by a dotted line.
Dashed line depicted the path $r = r_0$ which the spin precession Δ vanishes.

Between these regions one can find values of the angle (positive or negative) Δ, which
deteriorates the perfect anti-correlation in the directions that would be the same as each
other if the spacetime were flat.

4.3 Examples: Non-accelerating Kerr-Newman-(Anti)de Sitter-NUT Black Hole

The Kerr-Newman-de Sitter-NUT (KNdSNUT) spacetime is included in this large family of type D solutions. The KNdSNUT spacetime represents a non-accelerating black hole with mass m, electric and magnetic charges e and g, a rotation parameter a and a NUT parameter l in a de Sitter or anti-de Sitter background which non-zero cosmological constant Λ.

After setting the acceleration parameter equals to zero ($\alpha = 0$), the parameters in equation (4.2) become

$$
\begin{aligned}
a_3 &= -4\tfrac{\Lambda}{3}al, \\
a_4 &= -\tfrac{\Lambda}{3}a^2, \\
\kappa &= (1 - l^2\Lambda)(a^2 - l^2), \\
\epsilon &= 1 - \left(\tfrac{1}{3}a^2 + 2l^2\right)\Lambda, \\
n &= 1 + \tfrac{1}{3}(a^2 - kl^2)l\Lambda.
\end{aligned}
\tag{4.10}
$$

Thus, the metric (4.1) is reduced to

$$
ds^2 = -\frac{D}{\rho^2}[dt - (a\sin^2\theta + 4l\sin^2\tfrac{\theta}{2})d\phi]^2 + \frac{\rho^2}{D}dr^2 + \frac{P}{\rho^2}[adt - (r^2 + (a+l)^2 d\phi)]^2 + \frac{\rho^2}{P}\sin^2\theta d\theta^2,
\tag{4.11}
$$

where

$$
\begin{aligned}
\rho^2 &= r^2 + (l + a\cos\theta)^2, \\
P &= \sin^2\theta\left(1 + \frac{4}{3}\Lambda al\cos\theta + \frac{1}{3}\Lambda a^2\cos^2\theta\right), \\
D &= a^2 - l^2 + e^2 + g^2 - 2mr + r^2 - \Lambda\left[(a^2 - l^2)l^2 + (\tfrac{1}{3}a^2 + 2l^2)r^2 + \tfrac{1}{3}r^4\right].
\end{aligned}
\tag{4.12}
$$

We can notice that as $D \to 0$, the metric coefficient $g_{11} \to \infty$ and the metric fails to be strongly asymptotically predictable. This apparent singularity arise because the coordinate system are not valid at the radius r_+, which solve the equation $D = 0$. This singularity can be removed by a different choice of coordinates. In this work we consider particles only orbiting black holes and then we shall not remove the singularities considering r_+ as the event horizon of a black hole. Later, we will see that this horizon has relevance when spin precession angle is calculated.

For the Kerr-Newman-de Sitter-NUT spacetime, the spin precession angle $\Delta_{\mathrm{KNdSNUT}}$ of

equation (3.75) has coefficients

$$A_{\text{KNdSNUT}} = \frac{a\sqrt{D}}{2(r^2 + l^2)(D - a^2)^{3/2}} \left[(r^2 + l^2)D' - 2r(D - a^2) \right],$$

$$B_{\text{KNdSNUT}} = \frac{1}{2(r^2 + l^2)(D - a^2)^{3/2}} \left[4Dr(D - a^2) - (a^2 r^2 + Dr^2 + Dl^2 + a^2 l^2)D' \right],$$

(4.13)

where

$$D' = \frac{\partial D}{\partial r} = -\frac{4}{3}\Lambda r^3 + \left[2 - \Lambda \left(\frac{2}{3}a^2 + 4l^2 \right) \right] r - 2m,$$

(4.14)

and the relevant frame-dragging local inertial frame velocity Eqs. (3.46) and (3.47) can be expressed as

$$\cosh \eta_{\text{KNdSNUT}} = (r^2 + l^2)\sqrt{\frac{D}{(D - a^2)\left[(r^2 + a^2 + 2al + l^2)^2 - (a + 2l)^2 D \right]}}.$$

(4.15)

From this point it is easy to recover the Schwarzschild spin precession by setting $a, e, g, l, \Lambda = 0$. Then, the coefficients and frame-dragging are reduced to $A = 0$, $B = (r - 3m)/\sqrt{(r^2 - 2m)}$ and $\cosh \eta = 1$. After a few algebra, expression (3.75) is reduced to

$$\Delta_{\text{S}} = \Phi \left(\frac{r - 3m}{\sqrt{r^2 - 2mr}} \cosh \zeta - 1 \right),$$

(4.16)

which is precisely Eq. (51) from Ref. [31].

In the next subsections we will analyze the spin precession in different limiting cases in the parameters of the general solution. The plots presented below are dimensionless (unless the contrary is specified), the parameters presented are rates of the relevant parameter with respect to the mass m. Thus the mass parameter is used as a reference to express the charge and angular momentum ratio, represented by e/m for electric charge, a/m for angular momentum. One of the axis plots $v = v_{\text{EPR}}$ for the local inertial velocity due the EPR process and $0 < m/r < 1$ plots distance, with 0 corresponding to r distance at infinite and 1 for $r = m$, which is the smaller distance reached for extreme black holes.

4.3.1   Reissner-Nordström

This case corresponds to a Schwarzschild black hole with non-vanishing charges e and g, after setting l, Λ and a to zero. The Reissner-Nordström spacetime is also a spherically symmetric solution.

The spin precession angle is then reduced to

$$\Delta_{\text{RN}} = \Phi \left(\frac{r^2 - 3mr + 2e^2 + 2g^2}{r\sqrt{r^2 - 2mr + e^2 + g^2}} \cosh \zeta - 1 \right),$$ (4.17)

where the functions A and B are

$$A_{\text{RN}} = 0, \qquad B_{\text{RN}} = \frac{r^2 - 3mr + 2e^2 + 2g^2}{r\sqrt{r^2 - 2mr + e^2 + g^2}}$$ (4.18)
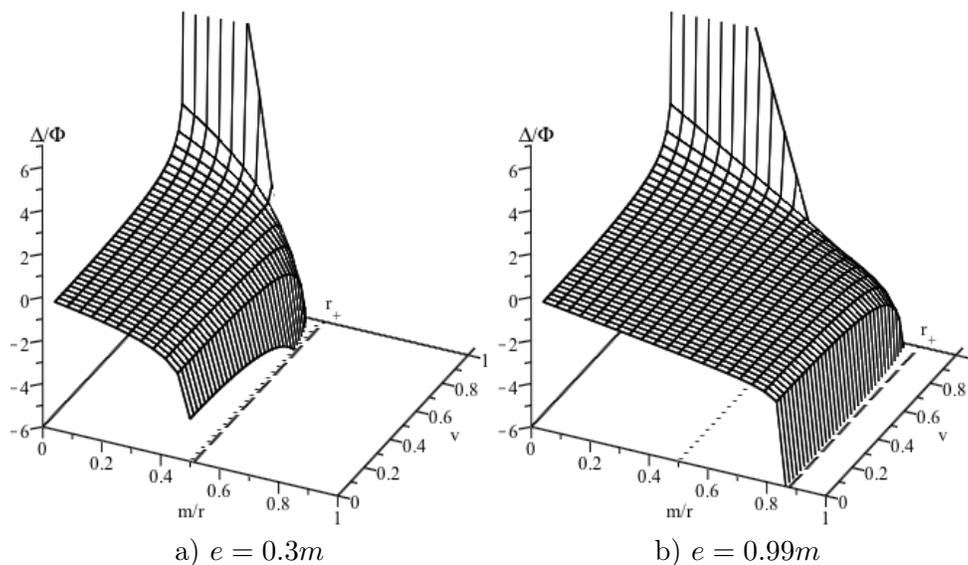
and $\cosh \eta_{\text{RN}} = 1$.

a) $e = 0.3m$ b) $e = 0.99m$

Figure 4.2: The precession angle Δ/Φ for a Reissner-Nordström black hole for two values of charge e. They are asymptotic to the horizon $r = r_+$ (dashed line), which is below the Schwarzschild radius $r_{\text{s}} = 2m$ (dotted line).

The angle Δ on Eq. (4.18) is plotted in Fig. 4.2 as function of the distance and local velocity $v = v_{\text{EPR}}$. When $m/r \to 0$ the experiment is placed far away from the black hole $(r \to \infty)$, and $m/r = 1$ corresponds to the limit of distance that we can reach for an extreme black hole with charge $e = m$, where, for simplicity, e represent the sum of both charges, electric and magnetic ones. When $v = 0$ the particles are static in the EPR source and for $v \to 1$ they are ultra-relativistic particles. In Fig. 4.2 the precession angle is plotted independently from the observer position angle Φ. For $e = 0$ we recover all results of the spin precession for a Schwarzschild black hole and the horizon is at $r = 2m$.

The plots are quite similar as in the Schwarzschild case (compare with Fig. 4.1). Analogous and interesting effects of spin precession can be compared with [31] using the previous reviewed regions:

Region I: The situation is identical to the Schwarzschild black hole. The spacetime is Minkowskian and $\Delta \to 0$.

Region II: Far away from the horizon r_+ with $v \neq 0$ we recover the spin precession found in special relativity and the plot is asymptotic (see Fig. 4.2), i.e. $\lim_{r \to \infty} \Delta = \cosh \zeta - 1$ in agreement to [76].

Region III: A new effect occurs near the black hole horizon. This effect corresponds to a shifting of horizon compared with the Schwarzschild case, from $r = 2m$ to $r = r_+ = m + \sqrt{m^2 - e^2}$. As the charge e is increased, we reach values of r below the Schwarzschild horizon, it means that we can calculate values of Δ at $r = r_+ < 2m$ (see Fig. 3.4 where the horizon would be located at $r = 2m$). The lowest value of r that we can reach is when $e = m$ for a extreme black hole, whose horizon is at $r = r_+ = m$. These values of r are not allowed for the Schwarzschild case. From Fig. 4.2 we see how the horizon is shifted as the charge is increased. $\Delta \to -\infty$ as the horizon is reached, no matter the velocity of the particles considered. EPR correlation then is totally lost. The same behavior of Δ was present in Schwarzschild radius in Ref. [31].

The divergence of the spin precession originates from the fact the vierbein (4.6) and the four-velocity (3.49) become singular at the horizon r_+. These singularities are connected with the breakdown of the coordinate system (t, r, θ, ϕ).
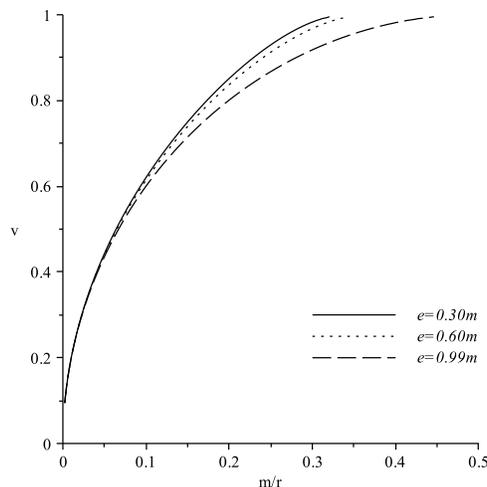

Figure 4.3: Parametric plot of position m/r and local inertial velocity v for path r_0 that keep a perfect anti-correlation ($\Delta = 0$) for a Reissner-Nordström black hole.

Region IV: It is still possible to keep circular orbits in the path $r = r_0$, with perfect anti-correlation $\Delta = 0$. Thus, for a particular position, the local inertial velocity

of particles v_{EPR} must be tuned at the beginning from the source. In Fig. 4.3 r_0 is plotted for three suitable values of charge e in function of position m/r and local inertial velocity v. We can see that for large distances $(m/r \to 0)$ is possible to have the perfect anti-correlation with low values of v. Meanwhile the horizon is reached, we must increase the local velocity of the particles to keep the perfect anti-correlation.

As in the Schwarzschild case, near the horizon there is a not null precession angle $(\Delta \neq 0)$, independently of the velocity of the particle. Then it is not possible to have a perfectly anti-correlated orbits. In Fig. 4.3 the limit circular orbits correspond to the point where r_0 ends on the top of the figure. For large values of e, we can have perfect anti-correlated orbits closer to the horizon, but there is no possible to find a r_0 below the Schwarzschild radius.

4.3.2   Kerr

Now we consider an axially symmetric spacetime with rotation parameter a. It corresponds to the Kerr spacetime. This parameter can be related to the rotation of a black hole and it is responsible for the dragging around of the spacetime near the hole discussed in Section 3.1.4.

If we review the metric of eq. (4.1) and simplify it setting the parameters $e = g = l = \Lambda = 0$, we obtain [69, 82]

$$ds^2 = -\frac{D}{\Sigma}(dt - a\sin^2\theta d\phi)^2 + \frac{\Sigma}{D}dr^2 + \Sigma d\theta^2 + \frac{\sin^2\theta}{\Sigma}[adt - (r^2 + a^2)d\phi]^2, \qquad (4.19)$$

where

$$\begin{aligned} D &= r^2 - 2mr + a^2, \\ \Sigma &= r^2 + a^2\cos^2\theta. \end{aligned} \qquad (4.20)$$

When $D \to 0$ the metric coefficient $g_{11} \to \infty$, and then Eq. (4.19) becomes problematic, the metric fails to be strongly asymptotically predictable, and thus it does not describe physical processes [69]. Therefore, this metric has physical meaning when $a^2 \leq m^2$, which is consequence of solving $D = r^2 - 2mr + a^2 = 0$ in g_{11}.

This component of the metric establishes two possible values of r for the Kerr black holes

$$r_\pm = m \pm \sqrt{m^2 - a^2}, \qquad (4.21)$$

whose horizon is denoted by r_+. As in the Schwarzschild case, $r > r_+$ is the region where

we can obtain sensible causal information of the system.

An important difference in Kerr spacetime is that the horizon is below the Schwarzschild radius $r_{\mathrm{s}} = 2m$, as can be seen from r_+ equation. When $a^2 = m^2$ it is called extreme Kerr black hole, hence $r_+ = r_-$ and the horizon is placed at $r = m$.

Another feature of Kerr-like spacetime is the *static limit surface*. Consider a stationary particle, i.e. $r = $ constant, $\theta = $ constant and $\phi = $ constant. Thus, from spacetime metric (4.19) we have

$$- d\tau^2 = g_{00} dt^2. \tag{4.22}$$

Then, for $g_{00} \geq 0$ this condition cannot be fulfilled, so a massive particle cannot be stationary within the surface $g_{00} = 0$, because, as we already know, such particle will acquire four-velocity due the frame-dragging (3.38). Photons however can satisfy this condition and only they can be stationary at the static limit. This is the reason why it is called static surface.

Solving the condition $g_{00} = 0$ for r gives us the radius of the static limit surface

$$r_{st} = m + (m^2 - a^2 \cos^2 \theta)^{1/2}. \tag{4.23}$$

It is important to emphasize that the static limit surface is not a horizon [80]. Later, we shall see why this is no a horizon for spin precession angle, but a limit for keeping the perfect anti-correlation.

The spin precession has the same form of (3.75), but with different coefficients A and B, that is, from equation (3.75) with coefficients (4.7) and parameters $e = g = l = \Lambda = 0$ the spin precession angle is reduced to

$$\Delta_{\mathrm{K}} = \Phi \left[\frac{-2\sqrt{D}am \sinh \zeta + (H - mD)\cosh \zeta}{(r^2 - 2mr)^{3/2}} \cosh \eta_{\mathrm{K}} + \frac{\sqrt{D}am}{(r^2 - 2mr)^{3/2}} \frac{\sinh \zeta \cosh \eta_{\mathrm{K}}}{\cosh^2 \eta_{\mathrm{K}} - \cosh^2 \zeta} - 1 \right], \tag{4.24}$$

where

$$D = r^2 - 2mr + a^2, \tag{4.25}$$

$$H = r^3 - 4mr^2 + 4m^2 r - a^2 m, \tag{4.26}$$

$$\cosh \eta_{\mathrm{K}} = \frac{r\sqrt{D}}{\sqrt{(r - 2m)(r^3 + a^2 r + 2ma^2)}} \neq 1, \tag{4.27}$$

with the coefficients A and B being

$$A_{\mathrm{K}} = -\frac{\sqrt{D}am}{(r^2 - 2mr)^{3/2}}, \qquad B_{\mathrm{K}} = \frac{H - mD}{(r^2 - 2mr)^{3/2}}. \tag{4.28}$$

The precession angle is plotted in Fig. 4.4 for two values of angular momentum parameter a, as a function of distance and local velocity $v = v_{\mathrm{EPR}}$. The distance is parameterized by m/r which means the experiment is placed at infinite when $m/r \to 0$, and $m/r = 1$ correspond to a extreme black hole, i.e. $a = m$. When $v = 0$ the particles are static at the EPR source and for $v \to 1$ they are ultra-relativistic. The precession angle was plotted independently from the observer position angle Φ. For $a = 0$ we recover all results of Schwarzschild spin precession [31] as expected.
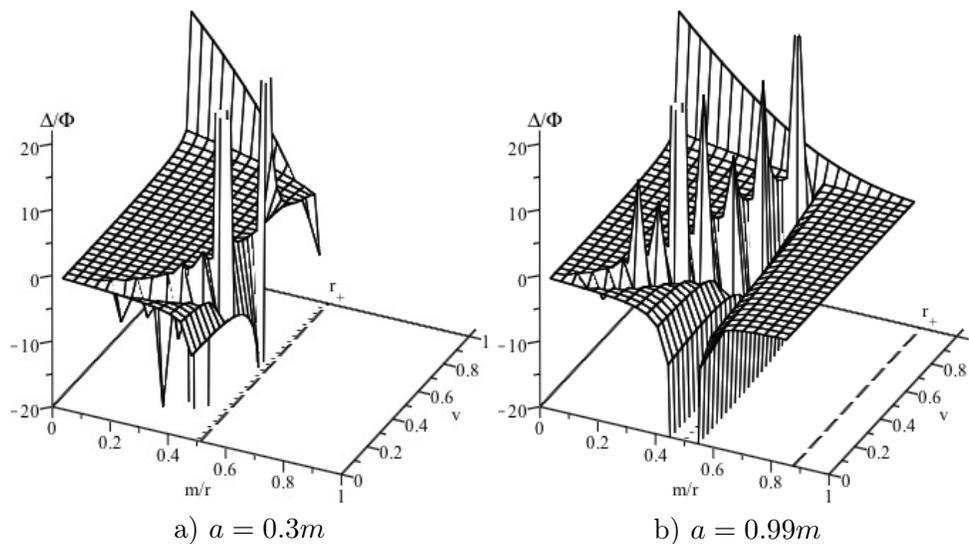

a) $a = 0.3m$ b) $a = 0.99m$

Figure 4.4: The precession angle Δ/Φ for a Kerr black hole for two values of angular momentum parameter a. They are asymptotic to the static limit $r_{st} = 2m$ and along a path $v = v_{fd}$. The peaks represent an asymptotic infinite wall.

The plot is quite similar to Fig. 4.1, but with important differences. The effects due the acceleration and gravity analyzed by regions are:

Region I: Again the situation is identical to the Schwarzschild's black hole. The frame-dragging has no contribution because it decreases with distance. Therefore the spacetime is Minkowskian and $\Delta \to 0$ as $v = v_{\mathrm{EPR}} \to 0$.

Region II: There are no new effects. The frame-dragging has no contribution and the angle Δ is asymptotic to infinite when $v \to 1$ for ultra-relativistic particles.

Region III: In the Schwarzschild and Reissner-Nordström spacetime, the divergence of the spin precession ($\Delta \to -\infty$) was at the horizon. Now, the divergence is present

in two locations, one of them at the static limit surface and the other one is through the path defined by $v_{\text{EPR}} = v_{fd}$.

The first divergence in Eq. (4.24) is related to the static limit surface. As mentioned in Section 3.1.4, any particle acquire velocity due the frame-dragging as it falls to the black hole. When this particle reaches the static limit surface at $r = 2m$ for equatorial plane, its velocity tends asymptotically to speed of light. In the left part of Eq. (4.24) it is easy to see why precession angle diverges when distance is evaluated at $2m$. The divergence of the spin precession in the Kerr spacetime originates from the fact that the frame-dragging component (4.27) of the four-velocity (3.49) becomes singular at the static limit r_{st}. This feature contrasts with the Reissner-Nordström case, where the singularities were connected with the breakdown of the coordinate system (t, r, θ, ϕ) at r_+.

Previously it was mentioned that the static limit is not a horizon. Beyond r_{st} it is still possible to get entangled particles in circular orbits. The region inside the interval $r_+ \leqslant r < 2m$ has a similar behavior as Region I and II (see in particular Fig. 4.4 b) where is more clear this feature). Frame-dragging has no effect and the precession angle Δ_{K} is asymptotic near the static limit at $2m$ and also for particles with $v_{\text{EPR}} \to 1$.

But near the horizon r_+ the function (4.24) is well defined. This is an unexpected result if we compare with Scharzschild and Reissner-Nordström cases, where the horizon represents an asymptotic limit.

For $r < r_+$ the coordinate system breakdowns and we are unable to find the precession angle for orbital particles.

The second divergence corresponds to a coupling between the EPR velocity and the frame-dragging. In Fig. 4.4 is represented by peaks an asymptotic infinite "wall". This wall follows a curved path defined by $\cosh^2 \zeta = \cosh^2 \eta$ in (4.24), which is easy to verify that corresponds to $v_{\text{EPR}} = v_{fd}$.

When the velocity of the first particle equals the velocity of the frame-dragging, Δ_{K} becomes asymptotically infinity. Physically, one particle remains static because v_{EPR} equals v_{fd}, meanwhile, the other particle continues his travel, as seen by the hovering observer. The static particle never reaches the observer, and therefore it is not possible to know the anti-correlation between the particles.

This situation represents a particular feature for Kerr-like spacetime. In

Schwarzschild, Reissner-Nordström and Ref. [32] the plots were very smooth until their functions reach their horizons. Here, the plot presents this infinite wall following the path which corresponds to the velocity that experience a free falling particle due the frame-dragging (see Fig. 4.5 a).
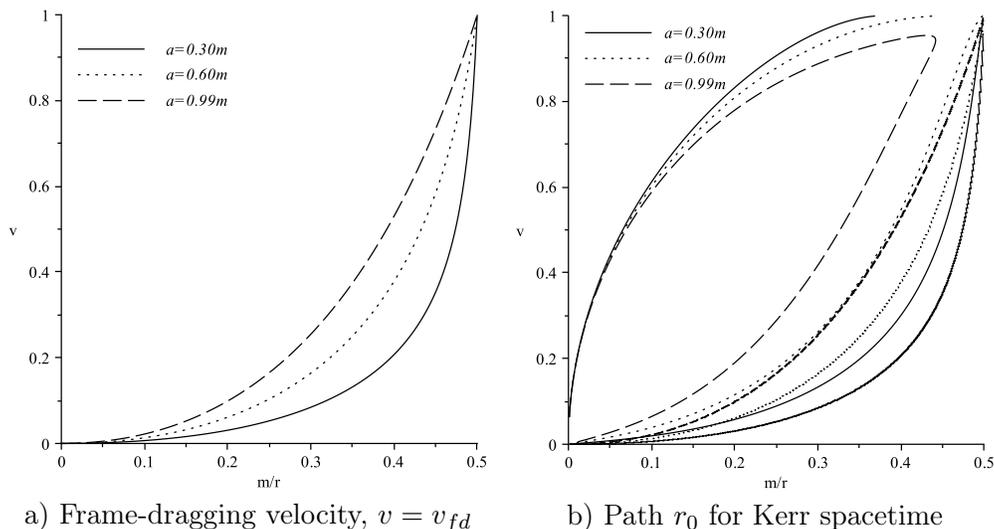

a) Frame-dragging velocity, $v = v_{fd}$ b) Path r_0 for Kerr spacetime

Figure 4.5: Frame-dragging velocity and perfect anticorrelation path for Kerr black hole. a) Local inertial velocity due the frame-dragging for three values of a. The infinite wall in Fig. 4.4 follow the path traced by this plot when $v_{\text{EPR}} = v_{fd}$. b) Parametric plot of position m/r and local inertial velocity v for path r_0 that keep a perfect anti-correlation ($\Delta = 0$) for a Kerr black hole.

Region IV: We can see in Fig. 4.5 b) that away from black hole, there is a low velocity that keeps the perfect anti-correlation, as in the Schwarzschild and Reissner-Nordström cases. As $r \to r_{st}$ there is a non-vanishing precession angle, independently of the velocity of the particle v_{EPR}. Perfectly anti-correlated orbits cannot be kept and r_0 has a limit value as in the Reissner-Nordström spacetime. We can see this limit value when r_0 ends on the right top the Fig. 4.5 b). Near the static limit, the contribution of the frame-dragging allows three values of v_{EPR} for the same value of angular momentum parameter a. This new effect is not present either in the Schwarzschild or Reissner-Nordström cases and in the previous work [32] was not mentioned. When the static limit is reached, the velocity due the EPR process must be the speed of light in order to get a perfect anti correlated particles.

4.3.3 Kerr-Newman

We are now in position to analyze the complete Kerr-Newman spacetime and its effects on entangled particles.

Simplifying Eq. (3.75) the spin precession angle is reduced to

$$
\Delta_{\mathrm{KN}} = \Phi \left\{ \frac{\cosh\eta}{r(D-a^2)^{3/2}} \left[A_{\mathrm{KN}} \cosh\zeta - B_{\mathrm{KN}} \sinh\zeta \left(\frac{2\cosh^2\zeta - \cosh^2\eta - \sinh^2\eta}{\cosh^2\zeta - \cosh^2\eta} \right) \right] - 1 \right\},
$$
(4.29)

where

$$
\begin{aligned}
A_{\mathrm{KN}} &= D^2 - (a^2 + mr - e^2 - g^2)D - a^2 r^2 + a^2 mr, \\
B_{\mathrm{KN}} &= a\sqrt{D}(e^2 + g^2 - mr), \\
\cosh\eta &= \frac{r^2\sqrt{D}}{\sqrt{(D-a^2)[(r^2+a^2)^2 - a^2 D]}}, \\
D &= r^2 - 2mr + a^2 + e^2 + g^2.
\end{aligned}
$$
(4.30)

From Eq. (4.29) it can be shown that Region I and II have the same behavior for a Minkowski spacetime. This is not surprising result since as we have seen in previous cases of this section, a and e decreases with distance.

For Region III the static limit (4.23) is reduced to $r_{st} = m + \sqrt{m^2 - e^2}$ on the equator, which coincides with the horizon of the Reissner-Nordström spacetime. The static limit r_{st} represents again an asymptotic limit for calculation of the precession angle Δ in the Kerr-Newman black holes. Contrary to Kerr spacetime where the static limit is placed at $r = 2m$, now it is below and this limit depends in the charge of black hole, depicted by a dotted line in Fig. 4.6. In this figure, 4.6a) and 4.6b) have the same horizon (4.21), as well as 4.6c) and 4.6d) between them. In a) r_{st} is too close to r_+ that dotted line cannot be distinguish. Fig. a) and c) have the same r_{st} because the electric charge parameter e is equal for both.

Once again, we can observe the infinite wall path due the coupling of v_{EPR} with v_{fd}. This asymptotic path is not constrained either to the region $r > 2m$ or above the horizon, but above the static limit.

Like in Kerr spacetime, the region between $r_+ \leqslant r < 2m$ is not affected by the frame-dragging and Δ tends asymptotically to infinity near r_{st}. Finally the coordinate system breakdown when r equals r_+.

4.3.4 NUT

There is still a controversy if the NUT parameter can be considered a gravo-magnetic monopole parameter of the central mass, or a twisting property of the surrounding spacetime
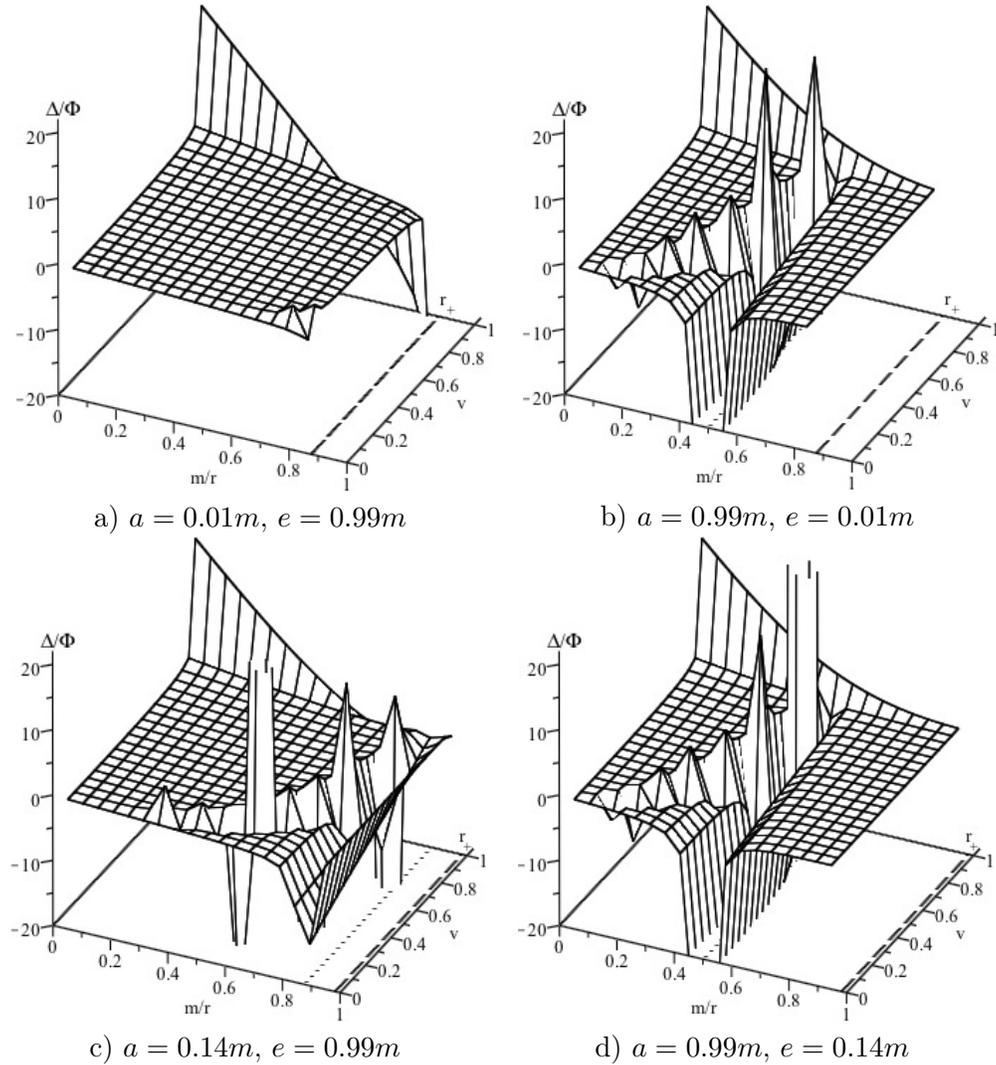
a) $a = 0.01m$, $e = 0.99m$

b) $a = 0.99m$, $e = 0.01m$

c) $a = 0.14m$, $e = 0.99m$

d) $a = 0.99m$, $e = 0.14m$

Figure 4.6: The precession angle Δ/Φ for a Kerr-Newman black hole for a pair of values of a and e, that keep r_+ constant (dashed line). The dotted line represents the static limit surface on equatorial plane. The plots are asymptotic at $r = r_{st}$ and along a path $v_{\mathrm{EPR}} = v_{fd}$. The peaks represent an asymptotic infinite wall. In a) r_{st} is too close to r_+ that dotted line cannot be distinguish.

[83]. For the purpose of this work we considered NUT parameter as similar as Kerr param-
eter, which induce a dynamic curvature of the spacetime due the frame-dragging. This is
more clearly when equation (3.75) is reduced by setting the parameters $e = g = a = \Lambda = 0$,

$$\Delta_{\mathrm{NUT}} = \Phi \left(\frac{r^3 - 3mr^2 - 3l^2r + ml^2}{(r^2 + l^2)\sqrt{r^2 - 2mr - l^2}} \cosh \zeta \cosh \eta - 1 \right), \qquad (4.31)$$

where

$$\cosh \eta = \frac{r^2 + l^2}{\sqrt{r^4 - 2l^2r^2 + 8ml^2r + 5l^4}}. \qquad (4.32)$$

and where functions A and B was

$$A_{\mathrm{NUT}} = 0, \quad B_{\mathrm{NUT}} = \frac{r^3 - 3mr^2 - 3l^2r + ml^2}{(r^2 + l^2)\sqrt{r^2 - 2mr - l^2}}. \qquad (4.33)$$

This equation (4.31) is quite similar to Schwarzschild spin precession angle, but now it
has integrated an additional factor due the frame-dragging of NUT. We must remember that
the NUT metric is also an axial-symmetrical and because of that, there is this additional
factor.

The equation (4.31) is asymptotic to infinity as $r \to m \pm \sqrt{m^2 + l^2}$. The positive root
represents the outer Schwarzschild-NUT horizon.

Although the $\cosh \eta$ term, with is due the frame-dragging, has a fourth degree polynomial
in the denominator, this quartic function does not have real roots. An elementary numerical
analysis shows that the roots o do not exist if one assumes that m and l are real and positive
numbers. Therefore the frame-dragging contribution to the NUT spin precession angle does
not has any asymptotic singularity for any value of r.

The NUT spin precession angle Eq. (4.31) is plotted in Fig. 4.7 for two values of v_{EPR}.
The distance once and again is parameterized by m/r which means the experiment is placed
at infinite when $m/r \to 0$; and the NUT parameter is plotted as m/l, where $m/l \to 0$
represents a infinitely large value this parameter.

We can see from Fig. 4.7 that for very large distance ($m/r \to 0$), the metric effects
vanish and the special relativity effects over entanglement prevail, like it was for Region I
and II in Schwarzschild case.

The most important feature that we can see is as NUT parameter increase, i.e. $m/l \to 0$,
the horizon shifts to larger distance and it is observed in the bottom of the plot as infinitely
asymptotic negative values of spin precession Δ. In fact when the NUT parameter is too
large, there is almost impossible to keep a perfect anticorrelation, even at slow motion.
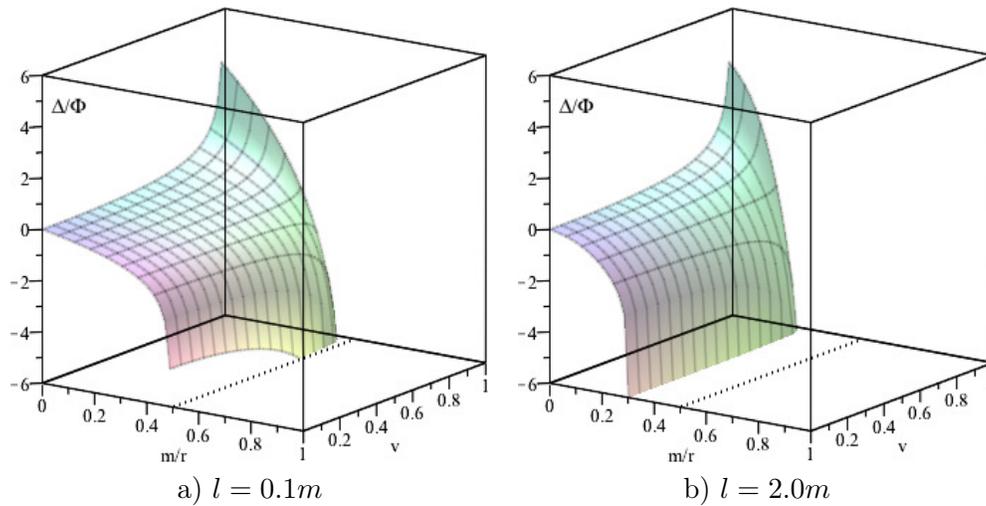
a) $l = 0.1m$ b) $l = 2.0m$

Figure 4.7: The precession angle Δ/Φ for a NUT black hole for two values of NUT parameter l as a function of distance m/r. Large values of the NUT parameter l shift the position of the Schwarzschild horizon event to r_{NUT}.

4.3.5 Schwarzschild-(Anti)de Sitter Black Hole

This is a spherically symmetric spacetime too, and has a cosmological observer (see Fig. 3.4). The Schwarzschild-de Sitter spacetime represents a black hole in asymptotically de Sitter space [84]. A positive cosmological constant Λ (de Sitter) is related to an accelerated universe, meanwhile negative value (anti-de Sitter) is related to negative vacuum energy and positive pressure. The spin precession angle in this case is given by

$$\Delta_{(\mathrm{A})\mathrm{dS}} = \Phi \left(\frac{r - 3m}{\sqrt{r^2 - 2mr - \frac{1}{3}\Lambda r^4}} \cosh \zeta - 1 \right), \tag{4.34}$$

where functions A and B are

$$A_{(\mathrm{A})\mathrm{dS}} = 0, \quad B_{(\mathrm{A})\mathrm{dS}} = \frac{r - 3m}{\sqrt{r^2 - 2mr - \frac{1}{3}\Lambda r^4}}. \tag{4.35}$$

For a distance near the black hole and positive Λ (de Sitter), is easy to show that the spin precession angle behaves in the same manner as in the case of Schwarzschild spacetime (see [31]) due the smallness of the cosmological constant. Nevertheless the cosmological constant has a significant effect only for a large distances which are of the order of 10^{26}m [85]. Here the Regions I and II differs.

We can see in Fig. 4.8-a) that for positive Λ, the spin precession angle is asymptotic
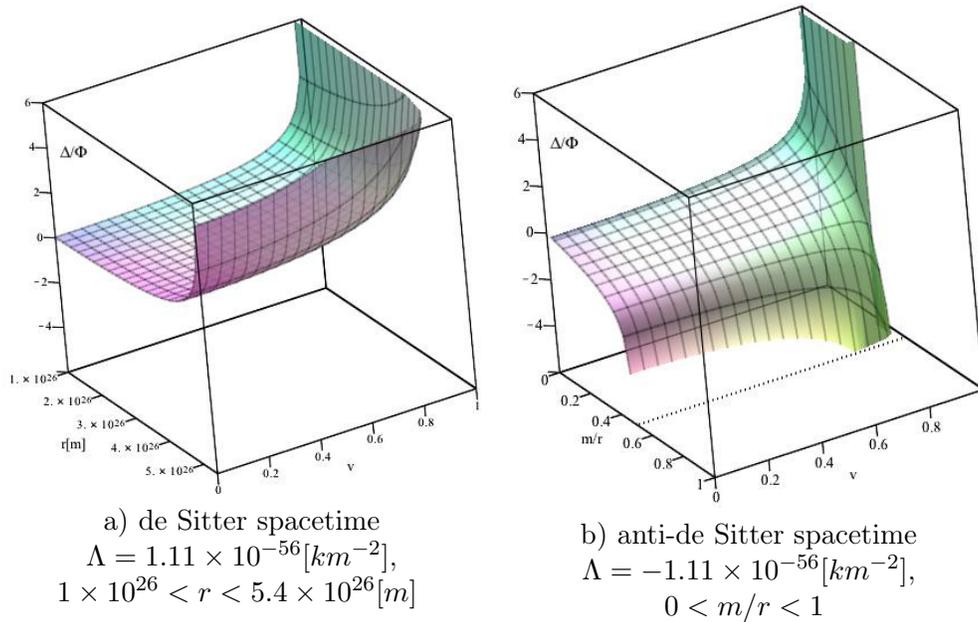
a) de Sitter spacetime
$\Lambda = 1.11 \times 10^{-56}[km^{-2}]$,
$1 \times 10^{26} < r < 5.4 \times 10^{26}[m]$

b) anti-de Sitter spacetime
$\Lambda = -1.11 \times 10^{-56}[km^{-2}]$,
$0 < m/r < 1$

Figure 4.8: The precession angle Δ/Φ for a Schwarzschild-de Sitter and anti-de Sitter spacetime. Both share a Schwarzschild horizon, but de Sitter has a cosmological horizon at 10^{26}m.

at the cosmological horizon, meanwhile for negative Λ (anti-de Sitter) in Fig. 4.8-b), the cosmological constant has despicable effects and the precession angle has the same behavior of the Schwarzschild spacetime previously mentioned.

4.4 Examples: Accelerating and rotating black holes

In Ref. [86] was shown that, when $\Lambda = 0$, the metric (4.1) represents an accelerating and rotating charged pair of black holes with a generally non-zero NUT parameter. We shall consider in this section the vacuum case ($\Lambda = e = g = l = 0$) where the background is Minkowski.

As Ref. [86] pointed out we can see that the parameters α and ω are related to the the acceleration and rotation of the source (mass m) respectively.

Therefore, with an arbitrary α and using the remaining scaling freedom to put $\omega = a$, the Plebański-Demiański metric is simplified to

$$ds^2 = \frac{1}{\Omega^2}\left(-\frac{D}{\rho^2}[dt - a\sin^2\theta d\phi]^2 + \frac{\rho^2}{D}dr^2 \right.$$
$$\left. +\frac{P}{\rho^2}[adt - (r^2 + a^2)d\phi]^2 + \rho^2\frac{\sin^2\theta}{P}d\theta^2\right), \tag{4.36}$$

where the parameters (4.2) are reduced to

$$\epsilon = 1 - a^2\alpha^2,$$
$$n = a\alpha m,$$
$$P = \sin^2\theta \left(1 - 2\alpha m \cos\theta + a^2\alpha^2 \cos^2\theta\right),$$

(4.37)

and

$$\rho^2 = r^2 + a^2 \cos^2\theta,$$
$$\Omega = 1 - \alpha r \cos\theta,$$
$$D = a^2 - 2mr + (1 - a^2\alpha^2)r^2 + 2\alpha^2 mr^3 - \alpha^2 r^4.$$

(4.38)

The metric (4.36) has four singularities when $\theta = \pi/2$, that is, we can factorize D as

$$D = (r - r_+)(r - r_-)(1 - \alpha^2 r^2),$$

(4.39)

where

$$r_\pm = m \pm \sqrt{m^2 - a^2}.$$

(4.40)

As we can remember, $r_\pm$ are the locations of the outer and inner horizons of the non-accelerating Kerr black hole. The other pair of horizons are related to the acceleration and is familiar in the context of the C-metric as an acceleration horizon:

$$r_{\text{Acc}} = \frac{1}{\alpha}.$$

(4.41)

On the other hand, after some calculation, the coefficients for the spin precession angle are

$$A_{\text{AccRot}} = \frac{a\sqrt{D}}{2r(D - a^2)^{3/2}}[rD' - 2(D - a^2)],$$
$$B_{\text{AccRot}} = \frac{1}{2r(D - a^2)^{3/2}}[4D(D - a^2) - r(a^2 + D)D'].$$

(4.42)

where

$$D' = \frac{\partial D}{\partial r} = -2m + 2(1 - a^2\alpha^2)r + 6\alpha^2 mr^2 - 4\alpha^2 r^3.$$

(4.43)

And the frame-dragging velocity is

$$\cosh\eta_{\text{PD}} = r^2 \sqrt{\frac{D}{(D - a^2)\left[(r^2 + a^2)^2 - a^2 D\right]}}.$$

(4.44)

But the horizons (4.40) and (4.41) have no physical relevance on the spin precession angle because equations (4.42) are not singular at these points. The horizons take importance when

the effect of each parameter is analyzed one by one.

We reviewed this kind of behavior for Kerr-Newman spacetime in our last work [33], where the Schwarzschild horizon and the frame-dragging effect produce an asymptotic spin precession angle instead of Kerr horizon.

It is easy to show that we can recover the Kerr spacetime results reviewed in previous section, after setting no acceleration ($\alpha = 0$). Therefore, we shall consider the effect of acceleration over the spin precession angle.

4.4.1   C-metric

From the pair of accelerated and rotating black holes represented by the metric (4.36), we can consider the limit when $a \to 0$. In this case, the metric has the form of the C-metric and thus the parameters (4.42) reduce to

$$A_{\text{C}-\text{metric}} = 0, \quad B_{\text{C}-\text{metric}} = \frac{\alpha^2 m r^2 + r - 3m}{\sqrt{(r^2 - 2mr)(1 - \alpha^2 r^2)}}, \quad \cosh \eta = 1. \qquad (4.45)$$

Then, the spin precession angle for the C-metric is

$$\Delta_{\text{C}-\text{metric}} = \Phi \left(\frac{\alpha^2 m r^2 + r - 3m}{\sqrt{(r^2 - 2mr)(1 - \alpha^2 r^2)}} \cosh \zeta - 1 \right). \qquad (4.46)$$

It is easy to see that this equation reduces to Schwarzschild case (4.16) when $\alpha = 0$.

In addition, we can see from equation (4.46) that is asymptotically predictable at the Schwarzschild radius and the acceleration horizon also, that is $\Delta_{\text{C}-\text{metric}} \to \infty$ as $r \to \alpha^{-1}$.

In Fig. 4.9 it is plotted the effect of acceleration α over the spin precession angle $\Delta_{\text{C}-\text{metric}}$ as function of the distance and local velocity of the particles. The acceleration is parameterized in function of acceleration per unit mass. As mentioned in Ref. [86], the acceleration can only have positive values. We can observe the same effects of the velocity of the particles that was already seen in all previous cases, that is, for high local velocity of the particles v_{EPR}, the $\Delta_{\text{C}-\text{metric}}$ increases.

The C-metric also has an horizon and corresponds to the Schwarzschild radius, that can be clearly observed in Eq. (4.46). But as was mentioned, there is another horizon due the acceleration parameter as $r \to \alpha^{-1}$.

The above behavior can suggest some insight about the physical interpretation of the acceleration parameter. In fact, because the acceleration horizon (4.41), we can see that a very small acceleration will have an important effect until a long distance is reached, even
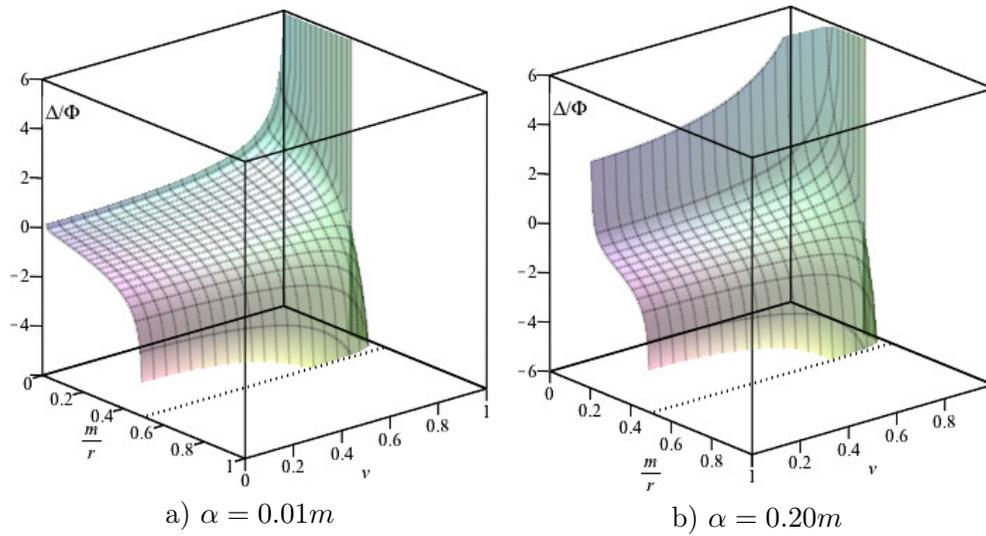
Figure 4.9: The precession angle Δ/Φ for C-metric for two values of the acceleration parameter α as function of distance m/r and local velocity $v = v_{\mathrm{EPR}}$. The dotted line is placed at Schwarzschild radius $r = 2m$.

when there is expected a flat spacetime with no effect over the spin precession angle. In reference [87] was noted that when $\alpha \neq 0$, it is difficult to uniquely determine the mass of each individual black hole since the spacetime is not globally asymptotically flat and one cannot expect to distinguish effects due to acceleration from those due to gravitational fields. By the calculation of the spin precession angle could be possible to distinguish indirectly the mass effects from those of the acceleration ones.

4.5 Uncertainties in observers' positions

As mentioned in Section 3.2.2 the uncertainty in the position will reflect in an increase (or decrease) of the violation of Bell's inequalities Eq. (3.78), and it should not be possible to compensate the direction of the measure instruments of the observers to extract the maximum violation of these inequalities.

It is important to note the near the Reissner-Nordström horizon, the static limit and infinitely wall path of Kerr and Kerr-Newman, the spin precession angle is asymptoticly divergent and is not possible to reach the maximum violation of Bell's inequality. In the same way, at the cosmological horizon of de Sitter could not get the perfect anticorrelation. In all these cases, any small variation in the position of the observers near the horizons will translate as a great variation in the measure of the spin precession angle, making virtually impossible adjust again the measure instruments of the observers.

For these cases it could be able to use free falling observers and different veirbeins in order to avoid dynamical and gravitation effects implied on spin precession angle. A future work could research these kind of observers.

Chapter 5

Conclusions

In this thesis, it was constructed an algorithm to calculate in a general way the spin precession angle of a EPR pair of spin-1/2 massive particles moving on the equator for very general axially symmetric spacetime without reference to any specific metric.

However even for the most general case, before applying it to Type D solutions, it was showed that when the frame-dragging is taken into account, then an additional velocity over particles must be incorporated. Therefore, hovering observers were introduced in order to have a fixed reference frames that ensures reliable directions to compare the measurements of the 1/2-spin quantum states. The total velocity measured by these observers was identified as the addition of the velocity of a ZAMO, plus the local velocity of the particles measured by the ZAMO. These ZAMOs co-rotate the black hole due the frame-dragging and were used as a preliminary step before calculating the total local inertial velocity of the particles moving on the equator of the black hole. Therefore it was obtained a general algorithm to calculate the total spin precession angle, which was measured from the perspective of these hovering observers. The result does not assume a particular coordinate system but only depends on the axially symmetric metric coefficients.

From the point of view of the hovering observers, there is a Wigner rotation Eq. (3.37) for each particle, because both particles travel with different velocities due the frame-dragging of the spacetime.

After that, these results were applied to the most general Type D Plebański-Demiański black hole. It was obtained the general expression for the spin precession angle Δ_{PD}, that describe the spacetime effects that deteriorate the perfect-anticorrelation of the entangled particles compared if they would be in the Minkowski spacetime, through the A and B coefficients (4.7) and the frame-dragging velocity $\cosh \eta_{\mathrm{PD}}$ (4.9). Both coefficients and $\cosh \eta_{\mathrm{PD}}$ are non-vanishing and they depend on the seven physical parameters arising in the Plebański-

Demiański metric.

It is important to mention again that the spin-singlet state is mixed up with the spin-triplet state, which it is easy to proof when $\Delta \to 0$ in the Eq. (3.74). This mixture is due exclusively by the effect of the curvature of spacetime on the quantum state of the particles

The explicit expression of Δ_{PD} in terms of the physical parameters can be written down but it is a huge expression. Thus it was prefered to write down a short formula, in terms of the quartic function D and its derivative D' with respect to r. It was studied two branches of this case according to Refs. [39, 40]. The first one correspond with $\alpha = 0$ and the second one with $l = 0$.

The first case (with $\alpha = 0$ and $l \neq 0$), corresponding to the non-accelerating Kerr-Newman-(Anti)de Sitter-NUT black hole, contains only six parameters and it is quite similar to the Plebański-Demiański case. It was studied different limits and it was computed the spin precession angle for different subfamilies of solutions. Among these cases it was included the Kerr solution with NUT and the NUT solution with rotation. Another cases included in the analysis were the Kerr, Schwarzschild-NUT, Schwarzschild(Anti)-de Sitter, Reissner-Nordström and Schwarzschild black holes.

In the Reissner-Nordström case, the electric charge parameter produces a shifting of the event horizon position from $r = 2m$ to $r = r_+$ as being contrasted with the Schwarzschild spacetime. But this horizon is still an asymptotic limit for the calculation of spin precession.

In the Kerr spacetime, the angular momentum parameter establishes the commonly named static limit surface, where two interesting physical processes occur: some results coincide with the Schwarzschild radius and it represents one limit for calculation of the precession angle, and the frame-dragging has the maximal value there, making massive particles ultra-relativistic and the spin precession angle $\Delta \to \infty$.

A remarkable difference was found when particles are close to the rotating black hole event horizon r_+. The precession angle is well defined, which contrasts with Scharzschild and Reissner-Nordström cases, where it tends to infinity.

Another effect in Kerr spacetime occurs when the velocity of the particles due the EPR process coincides with the velocity of the frame-dragging. One of the particles keeps their position relative to the hovering observer, meanwhile the other particle reach one observer. Then, the spin precession angle goes to infinity.

Another asymptotic limit is at $r = 2m$ because the equation of the spin precession angle is singular at this point, which was already observed for the Schwarzschild case.

For the Kerr-Newman spacetime, the static limit coincides with the horizon of the Reissner-Nordström spacetime, but this limit does not represent an asymptotic limit for

the spin precession angle.

It was still possible to find circular orbits with perfect anti-correlation for a and e parameters along a path called r_0, that is $\Delta(r = r_0) = 0$. Moreover, when only the angular momentum parameter a is considered, it can be reached a perfect anti-correlation close the static limit with three possible r_0 paths for the same value of a. This effect was not present in the Schwarzschild and Reissner-Nordström cases.

Even that the total electric charge in real black holes should be zero, it was considered as an arbitrary parameter in order to illustrate its effect on the spin precession. The electromagnetic interaction between charged particles and charged black hole was not taken into account and remain to be explored in a future work.

New results were found for Schwarzschild-NUT spacetime. The precession angle (4.31) has an asymptotic behavior at the Schwarzschild horizon shifted by NUT parameter i.e. at r_{NUT}. For Schwarzschild-(Anti)de Sitter spacetime there are also some interesting results in equations (4.34) and (4.35). For positive Λ there is a large increment of the spin precession angle at the cosmological horizon, meanwhile for negative Λ, the cosmological constant has negligible effects and the precession angle has the same behavior of the Schwarzschild spacetime.

For the second case of metrics previously mentioned, with $\alpha \neq 0$ and $l = 0$, there was analyzed an accelerating and rotating black hole. The subfamily discussed with detail was the C-metric, which most relevant effect was the acceleration horizon, where the spin precession angle was asymptotic.

This work showed that the choices of four-velocity of the particles, vierbein and observers are important to have a reliable measurements of the spin precession angle and obtain the perfect anti-correlation and the maximal violation of Bell's inequality. It is important to remember that as soon as the particles get closer to the event horizon for each case, their velocities increase very quickly until asymptotically reach speed of light, with a consequential rapid spin precession. Then, the hovering observers would not be able to adjust the direction of the measurements of the spin, making virtually impossible any measurements of the entanglement.

The results presented here derive from the doctoral research work developed in the Division of Graduate Studies, Faculty of Physics and Mathematics at the Universidad Autónoma de Nuevo León. Thus this thesis consists of the analysis and results presented in the two articles published during the doctoral fellowship. Each article contributes to this work as follows:

Entangled spinning particles in charged and rotating black holes, [33]

- The inclusion of frame-dragging in the computation of particle velocities of section 3.1.4.

- Selection of hovering observers and ZAMOs for the computation of spin precession for an axialsymmetrical spacetime of section 3.1.5.

- Results of spin precession for Reissner-Nordström and Kerr-Newman black holes of sections 4.3.1, 4.3.2 and 4.3.3.

- Plots 4.1, 4.2, 4.3, 4.4, 4.5 and 4.6.

Classical and Quantum Gravity, 01/2013; 30:235012

Quantum entanglement in Plebański-Demiański spacetimes, [81]

- General spin precession angle of Eq. (3.75).

- Results of spin precession for non-accelerating Kerr-Newman- anti)de Sitter-NUT and accelerating-rotating black holes of sections 4.3 and 4.4.

- Plots 3.4, 4.7, 4.8 and 4.9.

The argument presented in this research is strictly geometrical, because the quantum state is obtained through Lorentz transformations due the translation of states from one point to another. Although it was extensively analyzed the effects of the curvature of spacetime on entangled quantum states, it remains to determine the underlying mechanism of this interaction between the gravitational field and the states of the particles. An important line of research could use the results presented here in a quantum field theory of gravity.

Another line of researchn, that may be of interest, is in those regions close to a black hole and it still has no precession, as shown in Fig. 4.3. The inclusion of different physical parameters such as NUT and acceleration could create regions that compensate the effects between them, thus creating conditions to keep a perfect anticorrelation. Similarly it could be investigated systems with different mass-energy distributions, such binary black holes and metrics with arbitrary mass distribution.

In the present work it was considered only Type D solution with a congruence of geodesic curves with non-vanishing expansion and twisting. It would be interesting to study analytic continuations of these solutions in order to find the interior solution supporting the spin precession below the event horizons and the static limit surface and above the cosmological and acceleration horizons. Coordinates of the Kruskal-Szekeres type should be found for

these metrics. It would be interesting also to extend the analysis presented here to arbitrary non-equatorial orbits.

It is also known another different Type D solutions for the case of expansion but non-twisting. Among these solutions are the Robinson-Trautman Type D and the A-metrics. Moreover Type D solutions with non-expanding and non-twisting that emerge are the Kundt Type D and the B-metrics. It would be very interesting to generalize the results found in the present work to the description of entangled particles moving in these backgrounds. Future works would explore these scenarios.

Appendix A

Lorentz Transformations

A Lorentz transformation is a global coordinate transformation that connect two frames O and O', where the system O' moves respect to O without rotation and constant velocity. This implies that the primed coordinates $x^{\mu'}$ of O' is given in terms or elements of the original system O and its coordinates x^μ. It is said that they are linked by a lineal transformation or affine transformation[1]

$$x^{\mu'} = \Lambda^\mu_\nu x^\nu + a^\mu, \tag{A.1}$$

donde Λ^μ_ν y a^μ son constantes.

If $a^\mu = 0$, then the spatial origin of O matches with O' when $t = t' = 0$ and the Lorentz transformation is called *homogeneous*, meanwhile for $a^\mu \neq 0$ it is said that is an *nonhomogeneous* transformation. This last one is also called *Poincaré transformation* and the homogeneous transformations are simply called Lorentz transformations.

The constant Λ^μ_ν is a spacetime rotation equivalent to a "boost" in the direction of motion followed by a spatial rotation. This is in fact the Lorentz transformation.
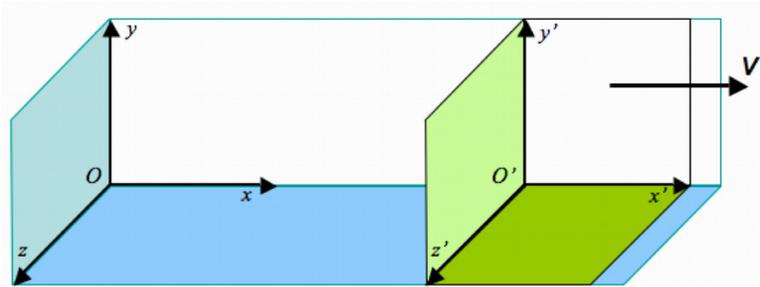

Figure A.1: Boost in x direction.

In order to get the equation (3.8) we follow the example of [88] and we consider the case

---

[1] An affine transformations is a lineal transformation that include a shift of origin between one system and the other one.

of a Lorentz transformation with a boost in the x direction as it is shown in Fig. A.1. The origin of O' moves along the x-axis of the system O in the positive direction with a constant velocity v relative to O. The axis of O and O' coincides at a initial time $t = t' = 0$. Therefore the transformation is homogeneous and can take the form

$$
\begin{aligned}
t' &= Bt + Cx, \\
x' &= A(x - vt), \\
y' &= y, \\
z' &= z.
\end{aligned}
\tag{A.2}
$$

Now, the first postulate of Special Relativity stays [68]:

The speed of light is the same in all inertial frames.

This implies that the measurement of spacetime intervals ds^2 are the same, regardless of the reference frame where we measure them, that is[2]

$$
ds^2 = -c^2 dt^2 + dx^2 + dy^2 + dz^2 = -c^2 (dt')^2 + (dx')^2 + (dy')^2 + (dz')^2.
\tag{A.3}
$$

Therefore, by replacing Eq. (A.2) in the last equation we get

$$
B^2 c^2 - A^2 v^2 = c^2, \quad BCc^2 + A^2 = 0, \quad C^2 c^2 - A^2 = 1.
\tag{A.4}
$$

After solving this system of equations we get

$$
A = B = \gamma, \quad C = -(v/c^2)\gamma,
\tag{A.5}
$$

where

$$
\gamma = (1 - v^2/c^2)^{-1/2}.
\tag{A.6}
$$

Thus, the boost (A.2) takes the form

$$
\begin{aligned}
t' &= \gamma(t - xv/c^2), \\
x' &= \gamma(x - vt), \\
y' &= y, \\
z' &= z.
\end{aligned}
\tag{A.7}
$$

---

[2]Note that the signature is $\eta_{ab} = \text{diag}(-, +, +, +)$, which applies throughout the whole thesis.

This system of equation can be expressed as a matrix array

$$
\begin{bmatrix} ct' \\ x' \\ y' \\ z' \end{bmatrix} = \begin{bmatrix} \gamma & -v\gamma/c & 0 & 0 \\ -v\gamma/c & \gamma & 0 & 0 \\ 0 & 0 & 1 & 0 \\ 0 & 0 & 0 & 1 \end{bmatrix} \begin{bmatrix} ct \\ x \\ y \\ z \end{bmatrix}
\tag{A.8}
$$

If we select[3] $\tanh\xi \equiv v/c$ we find that $\gamma = \cosh\xi$ and then the boost can be written as

$$
\begin{aligned}
t' &= ct\cosh\xi - x\sinh\xi, \\
x' &= x\cosh\xi - ct\sinh\xi, \\
y' &= y, \\
z' &= z,
\end{aligned}
\tag{A.9}
$$

and the Lorentz transformation matrix, i.e. the boost Λ^μ_ν is

$$
\Lambda^\mu_\nu = \begin{bmatrix} \cosh\xi & -\sinh\xi & 0 & 0 \\ -\sinh\xi & \cosh\xi & 0 & 0 \\ 0 & 0 & 1 & 0 \\ 0 & 0 & 0 & 1 \end{bmatrix},
\tag{A.10}
$$

where $\sinh\xi = -v\gamma/c$.

In this way the Lorentz transformation also can be expressed as

$$
\begin{aligned}
L(p)^0{}_0 &= \cosh\xi &&= \gamma, \\
L(p)^0{}_1 &= -\sinh\xi &&= -v_x\gamma/c = p^1/Mc = L(p)^1{}_0, \\
L(p)^1{}_1 &= \cosh\xi &&= \gamma = \delta_{11} + (\gamma-1)p^1p^1/\left((p^1)^2 + (p^2)^2 + (p^3)^2\right), \\
L(p)^2{}_2 &= 1 &&= \delta_{22} + (\gamma-1)p^2p^2/\left((p^1)^2 + (p^2)^2 + (p^3)^2\right), \\
L(p)^3{}_3 &= 1 &&= \delta_{33} + (\gamma-1)p^3p^3/\left((p^1)^2 + (p^2)^2 + (p^3)^2\right), \\
L(p)i_k &= 0 &&= \delta_{ik} + (\gamma-1)p^ip^k/|\vec{p}|^2, \text{ para } i, k = 2, 3,
\end{aligned}
\tag{A.11}
$$

where

$$
\begin{aligned}
v_x &= v, \\
v_y &= v_z = p^2 = p^3 = 0, \\
|\vec{p}| &= \sqrt{(p^1)^2 + (p^2)^2 + (p^3)^2}, \\
\gamma &= (1 - v_x^2/c^2)^{-1/2} = \sqrt{|\vec{p}|^2 + M^2c^2}/Mc.
\end{aligned}
\tag{A.12}
$$

---

[3]This substitution by hyperbolic functions was introduced by the very first time by Hermann Minkonski [89] in 1908 in his article "The Basic Equations of Electromagnetic Processes in Moving Bodies".

■

This is the boost in x-direction. It is easy to show that Eq. (3.8) has this form for a boost in any selected direction, after following the previous procedure.

Appendix B

Wigner Rotation

B.1 Wigner rotation definition

In the Section 3.1.1 we have a particle with a quantum state $|k, \sigma\rangle$ described in its own frame. The particle leaves the laboratory frame in x-direction with a speed v. In the frame of the laboratory the quantum state is $|p, \sigma\rangle = U(L(p))|k, \sigma\rangle$.

Later, an observer moves away from the laboratory in z-direction with speed V. Then, we want to get the unitary operator $U(\Lambda)$ that describe the quantum state of the particle with respect the a moving observer, where Λ is the Lorentz transformation which connects the moving observer frame with the laboratory frame.

Thus, the quantum state must be described by

$$|p', \sigma'\rangle = U(\Lambda)|p, \sigma\rangle, \tag{B.1}$$

where the primed state of the left is the state that see the moving observer, meanwhile the unprimed state is the laboratory description.

Now we can introduce the equivalence of the state in laboratory frame, that is, $|p, \sigma\rangle = U(L(p))|k, \sigma\rangle$, then

$$|p', \sigma'\rangle = U(\Lambda)U(L(p))|k, \sigma\rangle. \tag{B.2}$$

As we now, the product of two unitary operators is another unitary operator [75] which satisfy the condition $U(T_2)U(T_1)|\psi\rangle = U(T_2 T_1)|\psi\rangle$. Therefore

$$|p', \sigma'\rangle = U(\Lambda L(p))|k, \sigma\rangle. \tag{B.3}$$

Thus, it is possible to introduce a product of two unitary operators which effect is null,

that is, $U(T^{-1})U(T)|\psi\rangle = |\psi\rangle$. This is equivalent to multiply by a unitary matriz, i.e. $U(T^{-1})U(T) = U(T^{-1}T) = \mathbf{1}$. Thus, we can apply this kind of operator in Eq. (B.3).

$$|p', \sigma'\rangle = U\Big(L(\Lambda p)^{-1}L(\Lambda p)\Big)U(\Lambda L(p))|k, \sigma\rangle, \qquad (B.4)$$

where Λp is the Lorentz transformation that connects the 4-momentum $p^{\mu'}$, which is measured by the moving observer with el 4-momentum measured by the laboratory p^μ. That is, $p^{\mu'} = \Lambda^\mu{}_\nu p^\nu = (\Lambda p)^\mu$.

Now we can separate and arrange terms of Eq. (B.3) in order to get

$$\begin{aligned}|p', \sigma'\rangle &= U(L(\Lambda p)^{-1})U(L(\Lambda p))U(\Lambda)U(L(p))|k, \sigma\rangle \\ &= U(L(\Lambda p))\Big[U\Big(L(\Lambda p)^{-1}\Lambda L(p)\Big)\Big]|k, \sigma\rangle.\end{aligned} \qquad (B.5)$$

Finally it can be expressed as

$$|p', \sigma'\rangle = U(L(\Lambda p))U(W(\Lambda, p))|k, \sigma\rangle, \qquad (B.6)$$

$\blacksquare$

This way it is proved that $W(\Lambda, p) = L(\Lambda p)^{-1}\Lambda L(p)$ in Eq. (3.9). The product of Lorentz transformations $W(\Lambda, p)$ is known as Wigner rotation, in honor of the work of Eugene Wigner of 1939 *On unitary representations of the inhomogeneous Loretz group* [29].

The previous procedure can be summarized in the flow chart of the Figure B.1.

B.2 Wigner rotation for two inertial observers

In order to get the equation (3.13) from the Wigner rotation (3.9) for inertial observers, we will follow the flow chart of Fig. B.1.

In the "rest" frame of a particle[1], the 4-momentum is described by

$$k^\mu = (Mc, 0, 0, 0). \qquad (B.7)$$

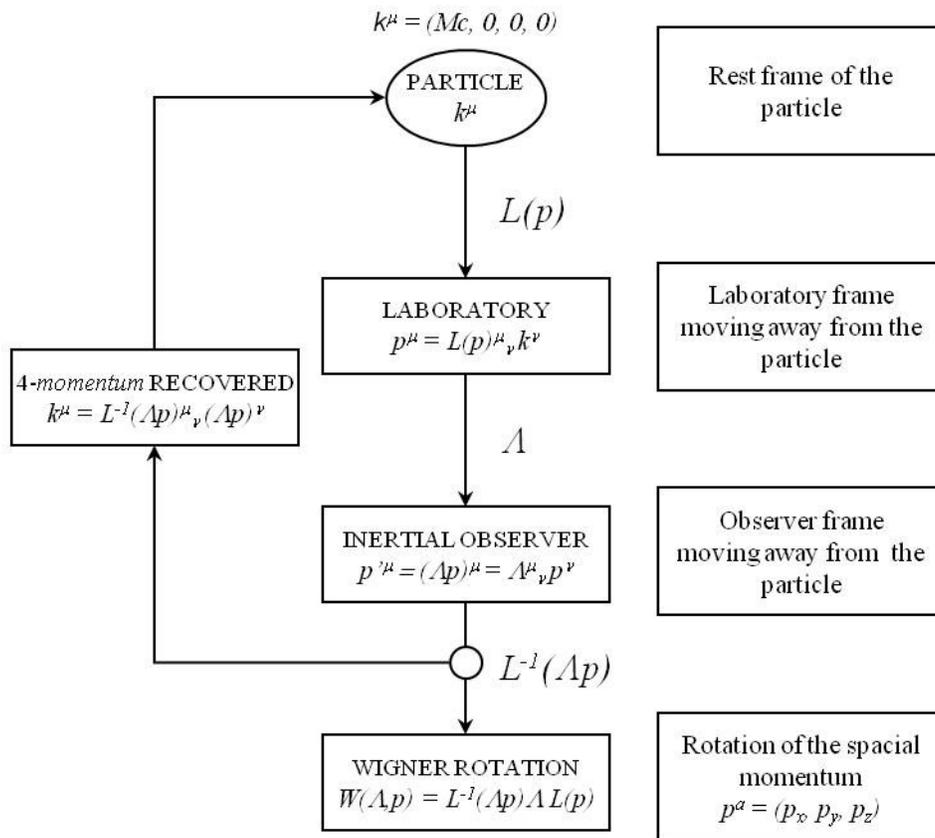[1]That is, the 4-momentum of the particle that an observer mounted in the particle measures itself.

Figure B.1: Flow chart from Lorentz transformations to Wigner rotation.

A Lorentz transformation (see Appendix A)

$$L(p) = \begin{bmatrix} \cosh\xi & \sinh\xi & 0 & 0 \\ \sinh\xi & \cosh\xi & 0 & 0 \\ 0 & 0 & 1 & 0 \\ 0 & 0 & 0 & 1 \end{bmatrix} \tag{B.8}$$

is then applied to get the 4-momentum $p^\mu = L(p)^\mu{}_\nu k^\nu$ of the laboratory that moves away relative to the particle in x-direction to the left, with speed $\tanh\xi = v/c$, that is,

$$p^\mu = (Mc\cosh\xi, Mc\sinh\xi, 0, 0). \tag{B.9}$$

After that in a similar way, an another Lorentz transformation

$$\Lambda = \begin{bmatrix} \cosh\chi & 0 & 0 & -\sinh\chi \\ 0 & 1 & 0 & 0 \\ 0 & 0 & 1 & 0 \\ -\sinh\chi & 0 & 0 & \cosh\chi \end{bmatrix} \tag{B.10}$$

is applied now over p^μ to get the 4-momentum $p^{\mu'} = \Lambda^\mu{}_\nu p^\nu$ of the particle as a inertial observer measures it when he/she moves away from the laboratory in the positive z-direction, with speed $\tanh\chi = V/c$:

$$p^{\mu'} = Mc(\cosh\sigma, \cos\theta\sinh\sigma, 0, \sin\theta\sinh\sigma), \tag{B.11}$$

where in a convenient way [23] it has been substituted

$$\begin{aligned} \cosh\sigma &= \cosh\chi\cosh\xi, \\ \sinh\sigma &= \sqrt{\cosh^2\chi\cosh^2\xi - 1}, \\ \sin\theta &= -\sinh\chi\cosh\xi/\sinh\sigma, \\ \cosh\theta &= \sinh\xi/\sinh\sigma. \end{aligned} \tag{B.12}$$

The 4-momentum $p^{\mu'}$ we call Λp. Next we apply to this momentum the standard Lorentz transformation $L(\Lambda p)$, which takes $k \to \Lambda p$ from the rest directly. From Eq. (3.8) we know

that $p^1 = \cos\theta \sinh\sigma$ and $p^3 = \sin\theta \sinh\sigma$, thus

$$
L(\Lambda p) = \begin{bmatrix}
\cosh\sigma & \cos\theta \sinh\sigma & 0 & \sin\theta \sinh\sigma \\
\cos\theta \sinh\sigma & 1 + (\cosh\sigma - 1)\cos^2\theta & 0 & (\cosh\sigma - 1)\cos\theta \sin\theta \\
0 & 0 & 1 & 0 \\
\sin\theta \sinh\sigma & (\cosh\sigma - 1)\cos\theta \sin\theta & 0 & 1 + (\cosh\sigma - 1)\sin^2\theta
\end{bmatrix}.
\tag{B.13}
$$

But its inverse matrix is the transformation of our interest to get the Wigner rotation, therefore

$$
L^{-1}(\Lambda p) = \begin{bmatrix}
\cosh\sigma & -\cos\theta \sinh\sigma & 0 & -\sin\theta \sinh\sigma \\
-\cos\theta \sinh\sigma & 1 + (\cosh\sigma - 1)\cos^2\theta & 0 & (\cosh\sigma - 1)\cos\theta \sin\theta \\
0 & 0 & 1 & 0 \\
-\sin\theta \sinh\sigma & (\cosh\sigma - 1)\cos\theta \sin\theta & 0 & 1 + (\cosh\sigma - 1)\sin^2\theta
\end{bmatrix}.
\tag{B.14}
$$

Then, is easy to show that the $L^{-1}(\Lambda p)^\mu{}_\nu (\Lambda p)^\nu = k^\mu$, as is concluded in the Fig. B.1.

In order to calculate the Wigner rotation, there is required the matrix product must satisfy

$$
\Lambda L(p) = \begin{bmatrix}
\cosh\xi \cosh\chi & \sinh\xi \cosh\chi & 0 & -\sinh\chi \\
\sinh\xi & \cosh xi & 0 & 0 \\
0 & 0 & 1 & 0 \\
-\sinh\xi \sinh\chi & \sinh\xi \sinh\chi & 0 & \cosh\chi
\end{bmatrix}.
\tag{B.15}
$$

Thus, the Wigner rotation obtained (3.9) for this case is

$$
W(\Lambda, p) = \begin{bmatrix}
1 & 0 & 0 & 0 \\
0 & \dfrac{\cosh\xi + \cosh\chi}{\cosh\xi \cosh\chi - 1} & 0 & \dfrac{\sinh\xi \sinh\chi}{\cosh\xi \cosh\chi - 1} \\
0 & 0 & 1 & 0 \\
0 & -\dfrac{\sinh\xi \sinh\chi}{\cosh\xi \cosh\chi - 1} & 0 & \dfrac{\cosh\xi + \cosh\chi}{\cosh\xi \cosh\chi - 1}
\end{bmatrix}.
\tag{B.16}
$$

In order to confirm that the Wigner rotation is reduced to a rotation around the y-axis, we can choose a spatial vector $z^\mu = (0, 0, 0, 1)$, which is mounted in the rest frame of the

particle. The product $W(\Lambda, p)^{\mu}{}_{\nu} z^{\nu}$ is given by

$$
W z = \begin{bmatrix} 0 \\ \dfrac{\sinh \xi \sinh \chi}{\cosh \xi \cosh \chi - 1} \\ 0 \\ \dfrac{\cosh \xi + \cosh \chi}{\cosh \xi \cosh \chi - 1} \end{bmatrix}.
\tag{B.17}
$$

This last result represents a pure rotation around the y-axis, because the two boost in Eq. (B.15) are in the plane xz [23]. This new vector $z^{\mu'} = (Wz)^{\mu}$ has components only in the axes x and z, with an rotation angle δ relative to the reference frame of the particle defined as

$$
\tan \delta = \frac{\sinh \xi \sinh \chi}{\cosh \xi + \cosh \chi}.
\tag{B.18}
$$

∎

Bibliography

[1] A. Einstein, B. Podolsky, and N. Rosen. Can quantum-mechanical description of physical reality be considered complete? *Phys. Rev.*, 47:777–780, 1935.

[2] D. Bohm and Y. Aharonov. Discussion of Experimental Proof for the Paradox of Einstein, Rosen, and Podolsky. *Phys.Rev.*, 108:1070–1076, 1957.

[3] J.S. Bell. On the Einstein Podolsky Rosen paradox. *Physics*, 1:195–200, 1964.

[4] Stuart J. Freedman and John F. Clauser. Experimental Test of Local Hidden-Variable Theories. *Phys.Rev.Lett.*, 28:938–941, 1972.

[5] Alain Aspect, Philippe Grangier, and Gérard Roger. Experimental Tests of Realistic Local Theories via Bell's Theorem. *Phys. Rev. Lett.*, 47:460–463, Aug 1981.

[6] W. Tittel, J. Brendel, H. Zbinden, and N. Gisin. Violation of Bell inequalities by photons more than 10 km apart. *Phys.Rev.Lett.*, 81:3563–3566, 1998.

[7] Sandu Popescu. Bell's inequalities versus teleportation: What is nonlocality? *Phys. Rev. Lett.*, 72:797–799, Feb 1994.

[8] Charles H. Bennett, Gilles Brassard, Claude Crepeau, Richard Jozsa, Asher Peres, et al. Teleporting an unknown quantum state via dual classical and Einstein-Podolsky-Rosen channels. *Phys.Rev.Lett.*, 70:1895–1899, 1993.

[9] G. Brassard, P. Horodecki, and T. Mor. TelePOVM -A generalized quantum teleportation scheme. *IBM J. Res. Dev.*, 48:87, 2004.

[10] Richard Jozsa. Entanglement and quantum computation. In S. Huggett and et.al., editors, *Geometric Issues in the Foundations of Science*. Oxford University Press, 1997. quant-ph/9707034.

[11] Robert Raussendorf and Hans J. Briegel. A one-way quantum computer. *Phys. Rev. Lett.*, 86:5188–5191, May 2001.

[12] D. Gottesman and I. L. Chuang. Quantum teleportation is a universal computational primitive. *Nature*, 402:390–393, 1999.

[13] R. Laflamme E. Knill and G. J. Milburn. A scheme for efficient quantum computation with linear optics. *Nature*, 409:46–52, 2001.

[14] Artur K. Ekert. Quantum cryptography based on Bell's theorem. *Phys. Rev. Lett.*, 67:661–663, Aug 1991.

[15] Charles H. Bennett, Gilles Brassard, and N. David Mermin. Quantum cryptography without bell's theorem. *Phys. Rev. Lett.*, 68:557–559, Feb 1992.

[16] R. Colella, A. W. Overhauser, and S. A. Werner. Observation of gravitationally induced quantum interference. *Phys.Rev.Lett.*, 34:1472–1474, 1975.

[17] A. Peters, K. Y. Chung, and S. Chu. Measurement of gravitational acceleration by dropping atoms. *Nature*, 400:849, 1999.

[18] T. L. Gustavson, A. Landragin, and M. A. Kasevich. Rotation sensing with a dual atom-interferometer Sagnac gyroscope. *Class. Quantum Grav.*, 17:2385, 2000.

[19] S. W. Hawking. Black hole explosions. *Nature*, 248:30–31, 1974.

[20] S. W. Hawking. Particle Creation by Black Holes. *Commun.Math.Phys.*, 43:199–220, 1975.

[21] N. D. Birrell and P. C. Davies. *Quantum Fields in Curved Space*. Cambridge University Press, London, 1982.

[22] R. M. Wald. *Quantum Field Theory in Curved Spacetime and Black Hole Thermodynamics*. The University of Chicago Press, Chicago, 1994.

[23] P. M. Alsing and G. J. Milburn. On entanglement and Lorentz transformations. *Quantum Inf. Compu.*, 2:487–512, 2002.

[24] H. Terashima and M. Ueda. Einstein-Podolsky-Rosen correlation seen from moving observers. *Quantum Inf. Comput.*, 3:224–228, 2003.

[25] Jakub Rembieliński and Kordian Andrzej Smoliński. Einstein-Podolsky-Rosen correlations of spin measurements in two moving inertial frames. *Phys. Rev. A*, 66:052114, Nov 2002.

[26] Robert M. Gingrich and Christoph Adami. Quantum entanglement of moving bodies. *Phys. Rev. Lett.*, 89:270402, Dec 2002.

[27] Doyeol Ahn, Hyuk-jae Lee, Young Hoon Moon, and Sung Woo Hwang. Relativistic entanglement and Bell's inequality. *Phys. Rev. A*, 67:012103, Jan 2003.

[28] Hui Li and Jiangfeng Du. Relativistic invariant quantum entanglement between the spins of moving bodies. *Phys. Rev. A*, 68:022108, Aug 2003.

[29] E. P. Wigner. On unitary representations of the inhomogeneous Loretz group. *Ann. Math.*, 40:149, 1939.

[30] S. Weinberg. *The Quantum Theory of Fields Vol. 1: Foundations*. Cambridge University Presss, 1995.

[31] Hiroaki Terashima and Masahito Ueda. Einstein-Podolsky-Rosen correlation in a gravitational field. *Phys. Rev.*, A69:032113, 2004.

[32] Jackson Said and Kristian Zarb Adami. Einstein-podolsky-rosen correlation in kerr-newman spacetime. *Phys. Rev. D*, 81:124012, Jun 2010.

[33] Felipe Robledo-Padilla and Hugo García-Compeán. Entangled spinning particles in charged and rotating black holes. *Physics Essays*, 26:1–21, 2013.

[34] J. F. Plebański and M. Demiański. Rotating, charged, and uniformly accelerating mass in general relativity. *Annals Phys.*, 98:98–127, 1976.

[35] D. Kramer, H. Stephani, M. MacCallum, and E. Herlt. *Exact Solutions of Einstein's Field Equations, 1st edition*. Cambridge University Presss, 1980.

[36] J. B. Griffiths and Jiri Podolsky. Accelerating and rotating black holes. *Class.Quant.Grav.*, 22:3467–3480, 2005.

[37] J. B. Griffiths and J. Podolsky. Global aspects of accelerating and rotating black hole space-times. *Class.Quant.Grav.*, 23:555–568, 2006.

[38] J. Podolsky and J. B. Griffiths. Accelerating Kerr-Newman black holes in (anti-)de Sitter space-time. *Phys.Rev.*, D73:044018, 2006.

[39] J. B. Griffiths and J. Podolsky. A New look at the Plebanski-Demianski family of solutions. *Int.J.Mod.Phys.*, D15:335–370, 2006.

[40] J. B. Griffiths and J. Podolský. *Exact Space-Times in Einstein's General Relativity*. Cambridge University Press, 2009.

[41] Dietmar Klemm. Rotating black branes wrapped on Einstein spaces. *JHEP*, 9811:019, 1998.

[42] Marco M. Caldarelli, Guido Cognola, and Dietmar Klemm. Thermodynamics of Kerr-Newman-AdS black holes and conformal field theories. *Class.Quant.Grav.*, 17:399–420, 2000.

[43] M.H. Dehghani. Rotating topological black holes in various dimensions and AdS / CFT correspondence. *Phys.Rev.*, D65:124002, 2002.

[44] W. Chen, H. Lu, and C.N. Pope. Kerr-de Sitter black holes with NUT charges. *Nucl.Phys.*, B762:38–54, 2007.

[45] W. Chen, H. Lu, and C.N. Pope. General Kerr-NUT-AdS metrics in all dimensions. *Class.Quant.Grav.*, 23:5323–5340, 2006.

[46] Don N. Page, David Kubiznak, Muraari Vasudevan, and Pavel Krtous. Complete integrability of geodesic motion in general Kerr-NUT-AdS spacetimes. *Phys.Rev.Lett.*, 98:061102, 2007.

[47] O.P. Santillan. Tri-Sasaki 7-metrics fibered over a QK limit Plebanski-Demianski metrics. *hep-th/0701126*, 2007.

[48] David Kubiznak and Pavel Krtous. On conformal Killing-Yano tensors for Plebanski-Demianski family of solutions. *Phys.Rev.*, D76:084036, 2007.

[49] Pavel Krtous, Valeri P. Frolov, and David Kubiznak. Hidden Symmetries of Higher Dimensional Black Holes and Uniqueness of the Kerr-NUT-(A)dS spacetime. *Phys.Rev.*, D78:064022, 2008.

[50] Marco Cariglia, Pavel Krtous, and David Kubiznak. Dirac Equation in Kerr-NUT-(A)dS Spacetimes: Intrinsic Characterization of Separability in All Dimensions. *Phys.Rev.*, D84:024008, 2011.

[51] Dietmar Klemm and Masato Nozawa. Supersymmetry of the C-metric and the general Plebanski-Demianski solution. *Journal of High Energy Physics*, 2013(5):1–21, 2013.

[52] Valeria Kagramanova, Jutta Kunz, and Claus Lammerzahl. Charged particle interferometry in Plebanski-Demianski space-times. *Class.Quant.Grav.*, 25:105023, 2008.

[53] J. Audretsch and C. Lämmerzahl. Local and nonlocal measurements of the Riemann Tensor. *Gen. Rel. Grav.*, 15:495, 1983.

[54] Hiroaki Terashima and Masahito Ueda. Spin decoherence by spacetime curvature. *J. Phys.*, A38:2029, 2005.

[55] Amir D. Aczel. *Entanglement.* Four Walls Eight Windows, 2002.

[56] N. Bohr. Can Quantum-Mechanical Description of Physical Reality be Considered Complete? *Physical Review*, 48:696–702, 1935.

[57] Gennaro Auletta. *Foundations and Interpretation of Quantum Mechanics*. World Scientific, 2009.

[58] J. J. Sakurai. *Modern Quantum Mechanics.* Addison-Wesley, 1994.

[59] Carl A. Kocher and Eugene D. Commins. Polarization Correlation of Photons Emitted in an Atomic Cascade. *Phys.Rev.Lett.*, 18:575–577, 1967.

[60] J. I. Cirac and P. Zoller. Preparation of macroscopic superpositions in many-atom systems. *Phys. Rev. A*, 50:R2799–R2802, Oct 1994.

[61] Amit Goswami. *Quantum Mechanics.* Waveland Press, Inc., 2003.

[62] Alan Aspect. Introduction: John Bell and the second quantum revolution. In J. S. Bell, editor, *Speakable and Unspeakable in Quantum Mechanics*. Cambridge University Press, 2004.

[63] Ramon Lapiedra. *Las carencias de la Realidad.* Tusquets Editores, 2008.

[64] Alain Aspect, Philippe Grangier, and Gérard Roger. Experimental Realization of Einstein-Podolsky-Rosen-Bohm *gedankenexperiment*: A New Violation of Bell's Inequalities. *Phys. Rev. Lett.*, 49:91–94, Jul 1982.

[65] Alain Aspect, Jean Dalibard, and Gérard Roger. Experimental Test of Bell's Inequalities Using Time-Varying Analyzers. *Phys. Rev. Lett.*, 49:1804–1807, Dec 1982.

[66] N. David Mermin. Is the moon there when nobody looks? Reality and the quantum theory. *Physics Today*, 38:38, 1985.

[67] Stephen W. Hawking. *Historia del Tiempo.* Editorial Crítica, 1988.

[68] Albert Einstein. *Relativity.* Three River Press, 1961.

[69] R. M. Wald. *General Relativity*. The University of Chicago Press, 1984.

[70] Charles W. Misner, Kip S. Thorne, and John Archibald Wheeler. *Gravitation*. W. H. Freeman and Company, 1973.

[71] Robert M. Wald. *Espacio, Tiempo y Gravitación: La teoría del "Big Bang" y los agujeros negros*. Fondo de Cultura Económica, 1998.

[72] Asher Peres and Daniel R. Termo. Quantum information and relativity theory. *Rev. Mod. Phys.*, 76:93–123, 2004.

[73] Horst von Borzeszkowski and Michael B. Mensky. EPR effect in gravitational field: nature of non-locality. *Phys. Lett. A*, 269:197–203, 2000. eprint arXiv:quant-ph/0007085.

[74] P. M. Alsing and G. J. Stephenson Jr. The Wigner rotation for photons in an arbitrary gravitational field. *eprint arXiv:quant-ph/0902.1399*, 2009.

[75] Steven Weinberg. *Quantum Theory of Fields*. Cambridge University Press, 1995.

[76] Hiroaki Terashima and Masahito Ueda. Einstein-Podolsky-Rosen correlation seen from movieng observers. *Quantum Inf.Comput.*, 3:224–228, 2003.

[77] Mikio Nakahara. *Geometry, Topololy and Physics*. Taylor & Francis Group, 2003.

[78] P.M. Alsing, Jr. Stephenson, G.J., and P. Kilian. Spin-induced non-geodesic motion, gyroscopic precession, Wigner rotation and EPR correlations of massive spin-1/2 particles in a gravitational field. *eprint arXiv: quant-ph/0902.1396*, 2009.

[79] Bernard F. Schutz. *A first course in general relativity*. Cambridge University Press, 2000.

[80] D. Raine and E. Thomas. *Black Holes, An Introduction*. Imperial College Press, 2010.

[81] Hugo García-Compeán and Felipe Robledo-Padilla. Quantum entanglement in Plebański-Demiański spacetimes. *Class.Quant.Grav.*, 30:235012, 2013.

[82] R. H. Rietdijk and J. W. van Holten. Killing tensors and a new geometric duality. *Nucl. Phys.*, B472:472–446, 1996. eprint arXiv:hep-th/9511166v1.

[83] A. Al-Badawi and M. Halilsoy. On the physical meaning of the NUT parameter. *Gen. Rel. Grav.*, 38:1729, 2006.

[84] G.W. Gibbons and S.W. Hawking. Cosmological Event Horizons, Thermodynamics, and Particle Creation. *Phys.Rev.*, D15:2738–2751, 1977.

[85] M. Mortazavimanesh and Morteza Mohseni. Spinning particles in Schwarzschild-de Sitter space-time. *Gen.Rel.Grav.*, 41:2697–2706, 2009.

[86] J. B. Griffiths and Jiri Podolsky. Accelerating and rotating black holes. *Class.Quant.Grav.*, 22:3467–3480, 2005.

[87] J. B. Griffiths, P. Krtous, and J. Podolsky. Interpreting the C-metric. *Class.Quant.Grav.*, 23:6745–6766, 2006.

[88] J. Foster and J. D. Nightingale. *A short course in General Relativity*. Springer, 1994.

[89] Hermann Minkowski. Die grundgleichungen für die elektromagnetischen vorgänge in bewegten körpern. *Nachrichten von der Gesellschaft der Wissenschaften zu Göttingen, Mathematisch-Physikalische Klasse.*, pages 53–111, 1908.

Articles

Quantum entanglement in Plebanski-Demianski spacetimes
Co-authors: Dr. H. García-Compeán

For an Einstein-Podolsky-Rosen pair of spin-1/2 particles in circular orbits in a general axially symmetric spacetime, the spin precession angle is obtained. Hovering observers are introduced for ensuring fixed reference frames to perform suitable reliable measurements. Frame-dragging of spinning holes is explicitly incorporated relative to hovering observers. The spin-singlet state is found to be mixedwith the spin-triplet by acceleration and gravity effects, which deteriorate the perfect anti-correlation of an entangled pair of spins measured by hovering observers. Finally, an algorithm to calculate spin precession for a general axially symmetric spacetime is proposed. This algorithm is applied to study the complete list of expanding and twisting Type-D Plebanski-Demianski black holes and their descendent limiting solutions with lower parameters.

Entangled spinning particles in charged and rotating black holes
Co-authors: Dr. H. García-Compeán

Spin precession for an Einstein-Podolsky-Rosen pair of spin-1/2 massive particles in equatorial orbits around a Kerr-Newman black hole is studied. Hovering observers are introduced to ensure static reference frames to measure or prepare the spin state. These observers also guarantee a reliable direction to compare spin states in rotating black holes. The velocity of the particles due to frame-dragging is explicitly incorporated by addition of velocities with respect the hovering observers and the corresponding spin precession angle is computed. The spin-singlet state is proved to be mixed with the spin-triplet by dynamical and gravity effects, thus it is found that a perfect anticorrelation of entangled states for these observers is explicitly deteriorated. Finally, an analysis concerning the different limit cases of parameters of spin precession including the frame-dragging effects is carried out.

Mass shift of sigma-Meson in Nuclear Matter
Co-authors: Dr. J. R. Morones, Dr. A. Santos-Guevara y M. Menchaca

The propagation of sigma meson in nuclear matter is studied in the Walecka model, assuming that the sigma couples to a pair of nucleon-antinucleon states and to particle-hole

states, including the in medium effect of sigma-omega mixing. We have also considered, by completeness, the coupling of sigma to two virtual pions. We have found that the sigma meson mass decreases respect to its value in vacuum and that the contribution of the sigma omega mixing effect on the mass shift is relatively small.

Revista INGENIERÍAS, 8 de julio 2007
UANL, Facultad de Ingeniería Mecánica y Eléctrica
Los Vectores en la Física
Coautores: Dr. J. R. Morones y M. Menchaca

Tomo una aplicación como de la invarianza de forma o covarianza, se muestra cómo el uso de cuadrivectores en el espacio-tiempo, conduce a una evidente manifestación de la unificación de los campos eléctrico y magnético, mostrándolos como aspectos diferentes de una entidad única: el campo electromagnético.

Entangled spinning particles in charged and rotating black holes

Felipe Robledo-Padilla[1,a)] and Hugo García-Compeán[2,b)]

[1]*Facultad de Ciencias Físico-Matemáticas, Universidad Autónoma de Nuevo León, Ciudad Universitaria, San Nicolás de los Garza, Nuevo León 66450, Mexico*
[2]*Departamento de Física, Centro de Investigación y de Estudios Avanzados del IPN, P.O. Box 14-740, 07000 México D.F., Mexico*

Abstract: Spin precession for an Einstein–Podolsky–Rosen pair of spin-1/2 massive particles in equatorial orbits around a Kerr–Newman black hole is studied. Hovering observers are introduced to ensure static reference frames to measure or prepare the spin state. These observers also guarantee a reliable direction to compare spin states in rotating black holes. The velocity of the particles due to frame-dragging is explicitly incorporated by addition of velocities with respect the hovering observers and the corresponding spin precession angle is computed. The spin-singlet state is proved to be mixed with the spin-triplet by dynamical and gravity effects, thus it is found that a perfect anticorrelation of entangled states for these observers is explicitly deteriorated. Finally, an analysis concerning the different limit cases of parameters of spin precession including the frame-dragging effects is carried out. © *2013 Physics Essays Publication*. [http://dx.doi.org/10.4006/0836-1398-26.1.86]

Résumé: La précession de spin pour une paire EPR des particules massives avec spin 1/2 en orbites équatoriales autour d'un trou noir de Kerr–Newman est étudiée. Des observateurs stationaires sont présents pour assurer des cadres de références fixes pour mesurer et préparer l'état de spin. Ces observateurs garantissent aussi une direction fiable pour comparer des états de spin dans des trous noirs en rotation. La vitesse des particules par l'effet Lense-Thirring est explicitement incorporée par l'addition des vitesses en ce qui concerne les observateurs stationaires et l'angle de précession de spin correspondant est calculé. L'état de spin singulet est observé pour être mélangé avec l'état de spin triplet par les effets de la dynamique et de la gravitation, ainsi il a été trouvé qu'une anti-corrélation parfaite d'états intriqués est explicitement détériorée selon ces observateurs. Finalement, une analyse concernant les différents cas limites des paramètres de précession de spin incluant les effets de Lense-Thirring est effectuée.

Key words: Entanglement; EPR Particles; Bell's Inequality; Spin; Frame-Dragging; Hovering Observers; Black Hole; Kerr–Newman Spacetime; Wigner Rotation; Vierbein; Angular Momentum; Charged Body.

I. INTRODUCTION

Entanglement of quantum states is a very interesting subject which has had a great deal of attention as a fundamental issue in physics since Einstein–Podolsky–Rosen (EPR) famous paper.[1] With the work by Bohm–Aharanov[2] for spin-entangled particles and Bell's hidden variables,[3] it was possible to realize that quantum mechanics is the correct description of the quantum phenomena and eventual experimental results[4–6] confirmed this fact. In recent years, a great deal of research on entangled states has been focused on quantum communication and teleportation,[7–9] quantum computation,[10–13] and quantum cryptography.[14,15]

More recently the some general behavior of the entangled behavior of quantum states has been studied in the literature. The first steps were taken in the context of special relativity[16–21] and later they were integrated within the framework of general relativity for the Schwarzschild spacetime[22] and for the Kerr–Newman spacetime.[23]

In particular for the case of the Schwarzschild spacetime, Terashima and Ueda[22] considered a pair of spinning particles in an entangled state moving on equatorial motion. Their results showed that the acceleration and the gravitational effects spoiled the EPR correlation precisely in the directions that are the same than in nonrelativistic theory, and it apparently decreases the degree of the violation of Bell's inequality. In the mentioned remarkable paper, they also found that near the event horizon of the black hole, the spin precession is extremely fast. Consequently, it can be argued that there exists a small uncertainty in the identification of the positions of the observers leading to a fatal error in the identification of the measurement directions needed to maintain the perfect EPR correlation. This implies that the choices of the four-velocity and the vierbein (or tetrad) are very important for nonlocal communication in a curved spacetime using an EPR pair of spins.[22]

The case of a rotating and charged black hole was studied in Ref. 23. There it was considered an observer at infinity and a free falling observer and it is found that the EPR correlation is unmeasurable for both cases at the event horizon and below. The spin precession approaches negatively to

a)felipe.robledopd@uanl.edu.mx
b)compean@fis.cinvestav.mx

infinity and that result implies an impossibility to extract the EPR correlation in that region.

The aim of the present paper is to extend previous work[22,23] by considering a different kind of observers (not at infinity) and by including the frame-dragging effects explicitly. For this, we consider Kerr–Newman spacetime in a different coordinate system from that it was used in Ref. 23 and then we study the effects in the different limiting cases.

The approach we used in the present paper follows mainly that of Terashima and Ueda[22] in analysis, notations, and conventions. The main idea is to look at the structure behind a Wigner rotation on the spin quantum state, which is locally well defined in the nonrelativistic theory. This transformation must preserve quantum probabilities of finding the spin state in the particular direction measured on a local inertial frame. In order to guarantee this, the transformation changing quantum state from a point to another one must be unitary. The Wigner rotation matrix[24] precisely achieves this. The rotation is composed by infinitesimal Lorentz transformations, which consist of a boost along the radial direction and a rotation in the angle direction of the orbital particle. Finally, it is found a precession of spin of a particle moving in curved spacetime due to the acceleration of the particle by an external force and due to the difference between local inertial frames at different points.

This paper is organized as follows. Section II is an overview of the Kerr–Newman black hole, its particular metric, their local inertial frames and event horizons. In Section III, the frame-dragging is discussed and the hovering observers are introduced. Section IV formulates step by step the spin precession in circular orbits of massive particles moving in equator and Section calculates the EPR correlation by Wigner rotations due to the motion and dragging velocity of each particle over the rotating spacetime. The relativistic addition of velocities is performed by the introduction of the zero angular momentum observers (ZAMOs) as a preliminary step. Our results are discussed in Section VI in terms of the limiting values of the different parameters. Then Reissner–Nordström, Kerr, and Kerr–Newman cases are analyzed independently and with these results the Bell's inequality is analyzed, closing the section. Conclusions and final remarks are presented in Section VII.

II. ROTATING AND CHARGED BLACK HOLES: THE KERR–NEWMAN GEOMETRY

The Kerr–Newman solutions form a three-parameter family of spacetime metrics, which in Boyer–Lindquist coordinates[25,26] is given by

$$ds^2 = -\frac{\bar{\Delta}}{\Sigma}(dt - a\sin^2\theta d\phi)^2 + \frac{\Sigma}{\bar{\Delta}}dr^2 + \Sigma d\theta^2 + \frac{\sin^2\theta}{\Sigma}[adt - (r^2 + a^2)d\phi]^2, \quad (1)$$

where

$$\bar{\Delta} = r^2 - 2mr + a^2 + e^2,$$
$$\Sigma = r^2 + a^2\cos^2\theta. \quad (2)$$

The three parameters of the family are electric charge e, angular momentum a, and mass m. The spacetime metric is expressed in geometric units ($G = 1$ and $c = 1$).

When $\bar{\Delta} \to 0$ the metric coefficient $g_{rr} \to 0$, then Eq. (1) becomes problematic and the metric fails to be strongly asymptotically predictable, and thus it does not describe black holes.[25] Therefore, this metric has physical meaning when $a^2 + e^2 \leq m^2$, which is consequence of solving $\bar{\Delta} = r^2 - 2mr + a^2 + e^2 = 0$ in g_{rr}. This component of the metric establishes two possible values of r for the Kerr–Newman black holes,

$$r_\pm = m \pm \sqrt{m^2 - a^2 - e^2}, \quad (3)$$

whose horizon is denoted by r_+. As in the Schwarzschild case, $r > r_+$ is the region where we can obtain sensible causal information of the system.

An important difference in Kerr–Newman is that the horizon is below the Schwarzschild radius $r_S = 2m$, as can be seen from r_+ equation. When $a^2 + e^2 = m^2$ it is called extreme Kerr–Newman black hole, hence $r_+ = r_-$ and the horizon is placed at $r = m$.

In order to describe the motion of spinning particles in a curved spacetime, the local inertial frame at each point is defined by a vierbein chosen as[26]

$$e_0^\mu(x) = \left(\frac{r^2 + a^2}{\sqrt{\bar{\Delta}\Sigma}}, 0, 0, \frac{a}{\sqrt{\bar{\Delta}\Sigma}}\right), \quad e_1^\mu(x) = \left(0, \sqrt{\frac{\bar{\Delta}}{\Sigma}}, 0, 0\right),$$
$$e_2^\mu(x) = \left(0, 0, \frac{1}{\sqrt{\Sigma}}, 0\right), \quad e_3^\mu(x) = \left(\frac{a\sin\theta}{\sqrt{\Sigma}}, 0, 0, \frac{1}{\sqrt{\Sigma}\sin\theta}\right). \quad (4)$$

It is easy to show that this vierbein satisfies the standard conditions,[27]

$$e_a^\mu(x)e_b^\nu(x)g_{\mu\nu}(x) = \eta_{ab},$$
$$e_\mu^a(x)e_a^\nu(x) = \delta_\mu^\nu, \quad (5)$$
$$e_\mu^a(x)e_b^\mu(x) = \delta_b^a,$$

where the Latin indices are Lorentz indices and take the values 0, 1, 2, 3; the Greek indices run over the four general-coordinate labels (t, r, θ, ϕ) and Einstein's sum convention on the repeated indices is assumed.

In Ref. 23, a similar analysis was carried out, but a different vierbein was chosen, where the frame-dragging effects were not explicitly taken into account.

III. FRAME-DRAGGING

Consider a freely falling test particle with four-velocity u^μ in the exterior of a Kerr–Newman black hole. The covariant component of a four-velocity in a direction of a given symmetry (Killing vector field) is a constant. For an observer at infinite, there are two conserved quantities: the relativistic energy per unit mass $E = -u_t$ and the angular momentum per unit mass $L_z = u_\phi$.

Since $g_{\mu\nu}$ is independent of ϕ, the trajectory of the particle still conserves angular momentum u_ϕ. But the presence of $g_{t\phi} \neq 0$ in the metric introduces an important new effect on the particle trajectories.[28] The free fall test particle will acquire angular momentum as it is approaching the black hole. To see this, consider the contravariant four-velocity for a test particle, which is

$$
\begin{aligned}
\frac{dt}{d\tau} &= u^t = g^{tt}u_t + g^{t\phi}u_\phi, \\
\frac{d\phi}{d\tau} &= u^\phi = g^{t\phi}u_t + g^{\phi\phi}u_\phi.
\end{aligned}
\tag{6}
$$

This test particle would be falling now from infinite with originally zero angular momentum, i.e., $u_\phi = 0$. Despite the fact that initially the particle falls radially with no angular momentum, it acquires an angular motion during the in fall,[29] that is, from Eq. (6) the angular velocity as seen by a distant observer is given by

$$
\omega(r, \theta) = \frac{d\phi}{dt} = \frac{d\phi/d\tau}{dt/d\tau} = \frac{u^\phi}{u^t} = \frac{g^{t\phi}}{g^{tt}}.
\tag{7}
$$

Equation (7) stands for a rotating relativistic body influences the surrounding matter through its rotation. Thus a particle dropped in a Kerr-like black hole from infinity (large distances) is dragged just by the influence of gravity so that it acquires an angular velocity ω in the same direction of rotation of the black hole. This effect decreases with distance.[28] From a physical point of view, we can interpret this phenomenon as a dragging of the local inertial frames by the rotating hole. This inertial frame rotates with an angular velocity ω relative to infinity, hence it is dragged with the rotation of the hole.[29]

Consider now the same particle in circular orbit around the rotating black hole ($u_r = u_\phi = 0$). From Eq. (6), we get

$$
u_{fd}^\phi = -\frac{g_{t\phi}}{g_{\phi\phi}}u_{fd}^t = \omega u_{fd}^t,
\tag{8}
$$

where we now identify u_{fd}^μ as the velocity of the particle due to this frame-dragging. Using the normalization condition for velocities $u^\mu u_\mu = -1$, it can be shown that

$$
u_{fd}^t = \sqrt{\frac{-g_{\phi\phi}}{g_{tt}g_{\phi\phi} - (g_{t\phi})^2}}.
\tag{9}
$$

Both Eqs. (8) and (9) constitute the components of the four-velocity of a test particle due to the frame-dragging as seen by a distant observer in the general frame.

We shall see later that the spin precession angle is calculated by infinitesimal Lorentz transformations of the velocity of a particle in a local inertial frame, because the spin is only defined in this kind of frames. Then, in order to find the velocity of a particle in a local inertial frame, we will consider a convenient set of hovering observers that will be useful to measure or prepare the relevant spin states. But first, as seen by long distances observers, the contravariant four-velocity is

$$
u_h^\mu = (dt/d\tau, 0, 0, 0) = ((-g_{tt})^{-1/2}, 0, 0, 0),
\tag{10}
$$

and their covariant four-velocity is obtained by lowering indices, that is,

$$
u_{\mu_h} = \left(-\sqrt{-g_{tt}}, 0, 0, \frac{g_{t\phi}}{\sqrt{-g_{tt}}}\right).
\tag{11}
$$

On the other hand, the energy of a particle with respect to a local observer is the time component of the four-momentum of the particle in the observer's frame of reference. It is obtained by projecting out the four-momentum of the particle on the four-velocity of the observer, i.e., $mu^\mu(u_\mu)_{\text{observer}} = -E$.

Thus, the energy of the particle per unit mass due to the frame-dragging velocity with respect to a hovering observer is

$$
u_{fd}^\mu u_{\mu_h} = -E_h = -\gamma_{fd},
\tag{12}
$$

where $\gamma_{fd} = (1 - v_{fd}^2)^{-1/2}$ is the usual relativistic gamma factor, v_{fd} is the local velocity of the particle due to the frame-dragging, and E_h is the relativistic energy per unit mass of the particle relative to a stationary hovering observer. It must not be confused with the energy E as seen by an observer at infinity, at the beginning of this section.

The local velocity due to the frame-dragging is then obtained from Eq. (12), and can be expressed as $\tanh\eta = v_{fd}$.

Consequently, the local inertial velocity due to the frame-dragging and measured by a hovering observer will be

$$
u_{fd}^a = \gamma_{fd}(1, 0, 0, v_{fd}).
\tag{13}
$$

The scalar product Eq. (12), the energy per unit mass E_h, is an invariant because it takes the same value, independently of the coordinate system used to evaluate it. If we choose another observer with known velocity 4-vector, like an inertial observer or a free falling observer, he/she will measure the same energy per unit mass due to the frame-dragging of the particle, by equivalent projection Eq. (12). This physical quantity in two local frames of the same event (hovering and inertial observers for example) will be connected by a Lorentz transformation between them even though one or both of the frames may be accelerating. This follows because the instantaneous rates of clocks and lengths of rods are not affected by accelerations and depend only on the relative velocities.[29]

Then, gathering previous results for Kerr–Newman metric, we can obtain the local inertial velocity as measured by a local observer.

The angular velocity Eq. (7) on equator $\theta = \pi/2$ is

$$\omega = a\left(\frac{2mr - e^2}{(r^2 + a^2)^2 - a^2\bar{\Delta}}\right), \tag{14}$$

where positive a implies positive ω, so the particle acquires an angular velocity in the direction of the spin of the hole.

Therefore, as seen by a distant observer, the general four-velocities components u_{fd}^ϕ and u_{fd}^t can be obtained from Eqs. (8) and (9), that is,

$$u_{fd}^\mu = \left(\frac{g_{\phi\phi}}{\bar{\Delta}}\right)^{1/2}(1,0,0,\omega), \tag{15}$$

and from Eqs. (11), (12), and (15), the relativistic gamma factor and the local inertial frame velocity are

$$\gamma_{fd} = \frac{r^2\sqrt{\bar{\Delta}}}{\sqrt{(\bar{\Delta} - a^2)[(r^2 + a^2)^2 - a^2\bar{\Delta}]}}, \tag{16}$$

$$v_{fd} = a\left(\frac{r^2 + a^2 - \bar{\Delta}}{r^2\sqrt{\bar{\Delta}}}\right).$$

Finally, from Eq. (13) the local four-velocity due to frame-dragging measured by a hovering observer is

$$u_{fd}^a = \frac{1}{\sqrt{(\bar{\Delta} - a^2)[(r^2 + a^2)^2 - a^2\bar{\Delta}]}}$$
$$\times (r^2\sqrt{\bar{\Delta}}, 0, 0, a(r^2 + a^2 - \bar{\Delta})). \tag{17}$$

Now if $\tanh\eta = v_{fd}$, Eq. (17) can be re-expressed as

$$u_{fd}^a = (\cosh\eta, 0, 0, \sinh\eta), \tag{18}$$

where

$$\cosh\eta = \frac{r^2\sqrt{\bar{\Delta}}}{\sqrt{(\bar{\Delta} - a^2)[(r^2 + a^2)^2 - a^2\bar{\Delta}]}},$$

$$\sinh\eta = \frac{a(r^2 + a^2 - \bar{\Delta})}{\sqrt{(\bar{\Delta} - a^2)[(r^2 + a^2)^2 - a^2\bar{\Delta}]}}. \tag{19}$$

But it can be found a relative motion between the hovering observer and the local frame given by

$$u_h^a = \eta^{ab}e_b^\mu u_{\mu_h} = \left(\sqrt{\frac{\bar{\Delta}}{\bar{\Delta} - a^2\sin^2\theta}}, 0, 0, -\frac{a\sin\theta}{\sqrt{\bar{\Delta} - a^2\sin^2\theta}}\right)$$
$$= (\cosh\kappa, 0, 0, -\sinh\kappa), \tag{20}$$

which implies that the hovering observer is not at rest in the local frame Eq. (4).

We can remove this relative motion by a local Lorentz transformation and its inverse, that is,

$$\Lambda_b^a = \begin{pmatrix} \cosh\kappa & 0 & 0 & \sinh\kappa \\ 0 & 1 & 0 & 0 \\ 0 & 0 & 1 & 0 \\ \sinh\kappa & 0 & 0 & \sinh\kappa \end{pmatrix},$$

$$\Lambda_a^b = \begin{pmatrix} \cosh\kappa & 0 & 0 & -\sinh\kappa \\ 0 & 1 & 0 & 0 \\ 0 & 0 & 1 & 0 \\ -\sinh\kappa & 0 & 0 & \sinh\kappa \end{pmatrix}. \tag{21}$$

Therefore, we shall consider a new vierbein $\tilde{e}_a^\mu = \Lambda_a^b e_b^\mu$, expressed by

$$\tilde{e}_0^\mu(x) = \left(\sqrt{\frac{\Sigma}{\bar{\Delta} - a^2\sin^2\theta}}, 0, 0, 0\right),$$

$$\tilde{e}_1^\mu(x) = \left(0, \sqrt{\frac{\bar{\Delta}}{\Sigma}}, 0, 0\right),$$

$$\tilde{e}_2^\mu(x) = \left(0, 0, \frac{1}{\sqrt{\Sigma}}, 0\right),$$

$$\tilde{e}_3^\mu(x) = \left(-\frac{a(r^2 + a^2 - \bar{\Delta})\sin\theta}{\sqrt{\bar{\Delta}\Sigma}\sqrt{\bar{\Delta} - a^2\sin^2\theta}}, 0, 0, \frac{\sqrt{\bar{\Delta} - a^2\sin^2\theta}}{\sqrt{\bar{\Delta}\Sigma}\sin\theta}\right). \tag{22}$$

We can confirm that in the new local frame defined by Eq. (22), the hovering observer is at rest, i.e., $\tilde{u}_h^a = \eta^{ab}\tilde{e}_b^\mu u_{\mu h} = (1, 0, 0, 0)$. Also it can be confirmed the local velocity of the freely falling particle $\tilde{u}_{fd}^a = \eta^{ab}\tilde{e}_b^\mu u_{\mu fd}$ is still given by Eq. (17), which is important because we have to know the velocity due to the frame-dragging measured by a hovering observer with the right static coordinate frame. Thus, we shall use the veirbein Eq. (22) from now on.

Another feature of Kerr-like spacetime is the *static limit surface*. Consider a stationary particle, i.e., $r = \text{constant}$, $\theta = \text{constant}$, and $\phi = \text{constant}$. Thus, from spacetime metric Eq. (1), we have

$$-d\tau^2 = g_{tt}dt^2. \tag{23}$$

Then, for $g_{tt} \geq 0$ this condition cannot be fulfilled, so a massive particle cannot be stationary within the surface $g_{tt} = 0$, because, as we already know, a particle will acquire four-velocity due to the frame-dragging Eq. (6). Photons can satisfy this condition and only they can be stationary at the static limit. This is the reason why it is called static surface.

Solving the condition $g_{tt} = 0$ for r gives us the radius of the static limit surface

$$r_{st} = m + (m^2 - e^2 - a^2\cos^2\theta)^{1/2}. \tag{24}$$

This radius is showed in Fig. 1 as r_{st} and is above the horizon r_+ as we can see. It is important to emphasize that the static limit surface is not a horizon.[29] Later, we shall see why
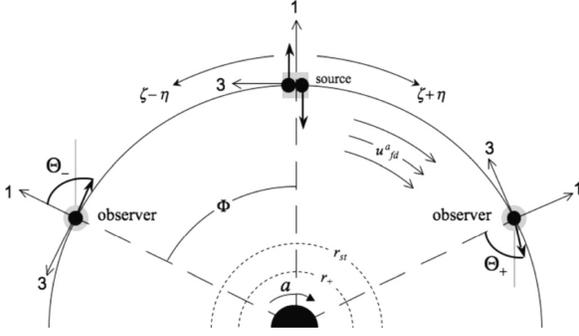
FIG. 1. An EPR gedanken experiment in the Kerr–Newman spacetime with an angular momentum parameter a. Two hovering observers (indicated by gray circles) and a static EPR source (gray square) are located at $\phi = \pm\Phi$ and 0, respectively. Both entangled particles are subject to the frame-dragging u^a_{fd} and leave the source with a local velocity $v = \tanh\xi = \tanh(\zeta \pm \eta)$ with regard to the hovering observers, which have plus sign for traveling on favor the rotation of black hole and minus for the opposite direction.

this is not a horizon for spin precession angle, but a limit for keeping the perfect anticorrelation.

IV. SPIN PRECESSION IN A KERR–NEWMAN BLACK HOLE

Now we consider massive particles with spin-1/2 in a Kerr–Newman black hole moving in a circular motion with radius r on the equatorial plane $\theta = \pi/2$. In spherical coordinates, the relevant velocity vector has two components, the temporal and the ϕ-coordinate at constant radius. The velocity vector field in Minkowski's flat-space determines the motion by the proper-velocity with $v = \tanh\xi = (1 - 1/\gamma^2)^{1/2}$, where $\gamma = (1 - v^2)^{-1/2}$.

Following Ref. 22, we will use the local velocity $u^a = (\cosh\xi, 0, 0, \sinh\xi)$. Any local vector can be described on a general reference frame through a vierbein transformation. Local velocity then transforms as $u^\mu = \tilde{e}^\mu_a u^a$. Then a general contravariant 4-velocity is obtained as

$$u^t = \frac{r}{\sqrt{\bar{\Delta} - a^2}}\cosh\xi - \frac{a(r^2 + a^2 - \bar{\Delta})}{r\sqrt{\bar{\Delta}}\sqrt{\bar{\Delta} - a^2}}\sinh\xi,$$
$$u^\phi = \frac{\sqrt{\bar{\Delta} - a^2}}{r\sqrt{\bar{\Delta}}}\sinh\xi, \tag{25}$$

and the covariant vector can be obtained by lowering indices of contravariant velocity by $u_\mu = g_{\mu\nu}u^\nu$. These velocities satisfy the normalization condition $u^\mu u_\mu = -1$ which ensure that any material particle travels with velocity lower than speed of light[1].

For the particle moving in orbital motion, we must apply an external force against the centrifugal force and the gravity. The acceleration due to this external force is given by

---

[1]By the relativistic addition of velocities, the frame-dragging velocity will be incorporated on $u^a_\pm = (\cosh\xi_\pm, 0, 0, \sinh\xi_\pm)$ in Sec. V, with the argument ξ redefined by $\xi_\pm = \zeta \pm \eta$. The positive sign corresponds to a particle corotating with respect to the rotation of the hole and negative for counter-rotation.

$$a^\mu(x) = u^\nu(x)\nabla_\nu u^\mu(x). \tag{26}$$

On equatorial plane the acceleration yields

$$a^r = \frac{1}{r^3(\bar{\Delta} - a^2)}[-\bar{\Delta}(e^2 - mr)\cosh^2\xi$$
$$+ 2\sqrt{\bar{\Delta}}a(e^2 - mr)\cosh\xi\sinh\xi$$
$$- (a^2(\bar{\Delta} + r^2 - mr) - \bar{\Delta}^2)\sinh^2\xi]. \tag{27}$$

In Section V, the frame-dragging velocity will be incorporated into velocity Eq. (25). The incorporation of the frame-dragging Eq. (17) leaves unchanged the structure of acceleration Eq. (26). This fact is due to the frame-dragging velocity u^a_{fd} is independent of t and ϕ. Thus the covariant derivatives of u^t and u^ϕ with respect to t and ϕ are not modified.

The change in the local inertial frame will be measured by χ^a_b and consists of a boost along the 1-axis and a rotation about the 2-axis and it is given by

$$\chi^a_b = -u^\nu \omega^a_{\nu b}, \tag{28}$$

where $\omega^a_{\nu b}$ are the connection one-forms which are defined as

$$\omega^a_{\mu b} = -\tilde{e}^\nu_b(x)\nabla_\mu \tilde{e}^a_\nu(x) = \tilde{e}^a_\nu(x)\nabla_\mu \tilde{e}^\nu_b(x). \tag{29}$$

In our particular situation, these connection components are easily computed,

$$\omega^0_{t1} = -\frac{(e^2 - mr)\sqrt{\bar{\Delta}}}{r^3\sqrt{\bar{\Delta} - a^2}}, \quad \omega^1_{t3} = \frac{a(e^2 - mr)}{r^3\sqrt{\bar{\Delta} - a^2}},$$
$$\omega^0_{\phi1} = \frac{a(e^2 - mr)\sqrt{\bar{\Delta}}}{r^3\sqrt{\bar{\Delta} - a^2}}, \quad \omega^1_{\phi3} = \frac{a^2r^2 - \bar{\Delta}r^2 + ma^2r - a^2e^2}{r^3\sqrt{\bar{\Delta} - a^2}}. \tag{30}$$

Therefore, the relevant boosts are described by the function,

$$\chi^0_1 = \frac{e^2 - mr}{r^2(\bar{\Delta} - a^2)}(\sqrt{\bar{\Delta}}\cosh\xi - a\sinh\xi), \tag{31}$$

while the rotation about the 2-axis is given by

$$\chi^1_3 = -\frac{1}{r^2(\bar{\Delta} - a^2)}$$
$$\times \left(a(e^2 - mr)\cosh\xi + \frac{[a^2(\bar{\Delta} + r^2 - mr) - \bar{\Delta}^2]}{\sqrt{\bar{\Delta}}}\sinh\xi\right). \tag{32}$$

Next step is to relate the boost and rotation[2] with the rotation of the local four-momentum on the plane traced by the general four-vectors of velocity and acceleration. Then we can compute the infinitesimal Lorentz transformation given by

---

[2]Which represent the change on the local inertial frame along $u^\mu(x)$.

$$\lambda_b^a(x) = -\frac{1}{m}[a^a(x)p_b(x) - p^a(x)a_b(x)] + \chi_b^a, \tag{33}$$

where the local four-momentum defined as $p^a(x) = (m\cosh\xi, 0, 0, m\sinh\xi)$.

The boost along the 1-axis and the rotation about the 2-axis are, respectively,

$$\lambda_1^0 = -\frac{\sinh\xi}{r^2\sqrt{\bar{\Delta}}(\bar{\Delta} - a^2)}$$
$$\times [A\sinh\xi\cosh\xi - B(\cosh^2\xi + \sinh^2\xi)],$$
$$\lambda_3^1 = \frac{\cosh\xi}{r^2\sqrt{\bar{\Delta}}(\bar{\Delta} - a^2)}$$
$$\times [A\sinh\xi\cosh\xi - B(\cosh^2\xi + \sinh^2\xi)], \tag{34}$$

where

$$A = \bar{\Delta}^2 - (a^2 + mr - e^2)\bar{\Delta} - a^2r^2 + a^2mr,$$
$$B = a\sqrt{\bar{\Delta}}(e^2 - mr). \tag{35}$$

Thus, we can get the change of the spin which is expressed as

$$\vartheta_k^i(x) = \lambda_k^i(x) + \frac{\lambda_0^i(x)p_k(x) - \lambda_{k0}(x)p^i(x)}{p^0(x) + m}. \tag{36}$$

In our case, it becomes a rotation about the 2-axis through an angle,

$$\vartheta_3^1 = \frac{1}{r^2\sqrt{\bar{\Delta}}(\bar{\Delta} - a^2)}[A\sinh\xi\cosh\xi - B(\cosh^2\xi + \sinh^2\xi)]. \tag{37}$$

Then, the complete rotation matrix due to the infinitesimal Lorentz transformations is given by

$$\vartheta_b^a(x) = \begin{pmatrix} 0 & 0 & 0 & 0 \\ 0 & 0 & 0 & \vartheta_3^1 \\ 0 & 0 & 0 & 0 \\ 0 & -\vartheta_3^1 & 0 & 0 \end{pmatrix}. \tag{38}$$

In nonrelativistic quantum mechanics, the only kinematic transformations of reference frames that are allowed to consider are translations and rotations, which are explicitly unitary. In relativistic quantum mechanics, one should also consider boosts, which are explicitly nonunitary. Regardless of this, the particle states undergoes an effective momentum dependent local unitary rotation under boosts governed by the *little group* of Wigner rotation for massive particles, which leaves the appropriate local rest momentum invariant. This group is SO(3) for massive particles which is the group of ordinary rotations in 3D.[16]

In the case of the curved spacetime, the quantum state of one particle $|p^a(x), \sigma; x\rangle$ transforms under a local Lorentz transformation as

$$U(\Lambda(x))|p^a(x), \sigma; x\rangle = \sum_{\sigma'} D_{\sigma'\sigma}^{(1/2)}(W(x))|\Lambda p^a(x), \sigma'; x\rangle, \tag{39}$$

where σ represents the spin state. The local Wigner rotation is calculated by $W_b^a(x) \equiv W^a{}_b(\Lambda(x), p(x))$.

If a particle moves along a path $x^\mu(\tau)$ from $x_i^\mu(\tau_i)$ to $x_f^\mu(\tau_f)$, the iteration of the infinitesimal transformation for a finite proper time gives the corresponding finite Wigner rotation,

$$W_b^a(x_f, x_i) = \lim_{N\to\infty}\prod_{k=0}^{N}\left[\delta_b^a + \vartheta_b^a(x_{(k)})\frac{h}{N}\right]$$
$$= T\exp\left(\int_{\tau_i}^{\tau_f}\vartheta_b^a(x(\tau))d\tau\right), \tag{40}$$

as proved in Ref. 22. Then a total argument Φ is computed by integrating out $\delta\phi = u^\phi d\tau$, and the operator T is not needed because ϑ_b^a is constant during the motion[3]. Therefore, the velocity u^ϕ represents a trivial rotation about the 2-axis,

$$u^\phi \equiv \varphi_3^1 = -\varphi_1^3 = \frac{\sqrt{\bar{\Delta} - a^2}}{r\sqrt{\bar{\Delta}}}\sinh\xi, \tag{41}$$

since the curved spacetime defines the parallel transport needed to compare local inertial frames from one point to another.

Thus, the Wigner rotation becomes a rotation about the 2-axis,

$$W_b^a(\pm\Phi, 0) = \exp\left(\int_0^\Phi \frac{\vartheta_b^a(x)}{\varphi_3^1(x)}d\phi\right) = \exp\left(\frac{\Phi}{u^\phi}\vartheta_b^a\right)$$
$$= \begin{pmatrix} 1 & 0 & 0 & 0 \\ 0 & \cos\Theta & 0 & \pm\sin\Theta \\ 0 & 0 & 1 & 0 \\ 0 & \mp\sin\Theta & 0 & \cos\Theta \end{pmatrix}, \tag{42}$$

where ϑ_b^a comes from Eq. (38), the angle of rotation is given by $\Theta = \Phi\vartheta_3^1/u^\phi$ and ϑ_3^1 for the Kerr–Newman spacetime was given by Eq. (37), that is,

$$\Theta = \frac{\Phi}{r(\bar{\Delta} - a^2)^{3/2}}[A\cosh\xi - B(\coth\xi\cosh\xi - \sinh\xi)]. \tag{43}$$

V. EPR CORRELATION

In the present work, we consider two observers and an EPR source on the equator plane $\theta = \pi/2$, at a fixed radius above horizon $(r > r_+)$, with azimuthal angles $\pm\Phi$ for observers and 0 for the EPR source. The observers and the EPR source are assumed to be hovering Eq. (10) over the black hole in order to keep them "at rest" in the Boyer–Linquist coordinate system (t, r, θ, ϕ) and to use the static local inertial frame Eq. (22) to measure or prepare the spin state. The inertial frame is defined at each instant since

---

[3]The Kerr metric is the unique stationary axial-symmetric vacuum solution as the Carter–Robinson theorem asserts[29] and then ϑ_b^a is independent of the time coordinate.

the observers and EPR source are accelerated to keep staying at constant radius, and they are not influenced by the frame-dragging.

The EPR source emits a pair of entangled particles in opposite directions. The particles adopt a circular orbit in the corotating frame of the black hole due to the frame-dragging Eq. (15). This frame corresponds to have a ZAMOs. The world line of these observers is orthogonal to the surface of constant t, that is, $dx_\mu u^\mu_{fd} = 0$. They have angular velocity ω as seen by a distant observer and the angular momentum of a particle is conserved in its local inertial frame. We will adopt a ZAMO observer as a preliminary step before we calculate the total local inertial velocity measured by the hovering observer. The local inertial velocity of the particles with constant four-momenta leaving the source by EPR process is $v_{\rm EPR} = \tanh\zeta$ from the point of view of a ZAMO, thus,

$$u^a_{\rm EPR} = (\cosh\zeta, 0, 0, \sinh\zeta). \qquad (44)$$

Therefore, from the point of view of a hovering observer, the particles will have a local velocity given by the relativistic addition of the velocity of ZAMOs Eq. (18) measured by this hovering observer, plus the local velocity of the particles measured by ZAMOs Eq. (44), that is, $\tanh\xi = \tanh(\zeta \pm \eta)$, where ξ comes from Section IV.

Once the particles leave the EPR source, one travels in direction of rotation of the black hole, and the other one travels in the opposite direction. Then, the final constant four-momenta is given by $p^a_\pm(x) = (m\cosh(\zeta \pm \eta), 0, 0, m\sinh(\zeta \pm \eta))$ measured by a hovering observer.

This incorporation of velocity due to the frame-dragging redefines Eq. (25) and all calculations of Section IV are consequently affected by the motion of the EPR particles. But the general structure is not modified and there appear no new terms, as previously mentioned for the acceleration computation.

Now, the spin-singlet state is defined by

$$|\psi\rangle = \frac{1}{\sqrt{2}} [|p^a_+, \uparrow; 0\rangle|p^a_-, \downarrow; 0\rangle - |p^a_+, \downarrow; 0\rangle|p^a_-, \uparrow; 0\rangle], \quad (45)$$

where for keeping a simple notation it was written only the φ coordinate in the argument. All the previous considerations are depicted in a gedanken experiment shown in Fig. 1.

After a proper time $\Phi/u^\phi_\pm$, each particle reaches the corresponding observer. The Wigner rotation Eq. (42) becomes

$$W^a_b(\pm\Phi, 0) = \begin{pmatrix} 1 & 0 & 0 & 0 \\ 0 & \cos\Theta_\pm & 0 & \pm\sin\Theta_\pm \\ 0 & 0 & 1 & 0 \\ 0 & \mp\sin\Theta_\pm & 0 & \cos\Theta_\pm \end{pmatrix}, \quad (46)$$

where the angle $\Theta_\pm$ is given by Eq. (43) with ξ substituted by $\xi_\pm = \zeta \pm \eta$. The sign depends on whether the motion of the entangled particle is in the same direction (or in the opposite sense) of the frame-dragging, that is,

$$\Theta_\pm = \frac{\Phi}{r(\bar{\Delta} - a^2)^{3/2}} [A\cosh(\zeta \pm \eta) \\ - B(\coth(\zeta \pm \eta)\cosh(\zeta \pm \eta) - \sinh(\zeta \pm \eta))]. \quad (47)$$

The Wigner rotation is represented in terms of the Pauli's matrix σ_y as

$$D^{(1/2)}_{\sigma'\sigma}(W(\pm\Phi, 0)) = \exp\left(\mp i\frac{\sigma_y}{2}\Theta_\pm\right). \qquad (48)$$

Therefore, each particle state is transformed by the corresponding Wigner rotation, and the new total state is given by $|\psi'\rangle = W(\pm\Phi)|\psi\rangle$. Hence, in the local inertial frame at $\phi = +\Phi$ and $-\Phi$, each particle state is transformed separately by

$$|p^a_\pm, \uparrow; \pm\Phi\rangle' = \cos\frac{\Theta_\pm}{2}|p^a_\pm, \uparrow; \pm\Phi\rangle \pm \sin\frac{\Theta_\pm}{2}|p^a_\pm, \downarrow; \pm\Phi\rangle, \qquad (49)$$

$$|p^a_\pm, \downarrow; \pm\Phi\rangle' = \mp\sin\frac{\Theta_\pm}{2}|p^a_\pm, \uparrow; \pm\Phi\rangle + \cos\frac{\Theta_\pm}{2}|p^a_\pm, \downarrow; \pm\Phi\rangle, \qquad (50)$$

and the entangled state is described by

$$|\psi\rangle' = \frac{1}{\sqrt{2}}\left[\cos\left(\frac{\Theta_+ + \Theta_-}{2}\right)(|p^a_+, \uparrow; \Phi\rangle|p^a_-, \downarrow; -\Phi\rangle \right. \\ - |p^a_+, \downarrow; \Phi\rangle|p^a_-, \uparrow; -\Phi\rangle) + \sin\left(\frac{\Theta_+ + \Theta_-}{2}\right) \\ \left. \times (|p^a_+, \uparrow; \Phi\rangle|p^a_-, \uparrow; \Phi-\rangle + |p^a_+, \downarrow; \Phi\rangle|p^a_-, \downarrow; -\Phi\rangle)\right]. \qquad (51)$$

This result includes the trivial rotation of the local inertial frames $\pm\Phi$, and it can be eliminated by rotating the basis at $\phi = \pm\Phi$ about the 2-axis through the angles $\mp\Phi$, respectively, consequently we have

$$|p^a_\pm, \uparrow; \pm\Phi\rangle'' = \cos\frac{\Phi}{2}|p^a_\pm, \uparrow; \pm\Phi\rangle \pm \sin\frac{\Phi}{2}|p^a_\pm, \downarrow; \pm\Phi\rangle, \qquad (52)$$

$$|p^a_\pm, \downarrow; \pm\Phi\rangle'' = \mp\sin\frac{\Phi}{2}|p^a_\pm, \uparrow; \pm\Phi\rangle + \cos\frac{\Phi}{2}|p^a_\pm, \downarrow; \pm\Phi\rangle. \qquad (53)$$

In this basis, the state is written as follows:

$$|\psi\rangle'' = \frac{1}{\sqrt{2}}[\cos\Delta(|p^a_+, \uparrow; \Phi\rangle'|p^a_-, \downarrow; -\Phi\rangle' \\ - |p^a_+, \downarrow; \Phi\rangle'|p^a_-, \uparrow; -\Phi\rangle') \\ + \sin\Delta(|p^a_+, \uparrow; \Phi\rangle'|p^a_-, \uparrow; \Phi-\rangle' \\ + |p^a_+, \downarrow; \Phi\rangle'|p^a_-, \downarrow; -\Phi\rangle')], \qquad (54)$$

where $\Delta = (\Theta_+ + \Theta_-)/2 - \Phi$. After some computations, the angle Δ is simplified and it yields

$$\Delta = \Phi\left\{\frac{\cosh\eta}{r(\bar{\Delta} - a^2)^{3/2}}\left[A\cosh\zeta - B\sinh\zeta \right.\right. \\ \left.\left. \times\left(\frac{2\cosh^2\zeta - \cosh^2\eta - \sinh^2\eta}{\cosh^2\zeta - \cosh^2\eta}\right)\right] - 1\right\}. \qquad (55)$$

This is precisely the general relativistic effect that deteriorates the perfect anticorrelation in the directions that would be the same as each other if the spacetime were flat with nonrelativistic particles. The spin-singlet state is mixed with the spin-triplet state. This is because while the spin-singlet state is invariant under spatial rotations, it is not invariant under Lorentz transformations Eq. (34).

This deterioration of the perfect anticorrelation is consequence of the manifest difference between the rotation matrix element ϑ_3^1 and trivial rotation ϕ_3^1. It is important to note that the entanglement is still invariant under local unitary operations, and then it does not mean to spoil the nonlocal correlation. Because the relativistic effect arises from acceleration and gravity, the perfect anticorrelation can be still employed for quantum communication, by rotating the direction of measurement about the 2-axis through the angles $\mp \Theta$ in the local inertial frames of the hovering observers. The parallel transport in general relativity Eq. (28) does not give the directions that maintain the perfect anticorrelation, because the rotation matrix elements Eq. (38) and the components of the change in local inertial frame Eq. (28) do not coincide.

VI. KERR–NEWMAN SPIN PRECESSION RESULTS

As Terashima and Ueda showed[22] for a Schwarzschild black hole, the acceleration and gravity deteriorate the EPR correlation for particles in a circular motion in equatorial plane. We summarize their results by describing in four important regions relative to the black hole plotted in Fig. 2.

- Region I: $r \rightarrow \infty$, $v \rightarrow 0$, or far away the black hole (no gravitational effects) and static particles. This region corresponds to the nonrelativistic limit, where there are no corrections to quantum mechanics and where EPR proposed their *gedanken* experiment.[1] The precession angle vanishes ($\Delta = 0$) and we get the maximal violation of Bell's inequality.
- Region II: $r \rightarrow \infty$, $v \rightarrow 1$, it is still far away from the black hole but relativistic corrections should be taken into

FIG. 2. The angle Δ/Φ for a Schwarzschild black hole as function of $2m/r$ and v, which is asymptotic to the event horizon $r_s = 2m$, indicated by a dotted line. Dashed line depicted the path $r = r_0$ which the spin precession Δ vanishes.

account, which were also studied by Terashima and Ueda in Ref. 17. The angle Δ is positive and becomes infinite. It is not possible to maintain perfect anticorrelation and the particles cannot be used for quantum communication.
- Region III: $r \rightarrow r_s$, where $r_s = 2m$ is the Schwarzschild radius (event horizon). Independently of local inertial velocity of the particles, the precession angle becomes infinite ($\Delta \rightarrow -\infty$). The static observers cannot extract the EPR correlation from circularly moving particles unless they have infinite accuracy in their own positions. To exploit the EPR correlation on and beyond the horizon, the observers must choose a four-velocity and a nonsingular vierbein at the horizon, and thus the observers must fall into the black hole together with the particles.
- Region IV: Although acceleration and gravity deteriorate the EPR correlation as Terashima and Ueda showed, it is still possible to find a combination of local inertial velocity and position respect to the black hole that keeps the perfect anticorrelation. They defined a path where at radius $r = r_0$ the angle Δ vanishes. We will identify this path as an additional region and it is between the other three regions.

Between these regions one can find values of the angle (positive or negative) Δ, which deteriorates the perfect anticorrelation in the directions that would be the same as each other if the spacetime were flat.

We shall compare the Schwarzschild and Kerr–Newman spacetimes and we will find interesting differences. Also, with the results of Section V, we will analyze the influence of each parameter on the spin precession. There will be remarkable differences among these regions.

The parameters presented in figures are rates of the relevant parameter with respect to m, thus the mass parameter is used as a reference to express the charge and angular momentum ratio, represented by e/m for electric charge, a/m for angular momentum. One of the axis plots $v = v_{EPR}$ for the local inertial velocity due to the EPR process and $0 < m/r < 1$ for distance, with 0 corresponding to r at infinite and 1 for $r = m$, which is the smaller distance reached for extreme black holes.

A. Reissner–Nordström case

This case corresponds to a Schwarzschild black hole with a nonvanishing charge e. From the Kerr–Newman spacetime, when $a = 0$, we recover the Reissner–Nordström solutions and spin precession Eq. (55) reduces to

$$\Delta_{RN} = \Phi \left[\frac{r^2 - 3mr + 2e^2}{r\sqrt{r^2 - 2mr + e^2}} \cosh \zeta - 1 \right]. \quad (56)$$

This expression has physical meaning when $e \leq m$, which is a direct consequence from the event horizon Eq. (3) for black holes.

The angle Δ on Eq. (56) is plotted in Fig. 3 as function of the distance and local velocity $v = v_{EPR}$. When $m/r \rightarrow 0$ the experiment is placed far away from the black hole ($r \rightarrow \infty$), and $m/r = 1$ corresponds to the limit of distance that we can reach for an extreme black hole with charge $e = m$. When
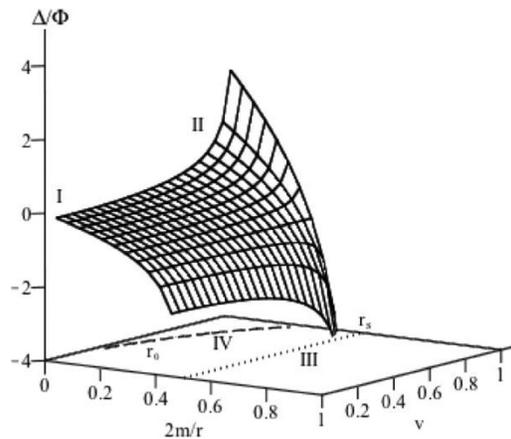
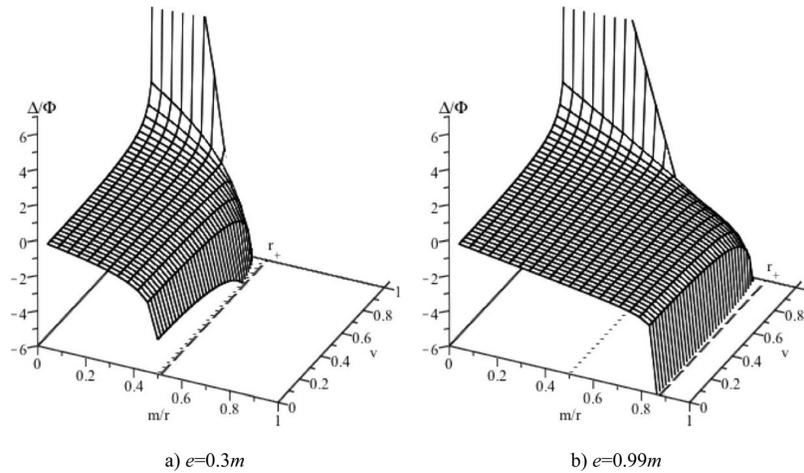a) $e=0.3m$ b) $e=0.99m$

FIG. 3. The precession angle Δ/Φ for a Reissner–Nordström black hole for two values of charge e. They are asymptotic to the horizon $r=r_+$ (dashed line), which is below the Schwarzschild radius $r_s=2m$ (dotted line).

$v=0$ the particles are static in the EPR source and for $v \rightarrow 1$, they are ultrarelativistic particles. In Fig. 3, the precession angle is plotted independently from the observer position angle Φ. For $e=0$, we recover all results of the spin precession for a Schwarzschild black hole and the horizon is at $r=2m$.

The plots are quite similar as in the Schwarzschild case (compare with Fig. 2). Analogous and interesting effects of spin precession can be compared with Ref. 22 using the previous reviewed regions:

- Region I: The situation is identical to the Schwarzschild black hole. The spacetime is Minkowskian and $\Delta \rightarrow 0$.
- Region II: Far away from the horizon r_+ with $v \neq 0$, we recover the spin precession found in special relativity and the plot is asymptotic (see Fig. 3), i.e., $\lim_{r \rightarrow \infty} \Delta = \cosh\zeta - 1$ in agreement to Ref. 17.
- Region III: A new effect occurs near the black hole horizon. This effect corresponds to a shifting of horizon compared with the Schwarzschild case, from $r=2m$ to $r=r_+=m+(m^2-e^2)^{1/2}$. As the charge e is increased, we reach values of r below the Schwarzschild horizon, it means that we can calculate values of Δ at $r=r_+<2m$ (see Fig. 1 where $r_{st}=2m$). The lowest value of r that we can reach is when $e=m$ for an extreme black hole, whose horizon is at $r=r_+=m$. These values of r are not allowed for the Schwarzschild case. From Fig. 3, we see how the horizon is shifted as the charge is increased. $\Delta \rightarrow -\infty$ as the horizon is reached, no matter the velocity of the particles considered. EPR correlation then is totally lost. The same behavior of Δ was present in Schwarzschild radius in Ref. 22.

The divergence of the spin precession originates from the fact the vierbein Eq. (22) and the four-velocity Eq. (25) become singular at the horizon r_+. These singularities are connected with the breakdown of the coordinate system (t, r, θ, ϕ).

- Region IV: It is still possible to keep circular orbits in the path $r=r_0$, with perfect anticorrelation $\Delta=0$. Thus, for a

particular position, the local inertial velocity of particles v_{EPR} must be tuned at the beginning from the source, In Fig. 4, r_0 is plotted for three suitable values of charge e in function of position m/r and local inertial velocity v. We can see that for large distances ($m/r \rightarrow 0$), it is possible to have the perfect anticorrelation with low values of v. Meanwhile, the horizon is reached, we must increase the local velocity of the particles to keep the perfect anticorrelation.

As in the Schwarzschild case, near the horizon there is a not null precession angle ($\Delta \neq 0$), independently of the velocity of the particle. Then it is not possible to have a perfectly anticorrelated orbits. In Fig. 4, the limit circular orbits correspond to the point where r_0 ends on the top of the
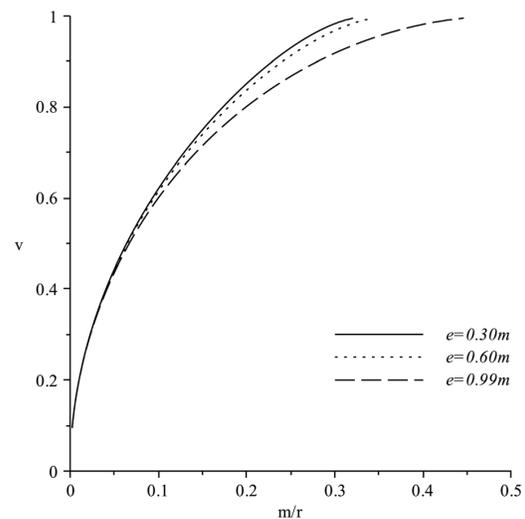

FIG. 4. Parametric plot of position m/r and local inertial velocity v for path r_0 that keep a perfect anticorrelation ($\Delta=0$) for a Reissner–Nordström black hole.

figure. For large values of e, we can have perfect anticorrelated orbits closer to the horizon, but there is no possible to find a r_0 below the Schwarzschild radius.

B. Kerr case

Now we consider a rotating black hole without charge. It corresponds to the Kerr spacetime. The spin precession has the same form of Eq. (55), but with different coefficients A and B, that is, after setting $e = 0$, we get

$$\Delta_K = \Phi\left\{ \frac{\cosh\eta}{r(r^2 - 2mr)^{3/2}}\left[A_K\cosh\zeta - B_K\sinh\zeta \right.\right.$$
$$\left.\left. \times\left(\frac{2\cosh^2\zeta - \cosh^2\eta - \sinh^2\eta}{\cosh^2\zeta - \cosh^2\eta}\right)\right] - 1\right\}, \quad (57)$$

where

$$\begin{aligned} A_K &= r^4 - 5mr^3 + 6m^2r^2 - 2a^2mr, \\ B_K &= -amr\sqrt{r^2 - 2mr + a^2}. \end{aligned} \quad (58)$$

The precession angle is plotted in Fig. 5 for two values of angular momentum parameter a, as a function of distance and local velocity $v = v_{EPR}$. The distance is parameterized by m/r which means the experiment is placed at infinite when $m/r \to 0$, and $m/r = 1$ correspond to a "extreme" black hole, i.e., $a = m$. When $v = 0$, the particles are static at the EPR source and for $v \to 1$, they are ultrarelativistic. The precession angle was plotted independently from the observer position angle Φ. For $a = 0$, we recover all results of Schwarzschild spin precession in Ref. 22 as expected.

The plot is quite similar to Fig. 2, but with important differences. The effects due to the acceleration and gravity analyzed by regions are:

- Region I: Again the situation is identical to the Schwarzschild's black hole. The frame-dragging has no contribution because it decreases with distance. Therefore, the spacetime is Minkowskian and $\Delta \to 0$ as $v = v_{EPR} \to 0$.

- Region II: There are no new effects. The frame-dragging has no contribution and the angle Δ is asymptotic to infinite when $v \to 1$ for ultrarelativistic particles.

- Region III: In the Schwarzschild and Reissner–Nordström spacetime, the divergence of the spin precession ($\Delta \to -\infty$) was at the horizon. Now, the divergence is present in two locations, one of them at the static limit surface and the other one is through the path defined by $v_{EPR} = v_{fd}$.

The first divergence in Eq. (57) is related to the static limit surface. As mentioned in Section III, any particle acquire velocity due to the frame-dragging as it falls to the black hole. When this particle reaches the static limit surface at $r = 2m$ for equatorial plane, its velocity tends asymptotically to speed of light. In the left part of Eq. (57), it is easy to see why precession angle diverges when distance is evaluated at $2m$. The divergence of the spin precession in the Kerr spacetime originates from the fact that the frame-dragging component Eq. (17) of the four-velocity Eq. (25) becomes singular at the static limit r_{st}. This feature contrasts with the Reissner–Nordström case, where the singularities were connected with the breakdown of the coordinate system (t, r, θ, ϕ) at r_+.

Previously, it was mentioned that the static limit is not a horizon. Beyond r_{st}, it is still possible to get entangled particles in circular orbits. The region inside the interval $r_+ \le r < 2m$ has a similar behavior as Region I and II (see in particular Fig. 5(b) where is more clear this feature). Frame-dragging has no effect and the precession angle Δ_K is asymptotic near the static limit at $2m$ and also for particles with $v_{EPR} \to 1$.

But near the horizon r_+ the function (57) is well defined. This is an unexpected result if we compare with Scharzschild and Reissner–Nordström cases, where the horizon represents an asymptotic limit.

For $r < r_+$, the coordinate system breaks down and we are unable to find the precession angle for orbital particles.

The second divergence corresponds to a coupling between the EPR velocity and the frame-dragging. In Fig. 5, it is represented by peaks an asymptotic infinite
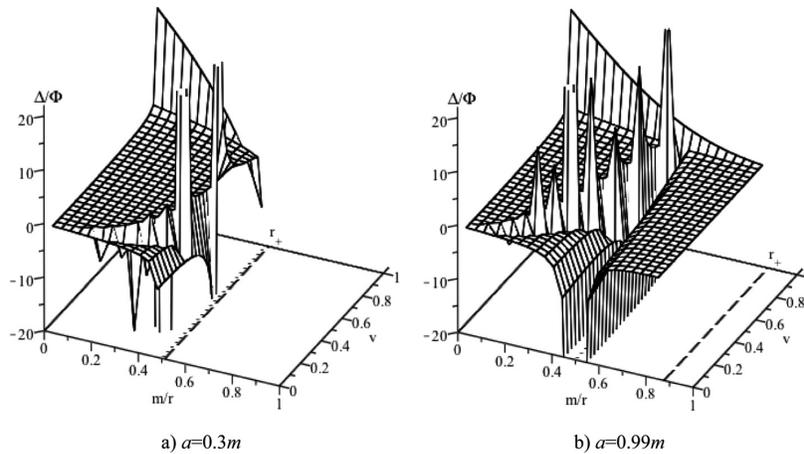

a) $a = 0.3m$ b) $a = 0.99m$

FIG. 5. The precession angle Δ/Φ for a Kerr black hole for two values of angular momentum parameter a. They are asymptotic to the static limit $r_{st} = 2m$ and along a path $v = v_{fd}$. The peaks represent an asymptotic infinite wall.
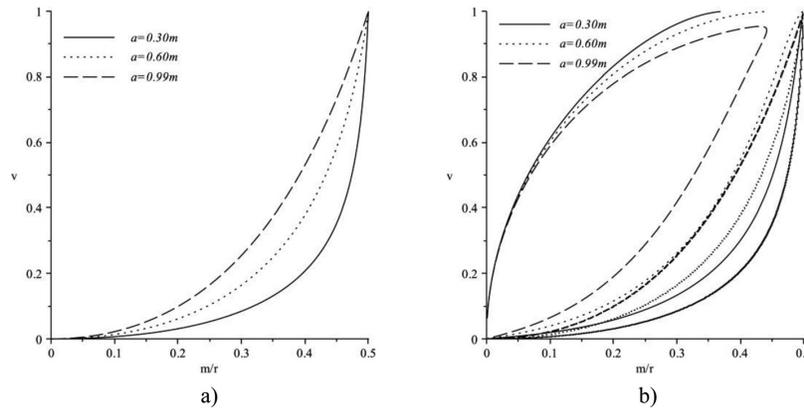
FIG. 6. (a) Local inertial velocity due to the frame-dragging for three values of a. The infinite wall in Fig. 5 follow the path traced by this plot when $v_{\mathrm{EPR}} = v_{fd}$. (b) Parametric plot of position m/r and local inertial velocity v for path r_0 that keep a perfect anticorrelation ($\Delta = 0$) for a Kerr black hole.

"wall." This wall follows a curved path defined by $\cosh^2\zeta = \cosh^2\eta$ in Eq. (57), which is easy to verify that corresponds to $v_{\mathrm{EPR}} = v_{fd}$.

When the velocity of the first particle equals the velocity of the frame-dragging, Δ_{K}, becomes asymptotically infinity. Physically, one particle remains static because v_{EPR} equals v_{fd}, meanwhile, the other particle continues his travel, as seen by the hovering observer. The static particle never reaches the observer, and therefore it is not possible to know the anticorrelation between the particles.

This situation represents a particular feature for Kerr-like spacetime. In Schwarzschild, Reissner–Nordström and Ref. 23, the plots were very smooth until their functions reach their horizons. Here, the plot presents this infinite wall following the path which corresponds to the velocity that experience a free falling particle due to the frame-dragging (see Fig. 6(a)).

- Region IV: We can see in Fig. 6(b) that away from black hole, there is a low velocity that keeps the perfect anticorrelation, as in the Schwarzschild and Reissner–Nordström cases. As $r \to r_{st}$ there is a nonvanishing precession angle, independently of the velocity of the particle v_{EPR}. Perfectly anticorrelated orbits cannot be kept and r_0 has a limit value as in the Reissner–Nordström spacetime. We can see this limit value when r_0 ends on the right top of the Fig. 6(b). Near the static limit, the contribution of the frame-dragging allows three values of v_{EPR} for the same value of angular momentum parameter a. This new effect is not present in the Schwarzschild and Reissner–Nordström cases and in the previous work in Ref. 23 neither. When the static limit is reached, the velocity due to the EPR process must be the speed of light in order to get a perfect anticorrelated particles.

C. Kerr–Newman case

We are now in position to analyze the complete Kerr–Newman spacetime and its effects on entangled particles. From Eq. (55), it can be shown that Region I and II have the same behavior for a Minkonski spacetime. This is

not a surprising result, as we have seen in previous cases of this section a and e decreases with distance.

For Region III, the static limit Eq. (24) is reduced to $r_{st} = m + (m^2 - e^2)^{1/2}$ on the equator. It coincides with the horizon for a Reissner–Nordström spacetime. The static limit r_{st} represents again an asymptotic limit for calculation of the precession angle Δ in the Kerr–Newman black holes. Contrary to Kerr spacetime where the static limit is placed at $r = 2m$, now it is below and this limit depends in the charge of black hole, depicted by a dotted line in Fig. 7. In this, Figs. 7(a) and 7(b) have the same horizon Eq. (3) as well as 7(c) and 7(d) between them. In (a) r_{st} is too close to r_+ that dotted line cannot be distinguished. Figures 7(a) and 7(c) have the same r_{st} because the electric charge parameter e is equal for both. Once again, we can observe the infinite wall path due to the coupling of v_{EPR} with v_{fd}. This asymptotic path is not constrained to the region $r > 2m$ nor above the horizon, but above the static limit.

Like in Kerr spacetime, the region between $r_+ \leq r < 2m$ is not affected by the frame-dragging and Δ tends asymptotically to infinity near r_{st}. Finally, the coordinate system breakdown when r equals r_+.

D. Uncertainties in observers' positions and Bell's inequality

When the hovering observers measure the spin of each entangled particle, in principle they could adjust the direction of the measure by Eq. (55) to get the perfect anticorrelation. As we have seen, near the static limit and on the infinite wall path the precession angle Δ will change very fast, making impossible to keep a position Φ without uncertainty for the hovering observers. As observed in Ref. 22, the error of the angle Θ to keep the perfect EPR correlation is given by

$$\delta\Theta = \delta\Phi \left| 1 + \frac{\Delta}{\Phi} \right|, \tag{59}$$

and near these asymptotic limits, $\delta\Theta$ must be less than π. If not, the hovering observers cannot set the directions of measurement in order to extract the EPR correlation. To utilize
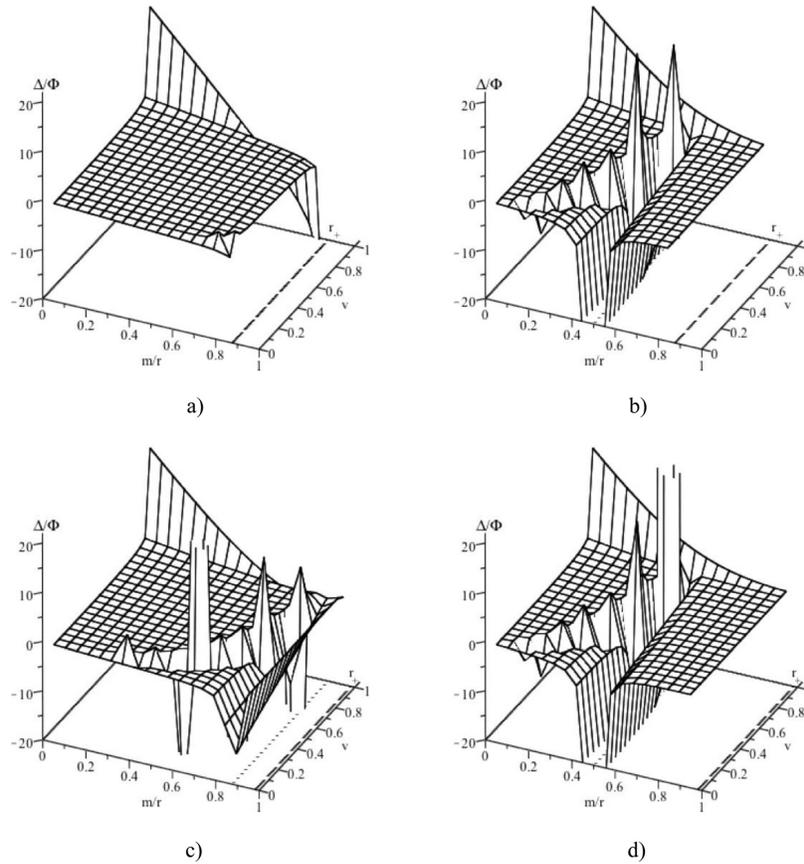
FIG. 7. The precession angle Δ/Φ for a Kerr–Newman black hole for a pair of values of a and e, that keep r_+ constant (dashed line). The dotted line represents the static limit surface on equatorial plane. The plots are asymptotic at $r = r_{st}$ and along a path $v_{\text{EPR}} = v_{fd}$. The peaks represent an asymptotic infinite wall. In (a) r_{st} is too close to r_+ that dotted line cannot be distinguished. a) $a = 0.01m$, $e = 0.99m$, b) $a = 0.99m$, $e = 0.01m$, c) $a = 0.14m$, $e = 0.99m$, d) $a = 0.99m$, $e = 0.14m$.

the EPR correlation for quantum communication, $\delta\Phi$ and r must satisfy

$$\delta\Phi < \pi \left| 1 + \frac{\Delta}{\Phi} \right|^{-1}. \tag{60}$$

When r_{st} is reached for the Kerr–Newman spacetime, $\delta\Phi$ must vanish because the velocity of the spin precession Eq. (25) is infinite due to the frame-dragging. Therefore, on the static limit, the hovering observers will not obtain the right EPR correlation from the particles, unless they can keep their positions Φ without uncertainty.

From the perspective of Bell's inequality, our previous results give rise to a decrement in the degree of the violation of that inequality, that is,

$$\langle \mathcal{Q}'\mathcal{S}' \rangle + \langle \mathcal{R}'\mathcal{S}' \rangle + \langle \mathcal{R}'\mathcal{T}' \rangle - \langle \mathcal{Q}'\mathcal{T}' \rangle = 2\sqrt{2}\cos^2\Delta, \tag{61}$$

where the trivial rotations of the local inertial frames $\pm\Phi$ has been discarded, the spin component of one particle is measured in the $(\cos\Phi, 0, -\sin\Phi)$ direction (component $\mathcal{Q}'$) or in the $(0, 1, 0)$ direction (component $\mathcal{R}'$), and the spin component of the other is measured in the $(-\cos\Phi, -1, \sin\Phi)/\sqrt{2}$

direction (component $\mathcal{S}'$) or in the $(\cos\Phi, -1, \sin\Phi)/\sqrt{2}$ direction (component $\mathcal{T}'$) as in Ref. 22 were established.

In order to use Eq. (61) for entanglement process (see Introduction), the hovering observers must take into account all reviewed effects due to the gravity, the frame-dragging and acceleration. As Ref. 22 showed, the spin component of one particle must be measured in the $(\cos\Theta, 0, -\sin\Theta)$ direction or in the $(0, 1, 0)$ direction in the local inertial frame at $\phi = \Phi$. For the other particle, the spin component must be measured in the $(-\cos\Theta, -1, -\sin\Theta)/\sqrt{2}$ direction or in the $(\cos\Theta, -1, \sin\Theta)/\sqrt{2}$ direction in the local inertial frame at $\phi = -\Phi$.

Finally, as soon the observers are placed near the asymptotic limits, it will be almost impossible to keep their position Φ, i.e., a small uncertainty $\delta\Phi$ translates to an uncertainty in $\delta\Theta$ from Eq. (59). This error in Θ decreases the degree of violation as $2\sqrt{2}\cos^2\delta\Theta$, and this error must be greater than two in order to restore the maximal violation of Bell's inequality. Thus, from Eq. (59), $\delta\Phi$ and r must be adjusted at least,

$$\delta\Phi < \sqrt{2} \left| 1 + \frac{\Delta}{\Phi} \right|^{-1}. \tag{62}$$

It is important to note that near the horizon for Reissner–Nordström and the static limit and the infinite wall path for Kerr and Kerr–Newman, the precession angle is asymptotically divergent and there is no possible the maximal violation of Bell's inequality. Thus free falling observers and different vierbeins can be chosen to avoid this divergence of spin precession angle.

VII. CONCLUSIONS

In this work, we constructed an equation that describe the spin precession of a pair of entangled massive spin 1/2-particles, under the gravitational and acceleration effects of the neighborhood of a charged and rotating black hole. Because the rotation of this compact relativistic object, the frame-dragging should be taken into account for the complete description of this spacetime. We considered the effects of the frame-dragging as an additional velocity over the entangled particles and later we incorporated this velocity in the computation of spin precession angle. Hovering observers were considered in order to have suitable reference frames that ensure reliable directions to compare the 1/2-spin quantum states.

The total velocity measured by the hovering observers was performed as the addition of the velocity of a ZAMO describing the frame-dragging velocity, plus the local velocity of the EPR particles measured by the ZAMO. These ZAMOs corotates the black hole due to the frame-dragging and they were used as a preliminary step before calculating the total local inertial velocity measured by the hovering observer. With this local velocity, it was possible to calculate the infinitesimal Lorentz transformations and therefore the boost and rotations that produce the Wigner rotation for the particles.

From the point of view of the hovering observers, there is a Wigner rotation for each particle, because both particles travel with different velocities due to the frame-dragging of the spacetime. After these considerations, we arrived to Eq. (55) that describe the spacetime effects that deteriorate the perfect anticorrelation of the entangled particles compared if they would be in the Minkowski spacetime.

We found that the perfect anticorrelation of the particles is deteriorated due to the acceleration and gravitational effects, as previous works found,[16,17,22] but now the charge and rotation parameter affect in particular ways the infinitesimal Lorentz transformations and therefore new features arise. These features contain new effects compared with the Schwarzschild spacetime[22] and Ref. 23 results. But as expected, in the case of $a = 0$ and $e = 0$, our results recover the equations of Ref. 22.

In the Reissner–Nordström case, the electric charge parameter produces a shifting of the event horizon position from $r = 2m$ to $r = r_+$ as being contrasted with the Schwarzschild spacetime. But this horizon is still an asymptotic limit for the calculation of spin precession.

In the Kerr spacetime, the angular momentum parameter establishes the commonly named static limit surface, where two interesting physical processes occur: it coincides with the Schwarzschild radius and represents one limit for calculation of the precession angle, and the frame-dragging has

the maximal value there, making massive particles ultrarelativistic and the spin precession angle $\Delta \to \infty$.

A remarkable difference was found when particles are close to the rotating black hole event horizon r_+. The precession angle is well defined, which contrasts with Scharzschild and Reissner–Nordström cases.

Another effect in Kerr spacetime occurs when the velocity of the particles due to the EPR process coincides with that of the frame-dragging. One of the particles keeps their position relative to the hovering observer, meanwhile the other particle reach one observer. Then, the spin precession angle goes to infinity. We found that the equation that describe the velocity of the frame-dragging Eq. (16), describes also a curved path where the spin precession angle is asymptotic.

Another asymptotic limit is at $r = 2m$ because the spin precession angle is singular at this point, which coincides with the Schwarzschild case.

For the Kerr–Newman spacetime, the static limit coincides with the horizon of the Reissner–Nordström spacetime, but this limit does not represent an asymptotic limit for the spin precession angle.

It still possible to find circular orbits with perfect anticorrelation for a and e parameters along a path called r_0, that is, $\Delta(r = r_0) = 0$. Moreover, when only the angular momentum parameter a is considered, it can be reached a perfect anticorrelation close the static limit with three possible r_0 paths for the same value of a. This effect is not present in the Schwarzschild and Reissner–Nordström cases.

Even that the total electric charge in real black holes should be zero, it was considered as an arbitrary parameter in order to illustrate its effect on the spin precession. The electromagnetic interaction between charged particles and charged black hole was not taken into account and remain to be explored in a future work.

It would be interesting to make an analytic continuation in order to find the interior solution supporting the spin precession below the event horizon r_+. Also one could consider a gedanken experiment mounted on ZAMOs for the Kerr-like spacetime.

Future work will extend the analysis discussed in the present paper to evaluate the behavior of spin precession on any general type D metric, making possible to investigate the EPR anticorrelation of particles in a seven parametric Plebański–Demiański spacetime.[30]

NOMENCLATURE

r	radial coordinate
t	time coordinate
θ	angular coordinate
ϕ	Azimutal coordinate
m	black hole mass

a	black hole angular momentum
e	black hole electric charge
G	universal gravitational constant
c	speed of light
$g_{\mu\nu}$	metric component
r_s	Schwarzschild radius
r_+	Kerr black hole external horizon
r_-	Kerr black hole internal horizon
$e_a^\mu(x)$	Vierbein
η_{ab}	Minkonski metric
$\delta_b^a, \delta_\beta^\alpha$	Kronecker delta
E	energy per unit mass
L_z	angular momentum per unit mass
u^μ, u_μ	four-vector velocity
$\Lambda_b^a, \chi_b^a, \lambda_b^a, \vartheta_b^a$	Lorentz transformation
r_s	radius of the static limit surface
ϑ_b^a	covariant derivative
$\omega_\nu{}^a{}_b$	one-form connection
ξ, ζ, κ, η	special relativity hyperbolic argument (hyperbolic angle)
W(x)	Wigner rotation
Θ	angle of rotation
Φ	angular distance from source to observers
Δ	spin precession angle of entangled particles
$\rightarrow$	tends to
∞	infinite
r_0	distance where $\Delta = 0$ near the black hole
$\mathcal{Q}, \mathcal{R}, \mathcal{S}, \mathcal{T}$	quantum spin directions of measure

[1]A. Einstein, B. Podolsky, and N. Rosen, Phys. Rev. **47**, 777 (1935).
[2]D. Bohm and Y. Aharonov, Phys. Rev. **108**, 1070 (1957).
[3]J. S. Bell, Physics **1**, 195 (1964).

[4]J. F. Clauser and S. J. Freedman, Phys. Rev. Lett. **28**, 938 (1972).
[5]A. Aspect, P. Grangier, and G. Roger, Phys. Rev. Lett. **47**, 460 (1981).
[6]W. Tittel, J. Brendel, H. Zbinden, and N. Gisin, Phys. Rev. Lett. **81**, 3563 (1998).
[7]S. Popescu, Phys. Rev. Lett. **72**, 797799 (1994).
[8]C. H. Bennet, G. Brassard, C. Crépeau, R. Jozsa, A. Peres, and W. K. Wooters, Phys. Rev. Lett. **70**, 1895 (1993).
[9]G. Brassard, P. Horodecki, and T. Mor, IBM J. Res. Dev. **48**, 87 (2004).
[10]R. Jozsa, "Entanglement and quantum computation," in *Geometric Issues in the Foundations of Science*, edited by S. Huggett (Oxford University Press, 1997).
[11]R. Raussendorf and H. J. Briegel, Phys. Rev. Lett. **86**, 51885191 (2001).
[12]D. Gottesman and I. L. Chuang, Nature **402**, 390–393 (1999), eprint quant-ph/9908010.
[13]E. Knill, R. Laflamme, and G. J. Milburn, Nature **409**, 46 (2001).
[14]A. K. Ekert, Phys. Rev. Lett. **67**, 661663 (1991).
[15]C. H. Bennet, G. Brassard, and N. D. Mermin, Phys. Rev. Lett. **68**, 557 (1992).
[16]P. M. Alsing and G. J. Milburn, Quantum Inf. Comput. **2**, 487 (2002).
[17]H. Terashima and M. Ueda, Quantum Inf. Comput. **3**, 224 (2003).
[18]J. Rembielinski and K. A. Smolinski, Phys. Rev. A **66**, 052114 (2002).
[19]R. M. Gingrich and C. Adami, Phys. Rev. Lett. **89**, 270402 (2002).
[20]D. Ahn, H. Lee, Y. H. Moon, and S. W. Hwang, Phys. Rev. A **67**, 012103 (2003).
[21]H. Li and J. Du, Phys. Rev. A **68**, 022108 (2003).
[22]H. Terashima and M. Ueda, Phys. Rev. A **69**, 032113 (2004).
[23]J. Said and K. Z. Adami, Phys. Rev. D **81**, 124012 (2010), eprint quant-ph/1001.0788v3.
[24]E. P. Wigner, Ann. Math. **40**, 149 (1939).
[25]R. M. Wald, *General Relativity* (The University of Chicago Press, 1984).
[26]R. H. Rietdijk and J. W. van Holten, Nucl. Phys. B **472** 427–446 (1996), eprint hep-th/9511166v1.
[27]M. Nakahara, *Geometry, Topology and Physics* (Taylor & Francis Group, 2003).
[28]B. F. Schutz, *A First Course in General Relativity* (Cambridge University Press, 2000).
[29]D. Raine and E. Thomas, *Black Holes, An Introduction* (Imperial College Press, 2010).
[30]J. F. Plebański and M. Demiański, Ann. Phys. **98**, 98 (1976).

Quantum entanglement in Plebański–Demiański spacetimes

Hugo García-Compeán[1] **and Felipe Robledo-Padilla**[2]

[1] Departamento de Física, Centro de Investigación y de Estudios Avanzados del IPN, P.O. Box 14-740, 07000 México D.F., México
[2] Facultad de Ciencias Físico-Matemáticas, Universidad Autónoma de Nuevo León, Ciudad Universitaria, San Nicolás de los Garza, Nuevo León, 66450, México

E-mail: compean@fis.cinvestav.mx and felipe.robledopd@uanl.edu.mx

Abstract
For an Einstein–Podolsky–Rosen pair of spin-1/2 particles in circular orbits in a general axially symmetric spacetime, the spin precession angle is obtained. Hovering observers are introduced for ensuring fixed reference frames to perform suitable reliable measurements. Frame-dragging of spinning holes is explicitly incorporated relative to hovering observers. The spin-singlet state is found to be mixed with the spin-triplet by acceleration and gravity effects, which deteriorate the perfect anti-correlation of an entangled pair of spins measured by hovering observers. Finally, an algorithm to calculate spin precession for a general axially symmetric spacetime is proposed. This algorithm is applied to study the complete list of expanding and twisting Type-D Plebański–Demiański black holes and their descendent limiting solutions with lower parameters.

PACS numbers: 03.65.Ud, 03.67.−a, 04.20.−q, 02.40.−k

(Some figures may appear in colour only in the online journal)

1. Introduction

For many years, quantum states of matter in a classical gravitational background have been of great interest in physical models. One of the famous experimental examples in this situation is the experiments of neutron interferometry in laboratories on the Earth. In such experiments, it is possible to capture the effects of the gravitational field into quantum phases associated with the possible trajectories of a beam of neutrons, following paths with different intensity of the gravitational field. The phase differences have information about how the gravitational field of Earth do affect the quantum states of neutrons [1]. Experiments using atomic interferometry were also reported later [2]. Another instance of the description of quantum states of matter in classical gravitational fields is Hawking's radiation [3] describing the process of black hole

evaporation. This process involves relativistic quantum particles and uses quantum field theory in curved spacetimes (see for instance, [4]).

Moreover, the study of the quantum properties of (non-)relativistic quantum matter has been studied in the literature along the years. For instance, in [5–10] the entanglement of a pair of non-relativistic spin-1/2 particles have been extended to special relativity through the uses of the Wigner rotation [11, 12]. Furthermore, the consideration of the general relativistic effects on the properties of the quantum states, as the entanglement and the spin precession angles, were discussed, for the Schwarzschild black hole, in [13]. In that paper, they considered a pair of spinning particles in an entangled state moving in equatorial motion of this black hole. As a result of their study, they found that the Einstein–Podolsky–Rosen (EPR) correlation [14] is deteriorated due to the acceleration of these spinning particles and the effect of the gravitational field of the black hole on them. This effect leads to a decrement in Bell's inequality degree of violation given by the quantum spin directions and is written as

$$\langle \mathcal{Q}'\mathcal{S}' \rangle + \langle \mathcal{R}'\mathcal{S}' \rangle + \langle \mathcal{R}'\mathcal{T}' \rangle - \langle \mathcal{Q}'\mathcal{T}' \rangle = 2\sqrt{2}\cos^2 \Delta.$$

All the information of the gravitational field is encoded in the precession angle Δ, which depends in general on all the parameters of the black hole of interest, on the radius r and on the frame-dragging velocity (if any). The case with $\Delta = 0$ corresponds with the result consistent with quantum mechanics. For $\Delta \neq 0$ and large, there is a deterioration of the prefect anti-correlation of the entangled pair of spin-1/2 particles.

For the simplest case of the Schwarzschild black hole, it depends only on the mass m parameter, and its strongest effect is localized on the Schwarzschild event horizon due to an extremely (infinite) rapid spin precession with $|\Delta_S| \to \infty$ producing the mentioned decrement of Bell's inequality. In this case there is no frame-dragging; however, Δ_S still depends on the local velocity of the particles with respect to the hovering observers. In the whole process it is observed that the choices of the 4-velocity vector and of the vierbein are important in order to be able to communicate non-locally in a curved spacetime using these spinning particles. Similar results, but also with subtle and important differences, were found for the case of Kerr–Newman black holes [15] and Kerr–Newman metric with frame-dragging [16].

The aim of this paper is to extend the description of spin precession mentioned above to the Plebański–Demiański black hole [17], which is the most general axially symmetric expanding and twisting Type-D solution of the Einstein–Maxwell equations according the Petrov–Penrose classification (see for instance, [18]). In order to do that, it is more convenient to write down the metric in Boyer–Lindquist coordinates. This description was studied by Griffiths and Podolský in a series of papers [19–21] (and reviewed in [22, 23]) with the purpose of clarifying the physical meaning of the parameters entering in the solution.

The Plebański–Demiański solution has been worked out previously in the literature connecting with higher dimensional theories. Some time ago, there was some interest of this metric in the study of some generalizations of the AdS/CFT correspondence [24–26]. More recently there has been a great deal of work in the context of higher dimensional solutions the Kerr–NUT–(anti-)de Sitter black hole in the context of brane and string theory [27–34].

The Plebański–Demiański family of Type-D solutions of the Einstein field equation describes a configuration of the gravitational fields characterized by seven parameters [17]. These configurations have null congruences of geodesic curves characterized in general by non-vanishing expansion, twist and shear parameters. In this paper, we will consider only expanding and twisting solutions. Under certain non-degenerate coordinate transformations of the original metric and the setting of constraints the metric is turned out into a new suitable form in Boyer–Lindquist coordinates and depending on seven parameters with almost direct physical interpretation [19–23].

Other kind of models involving the effects of the gravitational field on quantum matter properties precisely in Plebański–Demiański backgrounds is discussed in [35]. In that paper, the phase shift of charged particle interferometry described by complex scalar fields was computed. In there, the mentioned new form of the Plebański–Demiański spacetimes was also adopted and it was shown that all physical parameters contribute to the phase shift. The consideration of the interferometry of spin-1/2 particles in this context was worked out in [36].

The approach we will follow in this paper does adopt the notation and conventions from [13]. The main idea is to perform a series of consecutive local infinitesimal Wigner rotations [11] to give rise to the spin precession of a pair of entangled spin-1/2 particles on circular orbit around the equator of a general axially symmetric black hole, where the spin is locally well defined in the non-relativistic theory.

The Wigner rotation consists of an infinitesimal Lorentz transformation, which for the equatorial motion is written in terms of a boost along the radial direction and a rotation in the angle direction of the orbital particle. The final result is a spin precession of a particle moving in circular motion in curved spacetime due to the acceleration of the particle by an external force and due to the difference between local inertial frames at different points. These enable us to find the precession angle for a general axially symmetric spacetime. These results are then applied to describe the spin precession angle of an EPR pair of particles moving on the equator of an expanding and twisting Plebański–Demiański black hole. We will find that this angle depends on all the physical parameters of the black hole. Moreover, by making appropriate reductions we obtain the precession angle for all known subfamilies of this Plebański–Demiański black hole.

This paper is organized as follows. Section 2 presents some generalities about Plebański–Demiański spacetime. The effect of the axially symmetric component is reviewed in section 3 and the frame-dragging corrections over the velocity of a particle is calculated. In section 4, the Zero Angular Momentum Observers (ZAMOs) are introduced. We also present a gedanken experiment to describe the entangled pair of particles in circular orbit around a general axially symmetric black hole. Moreover, in this same section some calculations are performed which are necessary to propose an algorithm to find the spin precession angle without reference to any particular solution. Section 5 is devoted to calculate the EPR correlation by Wigner rotations due the motion of the particles in generalized spacetime. Finally, all results are integrated in section 6 to illustrate the use of the algorithm to get the spin precession angle for the Plebański–Demiański black hole. From this general case, the spin precession angle of the EPR pair is obtained for the complete list of subfamilies of non-expanding solutions. It is found that for the general case, this angle depends on all the physical parameters of the solution. Conclusions and final remarks are presented in section 7.

2. Plebański–Demiański spacetime

Among the solutions of the Einstein–Maxwell equations, the family of Type-D solutions are the most important ones. In particular, we will consider in the present paper those with non-vanishing expanding and twisting (ω) congruences of non-null electromagnetic field with two repeated principal null vectors coinciding with the two repeated principal null congruences of the Weyl tensor. These solutions were found in 1976 by Plebański and Demiański [17] and it is called Plebański–Demiański spacetime (or black hole). This spacetime is characterized by seven parameters which are found to be non-directly related to the physical parameters of a black hole. Recently, a new look of this metric was worked out [19, 20] (and reviewed in [22, 23]), allowed to give a Boyer–Lindquist form of the Plebański–Demiański metric in terms of the physical parameters, namely: a mass-like parameter m, a cosmological constant

Λ, a rotation-like parameter a, a NUT-like parameter l, the electric and magnetic charges e and g, and an acceleration-like parameter α. The following metric can be derived from the original Plebański–Demiański metric after some non-degenerate coordinate transformations and an appropriated treatment of the roots of the quartic function D, and it is given by

$$ds^2 = \frac{1}{\Omega^2}\left[-\frac{D}{\rho^2}\left(dt - (a\sin^2\theta + 2l(1-\cos\theta))\,d\phi \right)^2 + \frac{\rho^2}{D}\,dr^2 \right.$$
$$\left. + \frac{P}{\rho^2}\left(a\,dt - (r^2 + (a+l)^2)\,d\phi \right)^2 + \rho^2\frac{\sin^2\theta}{P}\,d\theta^2 \right], \tag{1}$$

with

$$\rho^2 = r^2 + (l + a\cos\theta)^2,$$
$$\Omega = 1 - \frac{\alpha}{\omega}(l + a\cos\theta)r,$$
$$P = \sin^2\theta(1 - a_3\cos\theta - a_4\cos^2\theta), \tag{2}$$
$$D = (\kappa + e^2 + g^2) - 2mr + \varepsilon r^2 - 2n\frac{\alpha}{\omega}r^3 - \left(\frac{\alpha^2}{\omega^2}\kappa + \frac{\Lambda}{3}\right)r^4,$$

and where

$$a_3 = 2a\frac{\alpha}{\omega}m - 4al\frac{\alpha^2}{\omega^2}(\kappa + e^2 + g^2) - 4\frac{\Lambda}{3}al,$$
$$a_4 = -a^2\frac{\alpha^2}{\omega^2}(\kappa + e^2 + g^2) - \frac{\Lambda}{3}a^2,$$
$$\varepsilon = \frac{\kappa}{a^2 - l^2} + 4l\frac{\alpha}{\omega}m - (a^2 + 3l^2)\left(\frac{\alpha^2}{\omega^2}(\kappa + e^2 + g^2) + \frac{\Lambda}{3}\right), \tag{3}$$
$$n = \frac{\kappa l}{a^2 - l^2} - (a^2 - l^2)\frac{\alpha}{\omega}m + (a^2 - l^2)l\left(\frac{\alpha^2}{\omega^2}(\kappa + e^2 + g^2) + \frac{\Lambda}{3}\right),$$
$$\kappa = \frac{1 + 2l\frac{\alpha}{\omega}m - 3l^2\frac{\alpha^2}{\omega^2}(e^2 + g^2) - l^2\Lambda}{\frac{1}{a^2 - l^2} + 3l^2\frac{\alpha^2}{\omega^2}}.$$

Equation (1) can be represented by the line element

$$ds^2 = g_{00}\,dt^2 + 2g_{03}\,dt\,d\phi + g_{11}\,dr^2 + g_{22}\,d\theta^2 + g_{33}\,d\phi^2, \tag{4}$$

which has a non-diagonal element that represents the axial symmetry and the metric coefficients are:

$$g_{00} = \frac{-D + Pa^2}{\Omega^2\rho^2},$$
$$g_{0i}\,dx^i = \frac{1}{\Omega^2}\left[\frac{D}{\rho^2}(a\sin^2\theta + 2l(1-\cos\theta)) - \frac{P}{\rho^2}a(r^2 + (a+l)^2) \right]d\phi,$$
$$g_{ij}\,dx^i\,dx^j = \frac{\rho^2}{\Omega^2 D}\,dr^2 + \rho^2\frac{\sin^2\theta}{\Omega^2 P}\,d\theta^2 + \frac{1}{\Omega^2}\left[-\frac{D}{\rho^2}(a\sin^2\theta + 2l(1-\cos\theta))^2 \right.$$
$$\left. + \frac{P}{\rho^2}(r^2 + (a+l)^2)^2 \right]d\phi^2. \tag{5}$$

This representation is a suitable way to work with the Plebański–Demiański metric (1). We shall use this representation in the next sections.

4

In order to describe the motion of spinning particles in a curved spacetime, we shall recall that the local inertial frame at each point is defined by a vierbein chosen as in [35]:

$$
\begin{aligned}
&e_0{}^\mu(x) = \frac{1}{\sqrt{-g_{00}}}(1,0,0,0), && e^0{}_\mu = \sqrt{-g_{00}}\left(1,0,0,\frac{g_{03}}{g_{00}}\right), \\
&e_1{}^\mu(x) = \frac{1}{\sqrt{g_{11}}}(0,1,0,0), && e^1{}_\mu = \sqrt{g_{11}}(0,1,0,0), \\
&e_2{}^\mu(x) = \frac{1}{\sqrt{g_{22}}}(0,0,1,0), && e^2{}_\mu = \sqrt{g_{22}}(0,0,1,0), \\
&e_3{}^\mu(x) = \sqrt{\frac{-g_{00}}{g_{03}^2 - g_{00}g_{33}}}\left(-\frac{g_{03}}{g_{00}},0,0,1\right), && e^3{}_\mu = \sqrt{\frac{g_{03}^2 - g_{00}g_{33}}{-g_{00}}}(0,0,0,1),
\end{aligned}
\tag{6}
$$

where x^μ runs over the spacetime coordinates $\{t, r, \theta, \phi\}$. It is easy to show that this vierbein satisfy the standard conditions:

$$
\begin{aligned}
e_a{}^\mu(x)e_b{}^\nu(x)g_{\mu\nu}(x) &= \eta_{ab}, \\
e^a{}_\mu(x)e_a{}^\nu(x) &= \delta_\mu{}^\nu, \\
e^a{}_\mu(x)e_b{}^\mu(x) &= \delta^a{}_b.
\end{aligned}
\tag{7}
$$

Here $\eta_{ab} = \mathrm{diag}(-1,1,1,1)$ is the Minkowski metric, and $a, b = 0, 1, 2, 3$ are tangent space indices.

The metric (1) is not written in its most general form. From this metric all the expanding and twisting Type-D solutions, including their different subfamilies as the accelerating and rotating black-hole, the Kerr solution with NUT, the NUT solution with rotation, the C-metric and the other well-known solutions like Kerr, NUT and Schwarzschild solutions, can be obtained. A more general treatment including the expanding but non-twisting solutions and non-expanding and non-twisting Type-D solutions is also possible. But only for simplicity, they will not be considered in this paper.

3. Frame-dragging

In this section, we consider the axially symmetric metric of the general form (4). This will be the only assumption, and all results will be valid for a generic metric of this form. The treatment will be general and it is only until section 6 when we will specialize in the Plebański–Demiański metric or subcases of it.

In the Kerr spacetime, the axial symmetry is related to the rotation of the black hole. When the metric is non-diagonal, the effect of frame-dragging has to be incorporated. This phenomenon can be interpreted as a dragging of local inertial reference frames [37] due the rotation. For instance, a distant observer will see a free-falling particle that acquires velocity, angular momentum and NUT parameter when it is near a spinning black hole. This happens in order to have suitable observers that make reliable measurements of the spin precession.

In a previous work, for the case of the Kerr–Newman spacetime with frame-dragging [16], we adopted a set of observers that hovered at fixed coordinate position. In this paper, we also use this kind of observers, which will be useful later to prepare (and measure) the relevant spin states. The hovering observers are not affected by frame-dragging, that is, as seen by long distance observers, the hovering position has a 4-velocity defined by

$$
u_{\mathrm{h}}^\mu = (\mathrm{d}t/\mathrm{d}\tau, 0, 0, 0) = ((-g_{00})^{-1/2}, 0, 0, 0).
\tag{8}
$$

It is worth mentioning that this hovering observer is at rest in the local frame (i.e. $u_h^a = \eta^{ab}e_b{}^\mu u_{\mu h}$), because the selected vierbein (6) will ensure the right measurements of the local infinitesimal Lorentz transformations of spin precession that we will discuss in section 4.

For a free-falling particle the 4-velocity due to frame-dragging, as seen by the same distant observers, was given (for instance) in [16, 37]

$$u^{\mu}_{\mathrm{fd}} = \sqrt{\frac{-g_{33}}{g_{00}g_{33} - (g_{03})^2}} \left(1, 0, 0, -\frac{g_{03}}{g_{33}}\right). \tag{9}$$

In this work, the frame-dragging velocity has to be measured by the hovering observer as a local inertial frame velocity and it can be obtained by projecting out the 4-momentum mu^{μ}_{fd} of the particle over the 4-vector velocity u_{μ_h} of the hovering observer

$$u^{\mu}_{\mathrm{fd}} u_{\mu_{\mathrm{h}}} = -E = -\gamma_{\mathrm{fd}}, \tag{10}$$

where E is the relativistic energy per unit mass of the particle with respect to a local observer (in this case, the hovering observer). This scalar product (10) is also the time component of the 4-momentum of the particle with respect to the hovering observer's reference frame, which is the usual relativistic gamma factor $\gamma_{\mathrm{fd}} = (1 - v^2_{\mathrm{fd}})^{-1/2}$.

Hence, our interest shall be focused in v_{fd}, which is the speed of the particle due to frame-dragging in the local inertial frame of the hovering observer. This frame-dragging speed is equivalent to $\tanh \eta = v_{\mathrm{fd}}$. Therefore, the local inertial frame velocity due to frame-dragging measured by a hovering observer can be represented in terms of hyperbolic functions as

$$u^a_{\mathrm{fd}} = (\cosh \eta, 0, 0, \ \sinh \eta). \tag{11}$$

Moreover, we shall see that this is a suitable way of expressing the frame-dragging velocity when this effect is incorporated in the spin precession angle in section 4.

Finally, the relevant hyperbolic functions are obtained after some straightforward algebra from equations (8)–(10) and they are given by

$$\begin{aligned}
v_{\mathrm{fd}} &= \tanh \eta = \frac{g_{03}}{\sqrt{(g_{03})^2 - g_{00}g_{33}}}, \\
\gamma_{\mathrm{fd}} &= \cosh \eta = \sqrt{\frac{g_{00}g_{33} - (g_{03})^2}{g_{00}g_{33}}}, \\
\sinh \eta &= \sqrt{\frac{-(g_{03})^2}{g_{00}g_{33}}}.
\end{aligned} \tag{12}$$

4. Spin precession

In this work, we consider two observers and an EPR source on the equator plane $\theta = \pi/2$. The observers are placed at azimuthal angles $\phi = \pm\Phi$ and the EPR source is located at $\phi = 0$. The observers and the EPR source are assumed to be hovering satisfying equation (8) over the black hole in order to keep them 'at rest' in the Boyer–Lindquist coordinate system (1). The EPR source emits a pair of entangled particles in opposite directions, describing a circular orbit on the equator at constant radius. The vierbein (6) works as a reference frame to prepare the spin state in the EPR source and to measure the new quantum states of the particles from the perspective of the hovering observers. This vierbein is defined at each point of spacetime since the observers, and consequently the EPR source, are accelerated on the equator and keep a constant radius, in such a way that they are not influenced by frame-dragging, as previously stated. The gedanken experiment depicting this situation is shown in figure 1.

From the perspective of ZAMOs, the local velocity of the entangled particles is given by

$$u^a_{\mathrm{EPR}} = (\cosh \zeta, 0, 0, \sinh \zeta), \tag{13}$$

where $v_{\mathrm{EPR}} = \tanh \zeta$ is the speed of particles in the local inertial frame of the ZAMO.
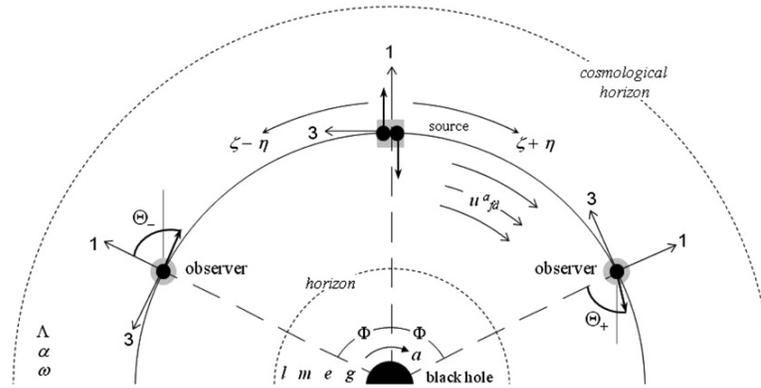
Figure 1. An EPR gedanken experiment in an axially symmetric spacetime. Two hovering observers (indicated by gray circles) and a static EPR source (gray square and hovering too) are located at $\phi = \pm\Phi$ and 0, respectively. The expanding and twisting Plebański–Demiański metric, represents a spacetime described through seven parameters: mass m, electric and magnetic charges e, g, rotation parameter a, cosmological constant Λ, NUT-like parameter l and acceleration-like parameter α. Both entangled particles feel frame-dragging with respect to the observers and they leave the source with a local velocity $\tanh(\zeta \pm \eta)$, where the positive sign stands for the particle traveling in the same direction as the rotation and the negative sign corresponds to the opposite one.

This ZAMO is mounted in a frame that is rotating around the black hole due to frame-dragging; therefore, the ZAMO has a local velocity described precisely by equation (11), as seen by the hovering observers. Moreover, it has the angular velocity $-g_{03}/g_{33}$, as seen by a distant observer. The world-lines of this kind of observers are orthogonal to the one of the surface of constant t (i.e. $dx_\mu u^\mu_{fd} = 0$), and the angular momentum of any particle is conserved in their local inertial frame [16, 37]. Due to this feature, we will adopt a ZAMO observer as a preliminary step before we calculate the total local inertial velocity of entangled particles measured by the hovering observers. When the particles leave the EPR source, their local velocity u^a_{EPR} remains constant in the ZAMO's frame.

Now, from the point of view of a hovering observer, the particles have a local inertial frame in which the velocity is given by the relativistic addition of the velocity of the ZAMO (11) plus the velocity of the particles measured by the ZAMOs (13). That is, $\tanh \xi_\pm$, where $\xi_\pm = \zeta \pm \eta$ is the total speed of the particle in the local inertial frame (see figure 1). The plus sign corresponds to the particle in the direction of the rotation of the black hole; meanwhile, the minus sign is for the other particle traveling in the opposite direction. In this way, the gravitational and frame-dragging effects are taken into account.

After the pair of entangled spin-1/2 particles is generated at the EPR source, they leave it and follow a circular path around a black hole. In spherical coordinates on the equatorial plane $\theta = \pi/2$, the velocity of particles has two relevant components, the temporal one and the spatial one with ϕ-coordinate at constant radius r. Thus, for the hovering observer, the motion is measured by the proper-velocity with $v = \tanh \xi$. That is, $u^a = (\cosh \xi, 0, 0, \sinh \xi)$, therefore the general contravariant 4-velocity is

$$
\begin{aligned}
u^t &= e_0{}^t \cosh \xi + e_3{}^t \sinh \xi, \\
u^\phi &= e_3{}^\phi \sinh \xi,
\end{aligned}
\tag{14}
$$

which satisfies the normalization condition $u^\mu u_\mu = -1$.

7

In order the particles describe circular motion, we must apply an external force that compensates both the centrifugal force and the gravity. The acceleration due to this external force is obtained from [13]

$$a^\mu(x) = u^\nu(x)\nabla_\nu u^\mu(x). \tag{15}$$

On the equatorial plane the acceleration then becomes

$$\begin{aligned}
a^r = (e_0{}^t)^2\Gamma^1_{00}\cosh^2\xi &+ \left[(e_3{}^t)^2\Gamma^1_{00} + (e_3{}^\phi)^2\Gamma^1_{33} + 2e_3{}^te_3{}^\phi\Gamma^1_{03}\right]\sinh^2\xi \\
&+ 2e_0{}^t\left(e_3{}^\phi\Gamma^1_{03} + e_3{}^t\Gamma^1_{00}\right)\sinh\xi\cosh\xi,
\end{aligned} \tag{16}$$

where $\Gamma^\mu_{\rho\sigma}$ are the usual Christoffel's symbols.

Once the frame-dragging velocity is incorporated into acceleration, it is interesting to note that (12) does not affect the structure of (16), i.e., the covariant derivatives ∇_μ in equation (15) act only over coordinates t and ϕ, and these variables are not present on the frame-dragging velocity. In the rest of this work, there will be no place where frame-dragging does affect another computation.

The change of the local inertial frame consists of a boost along the 1-axis and a rotation about the 2-axis calculated by

$$\chi^a{}_b(x) = -u^\nu\omega_\nu{}^a{}_b(x), \tag{17}$$

where the connection 1-forms are defined as

$$\omega_\mu{}^a{}_b(x) = -e_b{}^\nu(x)\nabla_\mu e^a{}_\nu(x) = e^a{}_\nu(x)\nabla_\mu e_b{}^\nu(x). \tag{18}$$

In our particular situation, the connections of interest are given by

$$\begin{aligned}
\omega_t{}^0{}_1 &= e_1{}^re^0{}_t\Gamma^0_{01} + e_1{}^re^0{}_\phi\Gamma^3_{01}, \\
\omega_t{}^1{}_3 &= e_3{}^te^1{}_r\Gamma^1_{00} + e_3{}^\phi e^1{}_r\Gamma^1_{03}, \\
\omega_\phi{}^0{}_1 &= e_1{}^re^0{}_t\Gamma^0_{13} + e_1{}^re^0{}_\phi\Gamma^3_{13}, \\
\omega_\phi{}^1{}_3 &= e_3{}^te^1{}_r\Gamma^1_{03} + e_3{}^\phi e^1{}_r\Gamma^1_{33}.
\end{aligned} \tag{19}$$

The relevant boost is described by

$$\begin{aligned}
\chi^0{}_1 = -e_0{}^te_1{}^r\left(e^0{}_t\Gamma^0_{01} + e^0{}_\phi\Gamma^3_{01}\right)\cosh\xi \\
- e_1{}^r\left[e_3{}^\phi\left(e^0{}_t\Gamma^0_{13} + e^0{}_\phi\Gamma^3_{13}\right) + e_3{}^t(e^0{}_t\Gamma^0_{01} + e^0{}_\phi\Gamma^3_{01})\right]\sinh\xi,
\end{aligned} \tag{20}$$

while the rotation about the 2-axis is given by

$$\begin{aligned}
\chi^1{}_3 = -e_0{}^te^1{}_r\left(e_3{}^t\Gamma^1_{00} + e_3{}^\phi\Gamma^1_{03}\right)\cosh\xi \\
- e^1{}_r\left[e_3{}^t\left(e_3{}^t\Gamma^1_{00} + e_3{}^\phi\Gamma^1_{03}\right) + e_3{}^\phi\left(e_3{}^t\Gamma^1_{03} + e_3{}^\phi\Gamma^1_{33}\right)\right]\sinh\xi.
\end{aligned} \tag{21}$$

The infinitesimal Lorentz transformation can be calculated easily by adding the rotation of the local 4-momentum $p^a(x) = mu^a(x)$ on the plane traced by the general 4-vectors of velocity and acceleration, that is [13]

$$\lambda^a{}_b(x) = -\frac{1}{m}[a^a(x)p_b(x) - p^a(x)a_b(x)] + \chi^a{}_b(x). \tag{22}$$

The boost along the 1-axis and the rotation about the 2-axis are respectively

$$\begin{aligned}
\lambda^0{}_1 = e^1{}_r\Big[(e_0{}^t)^2\Gamma^1_{00}\cosh^2\xi &+ \left((e_3{}^t)^2\Gamma^1_{00} + (e_3{}^\phi)^2\Gamma^1_{33} + 2e_3{}^te_3{}^\phi\Gamma^1_{03}\right)\sinh^2\xi \\
&+ 2e_0{}^t\left(e_3{}^\phi\Gamma^1_{03} + e_3{}^t\Gamma^1_{00}\right)\sinh\xi\cosh\xi\Big]\cosh\xi - e_0{}^te_1{}^r\left(e^0{}_t\Gamma^0_{01} + e^0{}_\phi\Gamma^3_{01}\right)\cosh\xi \\
&- e_1{}^r\left[e_3{}^\phi\left(e^0{}_t\Gamma^0_{13} + e^0{}_\phi\Gamma^3_{13}\right) + e_3{}^t\left(e^0{}_t\Gamma^0_{01} + e^0{}_\phi\Gamma^3_{01}\right)\right]\sinh\xi,
\end{aligned}$$

$$\begin{aligned}
\lambda^1{}_3 = -e^1{}_r\Big[(e_0{}^t)^2\Gamma^1_{00}\cosh^2\xi &+ \left((e_3{}^t)^2\Gamma^1_{00} + (e_3{}^\phi)^2\Gamma^1_{33} + 2e_3{}^te_3{}^\phi\Gamma^1_{03}\right)\sinh^2\xi \\
&+ 2e_0{}^t\left(e_3{}^\phi\Gamma^1_{03} + e_3{}^t\Gamma^1_{00}\right)\sinh\xi\cosh\xi\Big]\sinh\xi - e_0{}^te^1{}_r\left(e_3{}^t\Gamma^1_{00} + e_3{}^\phi\Gamma^1_{03}\right)\cosh\xi \\
&- e^1{}_r\left[e_3{}^t\left(e_3{}^t\Gamma^1_{00} + e_3{}^\phi\Gamma^1_{03}\right) + e_3{}^\phi\left(e_3{}^t\Gamma^1_{03} + e_3{}^\phi\Gamma^1_{33}\right)\right]\sinh\xi.
\end{aligned} \tag{23}$$

8

The change of the spin is obtained by computing the infinitesimal Wigner rotation [13]

$$\vartheta^i{}_k(x) = \lambda^i{}_k(x) + \frac{\lambda^i{}_0(x) p_k(x) - \lambda_{k0}(x) p^i(x)}{p^0(x) + m}. \tag{24}$$

In particular, the rotation about the 2-axis through a certain angle reads

$$
\begin{aligned}
\vartheta^1{}_3 = & -e^1{}_r \Big[\big(e_0{}^t\big)^2 \Gamma^1_{00} \cosh^2 \xi + \big(\big(e_3{}^t\big)^2 \Gamma^1_{00} + \big(e_3{}^\phi\big)^2 \Gamma^1_{33} + 2e_3{}^t e_3{}^\phi \Gamma^1_{03} \big) \sinh^2 \xi \\
& + 2e_0{}^t \big(e_3{}^\phi \Gamma^1_{03} + e_3{}^t \Gamma^1_{00} \big) \sinh \xi \cosh \xi \Big] \sinh \xi - e_0{}^t e^1{}_r \big(e_3{}^t \Gamma^1_{00} + e_3{}^\phi \Gamma^1_{03} \big) \cosh \xi \\
& - e^1{}_r \big[e_3{}^t \big(e_3{}^t \Gamma^1_{00} + e_3{}^\phi \Gamma^1_{03} \big) + e_3{}^\phi \big(e_3{}^t \Gamma^1_{03} + e_3{}^\phi \Gamma^1_{33} \big) \big] \sinh \xi \\
& + \left(\frac{\sinh \xi}{\cosh \xi + 1} \right) \Big\{ e^1{}_r \Big[\big(e_0{}^t\big)^2 \Gamma^1_{00} \cosh^2 \xi + \big(\big(e_3{}^t\big)^2 \Gamma^1_{00} + \big(e_3{}^\phi\big)^2 \Gamma^1_{33} + 2e_3{}^t e_3{}^\phi \Gamma^1_{03} \big) \sinh^2 \xi \\
& + 2e_0{}^t \big(e_3{}^\phi \Gamma^1_{03} + e_3{}^t \Gamma^1_{00} \big) \sinh \xi \cosh \xi \Big] \cosh \xi - e_0{}^t e_1{}^r \big(e^0{}_t \Gamma^0_{01} + e^0{}_\phi \Gamma^3_{01} \big) \cosh \xi \\
& - e_1{}^r \big[e_3{}^\phi \big(e^0{}_t \Gamma^0_{13} + e^0{}_\phi \Gamma^3_{13} \big) + e_3{}^t \big(e^0{}_t \Gamma^0_{01} + e^0{}_\phi \Gamma^3_{01} \big) \big] \sinh \xi \Big\}.
\end{aligned} \tag{25}
$$

Finally, from the tetrad given in equation (6), it can be shown, after some algebra, that the previous expression (25), can be expressed as

$$
\begin{aligned}
\vartheta^1{}_3 = & -\frac{\cosh(2\xi)}{2 g_{00} \sqrt{g_{11}[(g_{03})^2 - g_{00} g_{33}]}} \left(g_{03} \frac{\partial g_{00}}{\partial r} - g_{00} \frac{\partial g_{03}}{\partial r} \right) - \frac{\sinh(2\xi)}{4 g_{00}[(g_{03})^2 - g_{00} g_{33}]\sqrt{g_{11}}} \\
& \times \left[g_{00} \left(g_{33} \frac{\partial g_{00}}{\partial r} - g_{00} \frac{\partial g_{33}}{\partial r} \right) + 2 g_{03} \left(g_{03} \frac{\partial g_{00}}{\partial r} - g_{00} \frac{\partial g_{03}}{\partial r} \right) \right].
\end{aligned} \tag{26}
$$

5. EPR correlation

In this section, we will obtain the spin precession angle of a pair of spin-1/2 EPR particles moving on the equator of a general axial-symmetric spacetime. We will follow basically [13, 16] and the details will be not repeated here. However, we recall that in the case of the curved spacetime, the one-particle quantum states $|p^a(x), \sigma; x\rangle$ transform under a local Lorentz transformation as [11, 12]

$$U(\Lambda(x))|p^a(x), \sigma; x\rangle = \sum_{\sigma'} D^{(1/2)}_{\sigma' \sigma}(W(x)) |\Lambda p^a(x), \sigma'; x\rangle, \tag{27}$$

where $W^a{}_b(x) \equiv W^a{}_b(\Lambda(x), p(x))$ is the so-called local finite Wigner rotation.

If frame-dragging is taken into account on the local inertial frame velocity u^a, it will affect the previous local velocity transformation and then the total velocity will be written as $u^a_\pm = (\cosh \xi_\pm, 0, 0, \sinh \xi_\pm)$, where $\xi_\pm = \zeta \pm \eta$. Remember that the plus sign stands for a particle moving in the same direction of the rotation and the minus sign if the motion of the particles is in the opposite direction.

After a proper time $\Phi/u^\phi_\pm$, each particle reaches the corresponding observer. Thus, the finite Wigner rotation [13, 16] can be written as

$$W^a{}_b(\pm \Phi, 0) = \begin{pmatrix} 1 & 0 & 0 & 0 \\ 0 & \cos \Theta_\pm & 0 & \pm \sin \Theta_\pm \\ 0 & 0 & 1 & 0 \\ 0 & \mp \sin \Theta_\pm & 0 & \cos \Theta_\pm \end{pmatrix}. \tag{28}$$

Once again, the sign of the angle $\Theta_\pm = \frac{\Phi \vartheta^1{}_3}{u^\phi_\pm}$ depends if the motion of the entangled particle is in the direction (or in its opposite sense) of frame-dragging. Thus, one has

$$\Theta_\pm = \frac{\Phi}{2\sqrt{-(g_{00})^3 g_{11}}} \left\{ \left(g_{03}\frac{\partial g_{00}}{\partial r} - g_{00}\frac{\partial g_{03}}{\partial r} \right) \frac{\cosh(2\zeta \pm 2\eta)}{\sinh(\zeta \pm \eta)} + \left[g_{00}\left(g_{00}\frac{\partial g_{33}}{\partial r} - g_{33}\frac{\partial g_{00}}{\partial r} \right) \right. \right.$$
$$\left. \left. + 2g_{03}\left(g_{03}\frac{\partial g_{00}}{\partial r} - g_{00}\frac{\partial g_{03}}{\partial r} \right) \right] \frac{\cosh(\zeta \pm \eta)}{\sqrt{(g_{03})^2 - g_{00}g_{33}}} \right\}. \tag{29}$$

Then the required Wigner rotation is given in the following form:

$$D^{(1/2)}_{\sigma'\sigma}(W(\pm\Phi,0)) = \exp\left(\mp i\frac{\sigma_y}{2}\Theta_\pm \right), \tag{30}$$

where σ_y is the Pauli matrix.

Now we can define the 4-momentum of the particle as seen by each hovering observer. Thus, the spin-singlet state for entangled particles is given by

$$|\psi\rangle = \frac{1}{\sqrt{2}}[|p^a_+, \uparrow; 0\rangle|p^a_-, \downarrow; 0\rangle - |p^a_+, \downarrow; 0\rangle|p^a_-, \uparrow; 0\rangle], \tag{31}$$

where the sign on the lineal momentum stands for the direction of each particle and corresponds to the up and down of the spin direction. For notational simplicity, only the evaluation at $\phi = 0$ in the arguments of the position was written .

Therefore, after the finite Wigner rotation, the new total quantum state is given by $|\psi\rangle' = W(\pm\Phi)|\psi\rangle$. Consequently in the local inertial frames at the corresponding positions $\phi = \Phi$ and $-\Phi$, each particle state can be written as

$$|p^a_\pm, \uparrow; \pm\Phi\rangle' = \cos\frac{\Theta_\pm}{2}|p^a_\pm, \uparrow; \pm\Phi\rangle \pm \sin\frac{\Theta_\pm}{2}|p^a_\pm, \downarrow; \pm\Phi\rangle, \tag{32}$$

$$|p^a_\pm, \downarrow; \pm\Phi\rangle' = \mp\sin\frac{\Theta_\pm}{2}|p^a_\pm, \uparrow; \pm\Phi\rangle + \cos\frac{\Theta_\pm}{2}|p^a_\pm, \downarrow; \pm\Phi\rangle. \tag{33}$$

Thus, the entangled state is described by the combination

$$|\psi\rangle' = \frac{1}{\sqrt{2}}\left[\cos\left(\frac{\Theta_+ + \Theta_-}{2}\right) (|p^a_+, \uparrow; \Phi\rangle|p^a_-, \downarrow; -\Phi\rangle - |p^a_+, \downarrow; \Phi\rangle|p^a_-, \uparrow; -\Phi\rangle) \right.$$
$$\left. + \sin\left(\frac{\Theta_+ + \Theta_-}{2}\right) (|p^a_+, \uparrow; \Phi\rangle|p^a_-, \uparrow; \Phi-\rangle + |p^a_+, \downarrow; \Phi\rangle|p^a_-, \downarrow; -\Phi\rangle) \right]. \tag{34}$$

Now, in order to eliminate the spurious effect of the evident rotation of the local inertial frames leading to angles $\pm\Phi$, one has to compensate the rotation through a second transformation as in [13, 16].

It is easy to see that the final quantum state reads

$$|\psi\rangle'' = \frac{1}{\sqrt{2}}[\cos\Delta(|p^a_+, \uparrow; \Phi\rangle'|p^a_-, \downarrow; -\Phi\rangle' - |p^a_+, \downarrow; \Phi\rangle'|p^a_-, \uparrow; -\Phi\rangle')$$
$$+ \sin\Delta(|p^a_+, \uparrow; \Phi\rangle'|p^a_-, \uparrow; \Phi-\rangle' + |p^a_+, \downarrow; \Phi\rangle'|p^a_-, \downarrow; -\Phi\rangle')]. \tag{35}$$

Here $\Delta = (\Theta_+ + \Theta_-)/2 - \Phi$ and Δ is given by

$$\Delta = \Phi\left[(2A\sinh\zeta + B\cosh\zeta)\cosh\eta - A\frac{\sinh\zeta\cosh\eta}{\cosh^2\eta - \cosh^2\zeta} - 1 \right], \tag{36}$$

where

$$A = \frac{1}{2\sqrt{-(g_{00})^3 g_{11}}}\left(g_{03}\frac{\partial g_{00}}{\partial r} - g_{00}\frac{\partial g_{03}}{\partial r} \right),$$

$$B = \frac{1}{2\sqrt{-(g_{00})^3 g_{11}[(g_{03})^2 - g_{00}g_{33}]}}\left[g_{00}\left(g_{00}\frac{\partial g_{33}}{\partial r} - g_{33}\frac{\partial g_{00}}{\partial r} \right) \right.$$
$$\left. + 2g_{03}\left(g_{03}\frac{\partial g_{00}}{\partial r} - g_{00}\frac{\partial g_{03}}{\partial r} \right) \right]. \tag{37}$$

10

Thus, the spin precession angle Δ may contain the gravitational effects that deteriorate the perfect anti-correlation of the entangled particles [13]. The spin-singlet state is mixed up with the spin-triplet state. This is because while the spin-singlet state is invariant under spatial rotations, it is not invariant under Lorentz transformations (23).

As it was pointed out in [13], this deterioration is a consequence of the manifest difference between the rotation matrix element $\vartheta^1{}_3$ and the trivial rotation $\varphi^1{}_3$. It is important to note that the entanglement is still invariant under local unitary operations, and then the nonlocal correlation still holds. Because of the effects coming from acceleration, gravity and frame-dragging, the perfect anti-correlation can still be employed for quantum communication, by rotating the direction of measurement about the 2-axis through the angles $\mp\Theta$ in the local inertial frames of the hovering observers.

It is evident that formulas (36) and (37) can be applied to any axially symmetric black hole and in particular to the most general expanding and twisting Type-D solution of Einstein equations. This will be the goal of the next section.

6. Spin precession angle in expanding and twisting Plebański–Demiański black hole

6.1. Plebański–Demiański black hole

In this section, we study the spin precession angle of the spin-1/2 systems of entangled particles in the spacetime described by the Plebański–Demiański metric (1) with frame-dragging (12).

Thus, it is easy to show that the coefficients A and B from the spin precession angle Δ on the equator ($\theta = \pi/2$), given by equation (36), are written as

$$
\begin{aligned}
A_{\mathrm{PD}} &= \frac{a\sqrt{D}}{2(r^2+l^2)(D-a^2)^{3/2}}[(r^2+l^2)D' - 2r(D-a^2)], \\
B_{\mathrm{PD}} &= \frac{1}{2(r^2+l^2)(D-a^2)^{3/2}}[4Dr(D-a^2) - (a^2r^2 + Dr^2 + Dl^2 + a^2l^2)D'],
\end{aligned}
\tag{38}
$$

where D is a quartic polynomial of r and it can be read off from equation (2). Here D' is defined by

$$
D' = \frac{\partial D}{\partial r} = -4\left(\frac{\alpha^2\kappa}{\omega^2} + \frac{\Lambda}{3}\right)r^3 - \frac{6n\alpha r^2}{\omega} + 2\varepsilon r - 2m.
\tag{39}
$$

The frame-dragging local inertial frame velocity is given by

$$
\cosh\eta_{\mathrm{PD}} = (r^2+l^2)\sqrt{\frac{D}{(D-a^2)\left[(r^2+a^2+2al+l^2)^2 - (a+2l)^2D\right]}}.
\tag{40}
$$

Thus, the coefficients A_{PD}, B_{PD}, the spin precession angle Δ_{PD} and frame-dragging $\cosh\eta_{\mathrm{PD}}$ are finally written in terms of the seven parameters arising in the metric and which have a direct physical interpretation. It is well known from [22, 23] that the metric (1) represents a pair of accelerating black holes with the rotation, NUT and cosmological constant parameters, charge and mass. It is also known [22, 23] that in this situation there are two very different spacetime solutions. The first case is the one with $|l| \geqslant |a|$, which has non-singular curvature, this gives rise to an *accelerating NUT solution with rotation*. This also corresponds to the right branch of the diagram 1 of [22, 23]. In the second case, with $|l| \leqslant |a|$ we have an *accelerating and rotating black hole* including also the rest of the parameters. The types of solutions arising here correspond to the left branch and they are of singular nature. It can be shown that the coefficients and Δ_{PD} have the correct asymptotic limits.

We will analyze the associated spin precession angle of these two branches of these Type-D solutions of the Einstein equations. We start from the right branch and follow with

11

the left one. The more evident contribution to the spin precession angle will come from the exterior event, the cosmological and the acceleration horizons (obtained from the condition that the quartic polynomial D has at least two real roots which define the inner and outer horizons. The other vanishing terms define the cosmological and acceleration horizons). We will see that the main contribution to Δ_{PD} comes from precisely these horizons. Besides the horizon contribution, we will have an additional possibly non-trivial contribution coming from frame-dragging at $\cosh \eta_{\mathrm{PD}} = \cosh \zeta$ (36). In order to give a more detailed account of the entanglement behavior on these horizons, we shall study below the different limiting cases.

6.2. Non-accelerating Kerr–Newman–(anti-)de Sitter–NUT black hole

The Kerr–Newman–(anti-)de Sitter–NUT (KN(A)dSNUT) spacetime is included in this large family of Type-D solutions. The KN(A)dSNUT spacetime represents a non-accelerating ($\alpha = 0$) black hole with mass m, electric and magnetic charges e and g, a rotation parameter a and a NUT parameter l in a de Sitter or anti-de Sitter background with non-vanishing cosmological constant Λ. This case contains in turn two limits: $|a| > |l|$ and $|a| < |l|$, that correspond to the Kerr solution with NUT and the NUT solution with rotation, respectively.

After setting the acceleration parameter equal to zero i.e. $\alpha = 0$, the parameters in relation (3) become

$$
\begin{aligned}
\kappa &= (1 - l^2 \Lambda)(a^2 - l^2), \\
\varepsilon &= 1 - \left(\tfrac{1}{3} a^2 + 2l^2\right)\Lambda, \\
n &= l + \tfrac{1}{3}(a^2 - 4l^2) l \Lambda.
\end{aligned}
\tag{41}
$$

Thus, the metric (1) is reduced to

$$
\mathrm{d}s^2 = -\frac{D}{\rho^2}\left[\mathrm{d}t - \left(a \sin^2 \theta + 4l \sin^2 \frac{\theta}{2}\right)\mathrm{d}\phi\right]^2 + \frac{\rho^2}{D}\mathrm{d}r^2 + \frac{P}{\rho^2}[a\,\mathrm{d}t - (r^2 + (a+l)^2\,\mathrm{d}\phi)]^2
$$
$$
+ \frac{\rho^2}{P}\sin^2 \theta\,\mathrm{d}\theta^2,
\tag{42}
$$

where

$$
\begin{aligned}
\rho^2 &= r^2 + (l + a\cos\theta)^2, \\
P &= \sin^2 \theta \left(1 + \tfrac{4}{3}\Lambda al\cos\theta + \tfrac{1}{3}\Lambda a^2 \cos^2\theta\right), \\
D &= a^2 - l^2 + e^2 + g^2 - 2mr + r^2 - \Lambda\left[(a^2 - l^2)l^2 + \left(\tfrac{1}{3}a^2 + 2l^2\right)r^2 + \tfrac{1}{3}r^4\right].
\end{aligned}
\tag{43}
$$

We can notice that taking $D(r_+) \to 0$, the metric coefficient $g_{11} \to \infty$ and the metric fails to be strongly asymptotically predictable. This apparent singularity arises because the coordinates are not valid at the outer horizon r_+, and this singularity can be removed by a different choice of coordinates. In this work, we consider particles only orbiting black holes with $r > r_+$, and the Kruskal–Szekeres type extensions are not required here. Later, we will see that this horizon has relevance when the spin precession angle is calculated.

For the KN(A)dSNUT spacetime, the spin precession angle $\Delta_{\mathrm{KN(A)dSNUT}}$ with coefficients $A_{\mathrm{KN(A)dSNUT}}$, $B_{\mathrm{KN(A)dSNUT}}$ and the frame-dragging velocity $\cosh \eta_{\mathrm{KN(A)dSNUT}}$, are still given by equations (38) and (40), respectively. But now, D is given from equation (43) and

$$
D' = \frac{\partial D}{\partial r} = -\frac{4}{3}\Lambda r^3 + \left[2 - \Lambda\left(\frac{2}{3}a^2 + 4l^2\right)\right]r - 2m.
\tag{44}
$$

Thus the problem of the entanglement is completely expressed in terms of the remaining six physical parameters and the variable r. Finally, it is easy to check that with the coefficients $A_{\mathrm{KN(A)dSNUT}}$, $B_{\mathrm{KN(A)dSNUT}}$, the precession angle $\Delta_{\mathrm{KN(A)dSNUT}}$ has the correct asymptotic behavior at $r \to \infty$.

In the case when $e = g = \Lambda = 0$, the spin precession angle explicitly written in terms of the physical parameters is given by

$$
\begin{aligned}
\Delta_{\text{Kerr-NUT}} = \Bigg\{ & \frac{\cosh \eta_{\text{Kerr-NUT}}}{(r^2 + l^2)(r^2 - 2mr - l^2)^{3/2}} \Bigg[2a\sqrt{r^2 + a^2 - l^2 - 2mr}(mr^2 + 2l^2 r - ml^2) \sinh \zeta \\
& + [r^5 - 5mr^4 + (6m^2 - 4l^2)r^3 + (10l^2 m - 2a^2 m)r^2 \\
& + (-4a^2 l^2 + 3l^4 - 2m^2 l^2)r + 2a^2 l^2 m - l^4 m] \cosh \zeta \\
& + a\sqrt{r^2 + a^2 - l^2 - 2mr}(mr^2 + 2l^2 r - ml^2) \\
& \times \frac{\sinh \zeta}{\cosh^2 \eta_{\text{Kerr-NUT}} - \cosh^2 \zeta} \Bigg] - 1 \Bigg\} \Phi,
\end{aligned}
\tag{45}
$$

where

$$
\cosh \eta_{\text{Kerr-NUT}} =
$$

$$
\frac{(r^2 + l^2)\sqrt{r^2 - 2mr + a^2 - l^2}}{\sqrt{(r^2 - 2mr - l^2)[r^4 + (a^2 - 2l^2)r^2 + (8mal + 8l^2 m + 2a^2 m)r + 5l^4 + 3a^2 l^2 + 8al^3]}}.
\tag{46}
$$

Kerr black hole. Now we consider an axially symmetric spacetime with rotation parameter a. This parameter can be related to the rotation of a black hole and it is responsible for the dragging around the spacetime near the hole discussed in section 3.

This case was carried out also in our previous work [16], and we shall see that those results are confirmed in the present analysis.

From equation (36) with coefficients (38) and parameters $e = g = l = \Lambda = 0$ the spin precession angle is reduced to

$$
\Delta_{\text{K}} = \Phi \Bigg[\frac{-2\sqrt{D}am \sinh \zeta + (H - mD)\cosh \zeta}{(r^2 - 2mr)^{3/2}} \cosh \eta_{\text{K}} \\
+ \frac{\sqrt{D}am}{(r^2 - 2mr)^{3/2}} \frac{\sinh \zeta \cosh \eta_{\text{K}}}{\cosh^2 \eta_{\text{K}} - \cosh^2 \zeta} - 1 \Bigg],
\tag{47}
$$

where

$$
D = r^2 - 2mr + a^2,
\tag{48}
$$

$$
H = r^3 - 4mr^2 + 4m^2 r - a^2 m,
\tag{49}
$$

$$
\cosh \eta_{\text{K}} = \frac{r\sqrt{D}}{\sqrt{(r - 2m)(r^3 + a^2 r + 2ma^2)}} \neq 1,
\tag{50}
$$

with the coefficients A and B being

$$
A_{\text{K}} = -\frac{\sqrt{D}am}{(r^2 - 2mr)^{3/2}}, \qquad B_{\text{K}} = \frac{H - mD}{(r^2 - 2mr)^{3/2}}.
\tag{51}
$$

The detailed behavior of the spin precession angle Δ_{K} with the distance r and the local velocity $v = v_{\text{EPR}}$ coincides precisely with that described in [16] and it will be not repeated here. We only mention that the main sources of a divergent angle Δ_{K} are the effects on the outer event horizon of the Kerr metric in addition to the frame-dragging ones.

Schwarzschild-NUT black hole.   There is still a controversy if the NUT parameter can be considered a gravito-magnetic dual mass parameter, or a twisting property of the surrounding spacetime [38]. For the purpose of this work, we will find that the NUT parameter enters in the description of the spin precession similarly as the rotation parameter does. Consequently, it also might have important frame-dragging effects that are expected to contribute to the precession angle. This is more clearly stated when equation (36) is simplified by setting the parameters $e = g = a = \Lambda = 0$,

$$\Delta_{\mathrm{NUT}} = \Phi \left(\frac{r^3 - 3mr^2 - 3l^2 r + ml^2}{(r^2 + l^2)\sqrt{r^2 - 2mr - l^2}} \cosh \zeta \cosh \eta_{\mathrm{NUT}} - 1 \right), \qquad (52)$$

where

$$\cosh \eta_{\mathrm{NUT}} = \frac{r^2 + l^2}{\sqrt{r^4 - 2l^2 r^2 + 8ml^2 r + 5l^4}} \neq 1.$$

The coefficients A and B are given by

$$A_{\mathrm{NUT}} = 0, \qquad B_{\mathrm{NUT}} = \frac{r^3 - 3mr^2 - 3l^2 r + ml^2}{(r^2 + l^2)\sqrt{r^2 - 2mr - l^2}}. \qquad (53)$$

Equation (52) is a generalization of the Schwarzschild spin precession angle, but now it has integrated an additional factor due to frame-dragging.

The precession angle Δ_{NUT} diverges precisely at $r = r_{\mathrm{NUT}}$, where

$$r_{\mathrm{NUT}} = m \pm \sqrt{m^2 + l^2}. \qquad (54)$$

The positive root represents the outer Schwarzschild–NUT horizon.

Although the $\cosh \eta_{\mathrm{NUT}}$ term due to frame-dragging has a fourth-degree polynomial in the denominator, this quartic function does not have real roots. An elementary numerical analysis shows that the roots of this fourth-degree polynomial do not exist if one assumes that m and l are real and positive numbers. Therefore, frame-dragging contribution to the NUT spin precession angle does not have any asymptotic singularity for any particular value of r.

The NUT spin precession angle equation (52) is plotted in figure 2 for two values of NUT parameter l. The distance is parameterized by m/r which means that the experiment is placed at infinite when $m/r \to 0$. The local velocity of the particles v_{EPR} is indicated as v.

We can see from figure 2 the usual effect of the local velocity. As v_{EPR} increases, the absolute value of spin precession Δ_{NUT} increases too. Also, we can see that for small values of l, the spin precession has asymptotic values to the value of the Schwarzschild horizon figure 2(*a*). But now, for larger values of the NUT parameter figure 2(*b*), there is a shift in position of the horizon given by equation (54) to higher values of r. At the value r_{NUT}, $|\Delta_{\mathrm{NUT}}|$ increases without limit, deteriorating the perfect anti-correlation of the pair of the entangled particles.

Schwarzschild–(anti-)de Sitter black hole.   This is a spherically symmetric spacetime and therefore there is no non-diagonal element on the metric; consequently, there are no frame-dragging effects. The Schwarzschild–(anti-)de Sitter black hole represents a spacetime which is an asymptotically (anti-)de Sitter space [39]. A positive cosmological constant Λ is related to an accelerated universe, meanwhile a negative value is related to negative vacuum energy and positive pressure. The spin precession angle in this case is given by

$$\Delta_{\mathrm{(A)dS}} = \Phi \left(\frac{r - 3m}{\sqrt{r^2 - 2mr - \frac{1}{3}\Lambda r^4}} \cosh \zeta - 1 \right), \qquad (55)$$
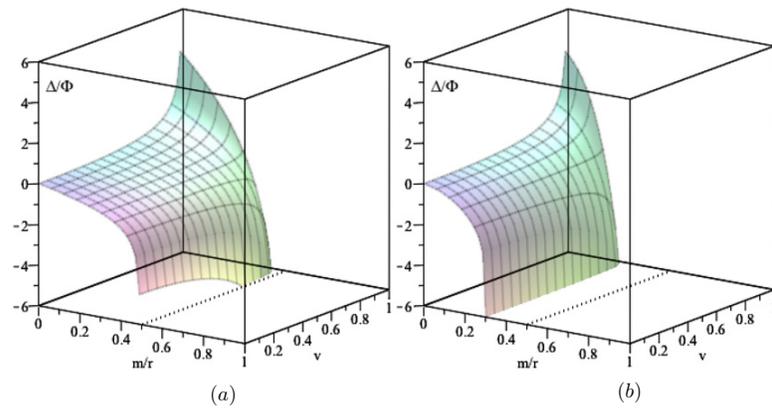
Figure 2. The precession angle Δ/Φ for a NUT black hole for two values of NUT parameter l as a function of distance m/r and local velocity $v = v_{\text{EPR}}$. The dotted line is placed at Schwarzschild radius $r = 2m$. Large values of the NUT parameter l shift the position of the Schwarzschild horizon event to r_{NUT}. (a) $l = 0.1m$; (b) $l = 2.0m$.

with A and B of the following form:

$$A_{\text{(A)dS}} = 0, \qquad B_{\text{(A)dS}} = \frac{r - 3m}{\sqrt{r^2 - 2mr - \frac{1}{3}\Lambda r^4}} \tag{56}$$

and $\cosh \eta_{\text{(A)dS}} = 1$.

For a distance near the black hole and positive Λ, it is easy to see that the spin precession angle behaves in the same manner as in the case of Schwarzschild spacetime (see [13]) due to the smallness of the cosmological constant Λ. But the cosmological constant has a significant effect only for large distances which are of the order of 10^{26} m [40].

We can see in figure 3(a) that for positive Λ, the spin precession angle is asymptotic at the cosmological horizon, meanwhile for negative Λ in figure 3(b), the cosmological constant has negligible effects and the precession angle has the same behavior as that of the Schwarzschild spacetime previously mentioned.

Reissner–Nordström black hole. This case corresponds to a Schwarzschild black hole with non-vanishing charges e and g, after setting l, Λ and a to zero. The Reissner–Nordström spacetime is also a spherically symmetric solution.

The spin precession angle is then reduced to

$$\Delta_{\text{RN}} = \Phi \left(\frac{r^2 - 3mr + 2e^2 + 2g^2}{r\sqrt{r^2 - 2mr + e^2 + g^2}} \cosh \zeta - 1 \right), \tag{57}$$

where the functions A and B are

$$A_{\text{RN}} = 0, \qquad B_{\text{RN}} = \frac{r^2 - 3mr + 2e^2 + 2g^2}{r\sqrt{r^2 - 2mr + e^2 + g^2}} \tag{58}$$

and $\cosh \eta_{\text{RN}} = 1$.

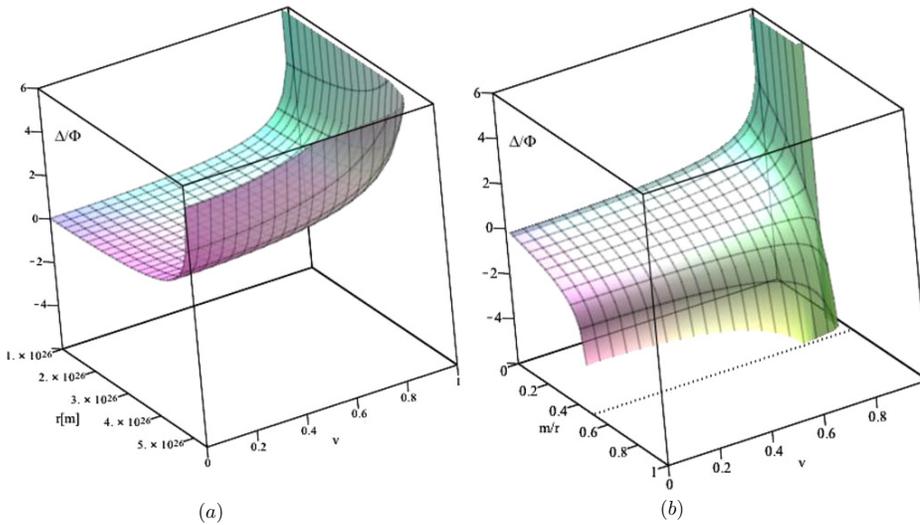This result reproduces completely our previous result of [16] after adding the magnetic charge g.

15

Figure 3. The precession angle Δ/Φ for a Schwarzschild–de Sitter and anti-de Sitter spacetime. (*a*) and (*b*) manifest the strong differences between these situations. (*a*) $\Lambda = 1.11 \times 10^{-56}$ (km^{-2}), $1 \times 10^{26} < r < 5.4 \times 10^{26}$ (m) (*b*) $\Lambda = -1.11 \times 10^{-56}$ (km^{-2}), $0 < m/r < 1$.

Schwarzschild black hole. Finally it is easy to recover the Schwarzschild spin precession by setting $a, e, g, l, \Lambda = 0$. The coefficients and frame-dragging are reduced to $A_S = 0$, $B_S = (r - 3m)/\sqrt{r^2 - 2mr}$ and $\cosh \eta_S = 1$. Consequently, the expression (36) is given by

$$\Delta_S = \Phi \left(\frac{r - 3m}{\sqrt{r^2 - 2mr}} \cosh \zeta - 1 \right), \tag{59}$$

which is precisely equation (51) from [13].

6.3. Accelerating and rotating black holes

In [41] it was shown that the metric (1) represents an accelerating and rotating charged pair of black holes with a generally non-zero NUT parameter. In order to simplify our analysis we shall consider in this subsection the case of vanishing parameters $\Lambda = e = g = l = 0$.

As [41] pointed out, we can see that the parameters α and ω are related to the acceleration and rotation of the source (mass m), respectively.

Therefore, with an arbitrary α and using the remaining scaling freedom to put $\omega = a$, the Plebański–Demiański metric is reduced to

$$ds^2 = \frac{1}{\Omega^2} \left(-\frac{D}{\rho^2} [dt - a \sin^2 \theta \, d\phi]^2 + \frac{\rho^2}{D} \, dr^2 + \frac{P}{\rho^2} (a \, dt - (r^2 + a^2) \, d\phi)^2 + \rho^2 \frac{\sin^2 \theta}{P} \, d\theta^2 \right), \tag{60}$$

where the parameters (2) and (3) are given by

$$\begin{aligned} \varepsilon &= 1 - a^2 \alpha^2, \\ n &= -a\alpha m, \\ P &= \sin^2 \theta (1 - 2\alpha m \cos \theta + a^2 \alpha^2 \cos^2 \theta), \end{aligned} \tag{61}$$

16

and

$$\rho^2 = r^2 + a^2 \cos^2 \theta,$$
$$\Omega = 1 - \alpha r \cos \theta, \tag{62}$$
$$D = a^2 - 2mr + (1 - a^2\alpha^2)r^2 + 2\alpha^2 mr^3 - \alpha^2 r^4.$$

The metric (60) has four singularities when $\theta = \pi/2$, that is, we can factorize D as

$$D = (r - r_+)(r - r_-)(1 - \alpha^2 r^2), \tag{63}$$

where

$$r_\pm = m \pm \sqrt{m^2 - a^2}. \tag{64}$$

As we can remember, $r_\pm$ are the locations of the outer and inner horizons of the non-accelerating Kerr black hole. The other pair of horizons are related to the acceleration α and it is familiar in the context of the C-metric as an acceleration horizon:

$$r_{\text{acc}} = \frac{1}{\alpha}. \tag{65}$$

After some easy manipulations, the coefficients for the spin precession angle are given by

$$A_{\text{AccRot}} = \frac{a\sqrt{D}}{2r(D - a^2)^{3/2}}[rD' - 2(D - a^2)],$$
$$B_{\text{AccRot}} = \frac{1}{2r(D - a^2)^{3/2}}[4D(D - a^2) - r(a^2 + D)D'], \tag{66}$$

where

$$D' = \frac{\partial D}{\partial r} = -2m + 2(1 - a^2\alpha^2)r + 6\alpha^2 mr^2 - 4\alpha^2 r^3 \tag{67}$$

and the frame-dragging velocity is

$$\cosh \eta_{\text{AccRot}} = r^2 \sqrt{\frac{D}{(D - a^2)[(r^2 + a^2)^2 - a^2 D]}}. \tag{68}$$

But the horizons (64) and (65) have no physical relevance on the spin precession angle because the coefficients (66) are not singular at these points.

We observed this kind of behavior for Kerr–Newman spacetime in our previous work [16], where the Schwarzschild horizon and the frame-dragging effect produce an asymptotic spin precession angle instead of Kerr horizons.

It is easy to show that we can recover the Kerr spacetime results reviewed in the previous section, after setting vanishing acceleration ($\alpha = 0$). Therefore, we shall consider the effect of acceleration over the spin precession angle.

C-metric. From the pair of accelerated and rotating black holes represented by the metric (60), we can consider the limit in which $a \to 0$. In this case, the metric has the form of the C-metric and thus the coefficients (66) reduce to

$$A_{\text{C-metric}} = 0, \qquad B_{\text{C-metric}} = \frac{\alpha^2 mr^2 + r - 3m}{\sqrt{(r^2 - 2mr)(1 - \alpha^2 r^2)}}, \tag{69}$$
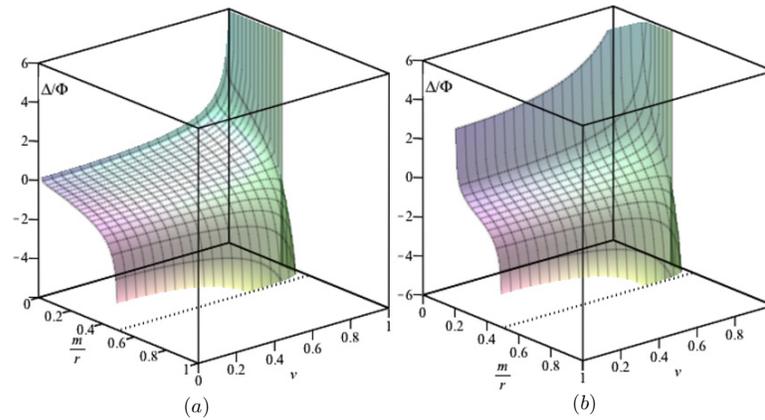
and

$$\cosh \eta_{\text{C-metric}} = 1. \tag{70}$$

Figure 4. The precession angle Δ/Φ for C-metric for two values of the acceleration parameter α as a function of distance m/r and local velocity $v = v_{\text{EPR}}$. The dotted line is placed at Schwarzschild radius $r = 2m$. (a) $\alpha = 0.01m$; (b) $\alpha = 0.20m$.

Then, the spin precession angle for the C-metric is

$$\Delta_{\text{C-metric}} = \Phi\left(\frac{\alpha^2 m r^2 + r - 3m}{\sqrt{(r^2 - 2mr)(1 - \alpha^2 r^2)}}\cosh\zeta - 1\right). \tag{71}$$

Moreover, it is easy to see that this equation reduces to the Schwarzschild case (59) when $\alpha = 0$.

In addition, we can see from equation (71) that it is divergent at the Schwarzschild radius $r = 2m$ and at the acceleration horizon, that is, $\Delta_{\text{C-metric}} \to \infty$ as $r \to \alpha^{-1}$.

In figure 4, the effect of acceleration α over the spin precession angle $\Delta_{\text{C-metric}}$ as function of the distance and local velocity of the particles is plotted. The acceleration is parameterized as a function of acceleration per unit mass. As mentioned in [41], the acceleration can only have positive values. We can observe the effect of the velocity of the particles that was already seen in all previous cases, that is, for high local velocity of the particles v_{EPR}, the $\Delta_{\text{C-metric}}$ increases.

The C-metric also has a horizon and corresponds to the Schwarzschild radius, that can be clearly observed in equation (71). But as was mentioned, there is another horizon due to the acceleration parameter as $r \to \alpha^{-1}$.

The above behavior can suggest some insight about the physical interpretation of the acceleration parameter. In fact, because of the acceleration horizon (65), we can see that a very small acceleration will have an important effect until a long distance is reached, even when a flat spacetime with no effect over the spin precession angle is expected. In [42], it was noted that when $\alpha \neq 0$, it is difficult to uniquely determine the mass of each individual black hole since the spacetime is not globally asymptotically flat and one cannot expect to distinguish effects due to acceleration from those due to gravitational fields. By the calculation of the spin precession angle it could be possible to distinguish indirectly the mass effects from those of the acceleration ones.

7. Conclusions

In this work, we found an algorithm to calculate in a general way the spin precession angle of an EPR pair of spin-1/2 massive particles moving on the equator for very general axially symmetric spacetime without reference to any specific metric.

18

However, even for the most general case, before applying it to Type-D solutions, we showed that when frame-dragging is taken into account, then an additional velocity over particles must be incorporated. Therefore, hovering observers were introduced in order to have a fixed reference frame that ensures reliable directions to compare the measurements of the 1/2-spin quantum states. The total velocity measured by these observers was identified as the addition of the velocity of a ZAMO, plus the local velocity of the particles measured by the ZAMO. These ZAMOs co-rotate the black hole due to frame-dragging and were used as a preliminary step before calculating the total local inertial velocity of the particles moving on the equator of the black hole. Therefore, we obtained a general algorithm to calculate the total spin precession angle, which is measured from the perspective of these hovering observers. The result does not assume a particular coordinate system but only depends on the axially symmetric metric coefficients.

After that, these results were applied to the most general Type-D Plebański–Demiański black hole. We obtained the general expression for the spin precession angle Δ_{PD} through the A and B coefficients (38) and the frame-dragging velocity $\cosh \eta_{PD}$ (40). Both coefficients and $\cosh \eta_{PD}$ are non-vanishing and they depend on the seven physical parameters arising in the Plebański–Demiański metric. The explicit expression of Δ_{PD} in terms of the physical parameters can be written down but it is a huge expression. Thus, we prefer to write down a short formula, in terms of the quartic function D and its derivative D' with respect to r. We study two branches of this case according to [22, 23]. The first one corresponds with $\alpha = 0$ and the second one with $l = 0$.

The first case (with $\alpha = 0$ and $l \neq 0$), corresponding to the non-accelerating Kerr–Newman–(anti-)de Sitter–NUT black hole, contains only six parameters and it is quite similar to the Plebański–Demiański case. In this right branch, we study different limits and we compute the spin precession angle for different subfamilies of solutions. Among these cases we have the Kerr solution with NUT and the NUT solution with rotation. Another cases included in the analysis were the Kerr, Schwarzschild–NUT, Schwarzschild–(anti-)de Sitter, Reissner–Nordström and Schwarzschild black holes. New results were found for Schwarzschild-NUT spacetime; the precession angle (52) has an asymptotic behavior at the Schwarzschild horizon shifted by the NUT parameter i.e. at r_{NUT}. For Schwarzschild–(anti)de Sitter spacetime there are also some interesting results (55) and (56). For positive Λ there is a large increment of the spin precession angle at the cosmological horizon, meanwhile for negative Λ, the cosmological constant has negligible effects and the precession angle has the same behavior as that of the Schwarzschild spacetime. For the second branch with $\alpha \neq 0$ and $l = 0$, we have the case of the accelerating and rotating black hole. The subfamily discussed in detail is the C-metric. We checked the consistency of our results by obtaining the Kerr, Reissner–Nordström and the Schwarzschild solutions also in this left branch.

The paper showed that the choices of 4-velocity, vierbein and observers are important to have a reliable measurement of the spin precession angle and obtain the perfect anti-correlation and the maximal violation of Bell's inequality. It is important to remember that as soon as the particles get closer to the event horizon for each case, their velocities increase very quickly until they asymptotically reach speed of light, with a rapid spin precession. The hovering observers would not be able to adjust the direction of the measurements of the spin, making virtually impossible any measurements of the entanglement.

In this paper, we considered only Type-D solution with a congruence of geodesic curves with non-vanishing expansion and twisting. It would be interesting to study analytic continuations of these solutions in order to find the interior solution supporting the spin precession below the event horizons and the static limit surface and above the cosmological

and acceleration horizons. Coordinates of the Kruskal–Szekeres type should be found for these metrics. It would be interesting also to extend our analysis to arbitrary non-equatorial orbits.

Another different Type-D solution is also known for the case of expansion but non-twisting. Among these solutions are the Robinson–Trautman Type D and the A-metrics. Moreover, Type-D solutions with non-expanding and non-twisting that emerge are the Kundt Type D and the B-metrics. It would be very interesting to generalize the results found in this paper to the description of entangled particles moving in these backgrounds. Future works would explore these scenarios.

Acknowledgments

References

[1] Collela R, Overhauser A W and Werner S A 1975 *Phys. Rev. Lett.* **34** 1472
[2] Peters A, Chung K Y and Chu S 1999 *Nature* **400** 849
     Gustavson T L, Landragin A and Kasevich M A 2000 *Class. Quantum Grav.* **17** 2385
[3] Hawking S W 1974 *Nature* **248** 30
     Hawking S W 1975 *Commun. Math. Phys.* **43** 199
[4] Birrell N D and Davies P C 1982 *Quantum Fields in Curved Space* (London: Cambridge University Press)
     Wald R M 1994 *Quantum Field Theory in Curved Spacetime and Black Hole Thermodynamics* (Chicage, IL: University of Chicago Press)
[5] Alsing P M and Milburn G J 2002 *Quantum Inform. Comput.* **2** 487
[6] Terashima H and Ueda M 2003 *Quantum Inform. Comput.* **3** 224
[7] Rembielinski J and Smolinski K A 2002 *Phys. Rev.* A **66** 052114
[8] Gingrich R M and Adami C 2002 *Phys. Rev. Lett.* **89** 270402
[9] Ahn D, Lee H, Moon Y H and Hwang S W 2003 *Phys. Rev.* A **67** 012103
[10] Li H and Du J 2003 *Phys. Rev.* A **68** 022108
[11] Wigner E P 1939 *Ann. Math.* **40** 149
[12] Weinberg S 1995 *The Quantum Theory of Fields: Foundations* vol 1 (Cambridge: Cambridge University Press)
[13] Terashima H and Ueda M 2004 *Phys. Rev.* A **69** 032113
[14] Einstein A, Podolsky B and Rosen N 1935 *Phys. Rev.* **47** 777
[15] Said J and Adami K Z 2010 *Phys. Rev.* D **81** 124012
[16] Robledo-Padilla F and García-Compeán H 2013 *Phys. Essays* **26** 86
[17] Plebański J F and Demiański M 1976 *Ann. Phys.* **98** 98
[18] Kramer D, Stephani H, MacCallum M and Herlt E 1980 *Exact Solutions of Einstein's Field Equations* 1st edn (Cambridge: Cambridge University Press)
[19] Griffiths J B and Podolský J 2005 *Class. Quantum Grav.* **22** 3467 (arXiv:gr-qc/0507021)
[20] Griffiths J B and Podolský J 2006 *Class. Quantum Grav.* **23** 555 (arXiv:gr-qc/0511122)
[21] Podolský J and Griffiths J B 2006 *Phys. Rev.* D **73** 044018 (arXiv:gr-qc/0601130)
[22] Griffiths J B and Podolský J 2006 *Int. J. Mod. Phys.* D **15** 335 (arXiv:gr-qc/0511091)
[23] Griffiths J B and Podolský J 2009 *Exact Space-Times in Einstein's General Relativity* (Cambridge: Cambridge University Press)
[24] Klemm D 1998 *J. High Energy Phys.* JHEP11(1998)019 (arXiv:hep-th/9811126)
[25] Caldarelli M M, Cognola G and Klemm D 2000 *Class. Quantum Grav.* **17** 399 (arXiv:hep-th/9908022)
[26] Dehghani M H 2002 *Phys. Rev.* D **65** 124002 (arXiv:hep-th/0203049)
[27] Chen W, Lu H and Pope C N 2007 *Nucl. Phys.* B **762** 38 (arXiv:hep-th/0601002)
[28] Chen W, Lu H and Pope C N 2006 *Class. Quantum Grav.* **23** 5323 (arXiv:hep-th/0604125)
[29] Page D N, Kubiznak D, Vasudevan M and Krtous P 2007 *Phys. Rev. Lett.* **98** 061102 (arXiv:hep-th/0611083)
[30] Santillan O P 2007 Tri-Sasaki 7-metrics fibered over the QK limit of the Plebański–demiański metrics (arXiv:hep-th/0701126)

H García-Compeán and F Robledo-Padilla

[31] Kubiznak D and Krtous P 2007 *Phys. Rev.* D **76** 084036 (arXiv:0707.0409 [gr-qc])

[32] Krtous P, Frolov V P and Kubiznak D 2008 *Phys. Rev.* D **78** 064022 (arXiv:0804.4705 [hep-th])

[33] Cariglia M, Krtous P and Kubiznak D 2011 *Phys. Rev.* D **84** 024008 (arXiv:1104.4123 [hep-th])

[34] Klemm D and Nozawa M 2013 *J. High Energy Phys.* JHEP05(2013)123

[35] Kagramanova V, Kunz J and Lämmerzahl C 2008 *Class. Quantum Grav.* **25** 105023

[36] Audretsch J and Lämmerzahl C 1983 *Gen. Rel. Grav.* **15** 495

[37] Raine D and Thomas E 2010 *Black Holes, An Introduction* (London: Imperial College Press)

[38] Al-Badawi A and Halilsoy M 2006 *Gen. Rel. Grav.* **38** 1729

[39] Gibbons G W and Hawking S W 1977 *Phys. Rev.* D **15** 2738

[40] Mortazavimanesh M and Mohseni M 2009 *Gen. Rel. Grav.* **41** 2697

[41] Griffiths J B and Podolský J 2005 *Class. Quantum Grav.* **22** 3467

[42] Griffiths J B, Krtous P and Podolský J 2006 *Class. Quantum Grav.* **23** 6745